



Sanderson, D., Cresswell, A., Seitz, B., Yamaguchi, K., Takase, T., Kawatsu, K., Suzuki, C., and Sasaki, M. (2013) Validated Radiometric Mapping in 2012 of Areas in Japan Affected by the Fukushima-Daiichi Nuclear Accident. University of Glasgow. ISBN 9780852619377

Copyright © 2013 University of Glasgow.

A copy can be downloaded for personal non-commercial research or study, without prior permission or charge

Content must not be changed in any way or reproduced in any format or medium without the formal permission of the copyright holder(s)

When referring to this work, full bibliographic details must be given

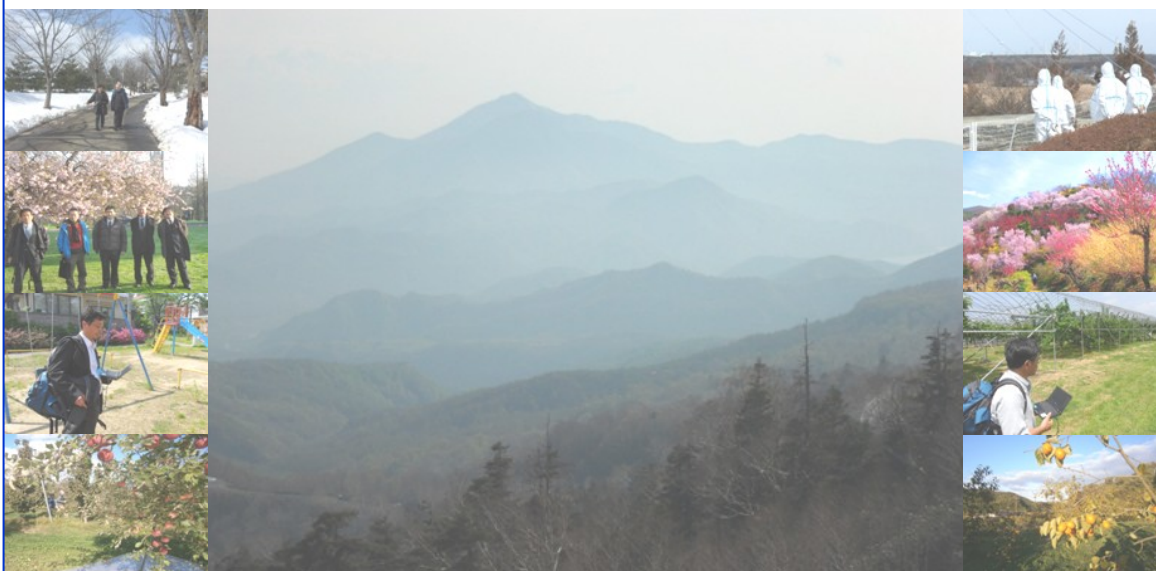
<http://eprints.gla.ac.uk/86365/>

Deposited on: 23 October 2013



Scottish Universities Environmental Research Centre

**Validated Radiometric Mapping in 2012 of Areas in
Japan Affected by the Fukushima-Daiichi
Nuclear Accident.**



D.C.W. Sanderson, A.J. Cresswell

Scottish Universities Environmental Research Centre

B. Seitz

SUPA School of Physics and Astronomy, University of Glasgow

K. Yamaguchi, T. Takase, K. Kawatsu, C. Suzuki, M. Sasaki

Faculty of Symbiotic System Science, Fukushima University

September 2013

East Kilbride Glasgow G75 0QF Telephone: 01355 223332 Fax: 01355 229898



The University of Glasgow, charity number SC004401



The University of Edinburgh is a charitable body, registered in Scotland, with registration number SC005336

© Scottish Universities Environmental Research Centre
East Kilbride, Glasgow, G75 0QF, UK

ISBN 978-0-85261-937-7

Published by:
University of Glasgow, Glasgow, G12 8QQ, UK, 2013.

要旨

2011年3月11日、日本の東北地方は、牡鹿半島の東70キロの海底の下を震源地とするマグニチュード9の地震に襲われた。本州北東部の海岸は、この地震による津波の被害にあった。その結果、福島第一原子力発電所の1号機から4号機までの原子炉は電源をすべて失い、冷却がまったく不可能になり、1号機、2号機、3号機で部分的な炉心溶融を起こし、一連の爆発が続き、大量の放射能が大気中に放出された。本事故は、国際原子力・放射線事象評価尺度（INES）レベル7（最高のレベル）と判断された。放出された放射能の多くは太平洋方向に拡散したが、かなりの量の放射性物質が日本の陸域に沈着し、局所的な放射線被曝を増大させた。

本報告書は、英国の大学の一チームが、2012年に日本を数次訪問し、日本の研究者と共に実施した、放射能計測および詳細な放射能マップ作成についての報告である。放射能マップは、作成時に、日本の地元の研究者に提供され、共有されている。本調査で得られたデータは、福島大学に設定された基準サイトから採取された土壌サンプルを基準に、クロス検証され、英国と日本で、それぞれ独自に分析された。本報告書では、上記のデータセットについて、また、セシウム134、セシウム137及びすべてのガンマ線線量率の検証済み放射分析マップについて、詳細に説明している。さらに、目盛り合わせ校正（キャリブレーション）サイトの設定についても、詳しく説明している。本書で報告される研究は、詳細な放射分析マップが、複雑な環境システムにおける放射性核種の拡散を理解する上で有効であることを明らかにしている。本報告書に収められた情報は、不必要な外部放射線被曝を防ぎ、除染復旧の対象地域を明らかにし、洗浄と土壌除去の効果を評価し、農業システムを介しての環境からの放射能摂取について調べ、環境放射能が時間とともに再拡散していくのをモニターする上で、有効である。本報告書には、本調査研究のデジタル・データがすべて含まれている。

放射分析法は、原子力の緊急事態において、放射能を計測し、環境への影響を理解する上で、有用であることが広く認められている。放射分析法は、原子力事故が起きた場合に、事故が環境に及ぼす影響について評価し、復旧方法の指針を出す上で、極めて重要である。スコットランド大学環境研究センター（The Scottish Universities Environmental Research Centre：略称SUERC）は、グラスゴー大学付属の研究センターであり、航空機モニタリングおよび陸域モニタリングを使用して、放射分析マップを作成する分野で、豊富な経験を有している。チェルノブイリ事故後の英国の放射能マップの殆どは、同センターが航空機モニタリングで作成したものである。また、原子力事故に緊急に対応するために、ヨーロッパ規模で制度の調整を行い、クロス・キャリブレーションも同センターがコーディネートした。大事故の直後、最も必要とされるのは、短時間に得られ、かつ広範囲にわたる情報である。福島第一原子力発電所の事故の場合、航空機モニタリングによる被害地域の調査は、当初は日米の合同チームによって、後に文部科学省と日本原子力研究開発機構によって行われ、全国規模の、数百メートル単位の空間解像度の放射能マップが作成された。事故の回復段階においては、より詳細な空間情報が求められる。客観的で、追跡可能で、クロス検証された分析が、より一層求められる。こうした調査を行うには、移動可能で、出来れば携帯可能で、効率がよく、頑丈で、きちんと

クロス・キャリブレーションされ、現場において詳細なリアルタイムの情報を直接提供できるシステムが必要である。SUERCの携帯ガンマ線スペクトロメトリ・システムは、以上の条件をすべて兼ね備えている。同システムは、10メートルの空間分解能以上の精度のものを提供し、10-20 cm単位の空間特性をリアルタイムで、確認することができる。

本書で報告される調査では、キャリブレーション・サイトを、福島大学のキャンパスと福島県果樹研究所に設定し、陸域モニタリング・システムについて、客観的かつ国際的に追跡可能な検証が出来るようにした。土壌サンプルの高分解能HPGeスペクトロメトリが福島大学の研究室とSUERCの研究室で実施され、それが、現場でのシステムの検証に使用された。両研究室で測定されたセシウム137の放射能濃度の値は、全く一致していた。セシウム134の放射能濃度の値の誤差は、5-10%の範囲内であった。この際に使用された土壌サンプルを詳細に調べた結果、放射能の大部分は土壌の表層に沈着していたものの、全放射能の約1%が表層より下に移行していることが明らかになった。このことは、土壌コラムにおける複雑な移行パターンについて、今後、さらに研究する必要があることを示唆している。本調査で設定したキャリブレーション・サイトは、将来も使用することができる。本報告書に収められたデータは、福島の地元の設備を、国際的に認知されている基準に照らして追跡可能にしたものであり、将来も使用することができる。

SUERCシステムを自動車に搭載して使用したが、比較的小型の検出器が、局所的な沈着パターンについて、1平方メートルあたり1万ベクレルから同1千万ベクレルまで、かなり広範囲の放射能レベルを計測できることを立証した。これらの放射能レベルは、全国規模の航空機モニタリングの当該地域の調査結果と、ほぼ同じであった。しかし、陸域モニタリングに基づくマップは、局所的な特徴についてかなり詳しく、局所的な差異を的確に捕捉し、土壌、覆域、構築環境に関連付けることが簡単である。2012年3月と同年7月に調査した地域は、福島県の一部であり、警戒区域と計画的避難区域の一部、および、2011年の津波の被災地域も含んでいる。市街区域における短時間のバックパック調査と、自動車による移動は、福島市(福島県の中心地)、大熊(福島第一原子力発電所の原子炉から3キロ以内)、南平、川内村(事故当初、警戒区域内)で行った。より詳細な情報が必要な場合に、自動車から降りてバックパックで調査することができ、同システムが融通性に富むことが立証された。

本調査では、スペクトロメトリ・システムが使われたが、ある放射性同位元素を特定し、自然放射線源のものと人工放射線源のものの放射能濃度を、1平方メートル当たり1万ベクレルから同1千万ベクレルまでの放射性セシウムまで、かなり広範囲にわたって、計量することが可能である。こうして得られた情報は、様々な発生源が線量率にどのような影響を与えているかを推定する際に使用された。自然界にある放射性物質(今回の事故には影響されていない)と、今回の事故により発生した放射性セシウム同位元素の影響とを比較することが容易に出来た。こうして得られた情報は、地元の人たちにとって大事なものである。復旧除染活動の指針を提供し、時と共に風化や放射性物質の崩壊により、徐々に事故による影響が減っていく度合いを観察できる。長期的には、こうした調査が、今回の事故による影響を広い

視野の中で理解し、改善の様子を記録することで被災地域に対する信頼が増していく上で、役に立つことを期待している。

市街区域では、バックパック・システムが、人々の生活空間の詳細な調査を行う上で最適の手段であった。福島大学と福島市飯坂町での調査では、詳細な放射分析マップにより、汚染度の高い配水管から、雨や雪解け水が沈着した放射能を取り除くため比較的汚染度の低い道路や表面が硬い場所まで、様々なレベルの汚染度を特定することができた。福島大学キャンパスでの復旧除染作業の効果は、明らかであった。放射分析マップは、復旧除染作業の効果を示し、今後、どこを除染すればいいかを特定することができた。同大学で行われた除染方法は、除染されていない場所に比べて、線量率を、3倍から4倍にまで低減していた。

果樹園や森林での除染は、とても難しい。しかし、福島県における農業の経済的な重要性、また、汚染された農作物が人体に入る可能性を考慮に入れると、局所的な放射能リスクを正確に把握することは、とても重要である。SUERCシステムは、福島県果樹研究所の果樹園、および、同県内の別の果樹園で使われた。茨城県つくば市の農業研究所とも調査が進められている。上記の諸サイトで、一年間にわたり計測を行った結果、沈着した放射性同位元素の半減や降水等の環境的要因による自力除染により、放射能が減少していることが分かった。上記の諸サイトで調査が継続されれば、土壌から果樹への移行の評価、果樹園を除染したり果樹の放射能摂取を削減する諸方策の効果の評価、果樹園で働く人々が接する外部線量率の評価等が可能になる。

本調査で収集されたデータは、特定の調査場所、特定の日時における、各同位体毎の特定の放射能のデータである。このデータは、本報告書の付録のCDに収められているが、透明性が高く、公開されており、独立的に検証されている。これらのデータは、参照のため、また、さらなる利用のために、利用することが可能である。

本報告書にまとめられた調査は、福島第一原子力発電所の事故により影響を受けた地域におけるモニタリング作業と除染復旧作業の困難さの多くを浮き彫りにしている。本調査は、日本の努力を助けるものとして、能力と方法を持つ国際コミュニティが存在していること、即ち、深刻な原子力発電所事故からの回復に伴う諸困難に取り組む国際協力の重要性を明らかにもしている。ここに収められたデータ、また、ここに紹介された方法が、将来の調査も含めて、今回の事故の環境への影響への理解が深まる上で役に立つことを願っている。日本の調査そして国際協力が、復興に貢献し、被災地域・コミュニティに対する信頼性の回復につながることを願っている。

Summary

On March 11 2011 the north-eastern region of Japan was hit by a magnitude 9 earthquake, which occurred underneath the sea-bed 70 km east of the Oshika peninsula in Tohoku. The north-eastern shore of Honshu was hit by a tsunami resulting from this earthquake. As a consequence, reactors 1-4 at the nuclear power station Fukushima-Daiichi suffered a completed loss of power and cooling causing a partial core meltdown in units 1, 2 and 3 followed by a series of explosions and the release of large quantities of radioactivity into the environment. The accident was rated level 7 (the highest level) on the International Nuclear Event Scale. While most of the emissions were driven towards the Pacific Ocean, a significant amount of radioactive material was deposited onto the Japanese land-mass, resulting in enhanced localised radiation exposure.

This report covers measurements and detailed radiation maps conducted by a UK University team working with Japanese colleagues during a series of visits in 2012. They have been presented and shared locally in Japan at time of acquisition. Since then the data have been cross-validated relative to soil samples from a reference site established at the University of Fukushima, and analysed independently in the UK and in Japan. This report provides detailed descriptions of the data sets, validated radiometric maps for ^{134}Cs , ^{137}Cs and the overall gamma dose rates, together with a full account of the establishment of the calibration site. The work reported here demonstrates the utility of detailed radiometric maps in helping to understand the distribution of radionuclides in complex environmental systems. This information is potentially of use to help avoid unnecessary external radiation exposure in the outdoor environment, to help to visualise and target areas for remediation, to evaluate the effectiveness of clean-up and soil removal activities, to examine uptake of radioactivity from the environment through agricultural systems, and to monitor redistribution over time of the activity in the environment. The report includes full copies of digital data sets for the demonstration surveys.

Radiometric methods provide means of measuring radioactivity with recognised roles in nuclear emergency response, and environmental applications. In the aftermath of nuclear accidents they are crucial to evaluate the environmental impact of the accident and guide remediation measures. The Scottish Universities Environmental Research Centre (SUERC) is a research centre attached to the University of Glasgow with extensive experience of radiometric mapping using airborne and ground based systems, conducting most of the UK post-Chernobyl radiation mapping using airborne systems and coordinating European projects to harmonise and cross-calibrate systems for nuclear emergency response purposes. In the early stages of major accidents the most pressing needs are for rapid, large scale, information. Airborne surveys of the affected area were conducted initially by a joint US/Japanese team and later on by The Ministry of Education Science and Technology (MEXT) and the Japanese Atomic Energy Agency (JAEA), eventually providing national scale radiation maps with a spatial resolution of several hundred meters. In later stages of accident recovery there are increasing needs for more detailed spatial information and increasing requirements for objective, traceable and cross validated analysis. Systems for this work need to be mobile, preferably portable, efficient, robust and well calibrated, providing detailed real time information directly on location. The SUERC Portable Gamma Spectrometry system fulfils these criteria. It provides a spatial resolution of better than 10 m for mapped data and allows a real time identification of spatial features down to 10-20 cm.

In the work reported here, calibration sites have been established in Fukushima at the campus of Fukushima University and the Fukushima Prefecture Fruit Tree Research Institute to provide objective and internationally traceable validation of ground based instruments. High resolution HPGe spectrometry of soil samples conducted at laboratories at Fukushima University and SUERC was used for validation of the field instrument. Values of ^{137}Cs activity concentration measured by the two laboratories were in full agreement to high precision. Agreement for the ^{134}Cs activity concentration values was within 5-10%. The soil samples used in this process were analysed as a function of depth, revealing that while the majority of activity was retained in near surface layers, a small component of approximately 1% of the total activity appears to have migrated more rapidly to greater depths. This suggests complex transport behaviour in the soil columns which should be investigated further. The calibration sites are open for future use. These data establish a traceable record between local facilities and internationally acknowledged standards for future use.

Deployment of the SUERC system in vehicles has demonstrated the ability of relatively small detectors to measure regional scale deposition patterns over a wide range of radioactivity levels, varying from 10,000 Bq per square meter up to more than 10 million Bq per square meter. These activity levels are broadly consistent with the national scale airborne maps for the study areas, but the ground based maps provide very high levels of local detail, which allow small scale changes to be readily observed and related to the local soils, land cover and built environment. Areas covered in two surveys in March and July 2012, respectively, cover parts of the Fukushima Prefecture including parts of the evacuation and exclusion zones as well as areas directly affected by the 2011 tsunami. Short backpack surveys in urban areas associated with the car trips were also conducted e.g. in Fukushima City (in the heart of the prefecture), Ōkuma (within 3 km of the Fukushima Daiichi reactors), Minami-Daira and Kawauchi-mura (within the initial evacuation zones). This demonstrates the versatility of a system which can be rapidly moved from a vehicle to backpack where further detailed information is needed.

With a fully spectrometric system as used in this study, it is possible to identify specific radioactive isotopes and to quantify the activity concentrations of natural and artificial sources spanning many orders of magnitude, from less than 10 kBq m⁻² to above 10 MBq m⁻² for radiocaesium. This information has been used to estimate the contribution to the dose rate from different sources, so that a comparison between the contributions from naturally occurring radioactive materials (not affected by the accident) and the different radiocaesium isotopes present following the accident can be readily made. These data provide vital information to the local population and emergency services in guiding remediation efforts, and also over the course of time, in observing the extent to which weathering and radioactivity decay processes are gradually reducing the relative contributions from the accident. In the long term it is hoped that this type of representation will help put the accident contributions into perspective, and to register improvements with time which may help to establish increased confidence in affected areas.

In urbanised areas backpack systems provide the means of producing detailed surveys in locations where people spend their time. Surveys conducted at Fukushima University and Fukushima Iizaka have demonstrated the ability of detailed radiometric mapping to identify locations with highly varying levels of contamination, from more highly contaminated areas around drain pipes to the relatively low levels of contamination on roads and other hard surfaces where rain and snow melt have removed deposited activity. The effectiveness of the remediation work conducted on the University campus was evident, showing the ability of

radiometric surveys to demonstrate the effectiveness of remediation and to identify where remaining activity is located. The remediation methods employed resulted in a three to four fold reduction in dose rate compared to untreated areas.

Remediation efforts in orchards or woodland are particularly challenging. Given the economic importance of agriculture in the Fukushima area and the possible pathways from contaminated produce into the human body, a precise evaluation of the local radiation risk is of prime importance. The SUERC system has been demonstrated in orchards at the Fukushima Prefecture Fruit Tree Research Institute, and at other orchards in the Prefecture. Work has also been undertaken with agricultural research institutions at Tsukuba, Ibaraki Prefecture. The comparison of measurements taken at these same sites over the time of a year show a decrease in activity following the half-life of the radioisotopes deposited, superimposed by environmental factors like precipitation and redistribution, illustrating self-remediation. Ongoing work on these sites will allow an assessment of transfer of activity in these systems, and the impact of measures to remediate the orchards or reduce uptake of activity in the fruit, and evaluate external doses to workers in the orchards.

The data collected during this work contain the activity per isotope at a given surveyed location and at a given moment in time. The data accompanying this report are transparent, open and independently validated. They are made available for reference purposes and further utilisation.

The work presented here highlights many of the difficult challenges ahead in the monitoring and remediation effort in the area affected by the accident in the Fukushima Dai-ichi nuclear power plant. It demonstrates the capabilities and methods at the disposal of the international community in aiding the Japanese efforts, demonstrating the value of international collaboration in helping to address some of the difficult problems associated with recovery from a serious nuclear accident. It is hoped that these data, and the methods which they demonstrate, will contribute, together with future work, to increased understanding of the environmental impacts of the accident, and that future cooperative work involving Japanese and international teams will contribute to recovery and restoration of confidence in affected areas and communities.

Overview

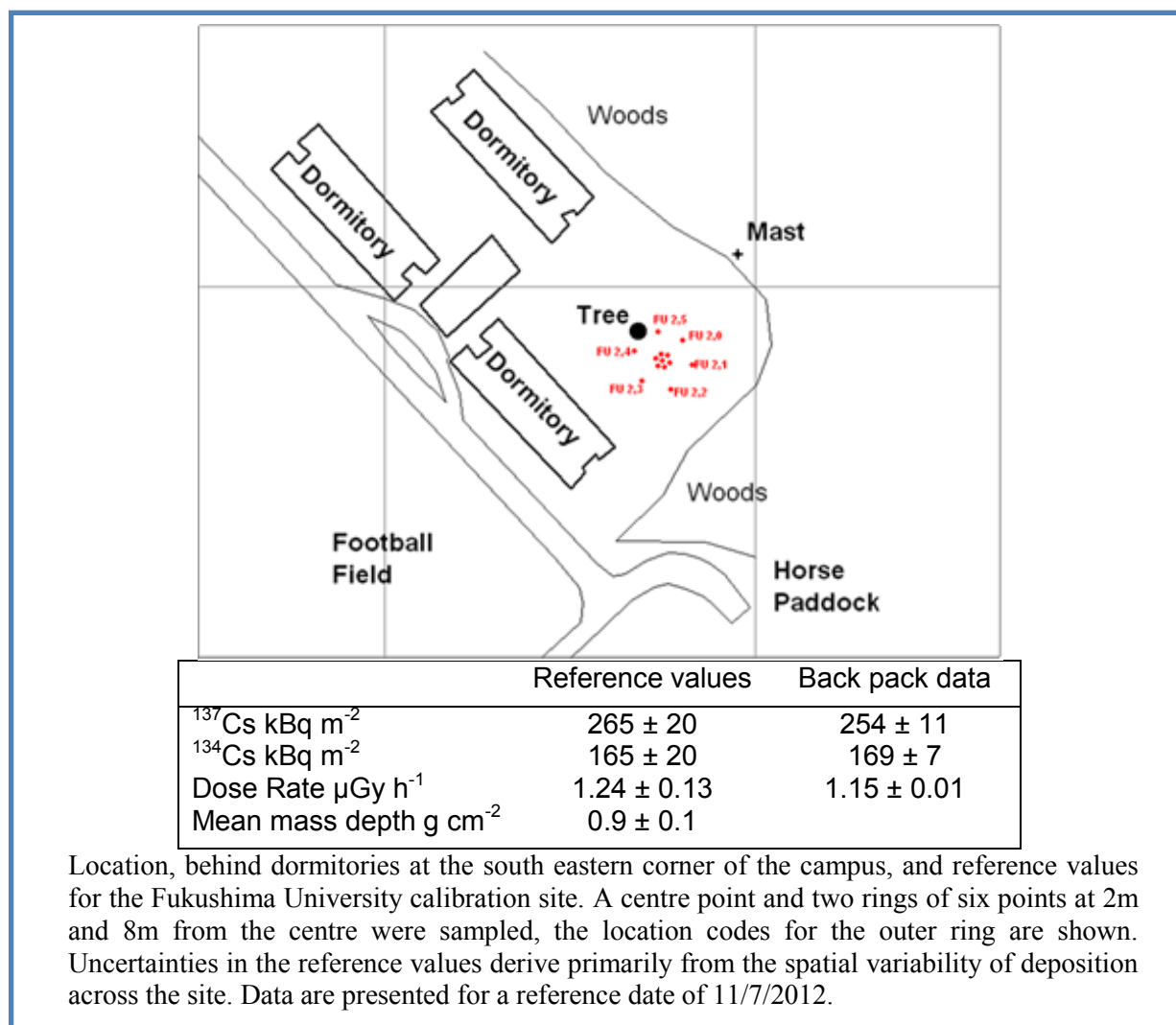
This report provides details of measurements and detailed radiometric maps undertaken by teams from the Scottish Universities Environmental Research Centre (SUERC) and the University of Glasgow in Japan in 2012. This was undertaken in support of work being conducted by Japanese institutions, including Fukushima University and the Fukushima Prefecture Fruit Tree Research Institution. SUERC is a research centre attached to the University of Glasgow with extensive experience of environmental radioactivity measurements including airborne and ground based radiometric mapping utilising sensitive gamma ray spectrometers on mobile platforms. SUERC conducted most of the UK post-Chernobyl radiation mapping using airborne systems, and subsequently coordinated European projects to harmonise and cross-calibrate airborne, vehicular and ground based radiation measurements for nuclear emergency response purposes.

Radiometric methods provide means of measuring natural and artificial radioactivity with recognised roles in nuclear emergency response, and other environmental applications. Airborne gamma spectrometry (AGS) is uniquely capable of recording deposited radioactivity patterns over very large areas. It therefore takes on vital roles, especially in the early stages of nuclear accident response, to defining the main features of national deposition, while minimising operator exposure to hazardous levels of radiation. In Japan in 2011 the AGS method was used effectively from March 2011, initially by a joint US/Japanese operation, and then by MEXT/JAEA to define the levels and locations of major deposition following the accident. Full national mapping was achieved by the early months of 2012, with the major features to the NW of the Fukushima Daiichi site being apparent by May 2011, and, together with ground based observations, informing decisions to confirm and extend evacuation zones. In the early stages of major accidents the most pressing needs are for rapid, large scale, information, for which AGS is the preferred method. In later stages of accident recovery there are increasing needs for more detailed spatial information including local radiation mapping at domestic scales, to target and evaluate remedial actions and to help understand agronomic impacts. Moreover in later stages there are also increasing requirements for objective, traceable and cross validated analysis in order to maintain confidence in the outcomes, and to support recovery.

The work reported here was conducted during visits to Japanese institutions and communities in March, May, July and November 2012. Calibration sites have been established in Fukushima to provide objective and internationally traceable validation of ground based instruments. Measurements were undertaken with the SUERC Portable Gamma Spectrometry system, a GPS-linked gamma ray spectrometer capable of operation for vehicular and backpack surveys to define the general levels and locations of radionuclides. The SUERC system includes a real time display that allowed local variations in the environment to be noted by the operator and others during the survey. This allowed immediate feedback of survey results to collaborators. In addition, preliminary results of the work reported here were presented at workshops and other occasions during 2012. The data collected are freely available, in an internationally defined exchange format, for further utilisation. This report presents and discusses the results of all these surveys.

Calibration sites

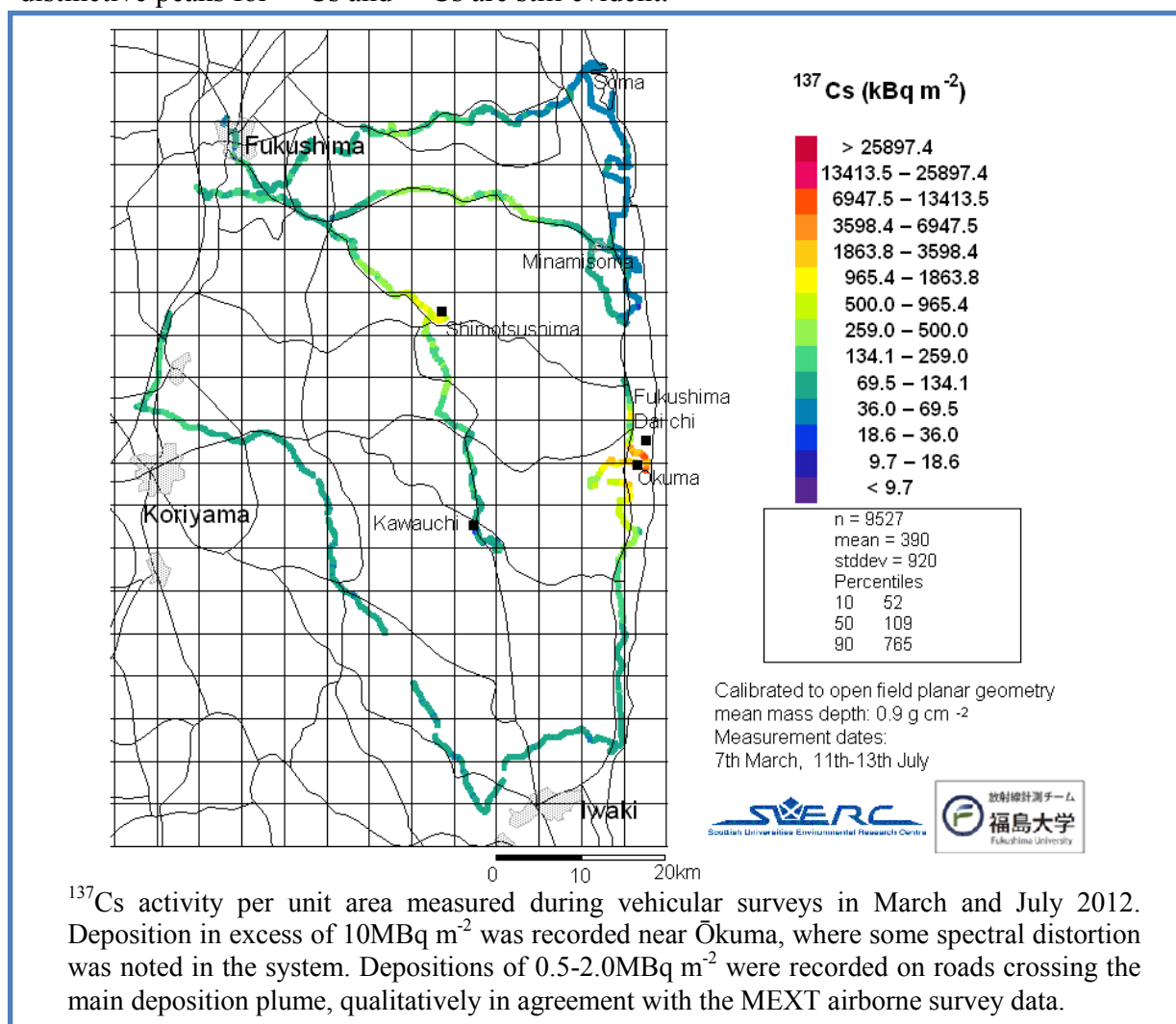
The rationale for the use of calibration sites has long been established. They allow verification of the calibration of instruments relative to international reference materials, such that quantified activity concentrations and dose rates may be reliably used. The use of calibration sites allows data collected by different instruments and organisations to be compared. Work conducted at SUERC in the early 1990s resulted in the development of a spatially representative sampling scheme for airborne and ground based system consisting of hexagonal sampling rings at increasing radii. Calibration sites using this pattern have been used for verification of the performance of SUERC radiometric systems and in International Intercomparison Exercises conducted in Europe in 1995 and 2002. A site was established at Fukushima University in July 2012, with soil samples analysed at Fukushima University and SUERC, and used to verify the performance of the backpack system used. The activity concentration determined with the SUERC system for ^{134}Cs and ^{137}Cs agree with the reference values, with the dose rate agreeing within 10%. A second site was identified at the Fruit Tree Research Institute, and sampled in November 2012 with the analysis of these samples ongoing. Performance of the SUERC system has also been verified against calibration sites in Scotland extensively sampled for an international intercomparison exercise.



Vehicular Surveys

Radiometric systems deployed in vehicles allow relatively rapid measurements over regional scale areas, albeit limited to areas accessible to vehicles. The fields of view of vehicular systems, typically 5-10m, include significant areas of the road surface which is not expected to be representative of local deposition due to self-remediation effects. Despite the effect of the road surface, it is recognised that vehicular measurements are able to measure regional scale deposition patterns and can play a valuable part in nuclear emergency response. The work in Japan using the SUERC Portable Gamma Spectrometry system was conducted to assess the ability of relatively small detectors to measure regional scale deposition patterns.

Measurements conducted in March and July 2012 confirm the ability of the small detector in the SUERC system to measure activity concentrations and dose rates across a range of several orders of magnitude, even in vehicles with additional shielding. Data collected from roads in the evacuation and exclusion zones produce data qualitatively similar to the national scale airborne maps. Short backpack surveys within these vehicular surveys demonstrate the higher level of detail available from close spaced surveys, and the versatility of a system that can be rapidly moved from a vehicle to backpack where further detail would be of particular value. The March 2012 measurements conducted within the exclusion zone showed activity concentrations and dose rates orders of magnitude greater than those observed in Fukushima City and surrounding areas. In the highest activity areas surveyed, around Ōkuma, the spectra show some distortion due to random summing of gamma-rays in the detector, however the distinctive peaks for ^{134}Cs and ^{137}Cs are still evident.



Backpack Measurements of Urbanised Areas

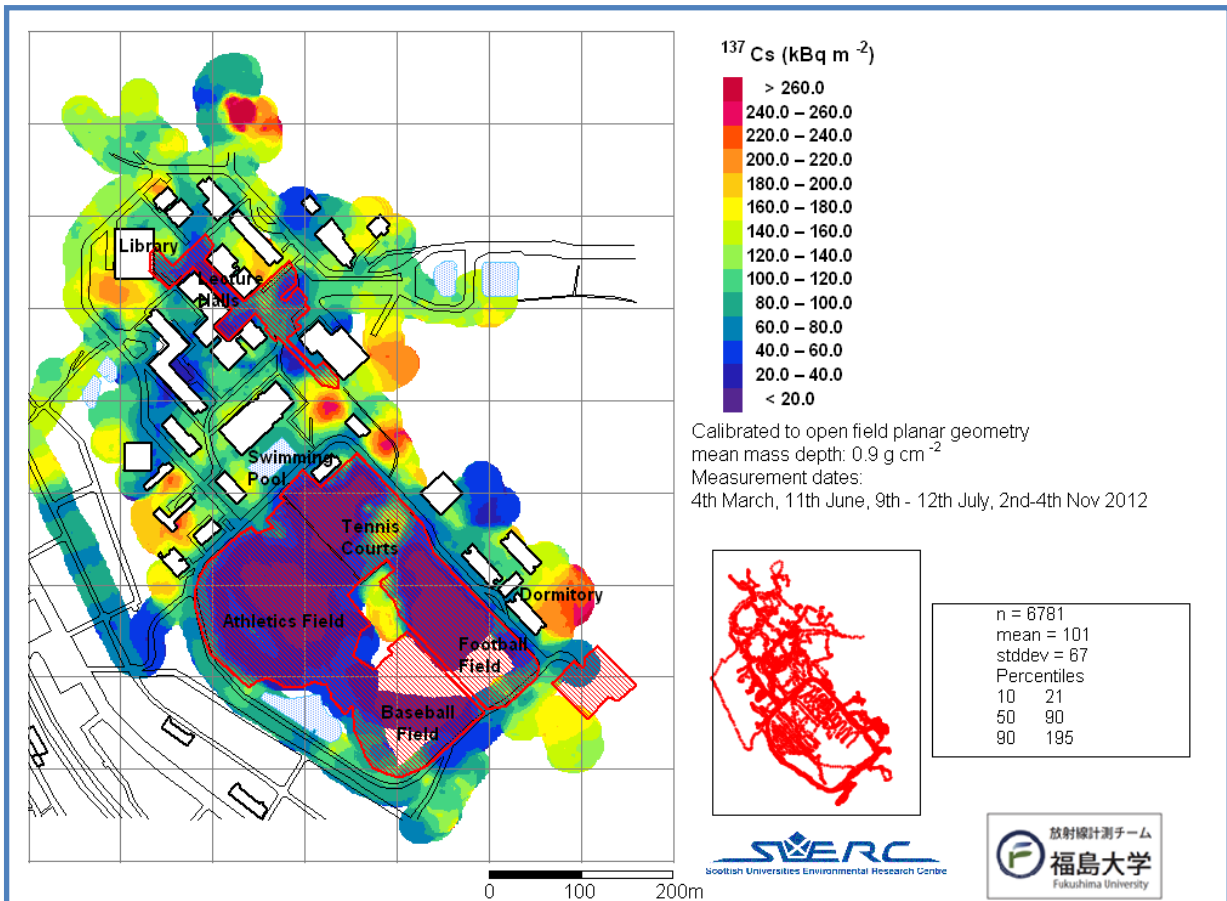
Radiometric systems can be used to produce detailed maps of the distribution of radioactivity over small areas. In urbanised areas backpack systems provide the means of producing such detailed surveys, allowing data collection to be conducted in locations where people spend their time. Such detailed mapping can be used to identify small locations with locally high activity concentrations, which if in areas of high use by members of the public may be considered for priority in remediation programmes. By conducting such surveys after remediation, the effectiveness of the remediation in reducing dose to members of the public can be evaluated. During the course of 2012, the SUERC system was used to collect data from two urbanised areas, the campus of Fukushima University and part of Fukushima City.

The majority of the campus of Fukushima University was surveyed in July 2012, with circuits of the sports fields and small areas around some of the buildings measured in March and November. The surveys showed most of the campus having levels of contamination $< 50 \text{ kBq m}^{-2} \text{ }^{134}\text{Cs}$ and dose rates $< 0.30 \text{ } \mu\text{Gy h}^{-1}$. Some small areas had higher activity concentrations ($> 100 \text{ kBq m}^{-2} \text{ }^{134}\text{Cs}$) and dose rates ($> 0.80 \text{ } \mu\text{Gy h}^{-1}$), mostly where access was limited and occupancy low. Part of Fukushima City was surveyed in May 2012, showing relatively low levels of deposited activity on road ways, with very low levels recorded inside buildings, and some areas of higher deposited activity on vegetated areas. These surveys demonstrate the ability of detailed radiometric mapping to identify locations with higher levels of contamination. When combined with information on human movements and occupancy of different areas this data could allow the identification of areas where contamination is most significant, and hence target remediation efforts.

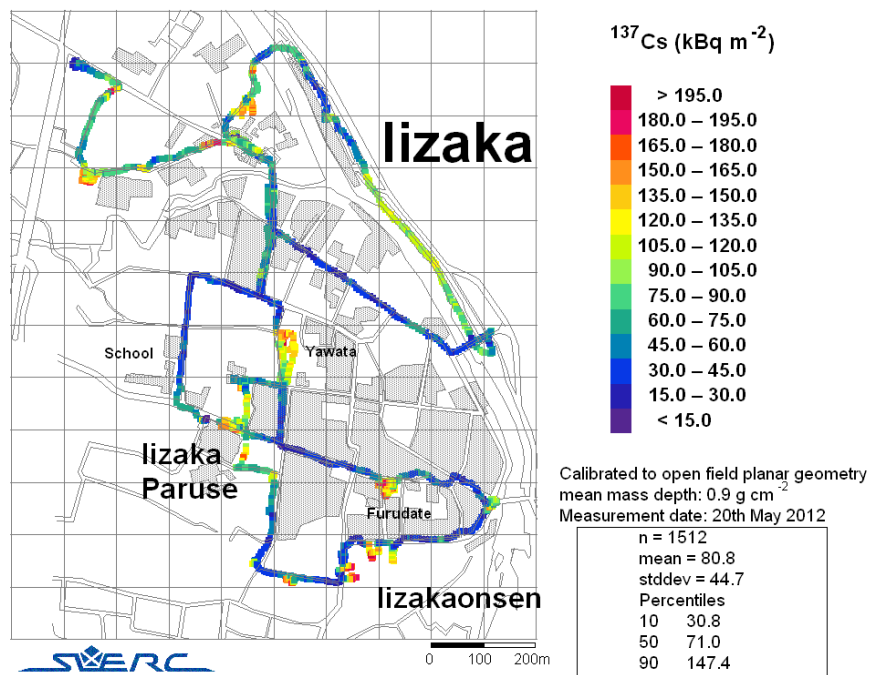
The effectiveness of the remediation work conducted on the University campus prior to the survey was evident, with most of the sports fields where turf had been replaced showing activity concentrations $< 5 \text{ kBq m}^{-2}$ and dose rates $< 0.05 \text{ } \mu\text{Gy h}^{-1}$. Remediation on other parts of the campus was less effective, with some of the tennis courts with artificial surfaces in particular showing very small reductions in activity concentrations compared to the unremediated parts of the campus. This has shown the ability of radiometric surveys to demonstrate the effectiveness of remediation and where remaining activity is located.

Deposited activity will not be permanently fixed in the environment. Natural processes will result in migration of activity, vertically to greater depth in soil and laterally. Rain and snow melt will wash activity from hard surfaces where it adheres less strongly, onto soils at verges or into river systems which can transport it to sediment traps downstream or into the sea. Detailed mapping reported here has shown that roads, and other similar hard surfaces, have lower levels of deposited activity compared to their immediate surroundings. Road drains with accumulated sediment have been shown to hold enhanced levels of activity, trapped from material removed from the roads by rain.

With a fully spectrometric system, such as the SUERC system, it is possible to quantify the activity concentrations of natural and artificial sources. This information has been used to estimate the contribution to the dose rate from radiocaesium and natural activity. A dose rate apportionment allows the significance of artificial contamination to the dose rate to be evaluated. Within the buildings where data has been collected, dose rates have been significantly reduced compared to the general area, with a reduced contribution from artificial activity.



^{137}Cs activity per unit area measured at Fukushima University campus, March-November 2012. The hashed areas indicate locations which had been remediated prior to the July 2012 survey, with significant reductions in activity concentrations and dose rates to 25-35% of the unremediated areas. The high activity feature at the north of the site is a restricted access area storing soil removed during remediation. The calibration site is located behind the dormitories at the south eastern corner of the campus.



^{137}Cs activity per unit area measured in Fukushima Iizaka, 20th May 2012, using the SUERC backpack system. Much of the survey was conducted on road surfaces that generally have lower activity concentrations. Vegetated areas beside the roads have higher activity concentrations. Small area surveys were conducted around a shrine at Yawata and a playground at Furudate where activity concentrations are higher.

Backpack Measurements of Fruit Cultivation Areas.

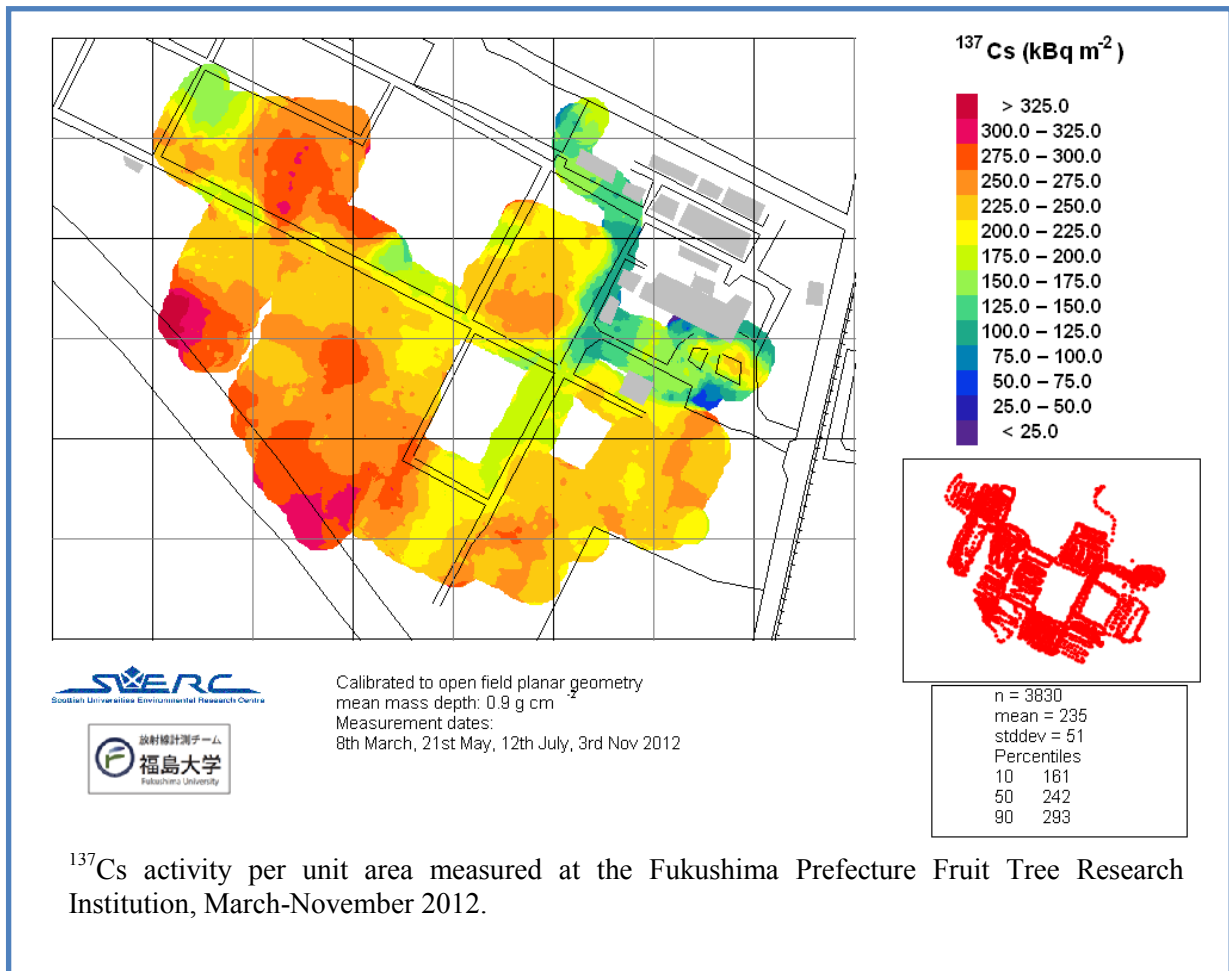
Fruit cultivation is a significant contribution to the economy of Fukushima Prefecture, and has been very heavily affected by the accident at Fukushima Daiichi. Uptake of activity into fruit, and methods of remediating orchards are major issues. Fukushima Prefecture operate a Fruit Tree Research Institute in the northern part of Fukushima city, which received a substantial deposition of activity following the accidents. An arrangement with staff at the research institute allowed the demonstration of the SUERC system at the institute orchards, and at orchards in more severely affected areas. Work has also been undertaken with agricultural research institutions at Tsukuba.

Activity transfer to fruit is a major concern. Some studies of transfer to fruit trees from soil and leaf were conducted following the Chernobyl accident. These showed that interception of activity by leaves was the most significant factor in initial contamination, with this activity translocating between different parts of the trees over the first 4-5 years. Thereafter, transfer from soil became a more important mechanism, with transfer rates controlled largely by soil type and chemistry. However, these studies may not be fully applicable to the particular varieties of fruit and soil types in Japan. It has been shown that immediately after the accident there was transfer from deposition on bark, which had not previously been observed. As the activity migrates further into the soil, especially as it enters the rooting zone of the trees, transfer from soil would be expected. Further work in understanding the particular mechanisms relevant for transfer of activity to fruit for the plant varieties and soils of Fukushima Prefecture would be of considerable benefit.

Mapping the deposition in fruit orchards allows the ratio of activity concentrations in fruit and on the ground to be measured. This is important data to help understand transfer processes, and hence develop methods to reduce such transfer that would be of a considerable benefit to fruit farmers in the area. Measurements were conducted at the Fukushima Prefecture Fruit Tree Research Institute in March, May, July and November 2012, and other areas of fruit cultivation in July and November. Ongoing work on these sites will allow an assessment of transfer of activity from to the fruit, and the impact of measures to remediate the orchards or reduce uptake of activity in the fruit. Mapping of deposition also allows the evaluation of external doses to workers in the orchards.

Isotopic Composition of Deposited Activity

Within a nuclear reactor, the relative composition of different radionuclides will depend upon irradiation history, and the isotopic composition of material in different locations within a reactor will vary. The isotopic composition of deposited activity can serve as a guide to the dynamics of the release processes during the accident. In addition, the production processes for ^{134}Cs and ^{137}Cs are different, and the isotopes may be released in different chemical forms and associations that could behave differently in the environment with implications for long term impacts. The data reported here, along with a brief review of data published elsewhere, has been used to evaluate any potential variation in the ratio of ^{134}Cs to ^{137}Cs activity concentrations. The measurements reported here show dispersion in the radiocaesium activity ratio of 10-15%, similar to other studies. Although partly explained by measurement precision, this suggests that there is some variation in isotope ratio reflecting different phases of release. The relatively small variation does, however, suggest that the terrestrial deposition was dominated by activity released from a single reactor core, with mixing within the reactor building prior to release.



Further Work

The data collected during this work have been prepared in a data exchange format designed during European collaborative work to facilitate exchange of fully-spectrometric radiometric data. These data sets are made available for reference purposes and utilisation in the ongoing work in Japan to remediate the environment, reduce dose to members of the public and restore normalcy to the life of the people of Japan.

The work presented here is a contribution to the beginning of the difficult challenges ahead. This work demonstrates the value of international collaboration in helping to solve difficult problems. There is a lot of work still to be completed. The work presented here demonstrates some of the approaches that will be of value in that work, and it is hoped that such approaches will be adopted to aid the work ahead.

Acknowledgements

The assistance of Yushin Toda (Japan Desk, Scotland) and Dr Sheng Xu (SUERC) in providing Japanese translation and assistance with Japanese scientific terminology is gratefully acknowledged.

The work reported here was supported by the Foreign and Commonwealth Office Prosperity Fund, the University of Glasgow Internationalisation Fund, the Great Britain Sasakawa Foundation.

We would also like to acknowledge the generous welcome which we received from scientists and individuals in all the Japanese institutions visited in 2012, and in particular the following organisations and individuals.

Faculty of Symbiotic System Science, Fukushima University.

Professor Katsushiko Yamaguchi for extending the initial invitation to visit Fukushima University and hosting and conducting reciprocal visits between SUERC and Glasgow University and Fukushima, T. Takase for preparing and analysing samples from cores collected at the calibration sites, Professor Kencho Kawatsu for arranging access to the exclusion zone and facilitating contact with prefecture institutions, Chika Suzuki and Miyuki Sasaki for assistance with data collection, Professors Takayuki Takahashi, Kenji Nanba, Yoshitaka Takagai, Osamu Nittono and Yamakawa Mitsuo, for their support and interest in the work.

Fukushima Prefecture Fruit Tree Research Institute.

Mamoru Sato and his team (Hiroyuki Ajito, Haruo Katsumata, Katsunori Takita, Abe Kazuhiro Minako Yuda) for arranging and facilitating measurements in the institute orchards and commercial orchards in the evacuation zone and in the vicinity of Fukushima.

NARO Food Research Institute, Tsukuba

Dr Setsuko Todoriki, Dr Kiyoshi Hayashi, Dr Toshio Ohtani, Dr Shinichi Kawamoto (National Food Research Institute), Katsushi Shirahata, Tomijiro Kubota (National Institute for Rural Engineering), Dr Yasuyuki Shibata (National Institute for Environmental Studies, Tsukuba) for facilitating exploratory work in Tsukuba.

Professor Masatoshi Morita (President, Society for Remediation of Radioactive Contamination in the Environment), for inviting David Sanderson to participate in the International Symposium on Remediation of Site Contamination Caused by the Fukushima Accident in May 2012. Dr John Cardarelli (US Environmental Protection Agency), Dr Hironori Kamemoto (EFA Laboratories, Tokyo) for assistance in collecting data at Fukushima Iizaka in May 2012 during the meeting.

Okuma town council and the police officers who escorted us safely into the exclusion zone.

Dr. Douglas MacGregor, SUPA School of Physics and Astronomy, University of Glasgow for accompanying and assisting in field work to remeasure the European (ECCOMAGS) reference sites in the Solway.

Contents

1. Introduction	1
1.1 Radiometric Mapping	1
1.2 Radiometrics and Nuclear Emergencies	1
1.3 March 2011 Nuclear Accidents	2
1.4 Calibration and Validation	8
1.5 This Work	8
2. Radiometric Methods	11
2.1 Summary of Systems and Analytical Approaches	14
2.1.1 Data Reduction Approaches	14
2.1.2 Gain monitoring and stabilisation	15
2.2 Relationship Between Airborne, Vehicular and Backpack Systems	16
2.3 SUERC Portable Gamma Spectrometry System	16
2.4 Data presentation and mapping	18
2.4.1 Mapping	18
2.4.2 Dose rate apportionment	19
3. Establishment of Calibration Sites in Fukushima	21
3.1 Reasons for Establishing Calibration Sites	21
3.2 Calibration Site at Fukushima University	22
3.2.1 Site selection and sampling	22
3.2.2 Sample preparation and measurements	22
3.2.3 Activity concentrations and $^{134}\text{Cs}/^{137}\text{Cs}$ ratios from the calibration samples ..	26
3.2.4 Depth profiles and activity per unit area for the calibration site	29
3.3 Additional Sites	32
4. Radiometrics and Recovery From Nuclear Accidents	35
4.1 Vehicular Surveys	35
4.1.1 Fukushima City, March 2012	36
4.1.2 Exclusion Zone, March 2012	38
4.1.3 Backpack Measurements Within the Exclusion Zone, March 2012	42
4.1.4 Carborne surveys in July and November 2012	50
4.1.5 Discussion of Vehicular Survey Results	54
4.2 Fukushima University Campus and Fukushima Iizaka	55
4.2.1 Fukushima University Surveys	56
4.2.2 Evaluation of Remediation	63
4.2.3 Fukushima Iizaka Survey	66
4.2.4 Discussion of Fukushima University and Fukushima Iizaka Surveys	71
4.3 Fruit Tree Cultivation	72
4.3.1 Fruit Tree Research Institute	74
4.3.2 Fruit Cultivation Areas in Fukushima Prefecture	87
4.3.3 Tsukuba	97
4.3.4 Discussion of Surveys of Areas of Fruit Cultivation	101
4.4 Assessment of Radionuclide Ratio	102
4.4.1 Vehicular survey results	105
4.4.2 Backpack measurements	108
4.4.3 Discussion of Radionuclide Ratios	111
5. Discussion and Conclusions	112
References	115

目次

1.	はじめに	1
1.1	放射性計測マッピング	1
1.2	放射線計測及び核緊急事態	1
1.3	2011年3月核事故	2
1.4	キャリブレーション及び妥当性	8
1.5	この研究	8
2.	放射性計測方法	11
2.1	システム及び分析アプローチのまとめ	14
2.1.1	デッタ生成アプローチ	14
2.1.2	ゲイン・モニタリング及び安定性	15
2.2	航空機と自動車に搭載システム及びバックパックシステム間の関係	16
2.3	SUERCの携帯ガンマ線スペクトロメトリ・システム	16
2.4	デッタ表現及びマッピング	18
2.4.1	マッピング	18
2.4.2	線量率配分	19
3.	福島にキャリブレーション地点の設置	21
3.1	キャリブレーション地点設置の理由	21
3.2	福島大学にキャリブレーション地点	22
3.2.1	地点選定及びサンプリング	22
3.2.2	サンプル準備及び測定	22
3.2.3	キャリブレーション試料の放射能濃度及び $^{134}\text{Cs}/^{137}\text{Cs}$	26
3.2.4	キャリブレーション地点の深度プロファイル及び単位面積当たり放射能濃度	29
3.3	他のサイト	32
4.	核事故の放射性計測及び除染	35
4.1	自動車に搭載システムによる調査	35
4.1.1	2012年3月福島市内	36
4.1.2	2012年3月警戒区域	38
4.1.3	2012年3月警戒区域以内のバックパックシステム測定結果	42
4.1.4	2012年7月と11月自動車に搭載システムによる測定結果	50
4.1.5	自動車に搭載システム測定結果の検討	54
4.2	福島大学と福島市飯坂町	55
4.2.1	福島大学での調査	56
4.2.2	除染の評価	63
4.2.3	福島市飯坂町での調査	66
4.2.4	福島大学と福島市飯坂町での測定結果の検討	71
4.3	果樹園	72
4.3.1	福島県果樹研究所	74
4.3.2	福島県内の別の果樹園	87
4.3.3	つくば	97
4.3.4	果樹園の測定結果の検討	101
4.4	放射性核種比の評価	102
4.4.1	自動車に搭載システム測定結果	105
4.4.2	バックパックシステム測定結果	108
4.4.3	放射性核種比の検討	111
5.	議論及び結論	112
	引用文献	115

Figures

Figure 1.1: Map of evacuation areas, and areas where restrictions have been removed.	5
Figure 1.2: Dose rates for the area within 80km of the Fukushima Daiichi NPP generated from airborne survey data collected by the US DOE and MEXT in the first few weeks after the accidents. Taken from MEXT 2011.	6
Figure 1.3: Dose rates for Japan generated from airborne survey data collected on behalf of MEXT by July 2012. Taken from MEXT 2012.	7
Figure 1.4: Location of areas surveyed using the SUERC Portable Gamma Spectrometry system in 2012.	9
Figure 1.5: Location of areas surveyed around Fukushima City in 2012. Showing the Fruit Tree Research Institute and Fukushima Iizaka (top centre), Mount Shinobu (top left), Fukushima University (bottom left) and areas of fruit cultivation surveyed near Date (right).	10
Figure 2.1: Typical 3x3" NaI(Tl) and Ge spectra showing the positions of characteristic peaks from natural activity (^{40}K , ^{214}Bi from the ^{238}U series, and ^{208}Tl from the ^{232}Th decay series), and peaks from ^{134}Cs and ^{137}Cs . The top spectrum is from an area of relatively low contamination. The middle spectrum is from an area with greater levels of contamination, and shows the interference between the ^{134}Cs 1365keV and the ^{40}K 1461keV peaks. The bottom spectrum is for a laboratory sample (sum of top samples from the Fukushima University calibration site), the 1038, 1167, 1175 and 1400.6 keV peaks are due to cascade summing in the close-coupled laboratory geometry.	13
Figure 2.2: Dose rate apportionment for the Fukushima University calibration site and SUERC.	20
Figure 3.1: Map of the calibration site, with the outer (8m) ring labelled.	23
Figure 3.2: The calibration site from the north west (left and centre) and south (right).	23
Figure 3.3: NaI(Tl) spectrum recorded from the Fukushima University calibration site and summed Ge spectrum for all the soil samples from the calibration site. The superior energy resolution of the Ge data are evident, as is the lower count rate. Note that the spectral peaks, in both cases, are explained by the combination of ^{134}Cs , ^{137}Cs and naturally occurring radionuclides.	24
Figure 3.4: ^{134}Cs and ^{137}Cs activity concentrations measured at Fukushima University and SUERC. The data cluster into the four depth sections of each core.	26
Figure 3.5: Distribution of standardised differences of the measured activity ratios between FU and SUERC relative to a ratio of 1.0 with a standard deviation of 0.15.	27
Figure 3.6: Cumulative distribution plots for the ratios of activity concentration determined at FU and SUERC. For ^{134}Cs (top) a normal distribution with a standard deviation of 0.15 and mean ratio of 1.07 is shown. For ^{137}Cs (bottom) a normal distributions with a standard deviation of 0.13 and a mean ratio of 1.02 is shown.	28
Figure 3.7: Depth profiles for ^{134}Cs and ^{137}Cs on the Fukushima University calibration site, showing activity concentrations (wet samples) from both laboratories and an exponential fit for a relaxation mass depth of 0.9 g cm^{-2}	30
Figure 3.8: Dose rate monitoring stations at Furudate (left) and Fukushima University with dose rates measured using the backpack system for the immediate areas (the playpark at Furudate and the lawn at the university) and next to the monitor.	32
Figure 3.9: Preparation of the calibration site at Fukushima Prefecture Fruit Tree Research centre in November 2012. A hexagonal sampling plan surrounding a central point was adopted with core samples taken at 2 metre and 8 meter radii, and split vertically. The site and orchard were mapped, and fruit samples collected.	34

Figure 4.1: Professor Yamaguchi with the SUERC backpack spectrometer at Mount Azuma, and Fukushima in March 2012	36
Figure 4.2: Transect of vehicular survey through Fukushima City, 5 th March 2012.....	37
Figure 4.3: Dose rate apportionment for the exploratory vehicular survey in Fukushima, 5 th March 2012.	38
Figure 4.4: Ōkuma Police escort for journey through the evacuation zone 7 th March 2012, Professor Kawatzu driving the car, preparing for entry to the exclusion zone.....	39
Figure 4.5: ¹³⁴ Cs activity per unit area determined from vehicular measurements, March 7 th 2012.....	40
Figure 4.6: ¹³⁷ Cs activity per unit area and dose rate determined from vehicular measurements, March 7 th 2012	41
Figure 4.7: Photographs in the immediate vicinity of Fukushima Daiichi Nuclear Power Station, 7 th March 2012.....	43
Figure 4.8: Location of measurements (bottom left) near the gate to Fukushima Daiichi, showing the damaged reactors 1 and 2 (far right).....	44
Figure 4.9: Average spectrum recorded near the gate to Fukushima Daiichi, 7 th March 2012.	44
Figure 4.10: Data collection at the Ōkuma Nuclear Centre, 7 th March 2012.	45
Figure 4.11: ¹³⁴ Cs, ¹³⁷ Cs activity per unit area and dose rate around the Ōkuma Nuclear Centre, 7 th March 2012.	45
Figure 4.12: Average spectra recorded outside (red) and inside (blue) the Ōkuma Nuclear Centre, 7 th March 2012.	46
Figure 4.13: Measurements at the day care centre, Ōkuma, 7 th March 2012	46
Figure 4.14: ¹³⁴ Cs, ¹³⁷ Cs activity per unit area and dose rate around the day care centre, Ōkuma, 7 th March 2012. Spectral distortion will reduce the accuracy of these values.	47
Figure 4.15: Average spectrum recorded at the day care centre, Ōkuma, 7 th March 2012.	48
Figure 4.16: Measurements at the district monitoring point visited, 7 th March 2012.....	48
Figure 4.17: ¹³⁴ Cs, ¹³⁷ Cs activity per unit area and dose rate around a monitoring point, 7 th March 2012.	49
Figure 4.18: Average spectrum recorded at the district monitoring point visited, 7 th March 2012.....	49
Figure 4.19: Observations of the effect of earthquake, tsunami and abandonment in the evacuation zone, 11 th -13 th July 2012.	51
Figure 4.20: Photographs from the November 2012 vehicular survey.....	52
Figure 4.21: ¹³⁴ Cs activity per unit area for vehicular surveys conducted 11 th -13 th July 2012.	53
Figure 4.22: ¹³⁷ Cs activity per unit area and dose rates for vehicular surveys conducted 11 th -13 th July 2012.....	54
Figure 4.23: Exploratory survey of Fukushima University on 6 th March 2012, with system demonstration and initial training.	57
Figure 4.24: ¹³⁴ Cs and ¹³⁷ Cs activity per unit area and dose rate for Fukushima University, measured 4 th March 2012.....	58
Figure 4.25: ¹³⁴ Cs and ¹³⁷ Cs activity per unit area and dose rate for Fukushima University, measured 11 th June 2012.....	59
Figure 4.26: ¹³⁴ Cs and ¹³⁷ Cs activity per unit area and dose rate for Fukushima University, measured 9 th -11 th July 2012.....	60
Figure 4.27: ¹³⁴ Cs and ¹³⁷ Cs activity per unit area and dose rate for Fukushima University, measured 2 nd and 4 th November 2012.....	61
Figure 4.28: Photographs of parts of the Fukushima University campus referred to in the text, taken in July 2012.	62

Figure 4.29: Dose rate apportionment for the four data sets from Fukushima University.	63
Figure 4.30: Areas of the Fukushima Campus that had been remediated by the July 2012 survey.	64
Figure 4.31: ^{134}Cs activity per unit area for the total data set for the July 2012 survey of Fukushima University, and for the unremediated and remediated areas with the tennis courts. The ^{137}Cs and dose rate show very similar distributions.	65
Figure 4.32: Dose rate apportionment for the remediated and unremediated (excluding the tennis courts) areas from the July 2012 Fukushima University survey.	66
Figure 4.33: Photographs associated with the Fukushima Iizaka surveys, 20 th May 2012.	67
Figure 4.34: ^{134}Cs and ^{137}Cs activity per unit area and dose rate for the demonstration surveys around Iizaka, 20 th May 2012.	68
Figure 4.35: ^{134}Cs and ^{137}Cs activity per unit area and dose rate around a children's play park at Furudate, 20 th May 2012, on Google Earth image.	69
Figure 4.36: ^{134}Cs and ^{137}Cs activity per unit area and dose rate around a shrine at Yawata, 20 th May 2012, on Google Earth image.	70
Figure 4.37: Dose rate apportionment for the data collected around Iizaka, 20 th May 2012, inside the conference venue and the small survey areas at Furudate and Yawata.	71
Figure 4.38: Radiometric data collection by Mamoru Sato and his team using the SUERC system, 8 th March 2012.	74
Figure 4.39: Radiometric survey at the Fruit Tree Research Institute, 21 st May 2012.	75
Figure 4.40: Radiometric surveys at the Fruit Tree Research Institute, 12 th July 2012.	76
Figure 4.41: Radiometric surveys at the fruit tree institute, 3 rd November 2012.	76
Figure 4.42: ^{134}Cs activity per unit area for the Fruit Tree Research Institute, measured 8 th March 2012.	77
Figure 4.43: ^{137}Cs activity per unit area and dose rate for the Fruit Tree Research Institute, measured 8 th March 2012.	78
Figure 4.44: ^{134}Cs activity per unit area for the Fruit Tree Research Institute, measured 21 st May 2012.	79
Figure 4.45: ^{137}Cs activity per unit area and dose rate for the Fruit Tree Research Institute, measured 21 st May 2012.	80
Figure 4.46: ^{134}Cs activity per unit area for the Fruit Tree Research Institute, measured 12 th July 2012.	81
Figure 4.47: ^{137}Cs activity per unit area and dose rate for the Fruit Tree Research Institute, measured 12 th July 2012.	82
Figure 4.48: ^{134}Cs activity per unit area for the Fruit Tree Research Institute, measured 3 rd November 2012.	83
Figure 4.49: ^{137}Cs activity per unit area and dose rate for the Fruit Tree Research Institute, measured 3 rd November 2012.	84
Figure 4.50: Time dependence of ^{134}Cs , ^{137}Cs and dose rate from all areas on the Fruit Tree research centre mapped in March, May, July and November 2012.	85
Figure 4.51: Fruit cultivation plots within the research station.	85
Figure 4.52: Time dependence of mean ^{134}Cs , ^{137}Cs activities and dose rates from the individual cultivation areas within the research institute (Figure 4.51).	86
Figure 4.53: Dose rate apportionment for the four data sets from the Fruit Tree Research Institute.	87
Figure 4.54: Photographs of Mount Shinobu taken in July and November 2012.	88
Figure 4.55: Persimmon orchard near Ryozenmachi Shimooguni, 3 rd November 2012.	88
Figure 4.56: ^{134}Cs activity per unit area distribution for citrus groves on Mount Shinobu, 12 th July 2012. Positions have been reconstructed from GPS locations with poor precision to within $\pm 20\text{m}$	89

Figure 4.57: ^{137}Cs activity per unit area and dose rate distribution for citrus groves on Mount Shinobu, 12 th July 2012. Positions have been reconstructed from GPS locations with poor precision to within $\pm 20\text{m}$	90
Figure 4.58: ^{134}Cs activity per unit area distribution for citrus groves on Mount Shinobu, 3 rd November 2012.....	91
Figure 4.59: ^{137}Cs activity per unit area and dose rate distribution for citrus groves on Mount Shinobu, 3 rd November 2012.....	92
Figure 4.60: ^{134}Cs and ^{137}Cs activity per unit area and dose rate distribution for the viewpoint and playparks on Mount Shinobu, 12 th July 2012. Positions have been reconstructed from GPS locations with poor precision to within $\pm 20\text{m}$	93
Figure 4.61: ^{134}Cs and ^{137}Cs activity per unit area and dose rate on an area of fruit cultivation near Hashirazawa, measured 24 th July 2012.....	94
Figure 4.62: ^{134}Cs and ^{137}Cs activity per unit area and dose rate on an area of fruit cultivation near Ryozenmachi Shimooguni, measured 24 th July 2012.....	95
Figure 4.63: ^{134}Cs and ^{137}Cs activity per unit area and dose rate on an area of fruit cultivation near Ryozenmachi Shimooguni, measured 3 rd November 2012.....	96
Figure 4.64: Average spectrum for data recorded at AFFRC, Tsukuba, in March 2012.....	97
Figure 4.65: Demonstration of SUERC radiometric system at Tsukuba, 5 th November 2012, with difference in activity concentrations on grass and hard surfaces apparent.....	97
Figure 4.66: Radiometric surveys on test plots at NIRE, AFFRC, Tsukuba, 5 th November 2012.....	98
Figure 4.67: ^{134}Cs and ^{137}Cs activity per unit area and dose rate for the NFRE, Tsukuba, measured 5 th November 2012.....	99
Figure 4.68: ^{134}Cs and ^{137}Cs activity per unit area and dose rate for the NIRE, Tsukuba, measured 5 th November 2012.....	100
Figure 4.69: Dose rate apportionment for the March and November 2012 data sets from Tsukuba. In March 2012 the interior dose rate (left hand side) from accident nuclides represent a smaller proportion than outside (centre) the NFRI building. By November the decay of ^{134}Cs can also be seen (right hand side).....	101
Figure 4.70: Count rate ratios of ^{134}Cs emissions (604keV in red, and 795keV in blue) to the ^{137}Cs 662keV peak, for air filter samples collected at Tsukuba in March 2011, measured at SUERC in January 2013.....	103
Figure 4.71: ^{134}Cs : ^{137}Cs activity ratio determined from vehicular survey using the SUERC Portable Gamma Spectrometry System in March 2012. Measurement uncertainties are typically ± 0.10 - 0.20	106
Figure 4.72: ^{134}Cs : ^{137}Cs activity ratio determined from vehicular survey using the SUERC Portable Gamma Spectrometry System in July 2012. Measurement uncertainties are typically ± 0.05 - 0.10	107
Figure 4.73: ^{134}Cs : ^{137}Cs activity ratio for the March 2012 survey of the Fukushima University campus. Uncertainties on individual measurements are typically ± 0.1	109
Figure 4.74: ^{134}Cs : ^{137}Cs activity ratio for the July 2012 survey of the Fukushima University campus. Uncertainties on individual measurements are typically ± 0.1	110

図一覧

図 1.1: 警戒区域地図.....	5
図 1.2: 事故後の最初の数週間で米国DOEと文部科学省が測定した航空調査データにより生成された福島第一原子力発電所の80キロ以内の地域の線量率。文部科学省2011年より.....	6
図 1.3: 2012年にSUERCポータブルガンマ線スペクトロメトリ・システムを使用して調査地域.....	7
図 1.4: エリアの場所は2012年にSUERCポータブルガンマ分析システムを使用して調査.....	9
図 1.5: 2012年に福島市周辺の調査地域。福島県果樹研究所と福島市飯坂町（上部中央）、信夫山（左上）、福島大学（左下）と伊達市近くの果樹園（右）.....	10
図 2.1: T典型的な3×3"のNaI (TI) とGeスペクトル。自然放射性濃度 (⁴⁰ K、 ²³⁸ Uシリーズから ²¹⁴ Bi、 ²³² Th崩壊系列から ²⁰⁸ Tl) 及び ¹³⁴ Csと ¹³⁷ Csからの特徴的なピークの位置が示された。上部スペクトルは比較的低い汚染の地域である。真ん中のスペクトルは、汚染の高いレベルで地域からのものであり、1365keVの ¹³⁴ Cs と1461keVの ⁴⁰ Kピーク間の干渉を示す。下のスペクトルは実験室サンプル（福島大学キャリブレーションサイトからトップのサンプルの合計）であり、その中に1038、1167、1175と1400.6 keVのピークが幾何学的なカスケード・サミングによるものである.....	13
図 2.2: 福島大学キャリブレーションサイトとSUERCの線量率の配分.....	20
図 3.1: ラベル付きアウター（8メートル）リング付きキャリブレーションサイトの地図.....	23
図 3.2: 北西（左と中央）と南（右）からキャリブレーションサイト.....	23
図 3.3: 福島大学キャリブレーションサイトから測定された NaI(Tl) スペクトル及びキャリブレーションサイトからすべての 土壌試料 について Ge のスペクトル。低い計数率は Ge のデータの エネルギー分解能を示す。スペクトルピークは、いずれの場合も、セシウム137と134及び天然放射性核種の組み合わせによって説明される.....	24
図 3.4: 福島大学とSUERCで測定した ¹³⁴ Csと ¹³⁷ Csの放射能濃度.....	26
図 3.5: 1.0の比及び0.15標準偏差に相対福島大学とSUERCで測定した放射能比の標準化された差の分布.....	27
図 3.6: 福島大学と SUERC で測定した放射能濃度の比の累積分布プロット。 ¹³⁴ Cs に対する標準偏差0.15と平均比率1.07の正規分布を示す（上）。 ¹³⁷ Cs に対する標準偏差0.13と平均比率1.02の正規分布を示す（下）.....	28
図 3.7: 福島大学キャリブレーションサイトから測定された ¹³⁴ Cs と ¹³⁷ Cs の深度プロファイルは、実験室や 0.9g cm ⁻² の質量深さ指数関数 フィットの両方から放射能濃度（ウェットサンプル）を示す.....	30
図 3.8: 古館（左）と福島大学のモニタリングステーションで観測された線量率、及び古館で遊び場と大学で芝生とモニタの隣にバックパックシステムを用いて測定した線量率.....	32
図 3.9: 2012年11月に福島県果樹研究センターでキャリブレーションサイトの準備。中心点の周囲の六角形のサンプリング計画は、2メートルと8メートルの半径で採取コア試料を採用し、垂直方向に分割された。サイトと果樹園がマッピングされ、果物のサンプルが収集された.....	34
図 4.1: 2012年3月吾妻山と福島でSUERCバックパックリュックスペクトロメータを持つ山口教授.....	36
図 4.2: 2012年3月5日に福島市を通して車両調査の横断する.....	37

図 4.3: 2012年3月5日に福島車両調査による線量率の配分.....	38
図 4.4: 2012年3月7日に大隈警察護衛により警戒禁止区域の旅の準備、河津教授は車を運転する.....	39
図 4.5: 2012年3月7日に車両の測定値から求めた単位面積あたりの ¹³⁴ Cs放射能濃度.....	40
図 4.6: 2012年3月7日車両の測定値から求めた ¹³⁷ Csの単位面積あたり放射能と線量率.....	41
図 4.7: 2012年3月7日に福島第一原子力発電所のすぐ近くの写真.....	43
図 4.8: 損傷した原子炉1号機と2号機（右端）を示した福島第一のゲート近くの測定場所（左下）.....	44
図 4.9: 2012年3月7日に福島第一原子力発電所のゲート近く観測された平均スペクトル.....	44
図 4.10: 2011年3月7日に大熊原子力センターのデータ収集.....	45
図 4.11: 2012年3月7日に大熊原子力センターの周りに単位面積あたり ¹³⁴ Csと ¹³⁷ Cs放射能濃度と線量率.....	45
図 4.12: 2012年3月7日に大熊原子力センター外（赤）と内（青）で記録された平均スペクトル.....	46
図 4.13: 2012年3月7日に大熊介護センターでの測定結果.....	46
図 4.14: 2012年3月7日に大熊介護センターの周りに単位面積あたり ¹³⁴ Csと ¹³⁷ Cs放射能濃度と線量率。スペクトルの歪みはこれらの値の精度が低下する.....	47
図 4.15: 2012年3月7日に大熊介護センターに記録された平均スペクトル.....	48
図 4.16: 2012年3月7日に訪問した地方監視ポイントでの測定.....	48
図 4.17: 2012年3月7日に監視ポイントの周りに単位面積あたり ¹³⁴ Csと ¹³⁷ Cs放射能濃度と線量率.....	49
図 4.18: 2012年3月7日に訪れた地区観測点で記録された平均スペクトル.....	49
図 4.19: 2012年7月11-13日に警戒区域の地震と津波の影響と遺棄の様子.....	51
図 4.20: 2012年11月車両調査からの写真.....	52
図 4.21: 2012年7月11-13日車両調査によりた単位面積あたり ¹³⁴ Cs放射能濃度.....	53
図 4.22: 2012年7月11-13日車両調査によりた単位面積あたり ¹³⁷ Cs放射能濃度.....	54
図 4.23: 2012年3月6日に福島大学の調査、システムの実演と初期トレーニング.....	57
図 4.24: 2012年3月4日に福島大学で測定した単位面積あたりの ¹³⁴ Csと ¹³⁷ Cs放射能濃度と線量率.....	58
図 4.25: 2012年6月11日に福島大学で測定した単位面積あたりの ¹³⁴ Csと ¹³⁷ Cs放射能濃度と線量率.....	59
図 4.26: 2012年7月9日-11日に福島大学で測定した単位面積あたりの ¹³⁴ Csと ¹³⁷ Cs放射能濃度と線量率.....	60
図 4.27: 2012年11月2日と4日に福島大学で測定した単位面積あたりの ¹³⁴ Csと ¹³⁷ Cs放射能濃度と線量率.....	61
図 4.28: 2012年7月に撮影した福島大学のキャンパスの一部の写真.....	62
図 4.29: 福島大学からの4つのデータセットの線量率配分.....	63
図 4.30: 2012年7月調査まで除染されていた福島大学キャンパスのエリア.....	64
図 4.31: 2012年7月調査には福島大学、除染されていないと除染されていた区域の全てのデータセットの単位面積あたりの ¹³⁴ Cs放射能濃度。 ¹³⁷ Cs放射能濃度と線量率が非常によく似た分布を示す.....	65
図 4.32: 2012年7月福島大学の調査から（テニスコートを除く）除染と未除染地域の線量率配分.....	66

図 4.33: 2012年5月20日に福島市飯坂町調査を関連する写真。	67
図 4.34: 2012年5月20日に飯坂周りのデモ調査の単位面積あたりの ¹³⁴ Csと ¹³⁷ Cs放射能濃度と線量率	68
図 4.35: 2012年5月20日にGoogle地球イメージで古館の子供の遊び場公園の周り単位面積あたりの ¹³⁴ Csと ¹³⁷ Cs放射能濃度と線量率	69
図 4.36: 2012年5月20日にGoogle地球イメージで八幡の周り単位面積あたりの ¹³⁴ Csと ¹³⁷ Cs放射能濃度と線量率	70
図 4.37: 2012年5月20日に飯坂（古館と八幡の会議会場と小さな調査エリア）で収集したデータの線量率の配分	71
図 4.38: 2012年3月8日にSUERCシステムを使用して放射データを収集していた佐藤さんと彼のチーム	74
図 4.39: 2012年5月21日に果樹研究所放射性調査	75
図 4.40: 2012年7月12日に果樹研究所放射性調査	76
図 4.41: 2012年11月3日に果樹研究所放射性調査	76
図 4.42: 2012年3月8日に果樹研究所で測定した単位面積あたりの ¹³⁴ Cs濃度	77
図 4.43: 2012年3月8日に果樹研究所で測定した単位面積あたりの ¹³⁷ Cs濃度と線量率	78
図 4.44: 2012年5月21日に果樹研究所で測定した単位面積あたりの ¹³⁴ Cs濃度	79
図 4.45: 2012年5月21日に果樹研究所で測定した単位面積あたりの ¹³⁷ Cs濃度と線量率	80
図 4.46: 2012年7月12日に果樹研究所で測定した単位面積あたりの ¹³⁴ Cs濃度	81
図 4.47: 2012年7月12日に果樹研究所で測定した単位面積あたりの ¹³⁷ Cs濃度と線量率	82
図 4.48: 2012年11月3日に果樹研究所で測定した単位面積あたりの ¹³⁷ Cs濃度と線量率	83
図 4.49: 2012年11月3日に果樹研究所で測定した単位面積あたりの ¹³⁷ Cs濃度と線量率	84
図 4.50: 2012年5月、7月と11月に果樹研究センターでマッピングされたすべての地域から ¹³⁴ Csと ¹³⁷ Cs放射能濃度及び線量率の時間依存性	85
図 4.51: 研究所内果樹栽培プロット	85
図 4.52: 研究所内の個々の栽培地からの平均 ¹³⁴ Csと ¹³⁷ Cs放射能濃度及び線量率の時間依存性（図4.51）	86
図 4.53: 果樹研究所から測定した四つのデータの線量率の配分	87
図 4.54: 2012年7月と11月に撮影した信夫山の写真	88
図 4.55: 2012年11月3日に霊山町下小国に近くの柿果樹園	88
図 4.56: 2012年7月12日に信夫山の柑橘類の果樹園で測定した単位面積あたりの ¹³⁴ Cs濃度の分布。位置は±20メートルの貧しい精度のGPSの地点から再修正された	89
図 4.57: 2012年7月12日に信夫山の柑橘類の果樹園で測定した単位面積あたりの ¹³⁷ Cs放射能濃度及び線量率の分布。位置は±20メートルの貧しい精度のGPSの地点から再修正された	90
図 4.58: 2012年11月3日に信夫山の柑橘類の果樹園で測定した単位面積あたりの ¹³⁴ Cs濃度	91
図 4.59: 2012年11月3日に信夫山の柑橘類の果樹園で測定した単位面積あたりの ¹³⁷ Cs放射能濃度及び線量率	92
図 4.60: 2012年7月12日に信夫山の眺望台と遊び場で測定した単位面積あたりの ¹³⁴ Csと ¹³⁷ Cs放射能濃度及び線量率の分布。位置は±20メートルの貧しい精度のGPSの地点から再修正された	93
図 4.61: 2012年7月24日に柱沢町近くに果樹栽培の地点で測定した単位面積あたりの ¹³⁴ Csと ¹³⁷ Cs放射能濃度及び線量率	94

図 4.62: 2012年7月24日に霊山町下小国近くに果樹栽培の地点で測定した単位面積あたりの ¹³⁴ Csと ¹³⁷ Cs放射能濃度及び線量率	95
図 4.63: 2012年11月3日に霊山町下小国近くに果樹栽培の地点で測定した単位面積あたりの ¹³⁴ Csと ¹³⁷ Cs放射能濃度及び線量率	96
図 4.64: 2012年3月つくばの AFFRCで記録されたデータの平均スペクトル	97
図 4.65: 2012年11月5日につくばで SUERC 放射 システムの 実演 により草や硬い表面の放射能濃度の違いが明らかになった	97
図 4.66: 2012年11月5日につくばのNIREとAFFRCでのテスト区域で放射性調査	98
図 4.67: 2012年11月5日につくばのNFREで測定した単位面積あたりの ¹³⁴ Csと ¹³⁷ Cs放射能濃度及び線量率	99
図 4.68: 2012年11月5日につくばのNIREで測定した単位面積あたりの ¹³⁴ Csと ¹³⁷ Cs放射能濃度及び線量率	100
図 4.69: 2012年3月と11月つくばのデータの線量率の配分。2012年3月に事故の核種より食品総合研究所の建物内部線量率（左手側）は外側（中央）より小さい割合を表す。11月まで ¹³⁴ Csの減衰も見る事ができる（右側）	101
図 4.70: 2013年1月にSUERCで測定した2011年3月につくばで採取されたエアフィルターのサンプルの ¹³⁴ Cs（604keV赤でと795keV青）と ¹³⁷ Cs（662keVピーク）のカウント比率	103
図 4.71: 2012年3月にSUERCポータブルガンマ分析システムを使用して車両の調査から求めた ¹³⁴ Cs/ ¹³⁷ Csの放射能比。測定の誤差は通常±0.10-0.20である	106
図 4.72: 2012年7月にSUERCポータブルガンマ分析システムを使用して車両の調査から求め ¹³⁴ Cs/ ¹³⁷ Csの放射能比。測定の誤差は通常±0.05-0.10	107
図 4.73: 福島大学キャンパスの2012年3月の測定結果に求めた ¹³⁴ Cs/ ¹³⁷ Csの放射能比。個々の測定誤差は一般的±0.1である	109
図 4.74: 福島大学キャンパスの2012年7月の測定結果に求めた ¹³⁴ Cs/ ¹³⁷ Csの放射能比。個々の測定誤差は一般的±0.1である	110

Tables

Table 1.1: Some of the reported estimates of ^{137}Cs and ^{131}I atmospheric releases, and total release where given.....	3
Table 2.1: Gamma ray energies and intensities used in gamma spectrometry. In this work, the short live iodine isotopes produced in the Fukushima Daiichi reactors had decayed and ^{60}Co was not detected. ^{134}Cs , ^{137}Cs and the natural radionuclides have been measured.....	12
Table 2.2: Spectral windows and background count rates used for the analysis presented here.....	17
Table 2.3: Stripping matrix used for the analysis presented here.....	18
Table 2.4: Sensitivity parameters for the backpack and vehicular measurements.....	18
Table 2.5: Dose rate apportionment for the Fukushima University calibration site.....	20
Table 3.1: Peaks present in the summed Ge spectrum (Figure 3.3) with corresponding intensity (net counts per kilosecond) and identification.....	25
Table 3.2: Summary statistics for activity ratios determined from the soil samples collected from the Fukushima University calibration site (52 samples).....	29
Table 3.3: Mean activity ratios and standard deviations from a small selection of published data, decay corrected to 15 th March 2011.....	29
Table 3.4: Activity per unit area and mean mass depth for each core from the Fukushima University calibration site, decay corrected to 11 th July 2012.....	31
Table 3.5: Reference values and observed values for ^{137}Cs and ^{134}Cs activity per unit area, activity ratio, dose rate and mean mass depth for the Fukushima University calibration site. Activity and dose rate data are presented for the sampling or measurement date (11/7/2012 or 03/11/2012), the activity ratio is also given for a reference date of 15/3/2011.....	32
Table 4.1: Summary statistics for the exploratory measurements in Fukushima City, 5 th March 2012.....	36
Table 4.2: Dose rate apportionment for the exploratory vehicular survey in Fukushima, 5 th March 2012.....	38
Table 4.3: Summary statistics for the vehicular measurements on a drive from Fukushima into the exclusion zone then to Iwaki and back to Fukushima, 7 th March 2012.....	39
Table 4.4: Mean and standard deviation for radiocaesium activity per unit area and dose rate for the four sets of backpack data recorded in the exclusion zone, 7 th March 2012.....	42
Table 4.5: Summary statistics for the vehicular measurements in the evacuation zone, 11-13 th July and 3 rd November 2012.....	50
Table 4.6: Summary statistics for backpack measurements at Kawauchi village and nearby pond, 11 th July 2012.....	50
Table 4.7: Summary statistics for the backpack surveys of Fukushima University in March, June, July and November 2012, and Fukushima Iizaka in May 2012.....	55
Table 4.8: Dose rate apportionment for the four data sets from Fukushima University.....	63
Table 4.9: Summary statistics for the regrided July 2012 Fukushima University survey, for the total area, the unremediated areas, and the remediated areas separating the tennis courts from the other areas.....	64
Table 4.10: Dose rate apportionment for the remediated and unremediated (excluding the tennis courts) areas from the July 2012 Fukushima University survey.....	66
Table 4.11: Dose rate apportionment for the data collected around Iizaka, 20 th May 2012, inside the conference venue and the small survey areas at Furudate and Yawata.....	71
Table 4.12: Summary statistics for the backpack surveys of areas of fruit cultivation in 2012: the Fukushima Prefecture Fruit Tree Research Institute in March, May, July and November; fruit cultivation areas at Mount Shinobu and near Date in July and November; the AFFRC at Tsukuba in March and November.....	73

Table 4.13: Dose rate apportionment for the four data sets from the Fruit Tree Research Institute.	87
Table 4.14: Dose rate apportionment for the two data sets from Tsukuba.	101
Table 4.15: Count rates for the 662keV (^{137}Cs) and 604keV and 795keV (^{134}Cs) peaks with associated ratios for air filter samples collected at Tsukuba in March 2011, measured at SUERC in January 2013.	102
Table 4.16: Activities for ^{134}Cs and ^{137}Cs in the samples of air filter material analysed at SUERC, with associated ratios at time of measurement (16-23 rd January 2013) and decay corrected to 15 th March 2011. Note that the ^{134}Cs activities are calculated without accounting for cascade summing, and are hence underestimates of the activity.	103
Table 4.17: Median values of ^{134}Cs : ^{137}Cs activity ratios from Yamana (2013), as reported and with a decay correction to 15 th March 2011.	104
Table 4.18: Weighted mean and standard deviation ^{134}Cs : ^{137}Cs activity ratio determined from vehicular measurements in March and July 2012, for the date measured and decay corrected to 15 th March 2011. Values at the top are for individual measurements, with values for regridded data below. The March data are presented for the whole survey, and excluding those data in the immediate vicinity of the Fukushima Daiichi Nuclear Power Plant where spectral distortion may affect the analysis.	105
Table 4.19: Weighted mean and standard deviation ^{134}Cs : ^{137}Cs activity ratio determined from backpack measurements in 2012, for the date measured and decay corrected to 15 th March 2011. Data in the top half of the table are for individual measurements, with regridded data in the bottom half.	108

表一覧

表 1.1: 報告された大気中の ¹³⁷ Cs と ¹³¹ I放出量.....	3
表 2.1: ガンマ線スペクトロメトリに使用するガンマ線エネルギー及び強さ。この研究に、福島第一原子力発電所に放出された短い半減期を持つ核種 ¹³¹ Iが既に放射壊変され、 ⁶⁰ Coが未測定である。 ¹³⁴ Csと ¹³⁷ Cs及びが天然の放射性核種が測定された.....	12
表 2.2: 本分析に関するスペクトル・ウィンドウ及びバックグラウンド計数率.....	17
表 2.3: 本分析に関するストリップ・マトリックス.....	18
表 2.4: バックパックシステム及び自動車に搭載システムの感度パラメーター.....	18
表 2.5: 福島大学にキャリブレーション・サイト線量率配分.....	20
表 3.1: Geスペクトル (図3.3) にピーク及びその強さ (単位キロ秒当たりネット・カウント) と同定.....	25
表 3.2: 福島大学にキャリブレーション・サイトに採集された 52土壌試料の核種濃度比のサマリー統計.....	29
表 3.3: 既報の一部データの平均核種濃度比及び標準偏差 (2011年3月15日に放射壊変校正).....	29
表 3.4: 福島大学にキャリブレーション・サイトにコアの単位面積当たり濃度及び平均質量深度 (2012年7月11日に放射壊変校正).....	31
表 3.5: 福島大学にキャリブレーション・サイトに ¹³⁴ Csと ¹³⁷ Csの単位面積当たり濃度、濃度比、線量率及び平均質量深度に対する基準値及び測定値。濃度及び線量率に対するサプリング或は測定日がそれぞれ2012年7月11日或は2012年11月3日であるが、濃度比が2011年3月15日に校正された.....	32
表 4.1: 2012年3月5日に福島市内での予備的な測定結果のサマリー統計.....	36
表 4.2: 2012年3月5日に福島市内での自動車に搭載システム線量率割合.....	38
表 4.3: 2012年3月7日に行われた福島-警戒区域-磐城-福島沿線の自動車に搭載システムの測定結果のサマリー統計.....	39
表 4.4: 2012年3月7日に行われた警戒区域で4セットのバックパックシステムによる単位面積当たり放射性セシウム濃度の平均値と標準偏差及び線量率.....	42
表 4.5: 2012年7月11-13日と11月3日に行われた警戒区域での自動車に搭載システムの測定結果のサマリー統計.....	50
表 4.6: 2012年7月11日に行われた川内村及び近くの池でのバックパックシステムの測定結果のサマリー統計.....	50
表 4.7: 2012年3月、6月、7月、11月に福島大学及び2012年5日に福島飯坂で行われたバックパックシステムの測定結果のサマリー統計.....	55
表 4.8: 福島大学で行われた4セットの線量率の配分.....	63
表 4.9: 2012年7月に福島大学の全体、未除染区域及び他の地域からのテニスコートを分ける除染区域で行われた測定結果のサマリー統計.....	64
表 4.10: 2012年7月に福島大学の除染した区域と除染していない区域 (テニスコートを除く) で測定された線量率の配分.....	66
表 4.11: 2012年5月20日に飯坂町 (コンファレンス会場内部、古館及び八幡) を中心に収集したデータの線量率の配分.....	71
表 4.12: 2012年にバックパックシステムにより得られた果樹園の測定結果のサマリー統計: 福島県果樹研究所 (3月、5月、7月、11月)、7月と11月の信夫山と伊達市近くの果樹園 (3月、5月、7月、11月)、つくばのAFFRC (3月と11月).....	73

表 4.13: 福島県果樹研究所に収集した4セットのデータの線量率の配分	87
表 4.14: つくばに収集した2セットのデータの線量率の配分	101
表 4.15: 2011年につくばで収集されたエアフィルターの 662keV (^{137}Cs) 及び 604keV と 795keV (^{134}Cs) ピークの計数率とその比率。測定が2013年1月に SUERC で行われた.....	102
表 4.16: SUERCで測定したエアフィルターの測定日 (2013年1月16-23日) 及び 放射壊変修正日 (2011年3月15日) の ^{134}Cs と ^{137}Cs の濃度とその比率。その中、 ^{134}Cs の計算についてカスケードが加算されないので、その濃度に対して過小評価する可 能性もある.....	103
表 4.17: Yamana (2013)による 2011年3月15日に放射壊変修正した $^{134}\text{Cs}/^{137}\text{Cs}$ 比.....	104
表 4.18: 2012年3と7月に自動車に搭載システムで測定した $^{134}\text{Cs}/^{137}\text{Cs}$ 比 (測定時点及 び2011年3月15日に修正日) の加重平均と標準偏差。上部と下部に示す値はそれぞれ 個々の測定結果と再グリッドデータである。3月のデータは全体の調査結果であるが 、スペクトル・ディストーションにより影響を受ける可能性があるために、福島第 一原子力発電所のすぐ近くのデータを除く.....	105
表 4.19: 2012年 にバックパックシステムで測定した $^{134}\text{Cs}/^{137}\text{Cs}$ 比 (測定時点及び 2011年3月15日に修正日) の 加重平均と標準偏差。表の 上半分と下半分の データはそれぞれ個々の 測定結果と再グリッドデータである.....	108

1. Introduction

1.1 Radiometric Mapping

Radiometric systems utilise sensitive gamma spectrometry systems on mobile platforms, producing continuous area mapping of radionuclide concentrations and dose rate. The technique exploits the penetrating nature of gamma radiation, for example the 662 keV gamma ray from ^{137}Cs has a half-distance in air of approximately 70m. Suitable gamma-ray detectors can measure this radiation from distances of up to 300m. Fully spectrometric systems, utilising scintillators such as NaI(Tl) or Ge semiconductor detectors, are capable of measuring activity concentrations for individual radionuclides. Deployed from aircraft such systems can rapidly collect data from large areas. Ground based deployment, on vehicles and backpacks, has a lower rate of area coverage but can provide greater spatial detail.

1.2 Radiometrics and Nuclear Emergencies

Radiometric systems deployed from aircraft to measure gamma radiation originating from ground surfaces were originally developed in the years immediately following the second world war for uranium exploration, and later for mineral resource evaluation and environmental studies. The ability of airborne gamma surveys to cover large areas under conditions was also recognised early on, with one of the first known airborne surveys in response to a nuclear emergency taking place shortly after the 1957 Windscale Fire (Williams *et.al.* 1958). Airborne systems were used to locate fragments of the Cosmos-954 satellite in Canada in 1978 (Bristow 1978, Grasty 1980), with radioactive fragments identified by ratios of counts in a low energy window (300-900 keV) to counts in a high energy window (900-1500 keV), and to map the distribution of CsCl salt from a radiotherapy source in Goiânia in Brazil in 1985 (IAEA 1988). The potential for using airborne systems to measure release rates during an accident have been explored, including the use of an airborne system developed by JAERI for field experiments at Tokai-mura in 1984 (Saito *et.al.* 1988).

Following the 1986 Chernobyl accident, radiometric systems deployed from aircraft and vehicles were widely used to determine the distribution of fallout throughout Europe, and beyond, in all phases of emergency response. In Scandinavia, geological survey groups used AGS with systems and procedures for natural-series activity mapping that required extensive post survey analysis often lasting several months. These systems and procedures were rapidly modified to allow measurement of artificial radionuclides, with large numbers of people to process data rapidly. The first airborne surveys of Chernobyl activity were conducted in Sweden, starting on the 1st May 1986, 4 days after the Chernobyl cloud was first detected over Sweden. Count rates in a window around the 795 keV ^{134}Cs peak were used to estimate radiocaesium deposition, with laborious data reduction and production of hand-contoured maps to rapidly produce deposition maps for the majority of the country with 100km spaced lines by the 8th May (Mellander 1989). The Geological Survey of Finland aircraft was returning from a survey in the north of the country to Helsinki on the 29th April 1986, where it recorded data from within the plume but was heavily contaminated (Grasty *et.al.* 1996). In Norway, an airborne survey was conducted between the 5th May and 6th June, with complementary carborne surveys of the entire country (Lindahl & Haabrekke 1986). Airborne surveys were also conducted around the Chernobyl site (Stukin 1991, Nagaoka *et.al.* 1994) from May 1986. In the UK, procedures were developed that extended the three window analysis used for geological prospecting to five windows including ^{134}Cs and ^{137}Cs

and allowed very rapid, near real time, generation of mapped data by a small survey team (Sanderson *et.al.* 1994a,b), with surveys of the most heavily contaminated areas of the UK from 1988 (Sanderson & Scott 1989, Sanderson *et.al.* 1989, 1990a, 1993).

Following the Chernobyl accident, many countries developed radiometric systems, and incorporated radiometric capability into their nuclear emergency response arrangements. This was accompanied by a considerable effort in developing systems and techniques to improve capability. In the UK, research was conducted at the Scottish Universities Environmental Research Centre (SUERC – formerly SURRC), supported by the nuclear industry and several government departments, to develop airborne survey capability. This included developing emergency response flight plans and baseline surveys for nuclear sites (Sanderson *et.al.* 1990b, 1992a,b, 1994c,d, 1997c); large area surveys of Cumbria funded by the Ministry of Agriculture, Fisheries and Food (Sanderson & Scott 1989) and southern Scotland funded by local authorities (Sanderson *et.al.* 1990a) and the Scottish Office (Sanderson *et.al.* 1993); investigations of the response of airborne detectors to complex sources with lead funding from the Department of the Environment, Transport and Regions (Sanderson *et.al.* 1997a) and the effects of survey parameters and temporal effects on airborne survey data (Sanderson *et.al.* 2001, 2008). Other countries developed more formal radiometric capabilities. During the 1990s this resulted in system developments running independently in several countries. In the mid 1990s, a European Commission funded project started work to coordinate developments, which included development of protocols for radionuclide deposition and dose rate mapping using AGS (Sanderson & McLeod 1997, ECCOMAGS 2002). A follow-on project included an international exercise to validate these protocols (Sanderson *et.al.* 2003, 2004).

1.3 March 2011 Nuclear Accidents

Following the Tōhoku earthquake and subsequent tsunami on the 11th March 2011, inundation of the emergency generators at the Fukushima Daiichi Nuclear Power Plant resulted in a loss of power to the cooling systems for the reactors and fuel storage ponds. Loss of power to the cooling systems resulted in significant increases in core temperature, fuel melting and a series of explosions. The accidents at Fukushima Daiichi resulted in the release of large quantities of radioactive material into the environment, with the greatest terrestrial deposition to the north west of the plant. The sequence of events has been described in detail in several reports (eg: NAIIC 2012, ONR 2011). The account of the accident summarised here is based on the NAIIC 2012 report, and provides a context for the measurements conducted and subsequent discussion.

The magnitude 9.0 Tōhoku earthquake occurred at 14:46 JST, on the 11th of March, with an epicentre approximately 130km off the coast to the north east of Fukushima Daiichi. At the time of the earthquake, reactors 1-3 had been operating at full power, with reactors 4-6 shut down for inspection. The earthquake triggered an automatic scram of the operating reactors, and backup diesel generators were started successfully. However, at 15:37 the peak tsunami wave, estimated at 14-15m, breached the tsunami defences rendering backup diesel generators and other equipment on the site inoperable, resulting in an almost total loss of active cooling capacity. At approximately 18:10 the core of reactor 1 was exposed. At approximately 14:30 on the 12th March controlled venting from reactor 1 was started, but was followed by a hydrogen explosion at 15:36. The explosion hampered recovery operations at reactors 1 and 2. At approximately 09:10 on the 13th March, the core of reactor 3 was

exposed, with venting started at approximately 09:20. A hydrogen explosion occurred at reactor 3 at 11:01 on the 14th March. This further hampered recovery operations at reactor 2, where the core was exposed at approximately 17:00. At 06:00 on the 15th March, a further hydrogen explosion occurred at reactor 4, and damage to the suppression chamber of reactor 2 resulted in a further discharge of radioactive material. The hydrogen explosion at unit 4 was initially attributed to the spent fuel store of unit 4, which was feared damaged in the earthquake with potential for further release had water levels not been restored. Later inspections, however, suggest that stored fuel damage was less severe suggesting that the hydrogen responsible for the unit 4 explosion may have come from reactor number 3.

On the 13th March the accident was classified as Level 4 on the International Nuclear Event Scale (INES), an “accident with local consequences”. On 18th March, the situation for units 1-3 was re-classified as Level 5, an “accident with wider consequences” with unit 4 as a Level 3 “serious incident”. Later in April the accident was reclassified as INES Level 7, a major accident.

The total activity released, and the proportions of this corresponding to different radionuclides (the source term), has been estimated several times and is still under investigation by several national and international organisations. Some of the estimates produced for the atmospheric release source term are given in Table 1.1. These estimates range from 6-15x10¹⁵ Bq for ¹³⁷Cs and 130-160x10¹⁵ Bq for ¹³¹I. The variation in ¹³⁷Cs estimates of a factor of 2.5 is similar to variations in the ¹³⁷Cs source term for the Chernobyl accident (Sanderson *et.al.* 1997), the variation in ¹³¹I estimates is very much smaller than the range for Chernobyl estimates which varied by a factor of 6.5.

Reporting organisation	Date of report	Activity released (x10 ¹⁵ Bq)			References and comments
		¹³⁷ Cs	¹³¹ I	Total [†]	
NISA	April 2011	6.1	130		NISA 2011a
NSC	April 2011	12	150		Reported in Chino <i>et.al.</i> 2011
JAEA	April 2011	13	150		Chino <i>et.al.</i> 2011
NISA	June 2011	15	160	218	NISA 2011b
NSC	Aug 2011	11	130		Reported in ICANPS 2011, Sugimoto 2013
JNES	Sept 2011	15	160	290	JNES 2011
WHO	2012	15.3	159	337	WHO 2012 Revised from NISA 2011b
WHO	2012	9.7	124		WHO 2012 Revised from Chino <i>et.al.</i> 2011

[†] Total excludes ¹³³Xe, estimated at >10¹⁹Bq

Table 1.1: Some of the reported estimates of ¹³⁷Cs and ¹³¹I atmospheric releases, and total release where given.

A sequence of evacuation orders was issued for residents in a rapidly increasing area around the nuclear power plant, the following description of the evacuations is taken from NAIIC (2012). At 20:50 on the 11th March an order was issued by the Prefecture governor to evacuate an area within 2km of the site. At 21:23 this was extended by the Prime Ministers Nuclear Emergency Response HQ to a 3km evacuation zone, with sheltering indoors for residents in the 3-10km radius zone, with an evacuation order to 10km issued at 05:44 on the 12th March. Following the first hydrogen explosion, the evacuation zone was again extended, to 20km, at 18:25 on the 12th. On March 15th residents in the 20-30km zone were ordered to shelter indoors, with voluntary evacuation advised on the 25th March. A deliberate evacuation area was established to the north west, covering areas identified as having highest deposition levels. Approximately 150,000 people were evacuated. On December 26th 2011, a policy was established by the NERHQ to review restricted and evacuated areas based on whether integrated annual doses could be maintained at less than 20mSv. From April 1st 2012 evacuation orders were lifted from several areas following review.

Radiometric methods played a vital part in monitoring deposited activity and dose rate following the accidents. On the 14th March, the US Department of Energy and National Nuclear Security Administration deployed the Aerial Measuring Systems (AMS) to Japan, with the first survey flights in the emergency zone flown on the 17th (Lyons & Colton 2012). These systems were used in cooperation with the Japanese Ministry of Education, Culture, Sports, Science and Technology (MEXT) to collect data initially within 80km of the Fukushima Daiichi plant, and then by a range of organisations on behalf of MEXT, and subsequently the Nuclear Regulation Authority (NRA), covering the majority of Japan. The dose rate measured for the initial surveys are shown in Figure 1.2 (taken from MEXT, 2011), with the data set for the majority of country shown in Figure 1.3 (taken from MEXT, 2012b). Monitoring was also conducted using vehicular radiometric and dosimetric systems, in-situ measurements and sampling, and hand-held dosimeters.

The airborne surveys were flown at ground clearances of 150-300m and 550-700m, for helicopter and fixed wing surveys respectively (Lyons & Colton 2012). Protocols for radionuclide deposition mapping produced and validated during European Community Framework Projects (Sanderson & McLeod 1999, ECCOMAGS 2002, Sanderson *et.al.* 2003, 2004), reflecting practices reported in IAEA (1991) and ICRU (1994) reports, recommends ground clearances of up to 100-150m for mapping natural activity. Anthropogenic radionuclides mostly produce lower energy gamma rays than natural sources, and lower ground clearances are required to produce a comparable measurement precision. The selection of ground clearance balances several factors including area coverage rate, desired measurement precision, radionuclides of interest, aircraft type, terrain, weather conditions and legal requirements.

The relatively high ground clearances used by the US Department of Energy National Security Administration (DOE/NNSA) Aerial Measuring System (AMS) and subsequent MEXT surveys are known to degrade spectral quality through reduced full-energy peak count rates and increased continuum count rates. This results in direct determination of radionuclide concentrations, especially for radionuclides with low energy gamma rays (eg ¹³¹I), more difficult than would be the case for lower level surveys. The DOE/NNSA AMS was not used to directly measure ¹³⁷Cs activity concentrations. Activity concentrations for ¹³⁴Cs were determined, with ¹³⁷Cs concentrations estimated by comparison with ground based measurements (MEXT 2011). In surveys conducted by MEXT, the spectrometric capability of the systems were barely utilised at all (MEXT 2012a). The systems were used to measure

dose rates, with the dose rate >1400keV used to estimate the natural component. ^{134}Cs and ^{137}Cs activity concentrations were then determined from the anthropogenic dose rate.

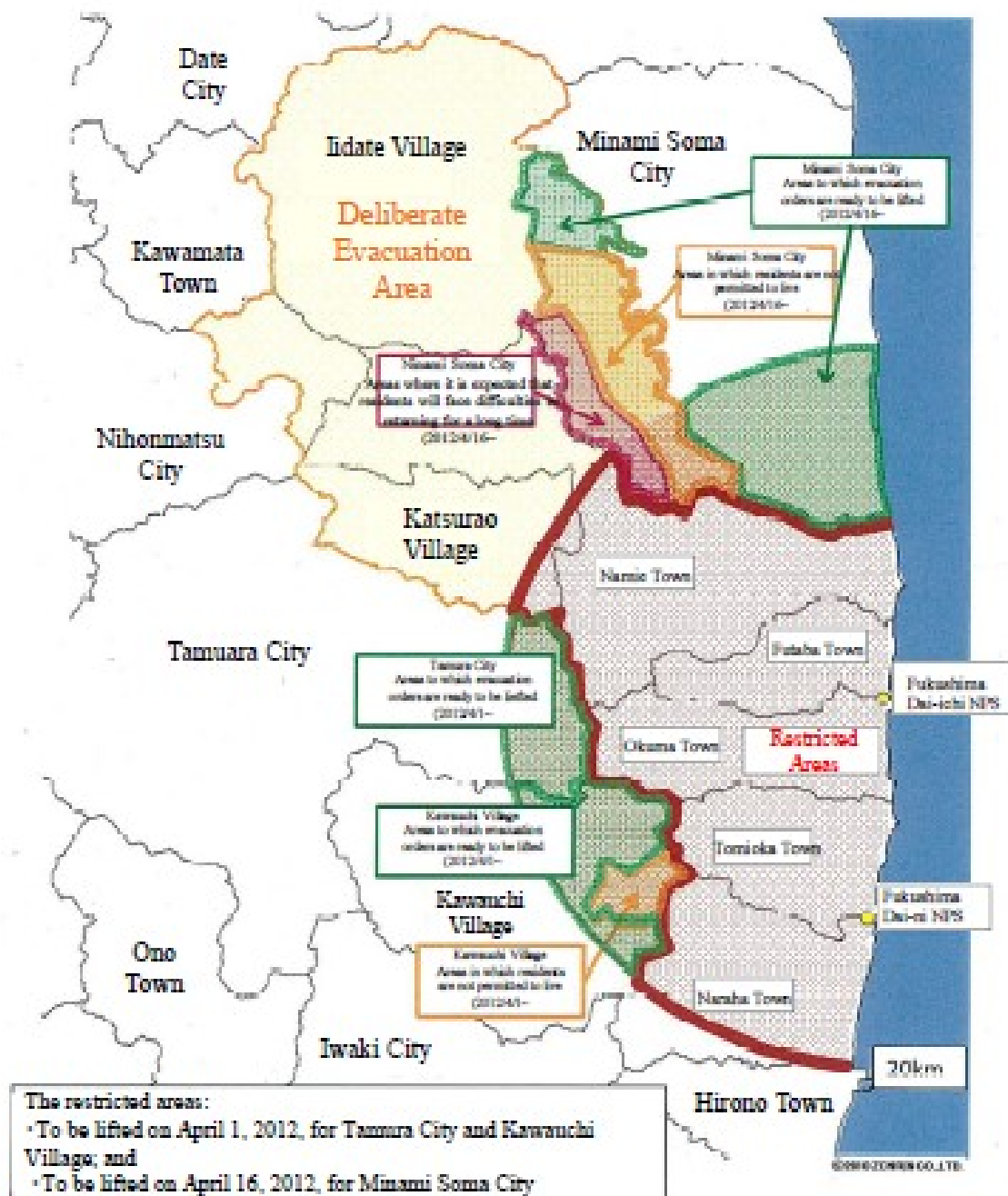


Figure 1.1: Map of evacuation areas, and areas where restrictions have been removed.

Results of airborne monitoring by MEXT and DOE
 (Readings of air dose monitoring inside 80km zone of Fukushima Dai-ichi NPP)

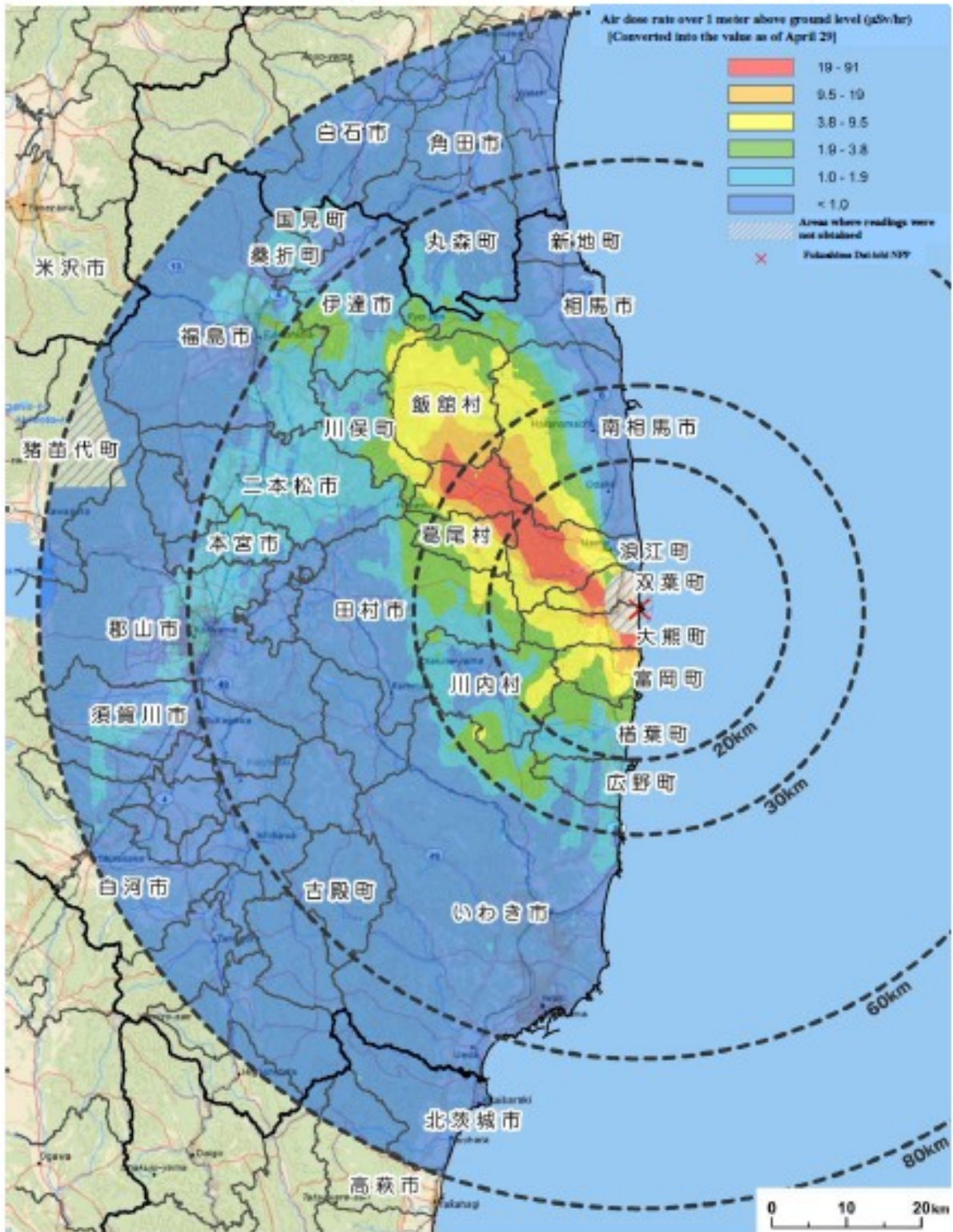


Figure 1.2: Dose rates for the area within 80km of the Fukushima Daiichi NPP generated from airborne survey data collected by the US DOE and MEXT in the first few weeks after the accidents. Taken from MEXT 2011.

**Measurement Results of the Airborne Monitoring Surveys Conducted by MEXT Nationwide
(Air dose rates at 1m height above the ground surface measured nationwide)**

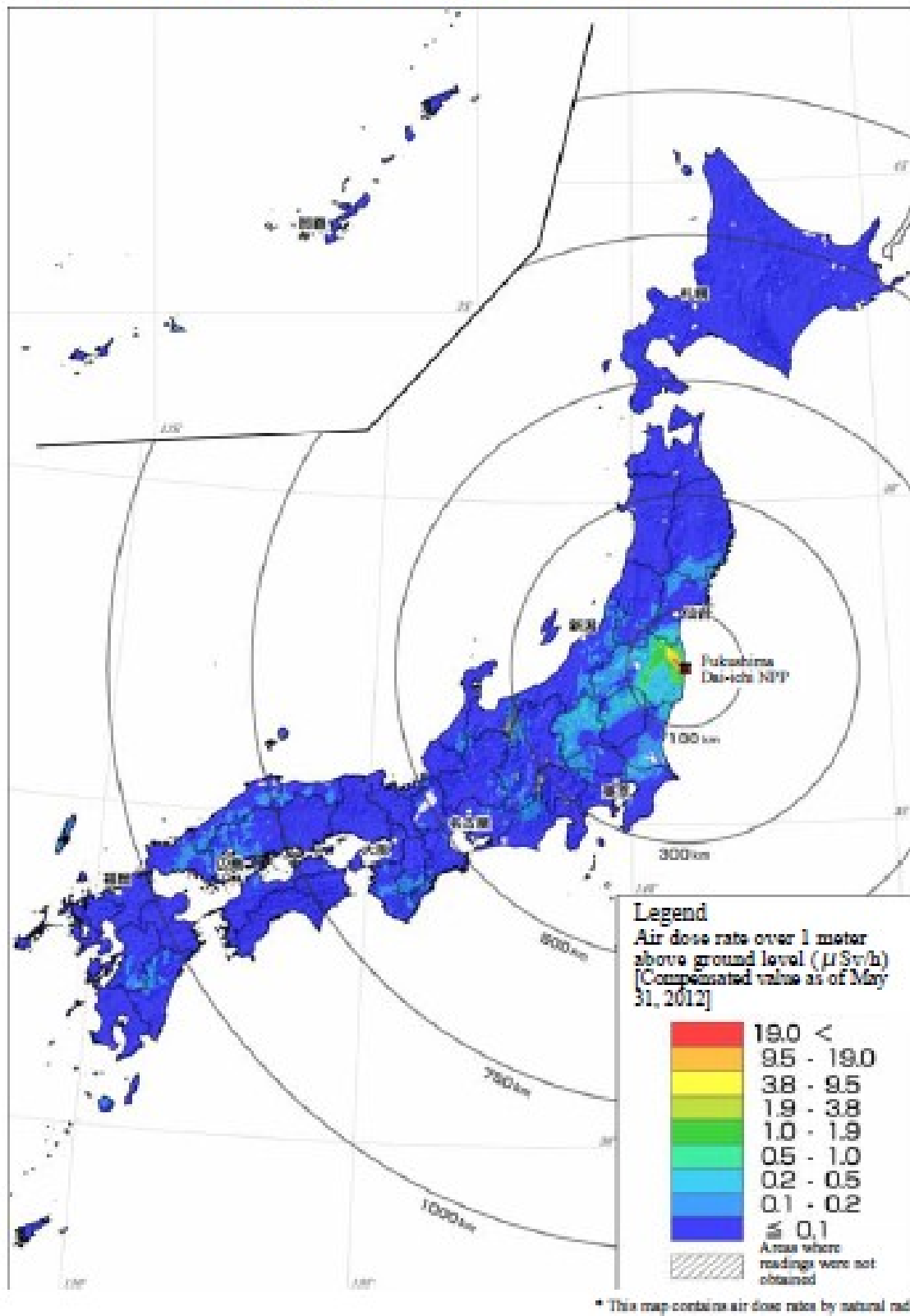


Figure 1.3: Dose rates for Japan generated from airborne survey data collected on behalf of MEXT by July 2012. Taken from MEXT 2012.

1.4 Calibration and Validation

Data collected by radiometric systems can be processed by several different methods to produce estimates of radionuclide concentration and dose rate. These methods all include parameters that reflect radiation transport and subsequent interactions in the detector, which can be determined by empirical or theoretical means. The activity concentration and dose rate estimates produced will depend upon the parameters used. During the early phases of nuclear emergency response the precision and accuracy of reported dose rates and activity concentrations may not be important. However, in later stages of the response it becomes more important that the calibration assumptions used in analyses are clearly stated, and that the analyses conducted can be validated.

In Europe, a series of projects funded under European Commission Framework Programmes has developed protocols for dose rate and activity deposition mapping (Sanderson & McLeod 1999), with a validation exercise held in 2002 (Sanderson *et.al.* 2003, 2004). These protocols defined essential requirements of systems and procedures, while recognising the variety of particular implementations. In particular, validation against independent, internationally traceable measurements was recommended.

1.5 This Work

This report documents a series of radiometric measurements conducted in Japan between March and November 2012, using the SUERC Portable Gamma Spectrometry System in collaboration with Fukushima University. These data include exploratory measurements in March 2012 at the National Food Research Institute in Tsukuba and at Fukushima University, surveys from vehicles into the evacuation and exclusion zones around the Fukushima Daiichi nuclear plant, surveys of the campus at Fukushima University and the Fukushima Prefecture Fruit Tree Research Institute. The areas surveyed are shown in Figure 1.4, with the areas surveyed around Fukushima Iizaka and the fruit cultivation areas near Date shown in Figure 1.5.

A calibration site established at Fukushima University is described, and data from this site used to assess the calibration of the SUERC system used for the work reported here.

A Technical Annex that accompanies this report details the analysis procedures and other information that may be helpful in a technical appraisal of the results presented here. The data sets are also available in processed (activity concentrations and dose rates for each measurement) and full spectral forms in the European Radiometrics and Spectral (ERS) data format (Guillot 2003), with images of all the mapped data for ^{134}Cs , ^{137}Cs and dose rate.

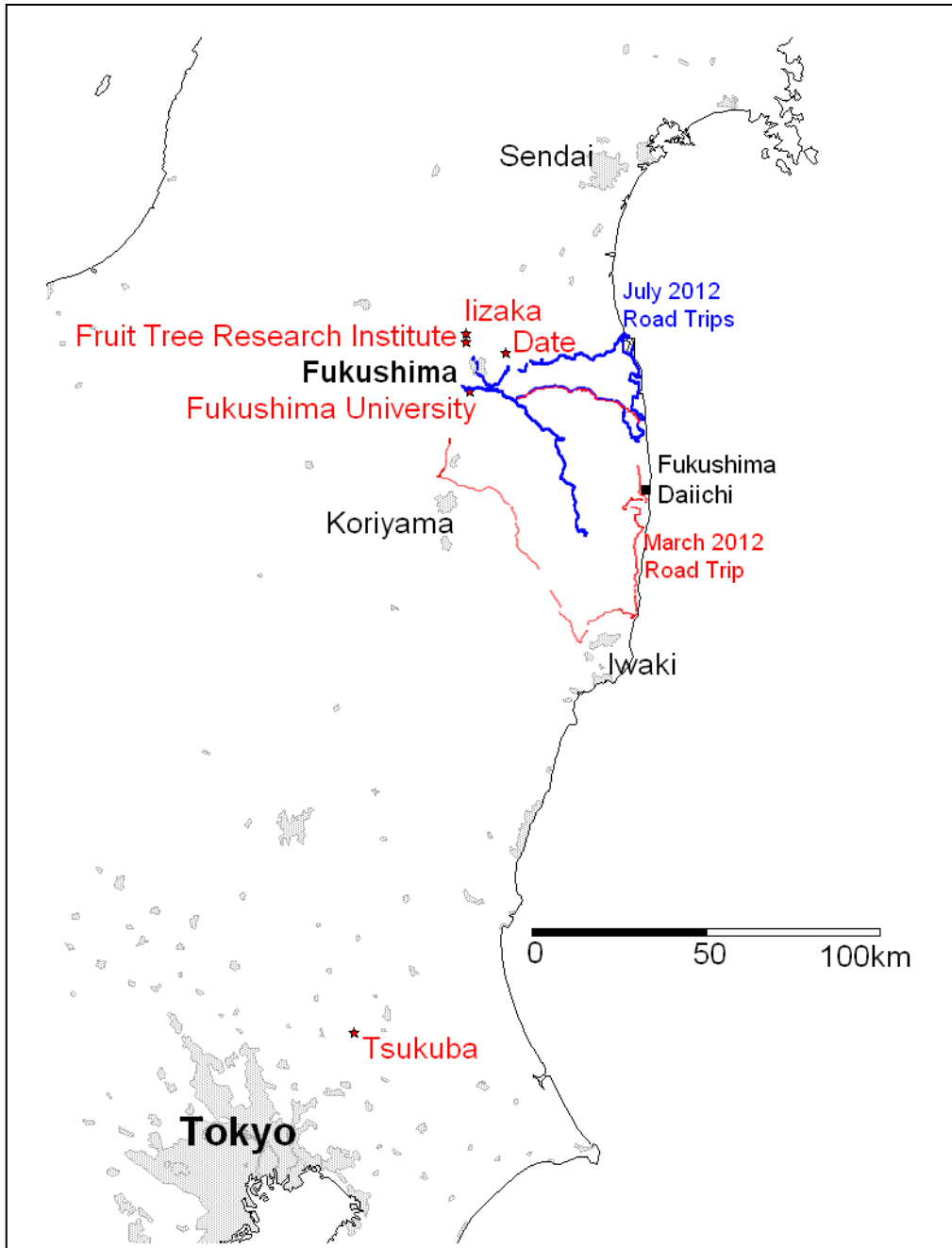


Figure 1.4: Location of areas surveyed using the SUERC Portable Gamma Spectrometry system in 2012.

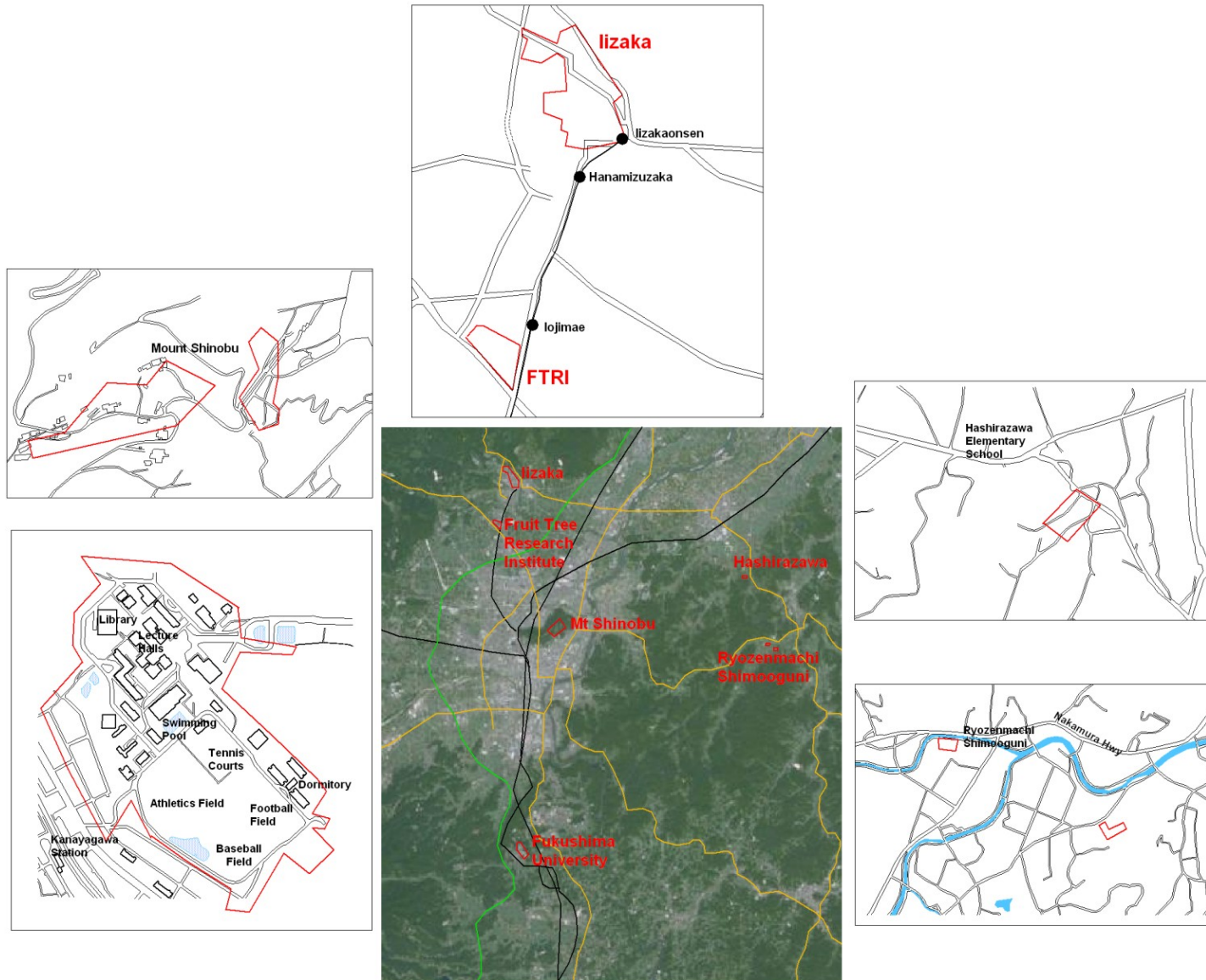


Figure 1.5: Location of areas surveyed around Fukushima City in 2012. Showing the Fruit Tree Research Institute and Fukushima Iizaka (top centre), Mount Shinobu (top left), Fukushima University (bottom left) and areas of fruit cultivation surveyed near Date (right).

2. Radiometric Methods

Many radionuclides decay with associated gamma rays with distinctive energies. The energies of principal gamma rays from nuclides relevant to environmental measurements are listed in Table 2.1. These gamma rays penetrate considerable distances in air, with for example the half length for the 662 keV gamma ray from ^{137}Cs being 72m in air, and distances of ~30cm in soil. Thus, suitable systems are capable of detecting these gamma rays remotely with large fields of view for activity within the top 30-40cm of soil. Gamma spectrometry measures the energy of gamma rays absorbed in the detector, producing a spectrum with full energy peaks and a continuum due to scattering between the source and detector and partial absorption in the detector. Radiometrics utilises sensitive gamma spectrometers measuring continuously mounted on mobile platforms to measure the distribution of radionuclides in the environment. Different detector types are used, with different characteristics that make them suitable for different tasks.

Scintillators are crystals that produce light as gamma rays are absorbed, photomultipliers or silicon photodiodes are used to collect the photons produced and generate a voltage pulse proportional to the energy deposited. Scintillators are sensitive detectors, robust, simple to operate, available in large volumes and relatively inexpensive. However, the peaks in spectra generated from scintillators are broad, resulting in the requirement to apply complex spectral analysis procedures. Thallium doped sodium iodide (NaI(Tl)) is the most commonly used scintillator for gamma spectrometry. Plastics and bismuth germanate (BGO) have poorer spectral resolution, and are often used for gamma-dosimetry where cost or volume are critical. Other scintillators often used include caesium iodide (CsI(Tl)) and lanthanum bromide (LaBr_3) with several other materials occasionally used. These have better spectral resolution, but are more expensive than NaI(Tl) and are not as readily available in large volumes.

Germanium semiconductor detectors produce electron-hole pairs as gamma rays interact with the crystal, which when a high voltage is applied generate voltage pulses. These detectors produce high resolution spectra, with the majority of peaks resolved allowing simple identification of isotopes. However, they require more sophisticated pulse processing electronics compared with scintillators, need to be cryogenically cooled requiring either a supply of liquid nitrogen or an electrical cooling system, are much less sensitive per unit volume than scintillators, are relatively fragile and significantly more expensive. They are routinely used for laboratory analysis, and for static in-situ field measurements, and can be used for radiometric measurements from vehicles or aircraft.

Spectra for a typical 3x3" NaI(Tl) detector and a Ge detector showing the distinctive peaks for natural and anthropogenic radionuclides are shown in Figure 2.1.

Studies of the response of NaI(Tl) and Ge detectors to fission products that may be released from reactor accidents (Sanderson *et.al.* 1997a, Cresswell *et.al.* 2001) have shown that, especially in the early period after release, the spectra measured may be very complex with several different radionuclides contributing. This results in compound peaks in NaI(Tl) detectors due to gamma rays from multiple radionuclides. Ge detectors are able to resolve these emissions and characterise the composition of the deposited activity. The practice at SUERC for many years has been to utilise both Ge and NaI(Tl) detectors (Sanderson *et.al.* 1994b, 1997b, 1997d, 1998, 2003) combining the sensitivity of NaI(Tl), allowing precise

spatial resolution of the location of deposited activity, with the spectral resolution of Ge detectors to characterise the composition.

Nuclide	Energy (keV)	Intensity	Comment
⁴⁰ K	1460.8	0.107	Natural
²¹⁴ Pb	241.9	0.745	Natural, ²³⁸ U decay series
	295.2	0.191	
	351.9	0.369	
²¹⁴ Bi	609.3	0.468	
	1120.3	0.154	
	1764.5	0.162	
	2204	0.052	
²²⁸ Ac	338.7	0.120	Natural, ²³² Th decay series
	911.3	0.290	
	964.8	0.055	
	969.2	0.175	
²¹² Pb	238.6	0.434	
²¹² Bi	727.2	0.068	
²⁰⁸ Tl	277.4	0.064	
	583.2	0.851	
	860.6	0.126	
	2614.5	0.999	
¹³⁷ Cs	661.7	0.85	Fission product, 30.04y half life
¹³⁴ Cs	563.2	0.084	Activation product, 2.065y half life
	569.3	0.154	
	604.7	0.976	
	795.8	0.855	
	801.9	0.087	
⁶⁰ Co	1173.2	0.999	Activation product, 5.27y half life
	1332.5	1	
¹³¹ I	364.5	0.812	Fission product, 8.04d half life
¹³² I/ ¹³² Te	228.2	0.88	Fission products in equilibrium, 3.26d half life
	522.7	0.16	
	630.2	0.133	
	772.6	0.756	
	954.6	0.176	

Table 2.1: Gamma ray energies and intensities used in gamma spectrometry. In this work, the short live iodine isotopes produced in the Fukushima Daiichi reactors had decayed and ⁶⁰Co was not detected. ¹³⁴Cs, ¹³⁷Cs and the natural radionuclides have been measured.

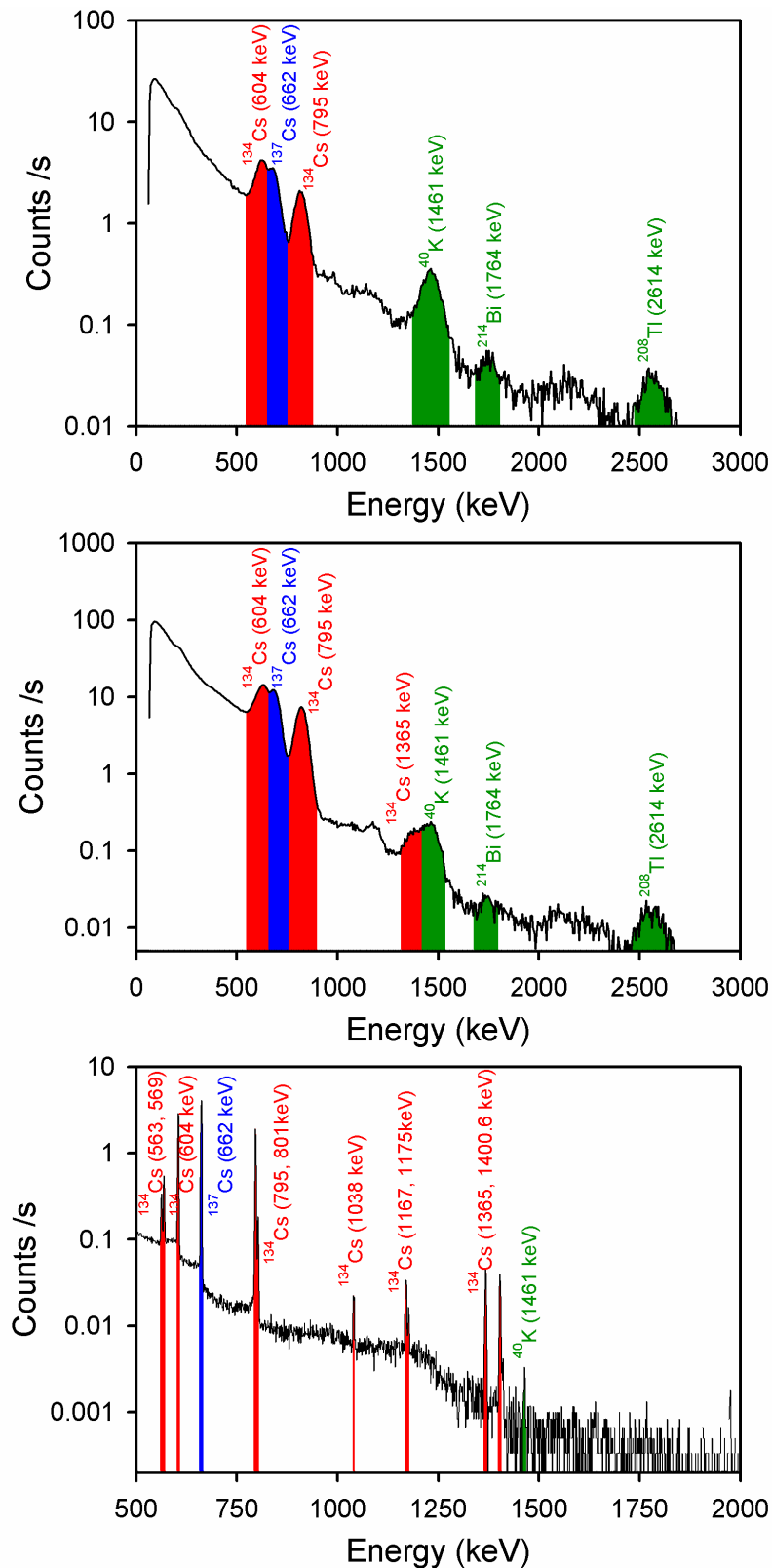


Figure 2.1: Typical $3\times 3''$ NaI(Tl) and Ge spectra showing the positions of characteristic peaks from natural activity (^{40}K , ^{214}Bi from the ^{238}U series, and ^{208}Tl from the ^{232}Th decay series), and peaks from ^{134}Cs and ^{137}Cs . The top spectrum is from an area of relatively low contamination. The middle spectrum is from an area with greater levels of contamination, and shows the interference between the ^{134}Cs 1365keV and the ^{40}K 1461keV peaks. The bottom spectrum is for a laboratory sample (sum of top samples from the Fukushima University calibration site), the 1038, 1167, 1175 and 1400.6 keV peaks are due to cascade summing in the close-coupled laboratory geometry.

2.1 Summary of Systems and Analytical Approaches

The requirements for radiometric systems are dependent upon the survey tasks. With a continually moving platform, spatial resolution is a function of speed, measurement time and the detector field of view, and the precision of activity estimates for single measurements is a function of integration time and detector sensitivity. General requirements for radiometric systems have been defined in protocols developed during projects funded by the European Commission (Sanderson & McLeod 1999, ECCOMAGS 2002). Radiometric systems comprise one or more gamma spectrometry instruments, positioning instrumentation and data acquisition and analysis computers. For airborne systems the spectrometry system is typically based on a large volume NaI(Tl) detector (between 8 and 32 litres), with additional Ge semiconductor detector systems also regularly used (ICRU 1994, IAEA 1996). Vehicular systems typically use smaller NaI(Tl) detectors (4 to 8 litres), again with Ge detectors also sometimes employed. Backpack systems are constrained by the weight an operator can carry, e.g. a 3x3" NaI(Tl) spectrometer. Positioning typically uses GPS receivers, with radar altimetry for airborne measurements. The computing system collects and records spectra, logged with positional information, and usually incorporates a real-time display for the operator.

2.1.1 Data Reduction Approaches

A variety of analytical approaches are used for processing measured spectra to generate dose rate and radionuclide activity concentration estimates.

Dose rate estimates can be determined from the total count rate in the spectrum, or the count rate above a defined threshold. Dose rate estimates can also be generated by a summation of the product of channel count rate with channel number (generating a Spectral Dose Index, SDI) or a summation of the product of the channel count rate with channel energy (generating an energy deposition in the detector). Alternatively, the dose rate corresponding to a given radionuclide activity concentration and distribution can be estimated and hence a total dose rate determined from radionuclide activity concentration measurements.

For estimates of radionuclide activity concentrations, the most common approaches to spectral analysis are:

Spectral Windows Methods with Stripping. This determines count rates within defined regions of interest in the spectrum corresponding to distinctive gamma rays for the radionuclides of interest. A stripping matrix is then used to subtract interferences between these windows as a result of scattered radiation and related full energy peaks. The resulting stripped count rates for each window can be scaled by a sensitivity parameter (and an altitude correction factor for airborne measurements) to produce activity concentrations. This method is simple to program and can be applied to individual spectra in real time (IAEA 1991, 2003, ICRU 1994, Sanderson *et.al.* 1994a,b). It requires prior knowledge of the radionuclides present in the environment, and an appropriate stripping matrix and set of sensitivity parameters. It can be very sensitive to detector gain drifts, especially where regions of interest are contiguous, and will produce erroneous results in the presence of radionuclides not included in the analysis.

Least Squares Fitting. This uses predetermined model spectra for each radionuclide of interest, which are then scaled and summed to fit the measured spectrum. For more than a few radionuclides, this approach requires matrix algebra. The model spectra need to be well matched to the response of the particular detector used.

Principal Components Methods. A statistical analysis across a large number of spectra identifies a large number of components that are then, either individually or in combination, identified with particular radionuclides. The method is commonly used in Minimum Noise Fraction (MNF) and Noise Adjusted Singular Value Deconvolution (NASVD) analyses (Hovgaard 1998, 2000). Because the methods require large numbers (>2000) of measurements, it can only be applied in post-processing. The noise reduction algorithm may also result in a loss of quantitative accuracy (Dickson 2004). In addition, the components extracted may not correspond to specific radionuclides or associated decay chains, and can reflect differing environmental compartments and other factors.

Peak Identification Methods. The spectra are processed to identify peaks, which may be due to individual gamma emission lines or be compound peaks of overlapping lines, with Gaussian or modified Gaussian shapes fitted to the peaks. The Peak Isolation Method (PIM) is an example of this approach (Guillot 2001). For spectra with intense peaks it produces results comparable to those from windows methods, but with greater statistical uncertainty at lower activity concentrations (Guillot 2001, Bourgeois *et.al.* 2003).

2.1.2 Gain monitoring and stabilisation

NaI(Tl) spectrometers are susceptible to gain instability, especially immediately after being powered up and with changes in operating temperature. These instabilities can be reduced by maintaining the detectors in a powered state and avoiding substantial temperature changes. However, for environmental monitoring applications air temperature is not controllable and with lightweight systems the installation of heating systems is impractical. The requirement to maintain maximum battery duration for the survey tasks may also limit the opportunity to leave the system with power on while not on survey.

Most of the methods used for data analysis are sensitive to gain instability in the detector, and therefore it is necessary to monitor gain and to stabilise spectra to compensate for these effects. Gain variations can be monitored by identifying peak positions of prominent gamma rays in the spectra, although in a post-emergency scenario care is needed as the natural series peaks routinely used for this purpose may experience interference from other gamma rays not usually present in the environment. Of particular importance in Japan for this work is the interference between the 1365 keV emission from ^{134}Cs and the 1461 keV peak from ^{40}K , as seen in Figure 2.1. In areas with ^{134}Cs contamination above approximately 50 kBq m^{-2} this interference precludes the reliable use of ^{40}K for automated gain stabilisation. A better approach under these circumstances is to use the 795 keV emission from ^{134}Cs to stabilise gain. Gain can be stabilised automatically or manually, by adjusting detector high voltage or amplifier gain, or in post processing by software. Detector gain can be stabilised to less than 1.5% drift (2 channels at 795keV), with corresponding a variation in activity concentrations for both ^{134}Cs and ^{137}Cs of less than 10% using the spectral windows stripping method.

2.2 Relationship Between Airborne, Vehicular and Backpack Systems

Airborne surveys provide an effective means of rapidly assessing the radionuclide activity concentrations and dose rates over large areas. Ground based methods, with vehicles or backpacks, generate data for smaller areas with finer spatial detail. The most significant factor in the relationship between radiometric measurements from different platforms is the detector field of view. As a rule of thumb, for airborne systems the field of view is a circle with radius approximately equal to the ground clearance elongated along the line of flight. Thus at a height of 100m an airborne system averages measurements across a track approximately 200m wide. For ground based systems the field of view is much smaller, at 5-10m radius.

The relationship between airborne and ground based measurements of ^{137}Cs activity concentration and dose rate has been extensively investigated (Sanderson *et.al.* 1994b, Tyler *et.al.* 1996, Hovgaard & Scott 1997, Bucher *et.al.* 2000, Mellander *et.al.* 2002, Sanderson *et.al.* 2003, 2004, Kock & Samuelsson 2011). AGS and in-situ or backpack measurements in open field conditions generally produce excellent agreement. Vehicular measurements on roads typically underestimate activity by 50% due to the influence of the road.

2.3 SUERC Portable Gamma Spectrometry System

The SUERC Portable Gamma Spectrometry System consists of a 3x3" NaI(Tl) detector with digital spectrometer and GPS receiver in a weather proof canister, connected via a USB cable to a netbook or tablet computer running a data acquisition and analysis program developed at SUERC. It can be deployed as a backpack system or in a vehicle. Spectra are continually logged with a measurement time of usually 5 or 10s, with the position and time of the start and end of each measurement and the midpoint recorded. The GPS system is WAAS enabled, with a nominal accuracy of 3-5 m, although in proximity to buildings and in mountainous terrain where signals from some satellites are impeded this accuracy may be reduced. The software includes an automatic gain stabilisation option, but due to uncertainties with respect to spectral interferences this was not used in this work. During acquisition, real time analysis is conducted using a spectral windows with stripping algorithm for radionuclide activity concentration estimates and a count rate above 400 keV for dose rate. Additional analysis using different methods are possible in post-processing. The real-time display shows activity concentrations and dose rates, gross and differential spectra with a waterfall plot time history, and moving map display. The response of the system to urban areas in Scotland has been studied through a series of projects (Cresswell *et.al.* 2013).

The algorithm for real time analysis uses three sets of parameters to convert count rates in defined spectral windows to calibrated activity concentration and dose rate values. These are count rates for each spectral window for the detector background, a stripping matrix that removes interferences between spectral windows producing pure nuclide count rates, and sensitivity parameters converting the nuclide specific count rates to activity concentrations.

Background count rates were determined from measurements collected from a plastic boat on Loch Lomond, and account for detector backgrounds and cosmic ray contributions.

The stripping matrix is derived from pure nuclide spectra. The matrix used is a reconciliation of elements derived from Monte Carlo simulations of the detector response using a code

developed at SUERC optimised for radiometric systems, and extensively validated (Allyson 1994, Allyson & Sanderson 1998, Cresswell *et.al.* 2001, Cresswell & Sanderson 2012), measurements conducted on calibration pads at SUERC, existing field measurements with similar detectors (Allyson 1994, Tyler 1994), and pure ^{134}Cs spectra generated from repeat measurements in Japan.

Sensitivity parameters have been derived from a combination of theoretical fluence rates presented in ICRU53 (ICRU 1994), modelled and measured response of detectors for in-situ measurements (Tyler 1994, Allyson 1994) and attenuation due to the detector canister, and measurements with point sources at SUERC. Analysis of data collected near the calibration site at Fukushima University in November 2012, with and without the operator present allowed the estimation of an operator effect. Additional studies of the operator shield factor have been undertaken as part of a physics student BSc dissertation in the University of Glasgow (Buchanan, 2013). These show an operator effect of 25-29% reduction in count rate for different spectral windows. Similarly, in locations where backpack and vehicular data have been collected, a vehicle shielding effect of 23-28% can be determined. The derivation of these factors are described in the Technical Annex.

Prior to use in Japan a working calibration was derived, and used for real-time analysis in the field. Data produced in the field with the working calibration are presented in the Technical Annex. A more thorough calibration was subsequently completed, accounting for operator effects not initially considered and with a gain stabilisation applied. This was used to produce the data presented in this report. The calibration parameters used are tabulated below.

Some data have also been processed using alternative methods, with results that are broadly compatible with the algorithm described here. These methods and comparisons between them are also presented in the Technical Annex. The windows stripping method has been used for this work because it generates activity concentrations for natural activity as well as radiocaesium. The total radiocaesium approach is marginally more stable with respect to gain drift, but can only generate natural activity concentrations when used in conjunction with other methods. The least squares fitting approach is very sensitive to gain variations, at least without detector gain being a parameter that is fitted along with the input spectra.

	Window range		Background count rates
	Energy (keV)	Channel [†]	
^{137}Cs 662keV	563-719	98-123	1.03 ± 0.02
^{134}Cs 795,802keV	720-869	124-147	0.32 ± 0.02
^{40}K 1461keV	1375-1550	228-256	0.39 ± 0.03
^{214}Bi 1764keV	1656-1856	273-305	0.14 ± 0.03
^{208}Tl 2614keV	2481-2775	405-444	0.10 ± 0.01
Total count rate (400-3000keV)	400-3000	70-512	5.7 ± 0.1

[†]Channel range for standard gain. Some data sets were collected with significantly higher or lower gain, and channel ranges were modified to match the energy range

Table 2.2: Spectral windows and background count rates used for the analysis presented here.

Source	Spectral Window				
	1 (¹³⁷ Cs)	2 (¹³⁴ Cs)	3 (⁴⁰ K)	4 (²¹⁴ Bi)	5 (²⁰⁸ Tl)
¹³⁷ Cs	1	0	0	0	0
¹³⁴ Cs	1.65	1	0.008	0	0
K pad	0.62	0.55	1	0	0
U pad	5.01	2.17	0.81	1	0.02
Th pad	4.55	2.81	0.65	0.62	1

Table 2.3: Stripping matrix used for the analysis presented here.

	Sensitivity parameter		
	Backpack	Vehicle	
¹³⁷ Cs 662keV	0.60	0.84	kBq m ⁻² cps ⁻¹
¹³⁴ Cs 795,802keV	0.61	0.85	kBq m ⁻² cps ⁻¹
⁴⁰ K 1461keV	106	150	Bq kg ⁻¹ cps ⁻¹
²¹⁴ Bi 1764keV	39.4	55	Bq kg ⁻¹ cps ⁻¹
²⁰⁸ Tl 2614keV	12.7	17.8	Bq kg ⁻¹ cps ⁻¹
Total count rate (400-3000keV)	0.0007	0.0008	μGy h ⁻¹ cps ⁻¹

Table 2.4: Sensitivity parameters for the backpack and vehicular measurements.

2.4 Data presentation and mapping

There are a range of methods employed for presenting radiometric data. Summary statistics and histograms can describe the entire data set, or portions of the data set. Individual data points can be plotted on a base map showing the location and value of measurements. Various interpolation routines can be used to smooth data, either for mapping or to generate regridded data with improved precision compared to individual measurements. With a fully spectrometric system, relationships between the activity concentrations of individual radionuclides and the dose rate may also be presented.

2.4.1 Mapping

Radiometric data are mapped to allow the geographical distribution of radiometric features to be visualised. Colour coding of values is common, with the practice at SUERC being to use a rainbow colour scale that runs from dark blue (lowest value) through greens, yellows, orange to red (highest value). Where the data set has a large range, a logarithmic scale may be used to allow variations at lower values to be visualised.

Individual data points may be displayed by plotting colour-coded symbols onto a suitable base map, or other image (eg: from Google Earth). This is an easily interpreted visualisation of the data with the location of each measurement evident. However, for areas of high data density such visualisations tend to result in data points being plotted overlapping which may be confusing.

Interpolation algorithms allow for the presentation of a smoothed map. The algorithm used at SUERC generates a weighted mean value for each pixel of the image from all data points within a defined maximum radius, using an inverse distance weighting function. The algorithm is described in the Technical Annex. Such approaches allow an estimate of activity concentration and dose rate to be made for locations between measurement points, assuming

that there is no substantial discontinuity in the radiation field between the data points. Survey design should allow for greater density of observations across expected boundaries in the radiation field (eg: across the boundary between roads and fields) so that the smoothed data set clearly show these boundaries.

Smoothing algorithms also allow the generation of regridded data sets, with the data presented on a regularly spaced grid analogous to a low resolution pixellated image. By combining several measurements, each cell in such data sets carry less uncertainty than the individual measurements that contribute to it. Regrided data sets can be used to compare data sets collected from the same area, either by different instruments to compare performance or at different times to assess environmental change.

2.4.2 Dose rate apportionment

The dose rate from the different natural and anthropogenic radionuclides in the environment can be calculated from the activity concentrations determined by spectral analysis. A dose rate apportionment can then be made, showing the contribution of each source of dose, and a residual dose rate that is not accounted for in the analysis. The dose rate apportionment shows the relative importance of different radionuclides to the dose rate. Contributions from ^{134}Cs , with a relatively short half life of 2.065 years will decrease quickly even without active remediation. ^{137}Cs , with a 30.04 year half life, will continue to contribute to the dose rate for longer.

Parameters to convert from activity concentration to dose rate for natural and anthropogenic activity, for different environmental geometries, are tabulated in several sources. For this work conversion parameters from ICRU (1994) and Aitken (1983) have been used, with parameters reconciled and applied as described in the Technical Annex. The method of dose rate apportionment can be illustrated using data from the calibration site at Fukushima University, in Table 2.5. Activity concentrations determined from the SUERC portable gamma spectrometer are scaled by the conversion parameter to give contributions to the dose rate from the U and Th decay series, ^{40}K , ^{137}Cs and ^{134}Cs , and a total calculated dose rate. The percentage of the total attributed to each of the components is also calculated. The residual is the difference between the measured and calculated dose rates, and would be positive if there were significant contributions to the dose rate from other sources. Such apportionments have been given in this report in the form of tables, including the uncertainties on each contribution, and as pie charts. Figure 2.2 shows the pie chart corresponding to the data in Table 2.5, with the corresponding dose rate apportionment for SUERC where natural processes have removed the environmental contamination from the 1986 Chernobyl accident.

Backpack Data		Conversion parameter	Calculated Dose rates ($\mu\text{Gy h}^{-1}$)		Apportionment
^{214}Bi	$6.5 \pm 1.1 \text{ Bq kg}^{-1}$	50.3×10^{-3}	$^{238}\text{U} + ^{235}\text{U}$ series	0.003 ± 0.001	$0.26 \pm 0.04 \%$
^{208}Tl	$3.5 \pm 0.3 \text{ Bq kg}^{-1}$	70.2×10^{-3}	^{232}Th series	0.007 ± 0.001	$0.55 \pm 0.05 \%$
^{40}K	$196 \pm 8 \text{ Bq kg}^{-1}$	444×10^{-3}	$^{40}\text{K} + ^{87}\text{Rb}$	0.009 ± 0.001	$0.70 \pm 0.03 \%$
^{137}Cs	$254 \pm 11 \text{ kBq m}^{-2}$	1.83×10^{-3}	^{137}Cs	0.465 ± 0.020	$37.7 \pm 1.6 \%$
^{134}Cs	$169 \pm 9 \text{ kBq m}^{-2}$	4.44×10^{-3}	^{134}Cs	0.750 ± 0.040	$60.8 \pm 3.2 \%$
dose rate	$0.152 \pm 0.002 \mu\text{Gy h}^{-1}$		Total	1.234 ± 0.062	
			Residual	-0.082 ± 0.076	$-6.6 \pm 6.2 \%$

Table 2.5: Dose rate apportionment for the Fukushima University calibration site.

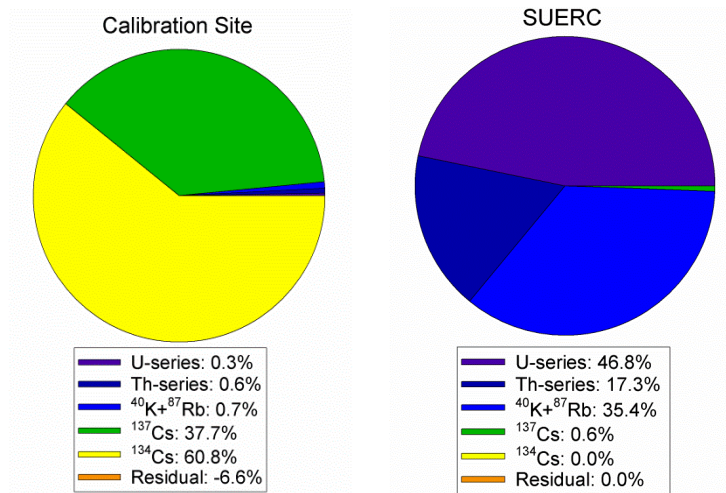


Figure 2.2: Dose rate apportionment for the Fukushima University calibration site and SUERC.

3. Establishment of Calibration Sites in Fukushima

3.1 Reasons for Establishing Calibration Sites

Calibration sites demonstrate the traceability of field measurements to international reference materials measured in controlled geometries and allow the validation of sensitivity parameters and models used to calculate activity concentrations and dose rates from gamma spectrometry measurements. The approach of mineral exploration calibration (as described, for example, in IAEA 1991, 2003) of using concrete reference pads to either directly calibrate radiometric instruments or to calibrate field instruments used to develop a calibration grid in the survey area does not allow direct calibration to the environmental systems of the survey. In particular, where soils differ significantly in density or geochemistry from concrete and where activity is stratified, for example as a result of fallout deposition and subsequent slow migration down the soil column. The use of calibration sites in environments representative of the whole survey area is preferred by SUERC.

The earliest radiometric surveys by SUERC used point to point comparison between radiometric data and several soil cores across the survey area (Sanderson *et.al.* 1988, 1989, Sanderson & Scott 1989). Individual soil cores are, however, poorly matched to the field of view of radiometric systems. A sampling scheme of concentric arcs with 17 cores collected was developed (Sanderson *et.al.* 1990a,b) which was later refined into an expanding hexagonal pattern (Tyler 1994, Sanderson *et.al.* 1994a, Tyler *et.al.* 1996).

Calibration sites can be used to determine calibration coefficients based on observations at the site. This has the advantage of providing a direct empirical means of tracing mapped data to laboratory results, which is independent of systematic errors in stripping matrices and other experimental system biases such as operator shielding. However, especially where only one site is used, it produces data relative to the conditions of the calibration site which may not be fully representative of source distributional effects elsewhere. ICRU53 (1994) suggests the expression of AGS results relative to calibration sites, but also recognises the use of modelled calibration data for expression of in-situ (static) gamma spectrometry results relative to a stated mass depth distribution as an alternative methodology.

A calibration site has been established at Fukushima University to allow validation of the calibration of field instruments against international reference materials. The sampling protocol follows the long established method employed at SUERC (Tyler 1994, Sanderson *et.al.* 1994a, Tyler *et.al.* 1996), which has been used for calibration verification for radiometric surveys by SUERC since 1992 and in international exercises comparing airborne and ground based radiometric methods (NKS 1997, Hovgaard & Scott 1997, Sanderson *et.al.* 2003, 2004). In this protocol, core samples are collected from a pattern of hexagonal rings around a centre point in a manner that allows for mean values of activity per unit mass, activity per unit area and associated mass depth, and dose rate representative of detectors at ground level and airborne survey altitudes to be determined. For airborne survey use, large sites of ~500m diameter are required. For use with ground based equipment, and potentially unmanned aircraft operating at low ground clearance, smaller sites can be used.

During the course of the work reported here, three internationally validated calibration sites established in SW Scotland for the European ECCOMAGS exercise (Sanderson *et.al.* 2003, 2004) were revisited. The instruments used in this work were checked over the centre points of the international reference sites and cores collected to allow an assessment of

environmental change since the exercise. In this way the calibration site at Fukushima is traced to the established European radiometrics reference sites.

3.2 Calibration Site at Fukushima University

3.2.1 Site selection and sampling

During a visit to Fukushima in July 2012, the possibility of developing a calibration site was explored. For the purposes of establishing a calibration site, an area was required that was open and level ground for at least 20m in all directions of the centre point (or, at least 250m for a site for use with aircraft), with approximately uniform activity and would be available for use for as long as possible. During the survey of the campus, two potential locations were identified. One was on a triangular platform beside a student accommodation block between the road by the tennis and the path to the canteen. This area was smaller than ideal, and is in an area of relatively high use. The second site identified is behind student accommodation blocks at the eastern side of the campus, with woodland to two sides. This area was large enough, in an area of relatively low use, and had only small variations in radiocaesium deposition across the site. It should be noted that while this site is suitable for backpack systems and for checking portable dose rate instruments, it is smaller than needed for calibrating airborne systems and difficult to access with vehicles.

A coring tool that removed cores of 10cm diameter to a depth of 20cm was used. Two rings of the SUERC calibration pattern, at 2m and 8m, were sampled, giving 13 cores including the centre point. The cores were assigned an identification code indicating the ring and position around the ring. Figure 3.1 shows the layout of the sampling pattern, with some photographs of the site in Figure 3.2.

3.2.2 Sample preparation and measurements

Each core was cut into depth intervals that would allow a depth profile to be approximated. It was expected that the majority of radiocaesium activity would be in the top 5cm of each core and so these were sectioned into small depth intervals (0-1cm, 1-3cm and 3-5cm) below that the core was sectioned into 5cm depth intervals (5-10cm, 10-15cm, 15-20cm). Each core section was weighed, and then dried and reweighed to determine water content. The dried sample was then ground to a powder and dispensed to sample containers for laboratory gamma spectrometry analysis.

All samples were analysed at Fukushima University and SUERC on 40% and 50% relative efficiency Ge detectors respectively. Figure 3.3 shows the NaI(Tl) spectrum recorded on the centre point of the calibration site together with a summed Ge spectrum combining all subsamples weighted by their mass fractions in each core. The full energy peaks in the spectra are all identified with natural activity or ^{134}Cs and ^{137}Cs , and are listed in Table 3.1 with the measured intensity and identification.

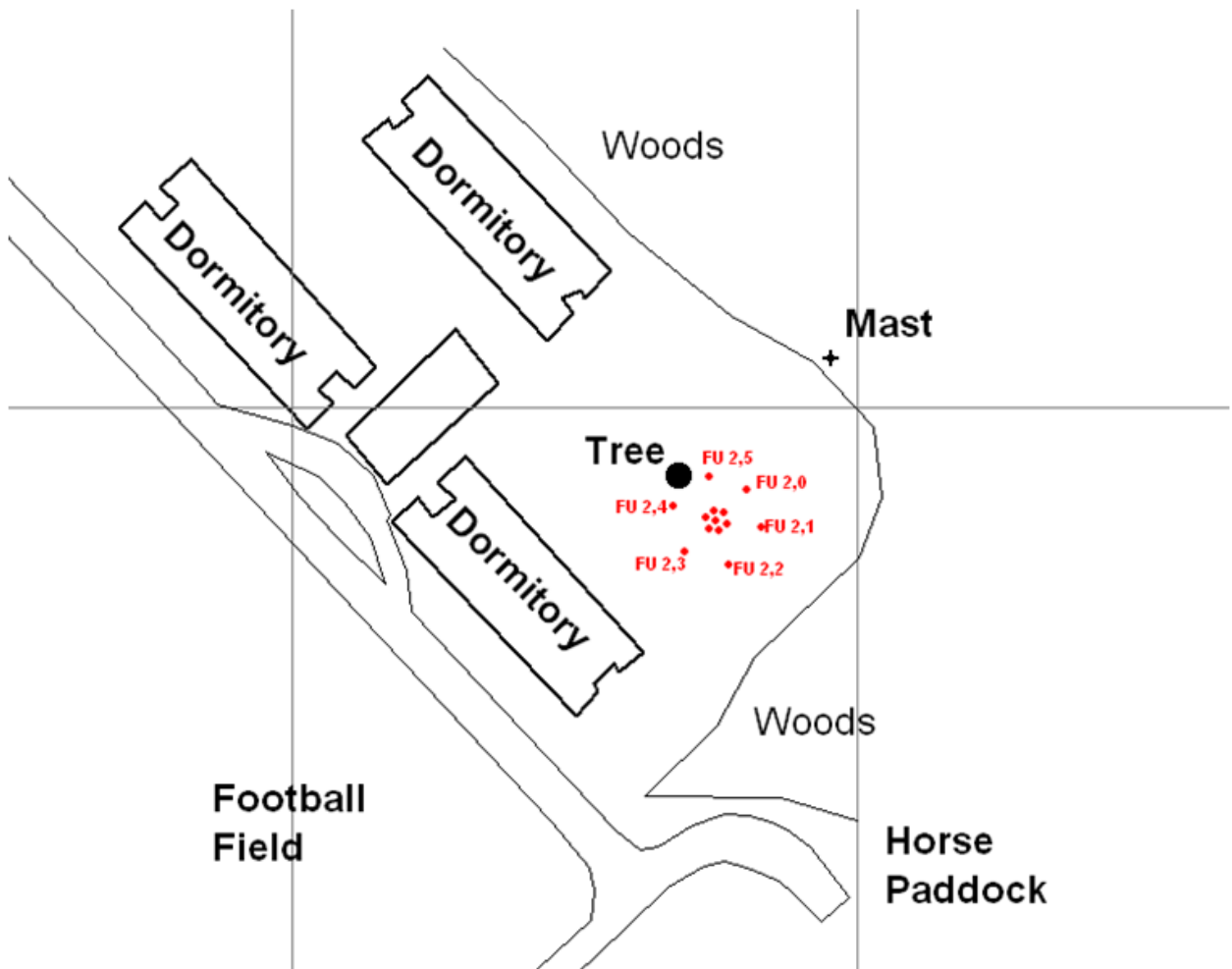


Figure 3.1: Map of the calibration site, with the outer (8m) ring labelled.



Figure 3.2: The calibration site from the north west (left and centre) and south (right).

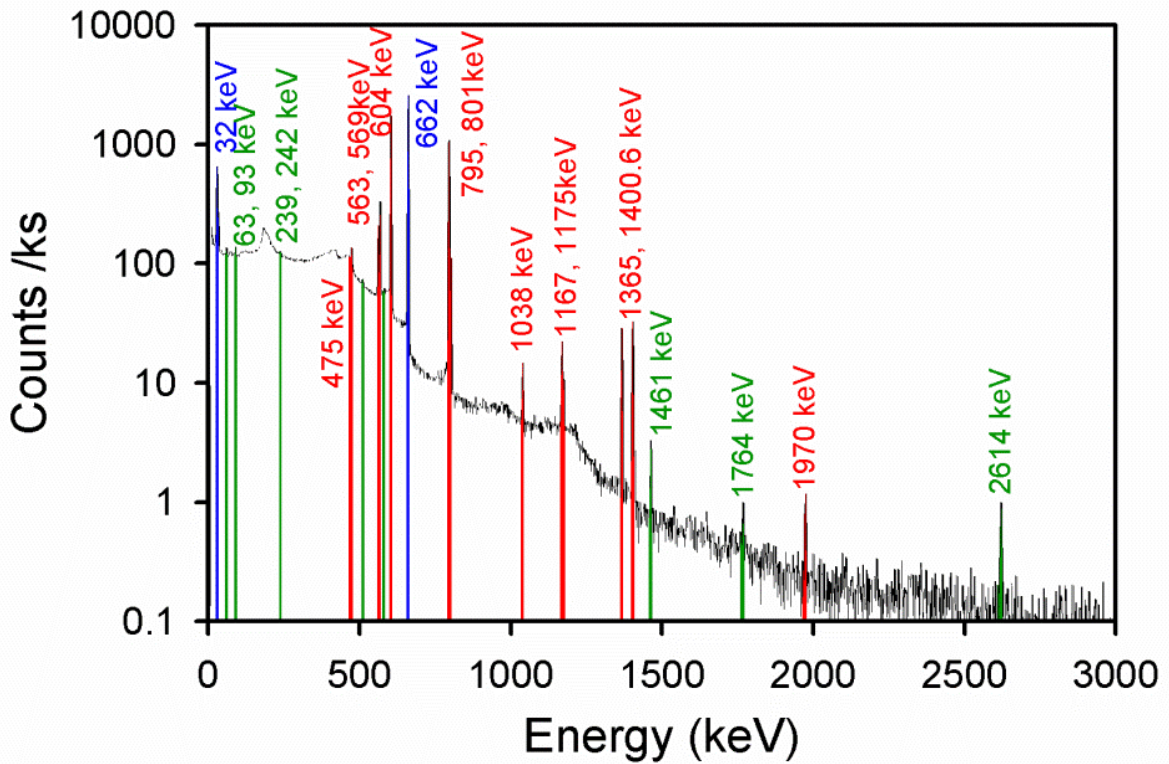
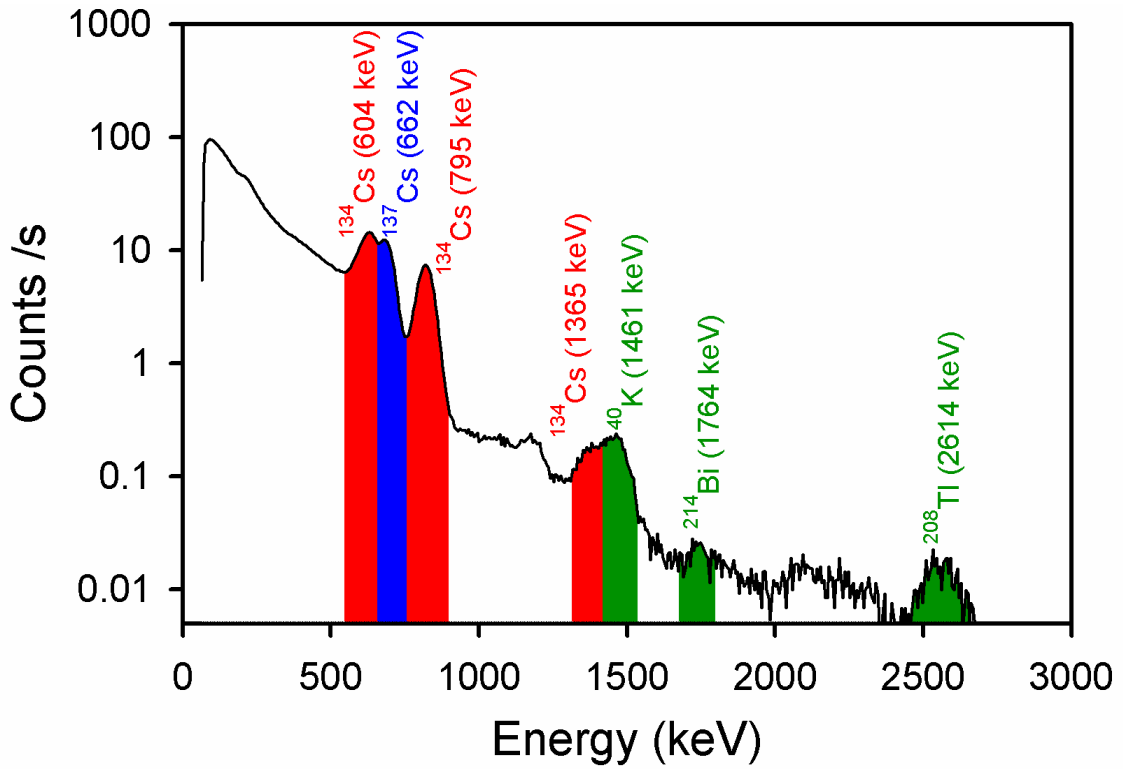


Figure 3.3: NaI(Tl) spectrum recorded from the Fukushima University calibration site and summed Ge spectrum for all the soil samples from the calibration site. The superior energy resolution of the Ge data are evident, as is the lower count rate. Note that the spectral peaks, in both cases, are explained by the combination of ^{134}Cs , ^{137}Cs and naturally occurring radionuclides.

Energy /keV	Intensity /ks ⁻¹	Identification
30.6, 31.0, 35.0	1848.4 ± 74.8	Ba x-rays (radiocaesium decay)
63.3	48.3 ± 46.4	²³⁴ Th (²³⁸ U decay series)
92.6	75.0 ± 48.6	²³⁴ Th (²³⁸ U decay series)
238.6	26.0 ± 49.4	²¹² Pb (²³² Th decay series)
241.9		²¹⁴ Pb (²³⁸ U decay series)
475.4	149.5 ± 45.8	¹³⁴ Cs
511.0	32.5 ± 36.7	Annihilation gamma rays
563.2	438.8 ± 33.2	¹³⁴ Cs
569.3	799.6 ± 39.6	¹³⁴ Cs
583.2	12.1 ± 21.5	²⁰⁸ Tl (²³² Th decay series)
604.7	5198.6 ± 76.0	¹³⁴ Cs
661.7	7567.7 ± 88.7	¹³⁴ Cs
795.8	3639.6 ± 61.9	¹³⁴ Cs
801.9	331.9 ± 21.3	¹³⁴ Cs
1038.6	37.1 ± 9.3	¹³⁴ Cs
1167.9	67.6 ± 10.7	¹³⁴ Cs
1175.0	33.9 ± 9.6	¹³⁴ Cs (cascade summing)
1365.2	114.4 ± 11.7	¹³⁴ Cs
1400.6	108.7 ± 11.8	¹³⁴ Cs (cascade summing)
1460.8	8.9 ± 4.5	⁴⁰ K
1764.5	1.7 ± 2.9	²¹⁴ Bi (²³⁸ U decay series)
1969.9	4.0 ± 2.8	¹³⁴ Cs (cascade summing)
2614.5	4.9 ± 2.7	²⁰⁸ Tl (²³² Th decay series)

Table 3.1: Peaks present in the summed Ge spectrum (Figure 3.3) with corresponding intensity (net counts per kilosecond) and identification.

Activity concentrations (Bq kg⁻¹) were determined from the Ge spectra from the net area of each peak, accounting for continuum components in the spectra and for laboratory background. At SUERC an internal standard (Sanderson *et.al.* 1993) on a sedimentary matrix was used. At Fukushima a multinuclide standard set on an alumina matrix was used. For peaks present in the standard, a scaling of count rates in the sample and standard give the activity concentration for the appropriate geometry. ¹³⁴Cs was not present in the internal standards. At SUERC energy dependent efficiency corrections were derived from the relative efficiencies of natural decay series lines from a Shap granite internal reference material. At Fukushima an efficiency correction curve was constructed from the nuclides within the standard material. In both cases efficiencies for ¹³⁴Cs peaks were thus determined. Analytical performance was checked relative to international reference materials. For SUERC this was done using IAEA Soil 375, IAEA Soil 6, and four retained reference samples from the international calibration sites established in the EU ECCOMAGS Project (Sanderson *et.al.* 2003, 2004). For Fukushima this was conducted using IAEA Soil 444 and JASC Soil 0471 samples. These measurements confirm that the measurement procedures produce activity concentrations consistent with the reference values. Full details of the analytical procedures used, and the activity concentrations for ¹³⁴Cs and ¹³⁷Cs for each subsample determined at Fukushima University and SUERC, are given in the Technical Annex.

3.2.3 Activity concentrations and $^{134}\text{Cs}/^{137}\text{Cs}$ ratios from the calibration samples

From the calibration site the 13 core samples, each subdivided into 4 depth sections, yielded 52 subsamples analysed both at Fukushima University and SUERC. The resulting 52 pairs of activity concentrations for ^{134}Cs and ^{137}Cs are shown on Figure 3.4. Both nuclides cover an activity concentration range of approximately 4 orders of magnitude from 10 to 10^5 Bq kg^{-1} . Taken together, the results from both laboratories are highly coherent across this large range, and the relationship between the isotopes appears coherent irrespective of the depth range of the samples. Both of these aspects will be explored in more detail here.

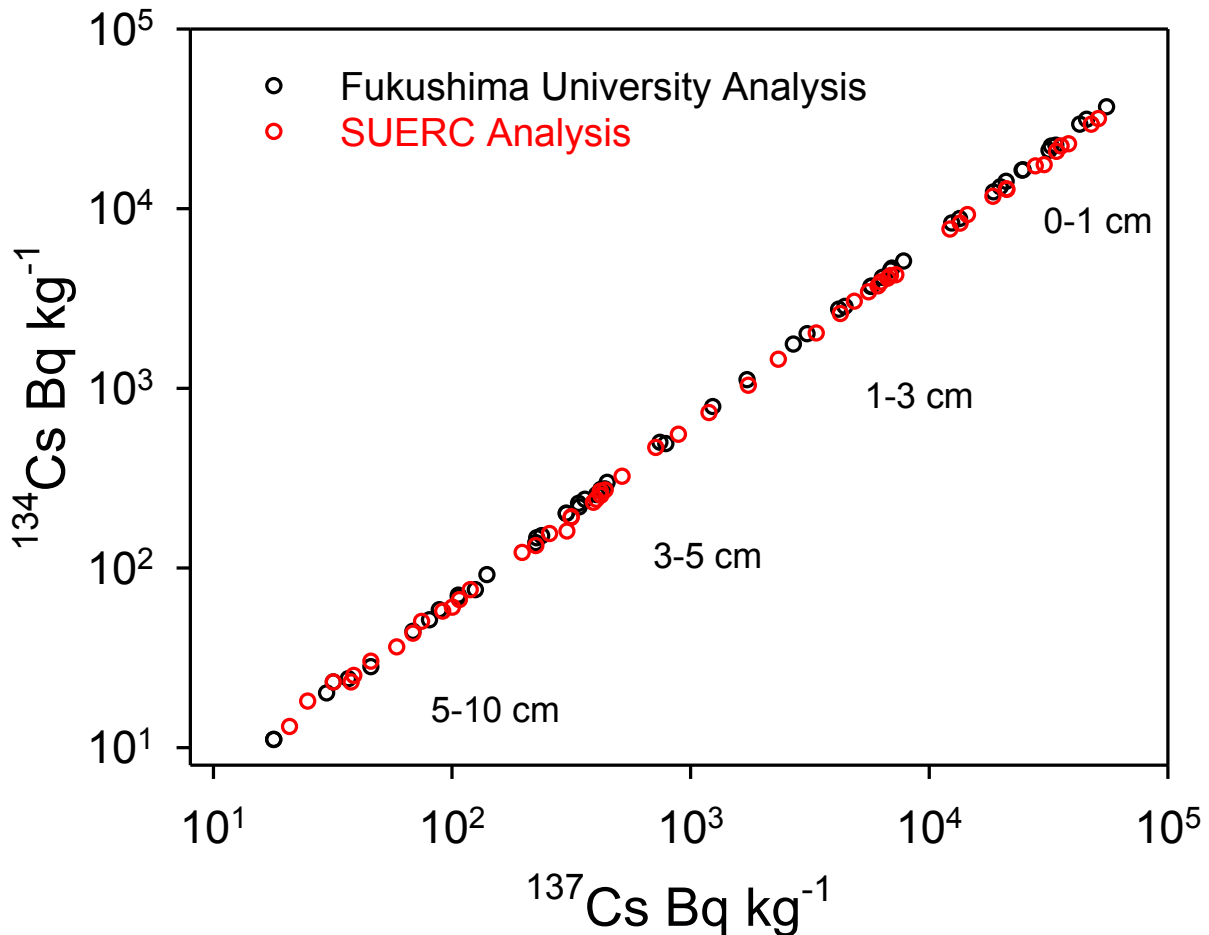


Figure 3.4: ^{134}Cs and ^{137}Cs activity concentrations measured at Fukushima University and SUERC. The data cluster into the four depth sections of each core.

The activity concentration data from each subsample and laboratory are tabulated in the Technical Annex. Prior to combining data from the laboratories to examine the activity distribution within cores and across the site it is important to establish the consistency between the two laboratories. Given the range of activities this has been assessed in two ways based on analysis of the ratios between the two laboratories for each sample.

The first approach adopted a method utilised during the international ECCOMAGS radiometrics intercomparison (Sanderson *et.al.* 2003, 2004). For this exercise, three calibration sites each represented by 31 cores samples subdivided into 5 measurement depths were analysed by a network of 10 European gamma spectrometry laboratories.

Each laboratory used their own protocol but was furnished with homogenised reference materials, with IAEA reference materials and a set of common samples, as well as unknown samples to analyse. Laboratory performance was evaluated using a standardised difference on measurements conducted using common materials. This expresses the difference between individual observations and a reference value, which can be based on a reduced mean or other fixed value, in units of standard deviation, which can be based on reference statistics including expected and observed measurement uncertainties. In the ECCOMAGS study, such differences were helpful in identifying outlying observations and ensuring that consensus values defined for the calibration sites were based on self consistent data sets from a network of international laboratories.

In applying standardised differences to the Fukushima calibration site a reference value of 1 has been used, which would correspond to the condition where both sets of data were equivalent, and a reference standard deviation of 0.15, based on the observed standard deviation of the ratio. The distribution for the standardised differences for the ^{134}Cs and ^{137}Cs measurements are shown in Figure 3.5. It can be seen that all the standardised differences fall within the ± 3 range, and the majority within ± 2 . This suggests that individual measurements are consistent between the two laboratories, within the uncertainties derived from the dispersion of the activity ratios. It is noted that individual measurement errors were smaller than the reference standard deviation observed across all observations. Also there is some evidence for asymmetry and a non-zero mean value, which merits further examination.

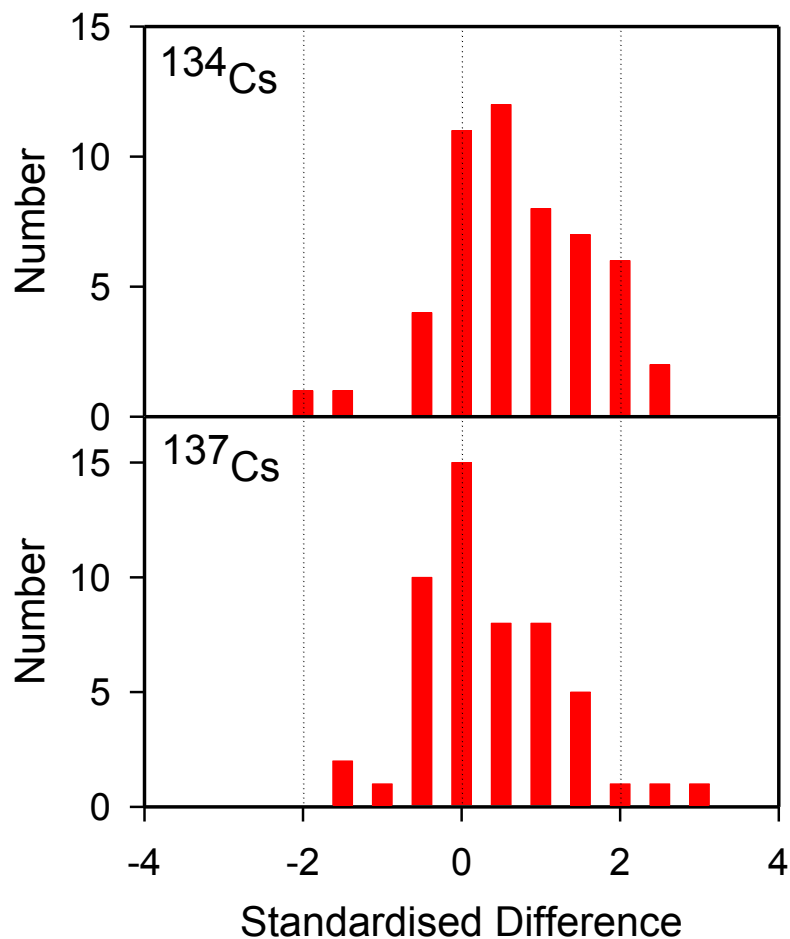


Figure 3.5: Distribution of standardised differences of the measured activity ratios between FU and SUERC relative to a ratio of 1.0 with a standard deviation of 0.15.

The second approach to examine the ratios utilised cumulative frequency distribution for the observed data in comparison with the expected form based on normal distribution. These are shown in Figure 3.6. The observations are well described by normal distributions, with means and standard deviations of 1.02 and 0.13 for ^{137}Cs and 1.07 and 0.15 for ^{134}Cs . This suggests that activity concentrations determined at Fukushima University are marginally higher than those determined at SUERC, by 2% for ^{137}Cs and 7% for ^{134}Cs . These differences are well contained within the measurement uncertainties, but may reflect small underlying methodological differences, which could, if necessary, be assessed further in future work.

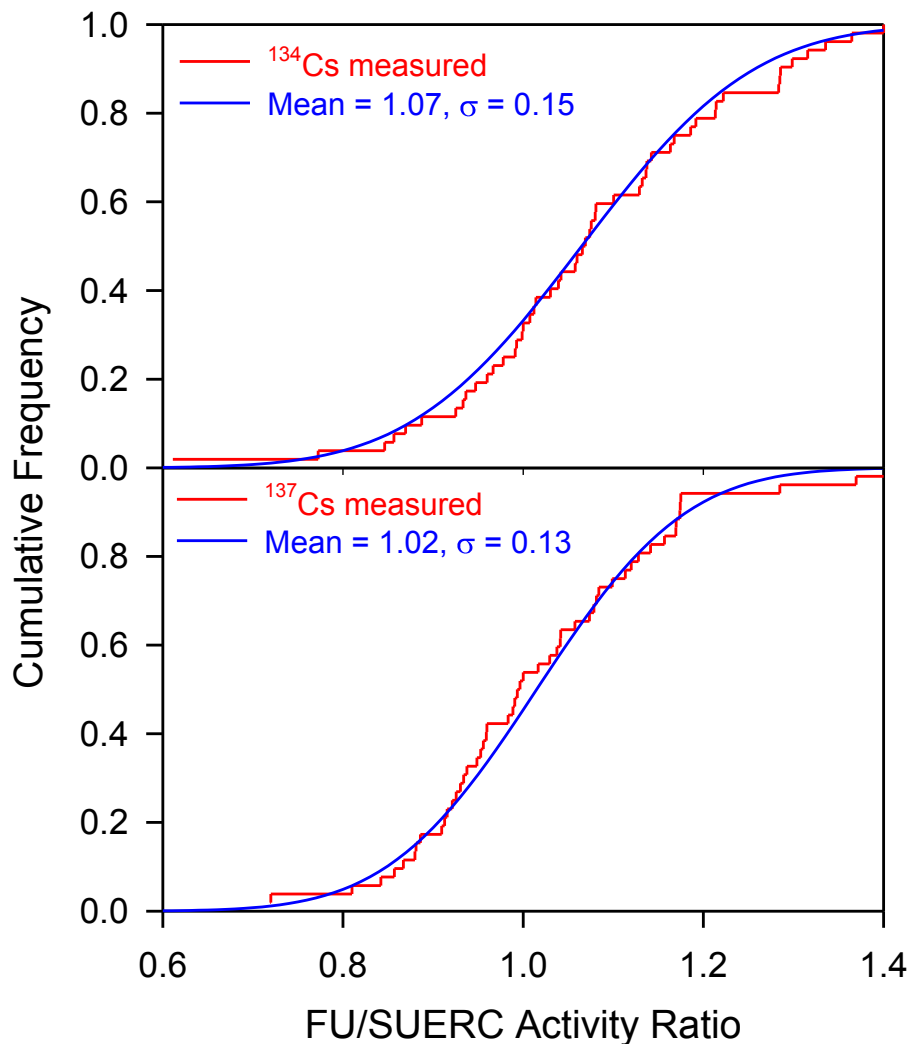


Figure 3.6: Cumulative distribution plots for the ratios of activity concentration determined at FU and SUERC. For ^{134}Cs (top) a normal distribution with a standard deviation of 0.15 and mean ratio of 1.07 is shown. For ^{137}Cs (bottom) a normal distributions with a standard deviation of 0.13 and a mean ratio of 1.02 is shown.

It is clear from the above that the comparison between two international laboratories, one in Japan the other in the U.K., has cross validated both data sets using independent internal standards and external reference materials. Given the good agreement between the laboratories with samples covering a wide activity concentration range, the mean value of each determination can be taken as the best estimate for the purpose of defining the calibration site.

Before turning to the depth distribution and summation to activity per unit area, it is useful to examine the ^{134}Cs to ^{137}Cs activity ratios for the samples. The full data set is given in the Technical Annex. Summary statistics from the activity ratios are given in Table 3.2 from which it can be seen that the majority of observations fall in the range from 0.922 to 0.988, decay corrected to March 2011. Note that the mean value of 0.952 ± 0.028 is slightly lower than the equal activity concentration assumption of the early calibration for US/Japanese AGS mapping during the emergency stage and the working calibrations for reconstructions of the source terms for atmospheric release (Katata *et.al.* 2012a,b, Terada *et.al.* 2012). It is, however, highly consistent with other published observations in the peer reviewed literature (eg: Table 3.3).

	$^{134}\text{Cs} : ^{137}\text{Cs}$ Activity Ratio	
	Measured (11 th July 2012)	Decay Corrected (15 th March 2011)
Mean	0.629	0.952
Std dev	0.018	0.028
10 th percentile	0.609	0.922
Median	0.627	0.948
90 th percentile	0.653	0.988

Table 3.2: Summary statistics for activity ratios determined from the soil samples collected from the Fukushima University calibration site (52 samples).

Reference	Location	$^{134}\text{Cs} : ^{137}\text{Cs}$ Activity Ratio
Tagami <i>et.al.</i> 2011	Chiba City (4 measurements)	0.887 ± 0.012
Ohno <i>et.al.</i> 2012	Koriyama (10 measurements)	0.994 ± 0.013
Kato <i>et.al.</i> 2012	Kawamata (5 measurements)	0.982 ± 0.011
Tazoe <i>et.al.</i> 2012	Various (7 measurements)	0.991 ± 0.020

Table 3.3: Mean activity ratios and standard deviations from a small selection of published data, decay corrected to 15th March 2011.

3.2.4 Depth profiles and activity per unit area for the calibration site

Activity released into the atmosphere is deposited on surfaces and migrates over time to greater depth. Depth profiles characterise the distribution of activity in the soil column, and vary with time since deposition, precipitation and soil characteristics. The depth profile is locally variable depending upon the precipitation, land use and soil characteristics at each site. The measured radiation field is dependent upon the depth profile, and detector calibrations should be made for a stated depth. The depth distribution is also an important factor in remediation, in particular in relation to the amount of soil that would need to be removed.

Gamma radiation is attenuated by matter, depending on its composition and density. Linear measured depth does not take these factors into account. A more useful quantity is the mass depth, which is the mass of material per unit area above the radiation source, and hence takes radiation attenuation into account. The mass depth for each subsample (β_i) in kg m^{-2} from a core can be simply obtained as the product of the linear depth and the bulk density, and is thus expressed in units of mass per unit area. Within each layer i , the activity concentration for each depth layer ($A_{m,i}$) in Bq kg^{-1} can be converted to activity per unit area ($A_{a,i}$) in Bq m^{-2} by multiplying by mass depth β_i .

The mass depth profiles for ^{134}Cs and ^{137}Cs for the Fukushima University calibration site cores are shown in Figure 3.7. Conventionally, mass depth profiles for undisturbed environments, such as the calibration site, have been parameterised using a single exponential function (eg: ICRU 1994, Walling & He 1999, Walling *et.al.* 2002, He & Walling 2003) characterised by a mean mass depth. Interestingly the data on Figure 3.7 from the upper 3 depths fall on a straight line on the log-linear scale, and are thus well described by an exponential distribution. They account for the majority of activity in the cores. However, the exponential profile underestimates the observed activities of the bottom sample sections from all core samples to a significant extent. This is reproduced by both laboratories, suggesting it is unlikely to be caused by the analytical method used. While the reasons for such excess activity at linear depths below 10cm and mass depths greater than $10\text{-}15\text{ g cm}^{-2}$ are not yet clear, and the possibility of transfer of activity during soil sampling and handling cannot be excluded, this would warrant further attention. If similar findings are observed elsewhere it may suggest the presence of more mobile components at depth than associated with the bulk of the activity in upper layers of soil. These could have implications for agronomic counter measures and for remediation activities. It is noted that Kato *et.al.* 2012 have reached similar conclusions.

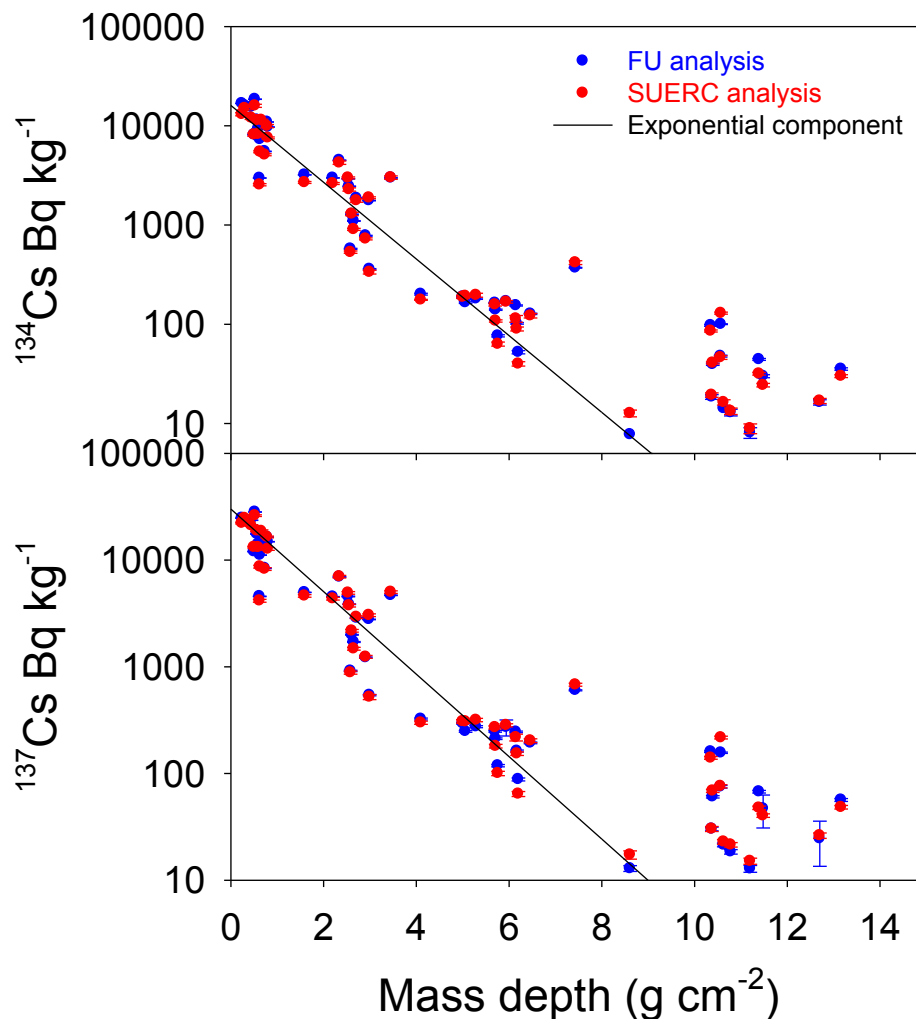


Figure 3.7: Depth profiles for ^{134}Cs and ^{137}Cs on the Fukushima University calibration site, showing activity concentrations (wet samples) from both laboratories and an exponential fit for a relaxation mass depth of 0.9 g cm^{-2} .

Mean mass depths for ^{134}Cs and ^{137}Cs for each core were then determined by the formula:

$$\bar{\beta} = \frac{\sum_i A_i \beta_i}{\sum_i A_i}$$

where A_i is the activity per unit mass of ^{134}Cs or ^{137}Cs .

Whereas for non-uniform distributions the activity concentrations $A_{m,i}$ are strongly dependent on the sampling depth and cannot be meaningfully summed or averaged, activity per unit area $A_{a,i}$ can. The total activity per unit area for each core, A_a , is thus the sum of the activities per unit area for each core section:

$$A_a = \sum_i A_{a,i} \rho_i d_i$$

where ρ_i is the wet density of each section, and d_i is the section thickness.

These are tabulated for each of the 13 cores on the calibration site below.

Core	Activity per unit area (kBq m^{-2})		Mean mass depth (g cm^{-2})	
	^{134}Cs	^{137}Cs	^{134}Cs	^{137}Cs
FU 0,0	142.6 ± 1.3	228.2 ± 1.8	0.50 ± 0.03	0.51 ± 0.03
FU 1,0	162.0 ± 1.7	256.1 ± 3.5	0.80 ± 0.06	0.80 ± 0.05
FU 1,1	201.3 ± 1.5	321.6 ± 3.3	1.36 ± 0.04	1.36 ± 0.12
FU 1,2	119.0 ± 0.9	184.6 ± 1.8	1.12 ± 0.03	1.13 ± 0.04
FU 1,3	97.6 ± 0.7	154.4 ± 1.5	1.59 ± 0.05	1.59 ± 0.06
FU 1,4	222.3 ± 2.2	359.3 ± 2.9	0.86 ± 0.04	0.86 ± 0.04
FU 1,5	122.0 ± 1.1	191.2 ± 2.3	0.76 ± 0.03	0.76 ± 0.04
FU 2,0	103.1 ± 0.9	163.0 ± 2.0	1.09 ± 0.05	1.10 ± 0.21
FU 2,1	192.5 ± 2.6	307.1 ± 2.3	0.94 ± 0.04	0.93 ± 0.03
FU 2,2	295.1 ± 3.6	470.9 ± 3.7	1.58 ± 0.07	1.59 ± 0.06
FU 2,3	205.8 ± 2.7	324.7 ± 2.9	1.22 ± 0.06	1.23 ± 0.05
FU 2,4	191.2 ± 2.4	302.2 ± 2.5	0.65 ± 0.03	0.66 ± 0.15
FU 2,5	226.2 ± 3.1	358.6 ± 2.5	0.72 ± 0.03	0.72 ± 0.03

Table 3.4: Activity per unit area and mean mass depth for each core from the Fukushima University calibration site, decay corrected to 11th July 2012.

These data can be combined to determine the reference values for the site taking account of weighting factors between the shells. Weighting factors are discussed by Tyler 1994, Tyler *et.al.* 1996. In this work the combined mean depth is $0.89 \pm 0.07 \text{ g cm}^{-2}$ ($8.9 \pm 0.7 \text{ kg m}^{-2}$), which is relatively shallow compared with the generic values given by ICRU 1994 (0-1 years 1.0 g cm^{-2} , 1-5 years 3.0 g cm^{-2}). For such a shallow distribution the weighting factors used were 15%, 45% and 40% for the central point, and the 2m and 8m shells respectively.

The dose rate on the calibration site was determined as described in Section 2. In addition to the calibration site the dose rate has been verified relative to fixed monitoring stations at Furudate in Fukushima Iizaka and on the University campus, with very good agreement between the SUERC instrument and the fixed monitor as can be seen in Figure 3.8.

The reference values for the calibration site are given in Table 3.5, with values from backpack measurements from July and November 2012. The backpack measurements conducted in July 2012 for ^{134}Cs and ^{137}Cs are within measurement uncertainties identical to the reference values, with the measured dose rate within 10%. In November 2012, under wetter environmental conditions, the measured activity concentrations and dose rate are suppressed.



Monitor reading: $0.674 \mu\text{Sv h}^{-1}$
 Area average: $0.68 \pm 0.02 \mu\text{Gy h}^{-1}$
 Next to monitor: $0.66 \pm 0.03 \mu\text{Gy h}^{-1}$

Monitor reading: $0.276 \mu\text{Sv h}^{-1}$
 Area average: $0.32 \pm 0.02 \mu\text{Gy h}^{-1}$
 Next to monitor: $0.24 \pm 0.01 \mu\text{Gy h}^{-1}$

Figure 3.8: Dose rate monitoring stations at Furudate (left) and Fukushima University with dose rates measured using the backpack system for the immediate areas (the playpark at Furudate and the lawn at the university) and next to the monitor.

	Reference values	Back pack data	
		July 2012	November 2012
^{137}Cs kBq m^{-2}	265 ± 20	254 ± 11	236 ± 6
^{134}Cs kBq m^{-2}	165 ± 20	169 ± 7	138 ± 2
$^{134}\text{Cs} : ^{137}\text{Cs}$	0.62 ± 0.09	0.66 ± 0.04	0.58 ± 0.03
$^{134}\text{Cs} : ^{137}\text{Cs}$ (15/3/11)	0.94 ± 0.14	1.01 ± 0.06	0.97 ± 0.05
Dose Rate $\mu\text{Gy h}^{-1}$	1.24 ± 0.13	1.15 ± 0.01	1.05 ± 0.01
Mean mass depth g cm^{-2}	0.9 ± 0.1		

Table 3.5: Reference values and observed values for ^{137}Cs and ^{134}Cs activity per unit area, activity ratio, dose rate and mean mass depth for the Fukushima University calibration site. Activity and dose rate data are presented for the sampling or measurement date (11/7/2012 or 03/11/2012), the activity ratio is also given for a reference date of 15/3/2011.

3.3 Additional Sites

A single calibration site represents a single environment with particular source distribution characteristics that may not be representative of other environments in the region. In addition, the site will change over time as the radionuclides are redistributed by natural processes, and potentially by human activity. Therefore, it is the practice at SUERC to develop several calibration sites representing different environmental conditions. Multiple calibration sites also provide the opportunity to cross compare these sites on a routine basis to account for potential environmental changes at these sites and provide security against significant environmental change at a single calibration site.

On the 12th July 2012, a location within the Fukushima Prefecture Fruit Tree Research Institute was identified as being suitable for a small calibration site. The open area is triangular, bounded by the boundary hedge of the institute on one side and orchard plots on the other two sides, and is smaller than the open area at Fukushima University. Samples, with contemporaneous backpack measurements, were collected from this site on the 3rd November 2012. The recommended values from this site will be reported separately, following the conclusion of the laboratory analysis. Photographs of the sampling and associated radiometric surveys for this site are shown in Figure 3.9. Like the site at Fukushima University, this is too small for calibration of airborne measurements. However, vehicular access may be more feasible.

The sites developed in this work at Fukushima University and the Fruit Tree Research Institute are small, relatively enclosed sites. While suitable for verification of the performance of ground based instruments they are not ideal for use with airborne systems, especially systems deployed on manned aircraft.

Measurements have also been conducted on calibration sites in south west Scotland developed for an international intercomparison exercise for airborne and ground based systems (Sanderson *et.al.* 2003, 2004). These sites had been extensively sampled in November 2001, with analyses conducted by ten laboratories with IAEA reference materials and common samples from the sites used to compare laboratory performance. In September 2012 a small number of additional samples were collected to assess any environmental change since 2001, and measurements with an SUERC system identical to that used in Japan conducted. These measurements are described in detail in the Technical Annex. After accounting for the differences in the mean mass depth on the calibration sites compared to the calibration assumption for the instrument, ¹³⁷Cs activity per unit area measurements on the sites agree to within 10% on the two sites with Chernobyl and Sellafield derived activity. On the third site with very low ¹³⁷Cs activity deposition from weapons testing fallout, agreement between the instrumental measurements and soil samples was poorer, but still within 3 σ .



Scientists from Fukushima University and the Fruit Tree Research Institute arriving to sample the calibration site



Laying out the calibration pattern and marking sampling points



Cutting a core into depth sections



Radiometric survey of the area around the calibration site, using two systems operated by Japanese and UK scientists



Radiometric survey within orchards



Preparation of fruit samples

Figure 3.9: Preparation of the calibration site at Fukushima Prefecture Fruit Tree Research centre in November 2012. A hexagonal sampling plan surrounding a central point was adopted with core samples taken at 2 metre and 8 meter radii, and split vertically. The site and orchard were mapped, and fruit samples collected.

4. Radiometrics and Recovery From Nuclear Accidents

During the course of 2012 a series of measurements were conducted using the SUERC portable gamma spectrometry system, as a backpack and from vehicles, in areas as illustrated in Figures 1.3 and 1.4. In addition to providing radiometric data of deposition and dose rates specific to the areas surveyed, of direct relevance to the communities using those areas, these measurements also illustrate some of the roles for radiometrics in nuclear accident response, especially during the recovery phases of the response.

Data from the vehicular surveys are presented in section 4.1, including data from small area mapping and measurement conducted with the backpack system during these vehicular surveys. Section 4.2 presents data collected using the backpack system in urbanised areas where members of the public spend time, specifically the campus of Fukushima University and part of Fukushima city. Data from agricultural research institutes and farms are presented in section 4.3. Section 4.4 presents data relating to isotope ratios that might show variations in the deposition resulting from different phases of release from the reactors at Fukushima Daiichi.

4.1 Vehicular Surveys

The use of radiometric systems in vehicles allows measurements to be conducted over regional scale areas relatively quickly. The areas accessible to most vehicles are limited to roads, car parks and similar surfaces. Measurements off-road are possible with a suitable vehicle. SUERC has conducted vehicular surveys using larger volume NaI(Tl) detector systems and complementary Ge detectors (Sanderson *et.al.* 1993, 1997, 1998), and carborne systems using 4 or 8 litre NaI(Tl) detectors are routinely used in other parts of Europe (Aage *et.al.* 2006, 2009a,b, Hjerpe & Samuelsson 2006). The fields of view of carborne systems, typically 5-10m, include significant areas of the road surface which is not expected to be representative of local deposition due to the effects of rain self-remediating hard road surfaces. The proportion of road surface contributing to the measurements depends upon several factors including the road width, the position of the detector relative to the edge of the road and the surrounding topography. Despite the effect of the road surface, it is recognised that carborne measurements are able to accurately measure regional scale deposition patterns and can play a valuable part in nuclear emergency response, allowing rapid measurements in areas where airborne data may not be available.

The work in Japan using the SUERC Portable Gamma Spectrometry system was conducted to assess the ability of relatively small detectors to measure regional scale deposition patterns. Carborne measurements were conducted in March 2012 in Fukushima city and on a circuit through the main deposition plume to the north west of Fukushima Daiichi, into the exclusion zone and south to Iwaki. Further carborne measurements were conducted on trips into the evacuation zone in July and November 2012.

The calibration includes an assessment of the shielding factor for the vehicle. However, it uses a stripping matrix calculated for a detector without the additional shielding, and associated scattered energy components, of the vehicle. The vehicle has not been taken onto a calibration site to independently verify the activity concentrations determined from measurements within the vehicle.

4.1.1 Fukushima City, March 2012

Some exploratory measurements were taken in Fukushima on the 5th March 2012, with the detector system deployed in a vehicle collecting spectra with 10s integration time. Data were recorded from a start point at Mount Azuma, driving through the city to a private residence. At both ends of the trip measurements were taken in backpack mode. There was snow on the ground during the survey, with deep drifts on Mount Azuma in particular. Snow attenuates radiation from the ground surface, reducing the apparent concentrations recorded by instruments above the snow. The attenuation of radiation by snow has been used since the 1960s to allow snow cover, and melt water run-off forecasting, using radiometric techniques (Dahl & Odegaard 1970, Abal'yan *et.al.* 1971, Bissell & Peck 1973, Nikiforov *et.al.* 1980, Peck *et.al.* 1980, Kuittinen & Vironmäki 1980, Saito 1991), most commonly by repeat surveys of the area in summer and winter conditions. In the University of Fukushima the campus dose rate meter was showing readings which were some 40% lower than they had been prior to snowfall.

Table 4.1 gives summary statistics for this survey.

The data have been plotted as transects along the route in Figure 4.2. This shows the variations of activity and dose rate along the survey route, with low activity registered on Mount Azuma due to considerable quantities of snow suppressing the radiation and within a house in Fukushima. In Fukushima City the data show a high degree of variability reflecting the complexities of urban environments.



Figure 4.1: Professor Yamaguchi with the SUERC backpack spectrometer at Mount Azuma, and Fukushima in March 2012

N.		Mean	Std. Dev.	10 th %tile	Median	90 th %tile
1608	¹³⁷ Cs kBq m ⁻²	56.4	48.3	31.6	40.1	116.8
	¹³⁴ Cs kBq m ⁻²	42.5	35.4	25.9	30.5	86.9
	Dose rate µGy h ⁻¹	0.275	0.197	0.190	0.205	0.541

Table 4.1: Summary statistics for the exploratory measurements in Fukushima City, 5th March 2012.

The dose rate apportionment for this survey is given in Table 4.2 and Figure 4.3. The snow cover, which was much deeper on Mount Azuma than in the city, significantly attenuates the radiation from both natural and anthropogenic sources with the higher energy natural gamma rays used in the SUERC analysis attenuated less strongly. The dose rate apportionments for Mount Azuma and Fukushima City are similar, with the small differences reflecting differences in attenuation by the snow and potential differences in the natural activity concentrations and deposition patterns. Within the private residence, overall radiation dose is significantly reduced compared to outside. However, the anthropogenic components still dominate the dose rate received.

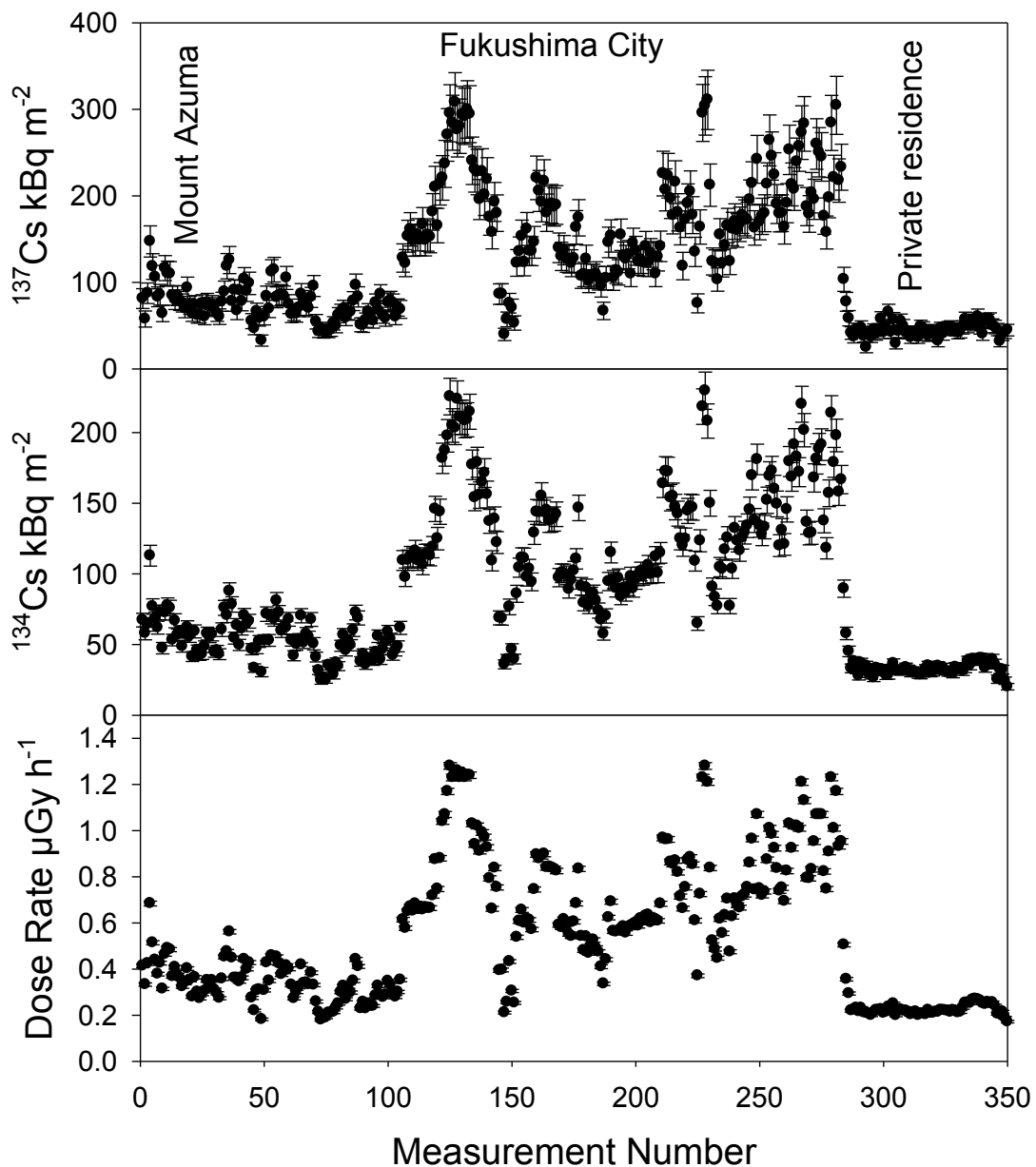


Figure 4.2: Transect of vehicular survey through Fukushima City, 5th March 2012.

	Mount Azuma	Fukushima City	Private Residence
Dose Rate $\mu\text{Gy h}^{-1}$	0.343 ± 0.009	0.753 ± 0.018	0.217 ± 0.002
$^{238}\text{U} + ^{235}\text{U}$ series	$1.06 \pm 0.20 \%$	$0.92 \pm 0.08 \%$	$2.86 \pm 0.40 \%$
^{232}Th series	$1.21 \pm 0.18 \%$	$0.85 \pm 0.08 \%$	$3.70 \pm 0.39 \%$
$^{40}\text{K} + ^{87}\text{Rb}$	$3.38 \pm 0.14 \%$	$2.24 \pm 0.07 \%$	$5.67 \pm 0.22 \%$
^{137}Cs	$29.50 \pm 0.79 \%$	$29.55 \pm 0.77 \%$	$27.69 \pm 0.55 \%$
^{134}Cs	$64.85 \pm 1.79 \%$	$66.45 \pm 1.69 \%$	$60.08 \pm 0.89 \%$
Residual	$6.14 \pm 3.68 \%$	$2.17 \pm 3.26 \%$	$8.35 \pm 2.73 \%$

Table 4.2: Dose rate apportionment for the exploratory vehicular survey in Fukushima, 5th March 2012.

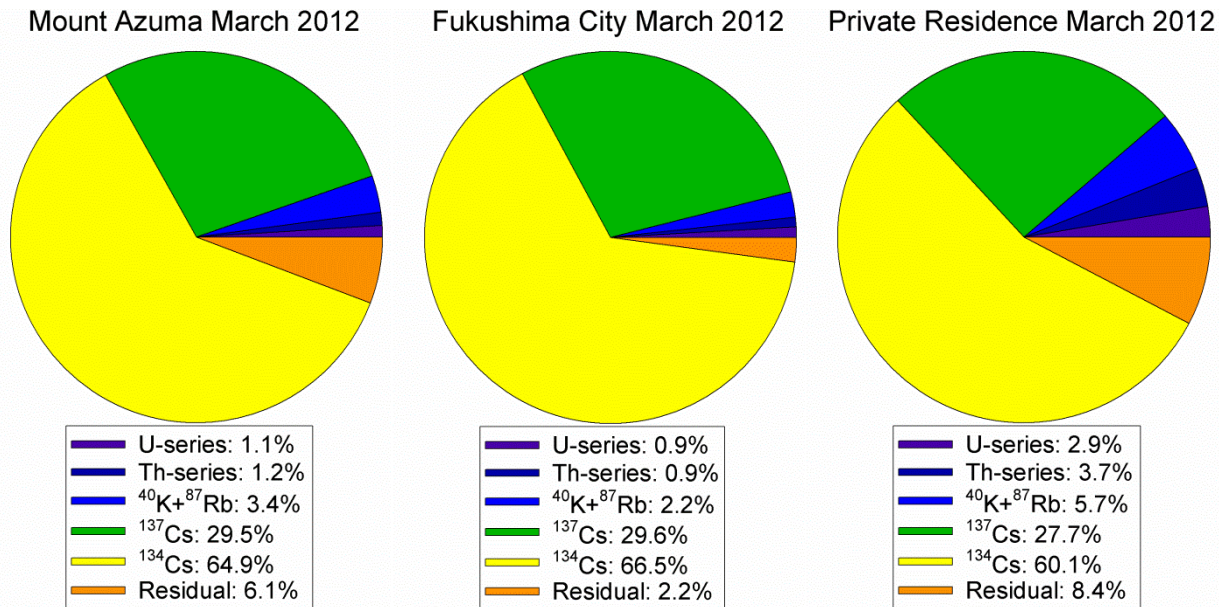


Figure 4.3: Dose rate apportionment for the exploratory vehicular survey in Fukushima, 5th March 2012.

4.1.2 Exclusion Zone, March 2012

The system was deployed within a vehicle on the 7th March 2012, collecting data with 5s integration time. On higher ground in particular, there was a considerable covering of snow to the sides of the roads that would reduce the apparent activity concentrations and dose rates the system would register compared to comparable measurements without the snow cover. The vehicle was then driven into the exclusion zone, to within 1km of the Fukushima Daiichi plant, to the south towards Iwaki and then back to Fukushima. The survey covered a total distance of approximately 200km. During this trip, the backpack was removed from the vehicle to map small areas at the Ōkuma Nuclear Centre and a day care centre at Ōkuma, and to collect spot measurements at monitoring stations and other locations. Table 4.3 gives the summary statistics for this survey, with the radiocaesium concentrations and dose rates determined from the vehicular measurements in Figures 4.5 and 4.6.

The measurements from the car show the same general pattern as that given by early airborne data (Figure 1.1). There are very high levels of deposition in the immediate vicinity of the plant, with highest levels observed in this survey around Ōkuma to the south. The main plume of deposition to the north west is crossed in Date and Iitate Districts with lower deposition nearer the coast. South of the NPP and towards Iwaki, there is elevated deposition

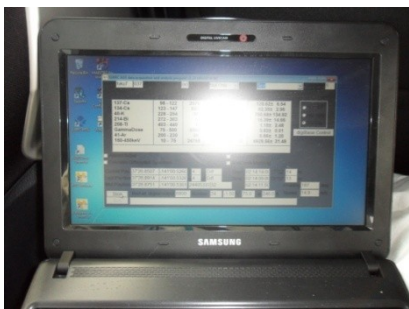
that is evident in the AGS data, although less pronounced on the colour scale used in Figure 1.1. The relatively high deposition measured here may relate to the relative lack of snow cover at these lower elevations nearer the coast. The airborne data also pick up the elevated deposition north of Koriyama that can be seen in the AGS map.



Police officers from Ōkuma who were escorts and guides into the exclusion zone



Professor Kawatzu, who drove the car through the evacuation and exclusion zones



Real-time display from the SUERC spectrometry system



Evacuated buildings and tsunami damage observed from the vehicular survey



Tsunami damage observed from the vehicular survey

Figure 4.4: Ōkuma Police escort for journey through the evacuation zone 7th March 2012, Professor Kawatzu driving the car, preparing for entry to the exclusion zone.

N.		Mean	Std. Dev.	10 th %tile	Median	90 th %tile
3974	¹³⁷ Cs kBq m ⁻²	708.1	1341.5	75.3	123.7	2798.6
	¹³⁴ Cs kBq m ⁻²	742.5	1956.0	56.5	87.2	2678.6
	Dose rate μGy h ⁻¹	4.168	10.816	0.346	0.529	15.000

Table 4.3: Summary statistics for the vehicular measurements on a drive from Fukushima into the exclusion zone then to Iwaki and back to Fukushima, 7th March 2012.

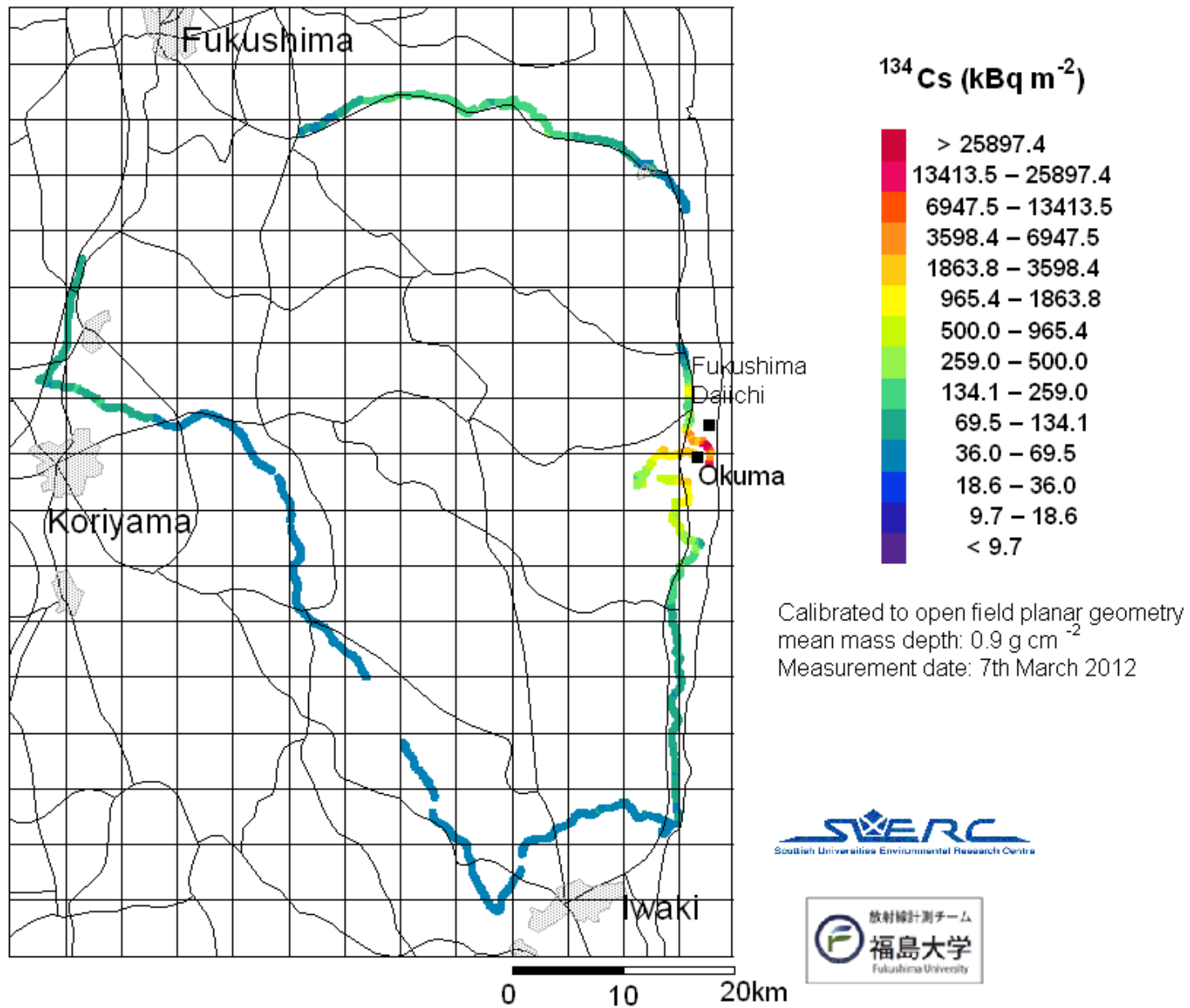


Figure 4.5: ^{134}Cs activity per unit area determined from vehicular measurements, March 7th 2012.

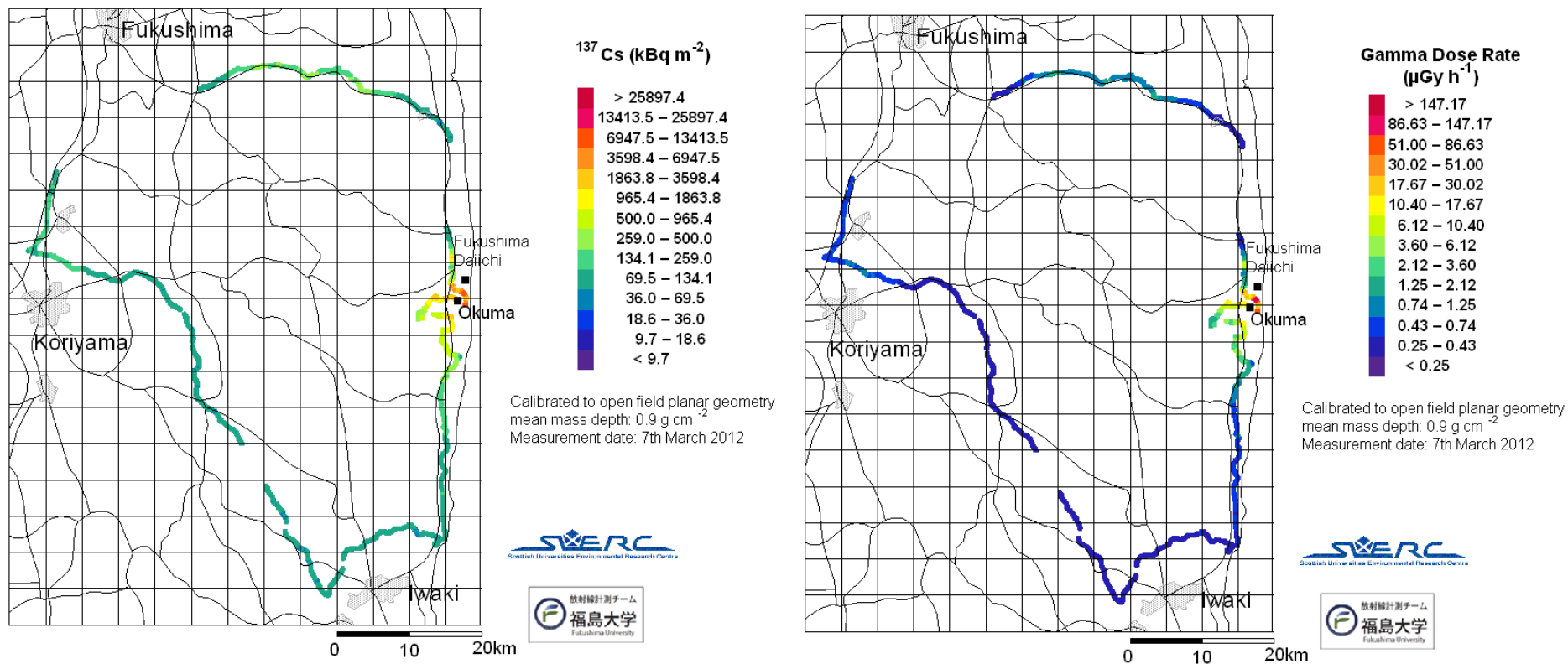


Figure 4.6: ^{137}Cs activity per unit area and dose rate determined from vehicular measurements, March 7th 2012

4.1.3 Backpack Measurements Within the Exclusion Zone, March 2012

The gamma spectrometry system was removed from the vehicle to collect spot measurements and short surveys for four locations within the exclusion zone during the vehicular survey. These locations are given in Table 4.4, with mean activity concentrations and dose rates recorded at each location.

Ten measurements, with a total of 50s integration time, were collected at a single location near the gates to Fukushima Daiichi, approximately 1km from Reactor 1. Figure 4.8 shows this location, with the average spectrum recorded there in Figure 4.9. The spectrum shows considerable distortion due to random summing of gamma rays, although the principle ^{134}Cs and ^{137}Cs peaks are still evident. A further twenty two measurements were collected from a location near Higashidaira, 2km south of the Fukushima Daiichi nuclear power plant.

A survey was conducted around the outside of the Ōkuma nuclear centre, with additional measurements recorded inside the building. Figure 4.11 shows the ^{134}Cs and ^{137}Cs activity per unit area and dose rate for this survey, on an image from Google Earth. The average spectra recorded inside and outside the building are shown in Figure 4.12. The spectrum recorded outside the building shows some evidence of random summing and spectral distortion due to the high count rate. The dose rate and deposition levels inside the building are an order of magnitude lower, and the spectral distortion is not present.

A short survey, collecting 313 spectra with 2s integration time, was conducted around a day care centre at Ōkuma. Figure 4.14 shows the ^{134}Cs and ^{137}Cs activity per unit area and dose rate for this survey, on an image from Google Earth. The average spectrum is shown in Figure 4.15, this shows distortion due to random summing. It should be noted that the spectral distortions will affect the accuracy of the activity per unit area shown in Figure 4.14.

A district monitoring site at Minamidaira, 7.3km south west of Fukushima Daiichi, was also visited. Figure 4.17 shows the ^{134}Cs and ^{137}Cs activity per unit area and dose rate measured on a short survey along track ways between fields. The average spectrum for these measurements is shown in Figure 4.18, which shows that even at this location deposition levels are sufficient to cause some spectral distortion in the 3x3" NaI(Tl) detector used.

Location	N	^{137}Cs kBq m ⁻² †	^{134}Cs kBq m ⁻² †	Dose rate μGy h ⁻¹
Fukushima Daiichi gates‡	14	1746 ± 108	1731 ± 115	12.6 ± 0.8
Higashidaira‡	23	6098 ± 648	11207 ± 1658	76 ± 11
Ōkuma nuclear centre (outside)	40	856 ± 228	1043 ± 266	6.4 ± 1.6
Ōkuma nuclear centre (inside)	147	121 ± 13	92 ± 8	0.65 ± 0.05
Day care centre, Ōkuma‡	313	2611 ± 645	2774 ± 849	17.9 ± 5.2
Monitoring point	153	877 ± 170	790 ± 160	5.1 ± 1.0

† Calibrated assuming open field, planar distribution with mean mass depth of 0.9 g cm⁻²

‡ Spectra show significant distortion that will affect the accuracy of derived activity concentrations and dose rate

Table 4.4: Mean and standard deviation for radiocaesium activity per unit area and dose rate for the four sets of backpack data recorded in the exclusion zone, 7th March 2012.



Near the main gate to Fukushima Daiichi



Dose rate measurement on the ground, $147 \mu\text{Sv h}^{-1}$.



Overlooking the nuclear power plant



Figure 4.7: Photographs in the immediate vicinity of Fukushima Daiichi Nuclear Power Station, 7th March 2012.



Figure 4.8: Location of measurements (bottom left) near the gate to Fukushima Daiichi, showing the damaged reactors 1 and 2 (far right).

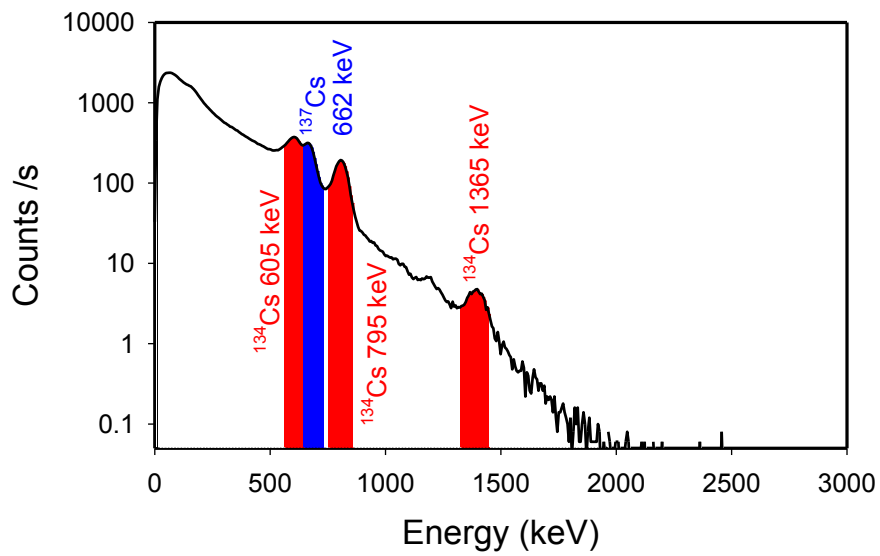


Figure 4.9: Average spectrum recorded near the gate to Fukushima Daiichi, 7th March 2012.



Figure 4.10: Data collection at the Ōkuma Nuclear Centre, 7th March 2012.

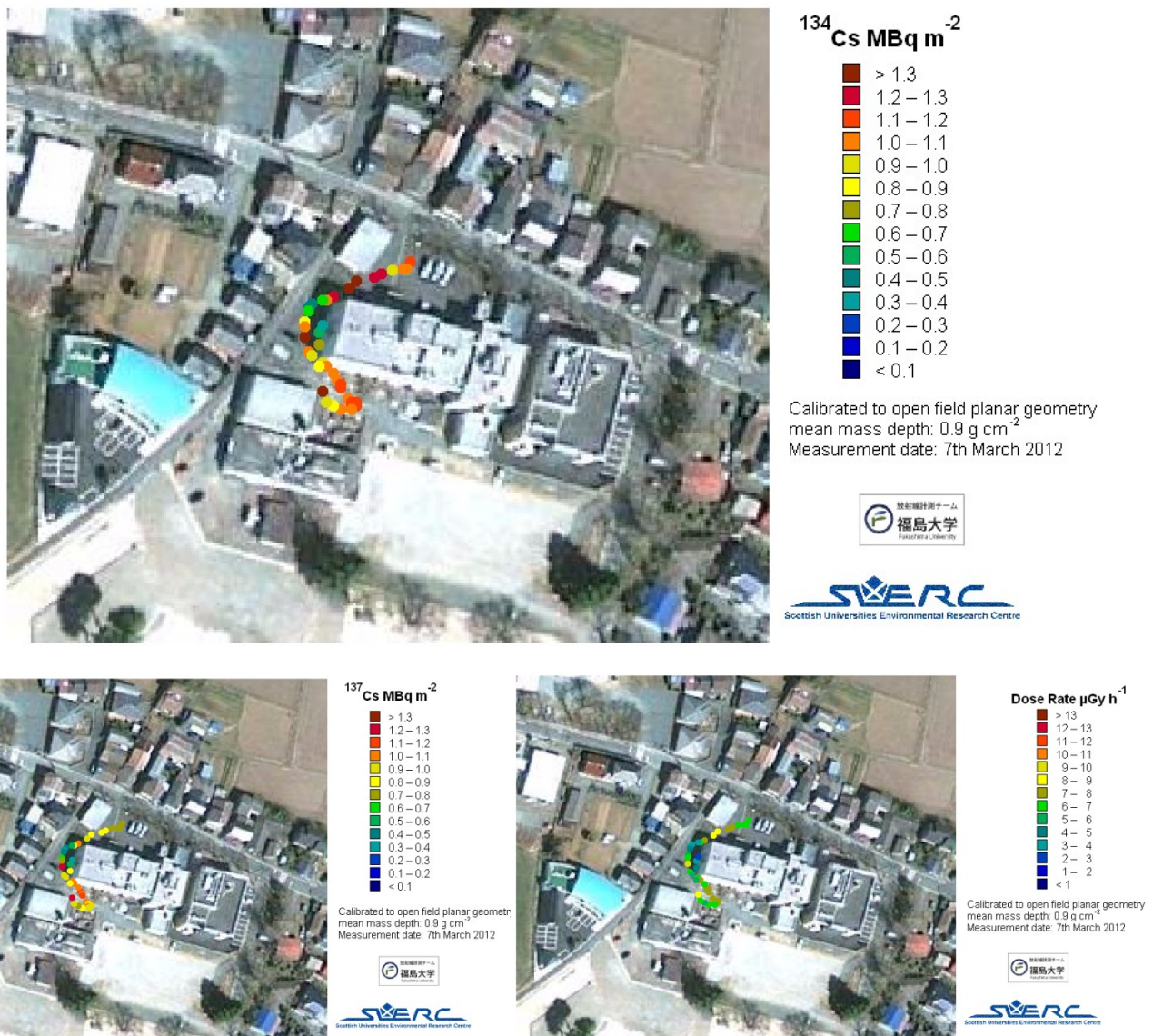


Figure 4.11: ^{134}Cs , ^{137}Cs activity per unit area and dose rate around the Ōkuma Nuclear Centre, 7th March 2012.

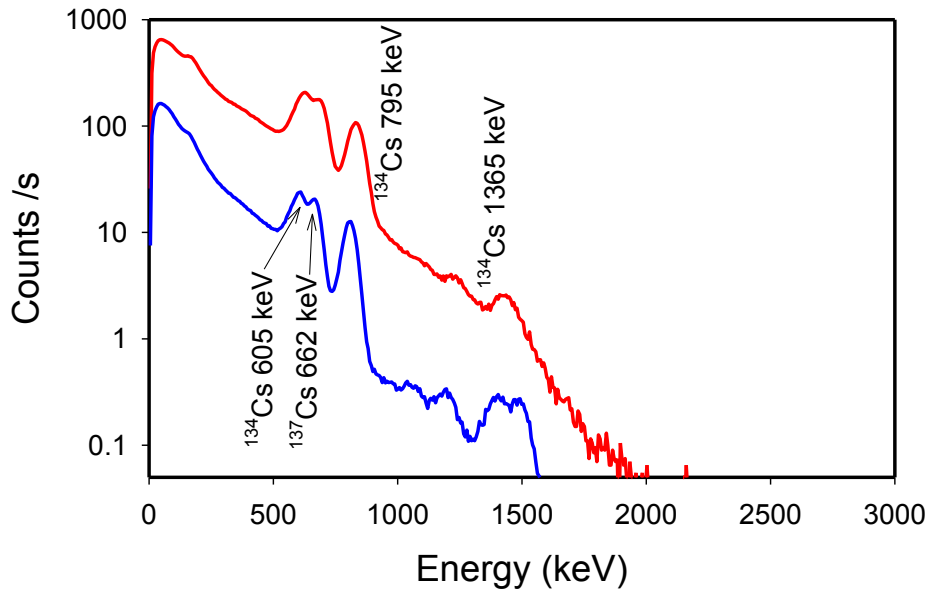


Figure 4.12: Average spectra recorded outside (red) and inside (blue) the Ōkuma Nuclear Centre, 7th March 2012.



Earthquake damage



Discussion of radiometric data



Discussion of data and explanation of the SUERC system



Figure 4.13: Measurements at the day care centre, Ōkuma, 7th March 2012



$^{134}\text{Cs MBq m}^{-2}$

- > 3.4
- 3.2 – 3.4
- 3.0 – 3.2
- 2.8 – 3.0
- 2.6 – 2.8
- 2.4 – 2.6
- 2.2 – 2.4
- 2.0 – 2.2
- 1.8 – 2.0
- 1.6 – 1.8
- 1.4 – 1.6
- 1.2 – 1.4
- 1.0 – 1.2
- < 1.0

Calibrated to open field planar geometry
 mean mass depth: 0.9 g cm^{-2}
 Measurement date: 7th March 2012



$^{137}\text{Cs MBq m}^{-2}$

- > 3.4
- 3.2 – 3.4
- 3.0 – 3.2
- 2.8 – 3.0
- 2.6 – 2.8
- 2.4 – 2.6
- 2.2 – 2.4
- 2.0 – 2.2
- 1.8 – 2.0
- 1.6 – 1.8
- 1.4 – 1.6
- 1.2 – 1.4
- 1.0 – 1.2
- < 1.0

Calibrated to open field planar geometry
 mean mass depth: 0.9 g cm^{-2}
 Measurement date: 7th March 2012



$\text{Dose Rate } \mu\text{Gy h}^{-1}$

- > 26
- 24 – 26
- 22 – 24
- 20 – 22
- 18 – 20
- 16 – 18
- 14 – 16
- 12 – 14
- 10 – 12
- 8 – 10
- 6 – 8
- 4 – 6
- 2 – 4
- < 2

Calibrated to open field planar geometry
 mean mass depth: 0.9 g cm^{-2}
 Measurement date: 7th March 2012



Figure 4.14: ^{134}Cs , ^{137}Cs activity per unit area and dose rate around the day care centre, Ōkuma, 7th March 2012. Spectral distortion will reduce the accuracy of these values.

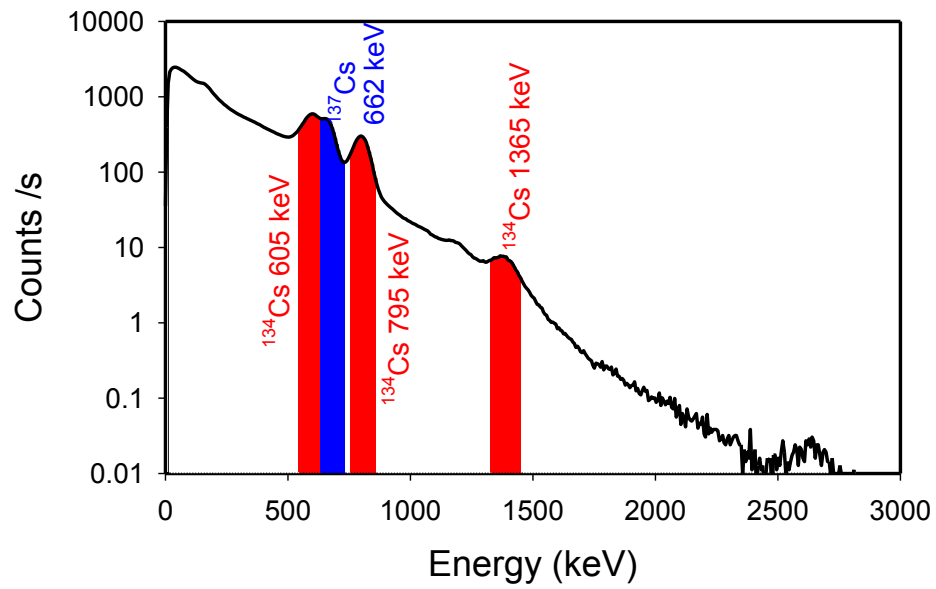


Figure 4.15: Average spectrum recorded at the day care centre, Ōkuma, 7th March 2012.



Figure 4.16: Measurements at the district monitoring point visited, 7th March 2012.

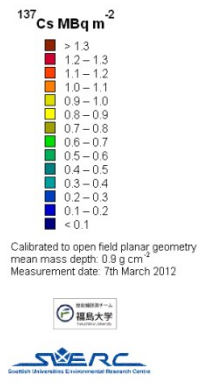


Figure 4.17: ^{134}Cs , ^{137}Cs activity per unit area and dose rate around a monitoring point, 7th March 2012.

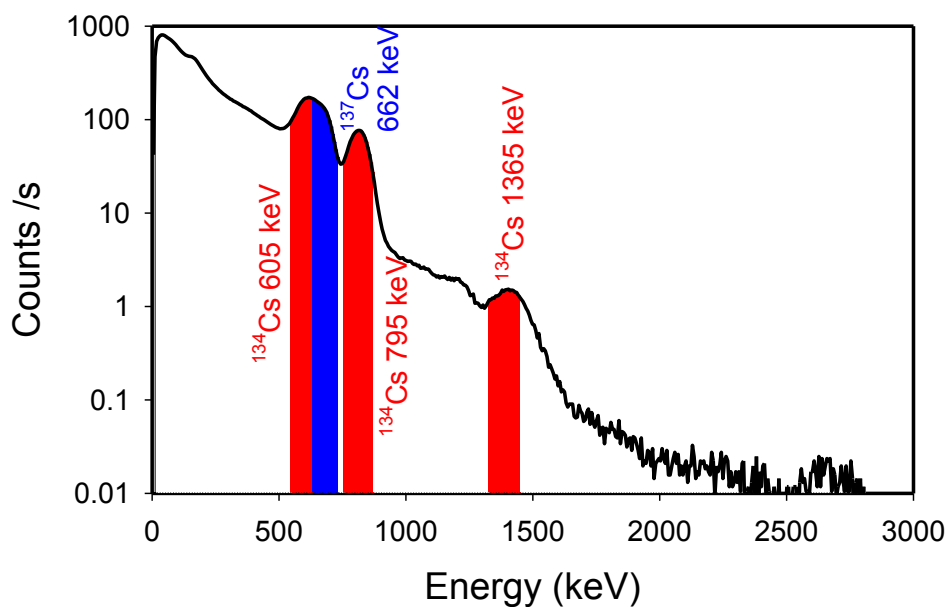


Figure 4.18: Average spectrum recorded at the district monitoring point visited, 7th March 2012.

4.1.4 Carborne surveys in July and November 2012

Data were also collected with the system deployed in a vehicle during the subsequent visits to Fukushima, between the 11th and 13th July and the 3rd November, with some backpack measurements included. The July data include measurements within areas of tsunami damage at Minami Soma and Soma. The November data were collected on a short drive travelling to fruit cultivation areas near Date. Summary statistics for these surveys are given in Table 4.5. The ¹³⁴Cs and ¹³⁷Cs activity per unit area and dose rates for the July vehicular surveys are shown in Figures 4.21 and 4.22.

Again, the July 2012 carborne data reproduce the general pattern of deposition produced from airborne systems (Figure 1.1). Low levels of deposition (often <10 kBq m⁻² ¹³⁴Cs) are observed along the coastal areas between Soma and Minamisoma. The main north westerly deposition plume is crossed in Date and Iitate Districts, with the highest deposition measured in this data set (>500 kBq m⁻² ¹³⁴Cs) near Shimotsushima which again corresponds to the airborne pattern. The northern leg between Soma and Fukushima, crossing into Miyagi Prefecture, records much lower deposition levels compared to the road 10-15km south of here, corresponding to the northern reach of the main deposition plume seen in Figure 1.1 with much lower deposition levels in that part of Miyagi Prefecture.

Backpack data were collected with inaccurate GPS locations at Kawauchi, in the vicinity of the Kawauchi Village Office, some of the fallow rice paddies across the river from the village office, and near the hotel, and also at a small pond approximately 3km south east of the village. Summary statistics for these data are given in Table 4.6.

Date and number of measurements		Mean	Std. Dev.	10 th %tile	Median	90 th %tile
July 2012 5553	¹³⁷ Cs kBq m ⁻²	161.8	196.0	46.4	97.4	336.0
	¹³⁴ Cs kBq m ⁻²	107.4	135.4	31.1	63.3	218.9
	Dose rate μGy h ⁻¹	0.666	0.801	0.211	0.409	1.330
Nov 2012 130	¹³⁷ Cs kBq m ⁻²	125.4	50.0	73.7	108.7	193.9
	¹³⁴ Cs kBq m ⁻²	73.3	29.6	43.4	59.2	116.7
	Dose rate μGy h ⁻¹	0.454	0.198	0.275	0.376	0.799

Table 4.5: Summary statistics for the vehicular measurements in the evacuation zone, 11-13th July and 3rd November 2012.

Date and number of measurements		Mean	Std. Dev.	10 th %tile	Median	90 th %tile
Kawauchi Village 897	¹³⁷ Cs kBq m ⁻²	30.5	14.8	11.8	29.3	50.6
	¹³⁴ Cs kBq m ⁻²	14.6	7.1	6.6	14.0	23.5
	Dose rate μGy h ⁻¹	0.163	0.059	0.085	0.159	0.237
Pond 242	¹³⁷ Cs kBq m ⁻²	130.8	24.7	94.7	130.8	163.5
	¹³⁴ Cs kBq m ⁻²	62.0	11.6	45.3	62.4	76.7
	Dose rate μGy h ⁻¹	0.571	0.098	0.432	0.569	0.699

Table 4.6: Summary statistics for backpack measurements at Kawauchi village and nearby pond, 11th July 2012.



Disused bus stop at Kawauchi Mura



Overgrown train line at Minasoma



Earthquake damage in Minamisoma



Tsunami damage at Soma



Figure 4.19: Observations of the effect of earthquake, tsunami and abandonment in the evacuation zone, 11th-13th July 2012.



Figure 4.20: Photographs from the November 2012 vehicular survey.

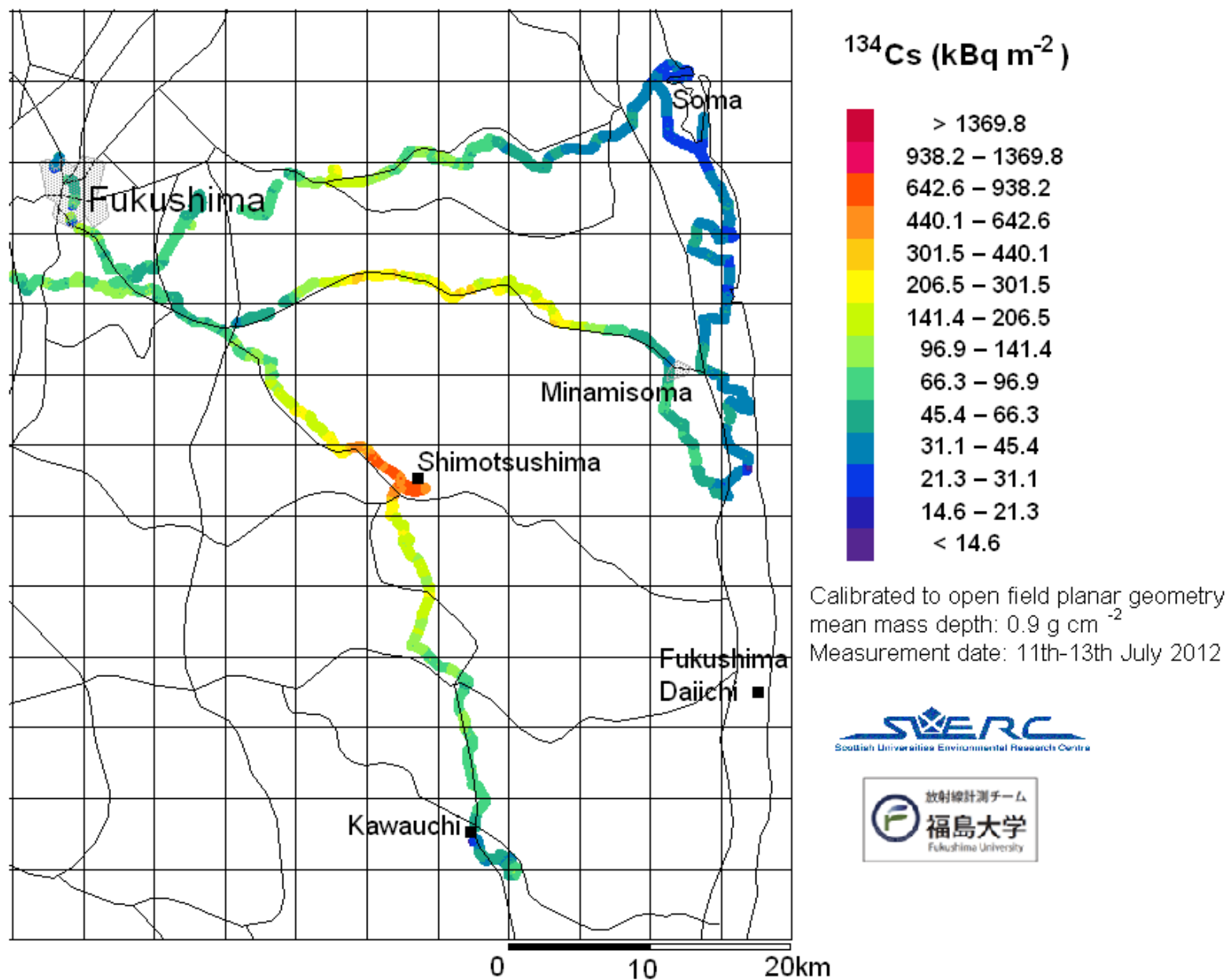


Figure 4.21: ^{134}Cs activity per unit area for vehicular surveys conducted 11th-13th July 2012.

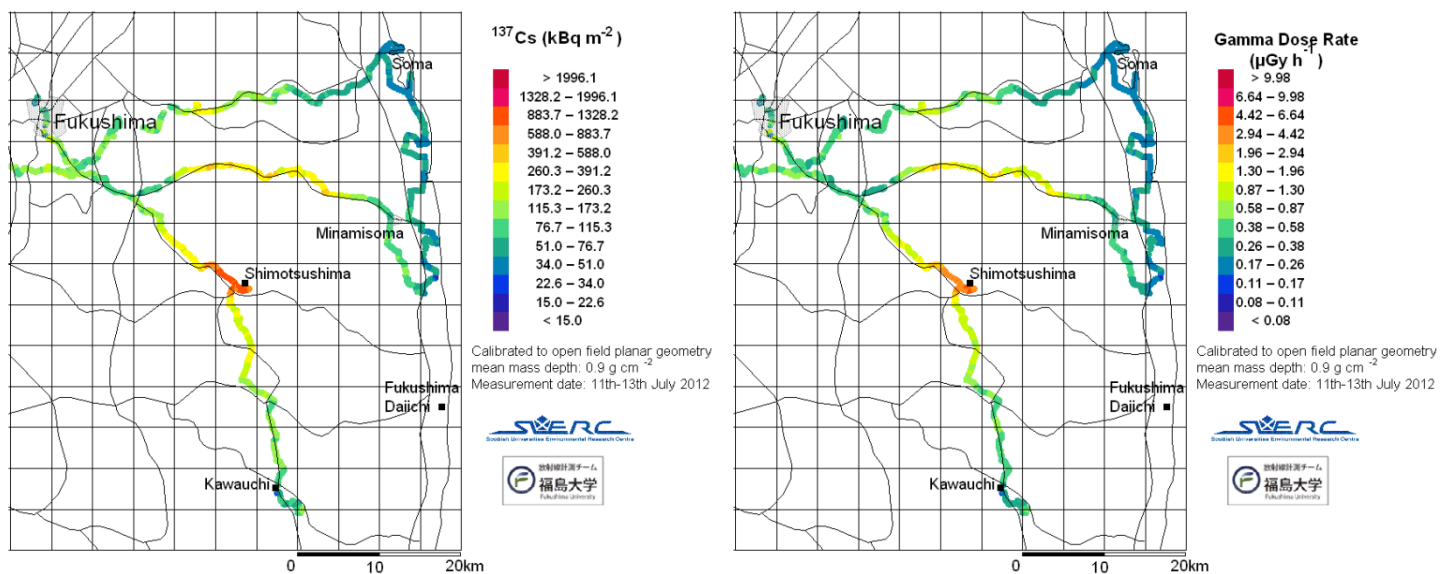


Figure 4.22: ^{137}Cs activity per unit area and dose rates for vehicular surveys conducted 11th-13th July 2012.

4.1.5 Discussion of Vehicular Survey Results

The SUERC Portable Gamma Spectrometry system has been successfully used to conduct surveys that qualitatively reproduce the general regional scale deposition patterns recorded using airborne systems, despite the vehicular field of view being dominated by the road surfaces. Quantitative comparisons between the airborne data and the vehicular survey data presented here could be conducted using spatial matching methods similar to those used for the ECCOMAGS Exercise (Sanderson *et.al.* 2003, 2004) and other ground to air comparisons, but would require access to the airborne data. This has not been done at present.

This work has demonstrated that small gamma spectrometry systems that can be rapidly deployed into any available vehicle can be used for regional scale deposition mapping, with a good response over a wide range of deposition activity concentrations, from 10 to 10000 kBq m^{-2} ^{137}Cs , with some spectral distortion at higher deposition levels.

The surveys have also demonstrated the utility of using a system that can also be used in a backpack configuration for such work. The system can be easily removed from the vehicle for detailed surveys, either at locations where detailed data is known to be required or to investigate features observed during the vehicular survey.

4.2 Fukushima University Campus and Fukushima Iizaka

Radiometric systems can be used to produce detailed maps of the distribution of radioactivity over small areas. In urbanised areas backpack systems provide the means of producing such detailed surveys, allowing data collection to be conducted in locations where people spend their time. Such detailed mapping can be used to identify small locations with locally high activity concentrations, which if in areas of high use by members of the public may be considered for priority in remediation programmes. By conducting such surveys after remediation, the effectiveness of the remediation in reducing dose to members of the public can be evaluated. During the course of 2012, the SUERC system was used to collect data from two urbanised areas, the campus of Fukushima University and part of Fukushima City.

Data were collected from the Fukushima University campus on four occasions. An exploratory circuit of the sports fields in March 2012, a short investigation to the west of the campus in June 2012, an extensive survey of the majority of the area in July 2012 and a further circuit of the sports field and calibration site in November 2012. The backpack system was also demonstrated during the International Symposium on Remediation of Site Contamination Caused by the Fukushima Accident, organised by the Society for Remediation of Radioactive Contamination in the Environment, held in Paruse Iizaka, Fukushima City in May 2012. Summary statistics for these surveys are given in Table 4.7.

Date and number of measurements		Mean	Std. Dev.	10 th %tile	Median	90 th %tile
Fukushima University Campus						
March 2012 600	¹³⁷ Cs kBq m ⁻²	61.2	30.1	30.2	55.4	99.5
	¹³⁴ Cs kBq m ⁻²	51.7	26.3	25.1	46.8	87.4
	Dose rate µGy h ⁻¹	0.380	0.177	0.198	0.354	0.615
June 2012 171	¹³⁷ Cs kBq m ⁻²	101.8	37.7	54.0	97.3	149.2
	¹³⁴ Cs kBq m ⁻²	66.3	25.5	36.8	63.8	95.9
	Dose rate µGy h ⁻¹	0.483	0.169	0.278	0.465	0.696
July 2012 4988	¹³⁷ Cs kBq m ⁻²	103.1	70.9	16.6	95.2	200.2
	¹³⁴ Cs kBq m ⁻²	68.1	47.5	10.3	62.6	132.1
	Dose rate µGy h ⁻¹	0.496	0.323	0.105	0.461	0.918
Nov 2012 1020	¹³⁷ Cs kBq m ⁻²	106.0	60.3	41.3	87.0	199.8
	¹³⁴ Cs kBq m ⁻²	61.7	38.9	17.1	51.7	125.7
	Dose rate µGy h ⁻¹	0.539	0.269	0.230	0.467	0.972
Iizaka						
May 2012 1513	¹³⁷ Cs kBq m ⁻²	80.8	44.7	30.8	71.0	147.4
	¹³⁴ Cs kBq m ⁻²	55.5	30.5	21.6	48.3	103.1
	Dose rate µGy h ⁻¹	0.406	0.206	0.177	0.361	0.732

Table 4.7: Summary statistics for the backpack surveys of Fukushima University in March, June, July and November 2012, and Fukushima Iizaka in May 2012.

4.2.1 Fukushima University Surveys

The exploratory circuit on 6th March 2012 was conducted in unfavourable conditions, with significant quantities of snow on the ground to either side of the roads and footpaths. This attenuates radiation from soil beneath the snow. Data were collected from pathways between buildings near the Faculty of Symbiotic System Science, and the road way around the athletics and sports fields, a total distance of almost 3.5km. The distribution of ^{134}Cs , ^{137}Cs and dose rate determined from this survey is shown in Figure 4.24. The survey demonstrates the ability of the system to identify localised areas of relatively high radiocaesium concentration; by the pond to the south of the athletics field, in a car park to the south of the baseball field, outside dormitories to the north of the football field and on the plaza outside the lecture theatres. Analysis of the preliminary data suggested some spatially coherent variations in the ratio of ^{134}Cs : ^{137}Cs activity concentrations. These variations will be explored more fully in section 4.4 of this report.

A short survey was conducted by Fukushima University staff and students to gain familiarity with the instrument, and consisted of a short circuit of roads and paths on the western side of the campus and the residential areas just west of the campus. The distribution of ^{134}Cs , ^{137}Cs and dose rate determined from this survey is shown in Figure 4.25.

The survey in July 2012 covered a large proportion of the campus in approximately 8h survey time. The distribution of ^{134}Cs , ^{137}Cs and dose rate determined from this survey is shown in Figure 4.26. The data show that the radiocaesium activity is mostly located on vegetated areas, with the roads and paths, and the paved plazas within the campus showing much lower activity concentrations. The remediated sports fields, where surface soils have been removed and replaced with uncontaminated soils, have the lowest activity concentrations. Many of the areas with the highest radiocaesium concentrations were relatively inaccessible to students, these included an area behind the music building where a drain pipe outlet had produced a small patch of radiocaesium with $>150 \text{ kBq m}^{-2} \text{ }^{134}\text{Cs}$, a fenced off area beside the music department, and behind the water tower at the northern edge of the campus where soil removed during remediation was stored in plastic bags behind a barrier. However, there were several areas identified with some of the highest radiocaesium concentrations that were relatively accessible to students. There were two areas of open ground adjacent to dormitories with $>100 \text{ kBq m}^{-2} \text{ }^{134}\text{Cs}$; one just to the north of the tennis courts and a second larger area behind the dormitories to the north of the football pitch, which is where a calibration site was established. The sloping area south of the cafeteria towards the sports pitches had similar radiocaesium concentrations. Most of the grassed and lightly wooded areas around buildings on the campus had activity concentrations $>75 \text{ kBq m}^{-2} \text{ }^{134}\text{Cs}$, with some localised patches of much higher activity concentrations, one of which was identified with a slight depression among trees near the computer laboratory. The car park to the south of the baseball field registers $>50 \text{ kBq m}^{-2} \text{ }^{134}\text{Cs}$, consistent with the March data, with a distinct linear feature across the area, which was identified as a covered drain that had accumulated soil, with grass and other vegetation growing from it. A few paths through woodland around the campus were surveyed, these all had activity concentrations $>75 \text{ kBq m}^{-2} \text{ }^{134}\text{Cs}$. A section of a car park in front of buildings to the north east of the lecture theatres had been excavated with some of the soil removed from the sports fields during remediation buried there prior to resurfacing. The dose rate and activity concentrations recorded here are consistent with the other remediated hard surfaces on the campus, showing that contaminated soil may be disposed of by burial under hard surfaces away from plant rooting zones with negligible

external dose rate to people using these areas. Figure 4.28 shows some of the features referred to here.

On the 2nd and 4th November 2012 a repeat survey was conducted of the circuit from March, with repeat measurements on the calibration site sampled in July. The distribution of ^{134}Cs , ^{137}Cs and dose rate determined from this survey is shown in Figure 4.27. This shows a distribution of activity that is broadly similar to the March survey, an exception would be near a dormitory to the north of the tennis courts where the activity concentration recorded is significantly lower. This is next to one of the small open areas with $>100 \text{ kBq m}^{-2}$ ^{134}Cs identified in the July survey, the raised platform shown in Figure 4.28.



Figure 4.23: Exploratory survey of Fukushima University on 6th March 2012, with system demonstration and initial training.

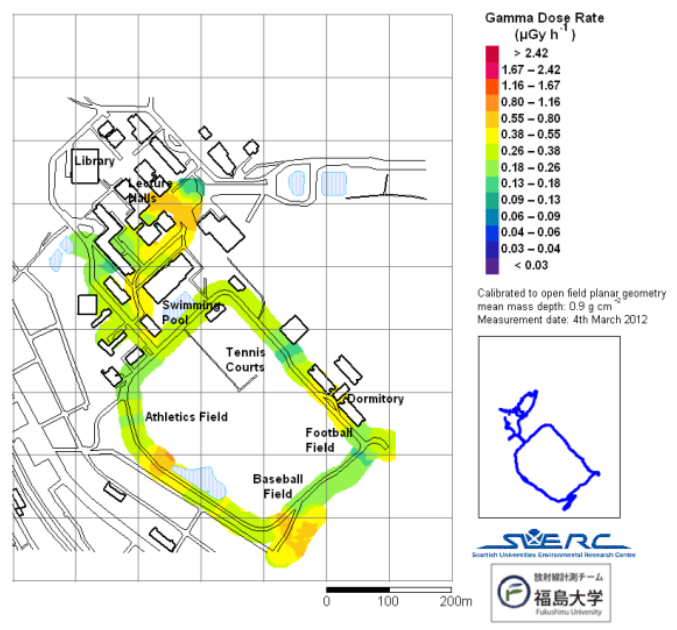
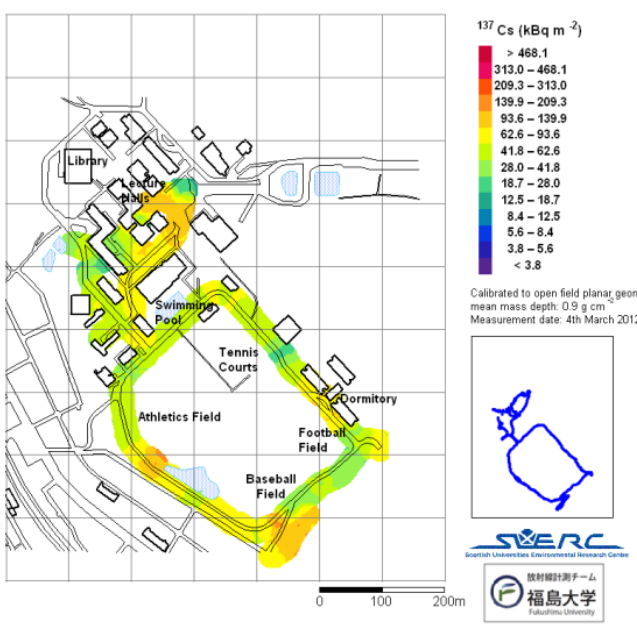
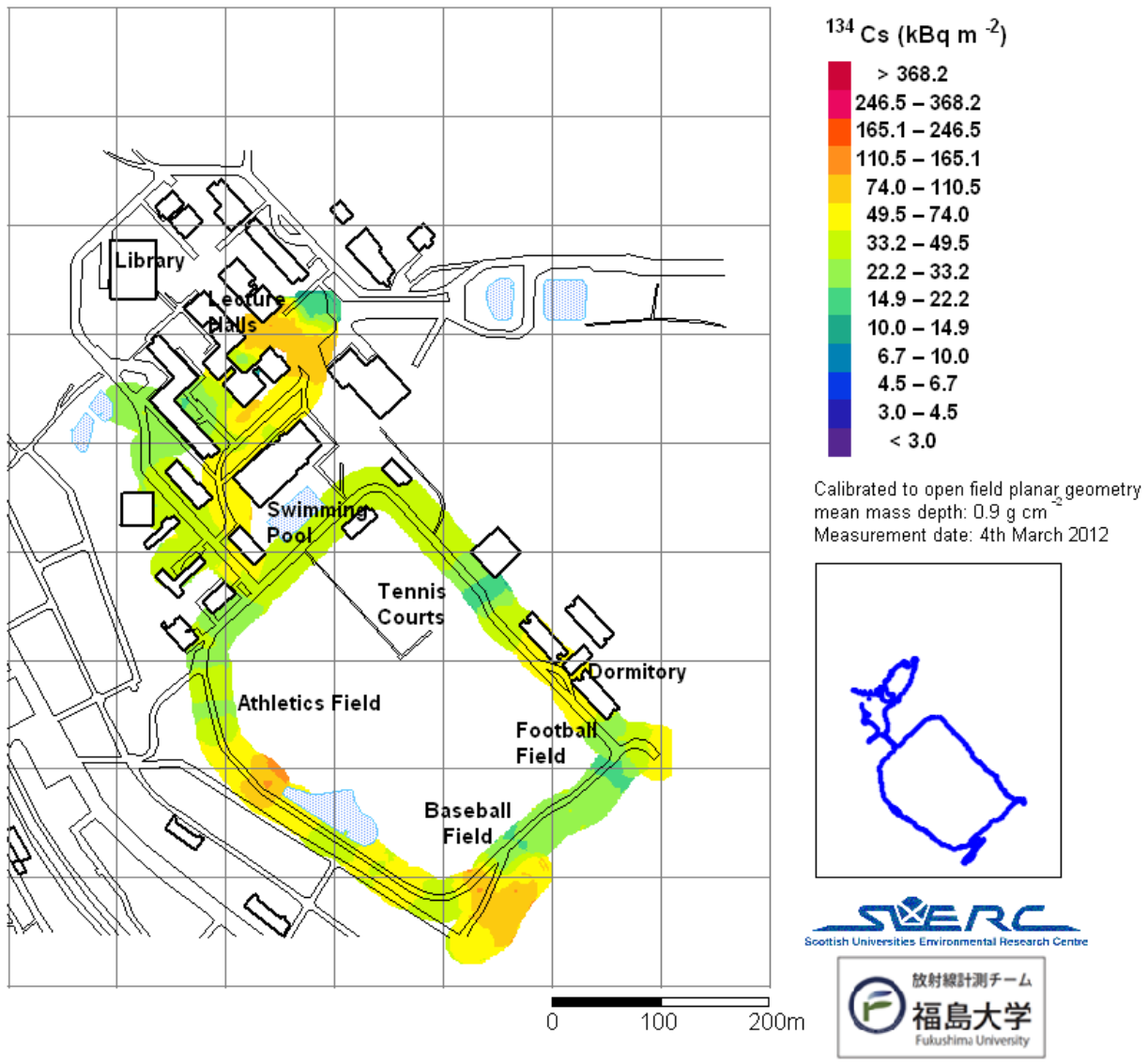


Figure 4.24: ^{134}Cs and ^{137}Cs activity per unit area and dose rate for Fukushima University, measured 4th March 2012.

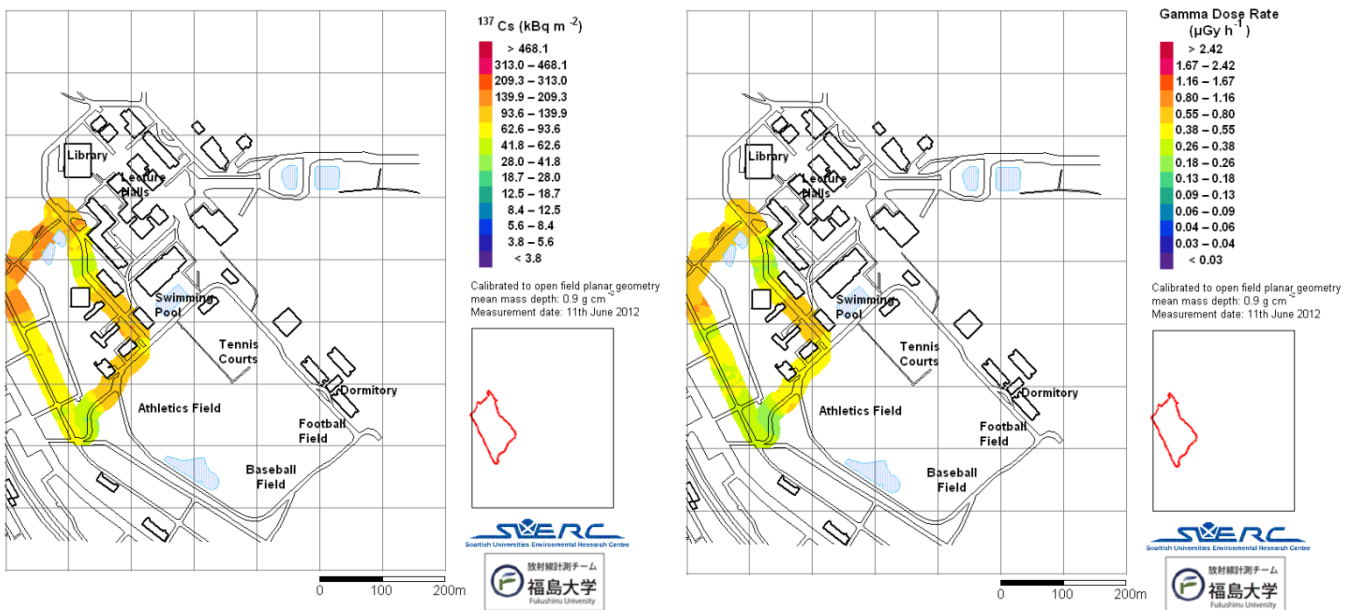
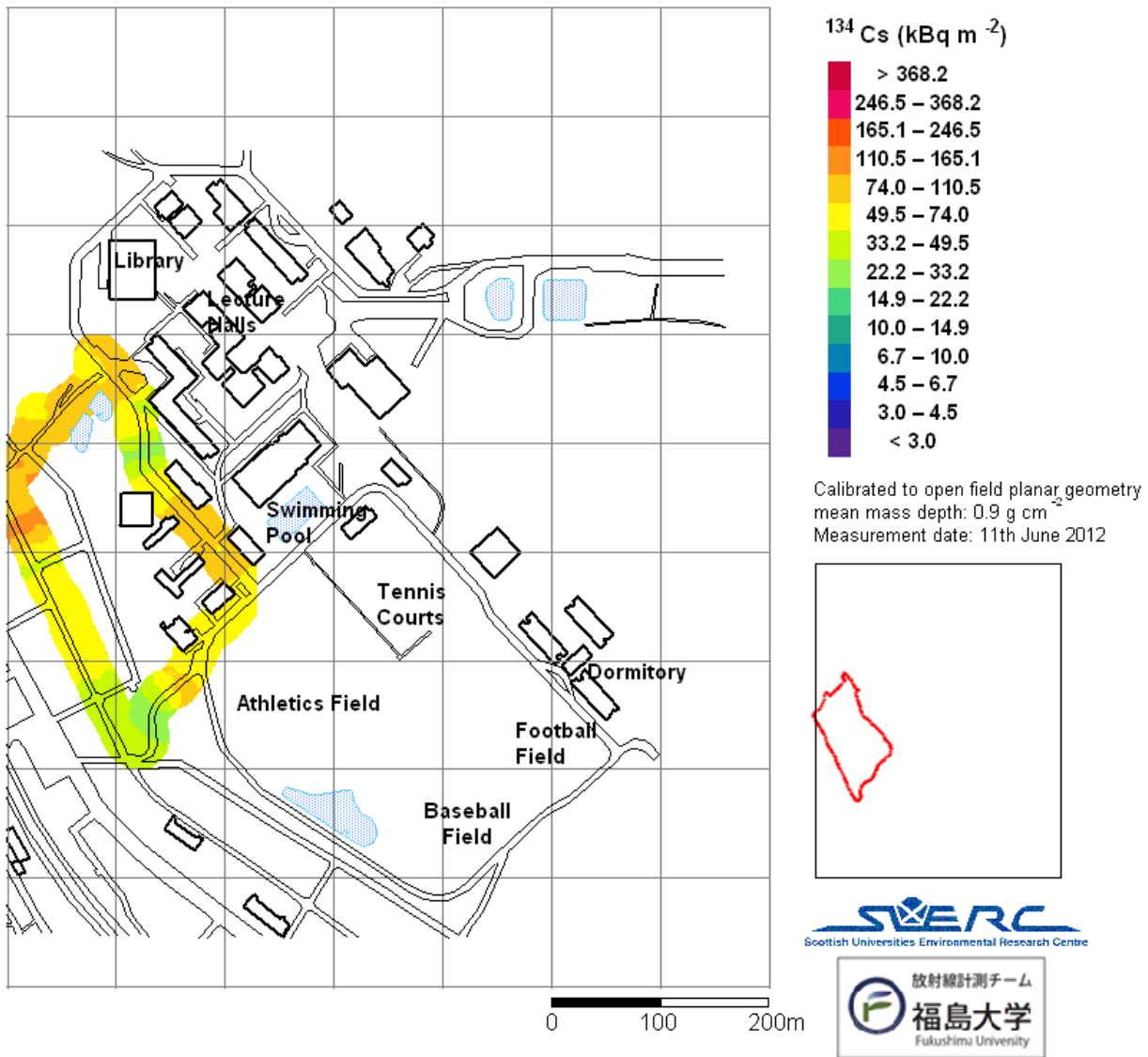


Figure 4.25: ^{134}Cs and ^{137}Cs activity per unit area and dose rate for Fukushima University, measured 11th June 2012.

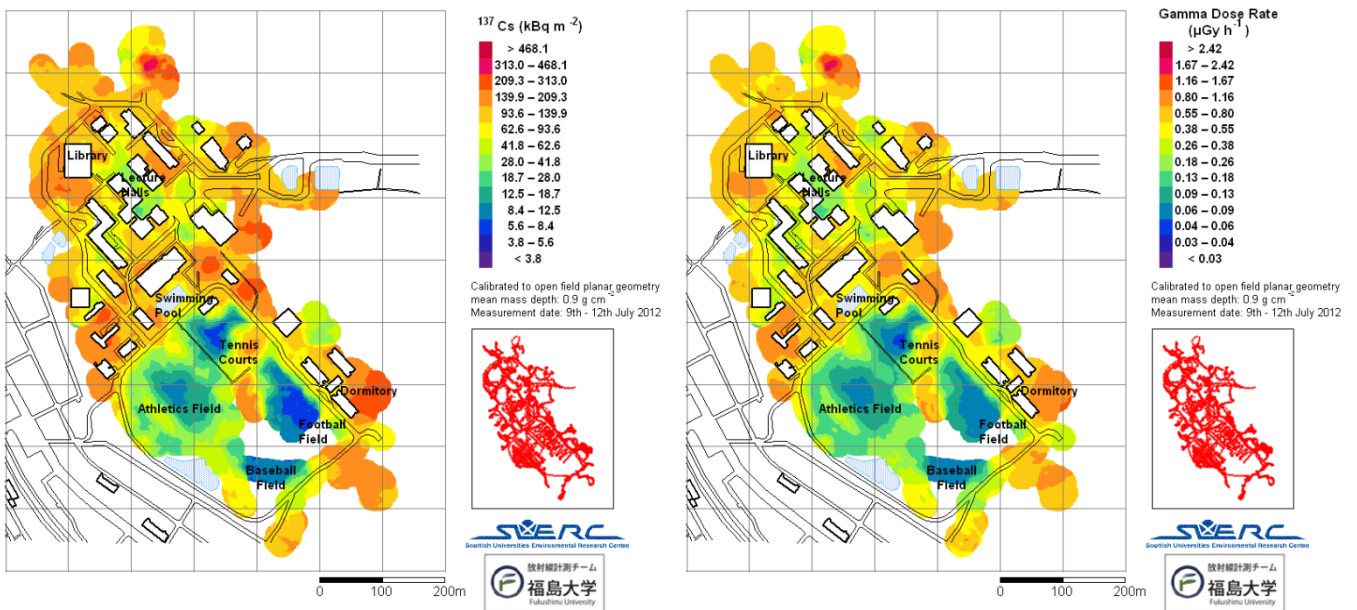
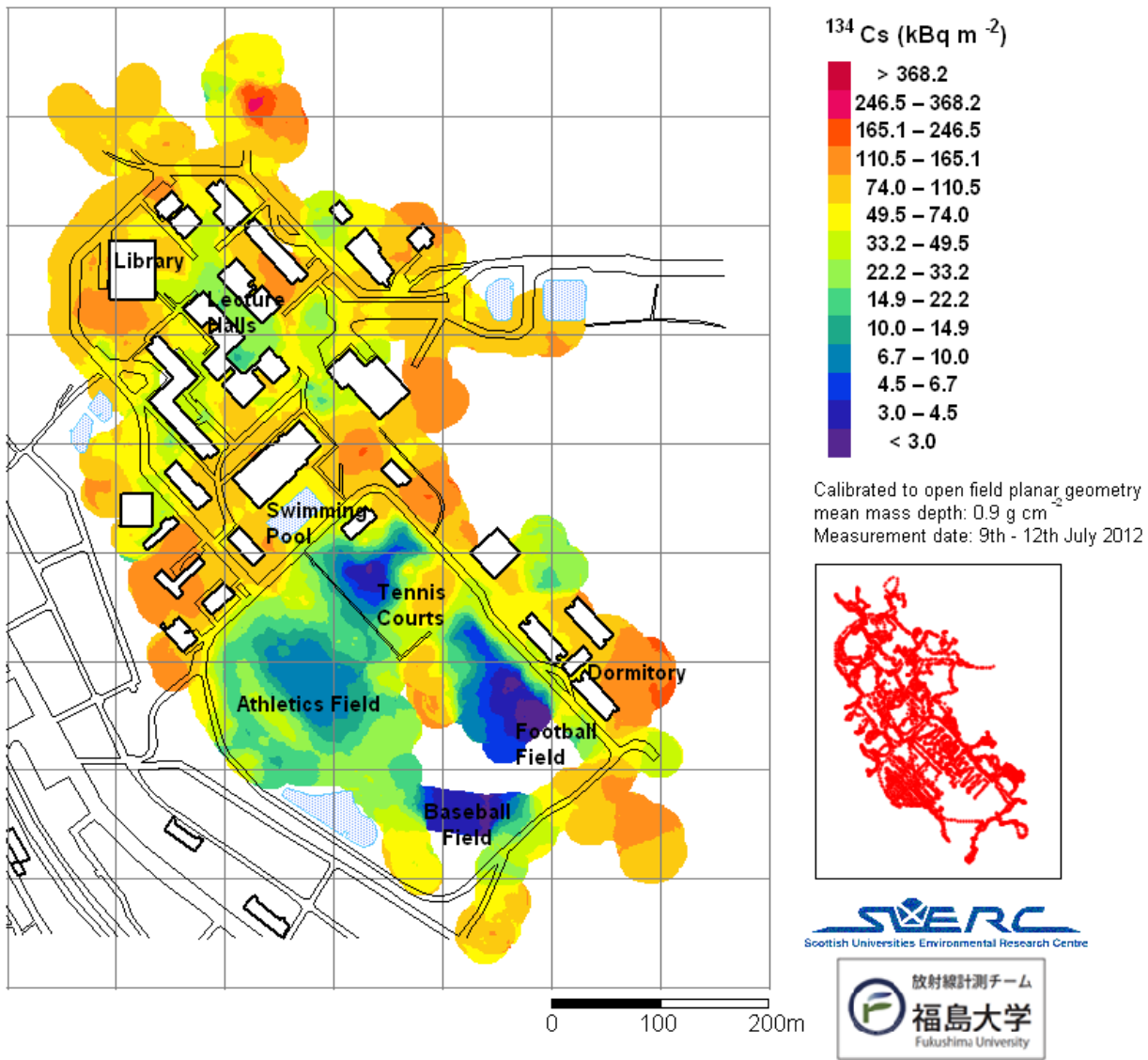


Figure 4.26: ^{134}Cs and ^{137}Cs activity per unit area and dose rate for Fukushima University, measured 9th-11th July 2012.

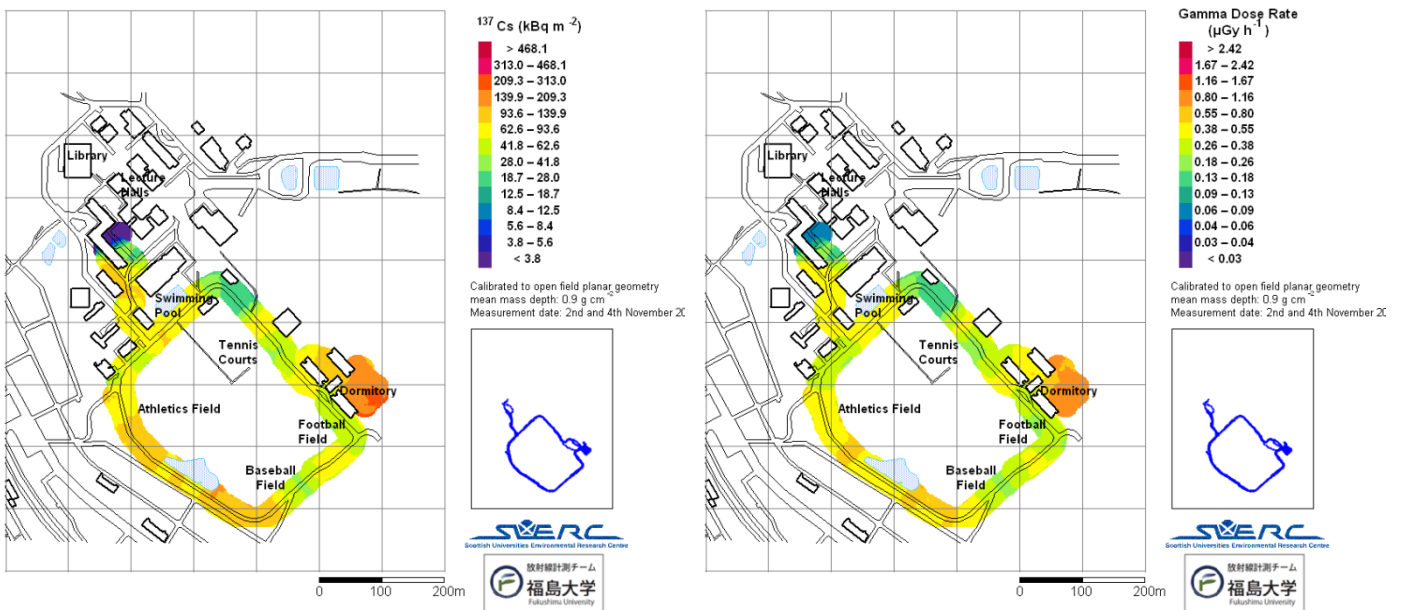
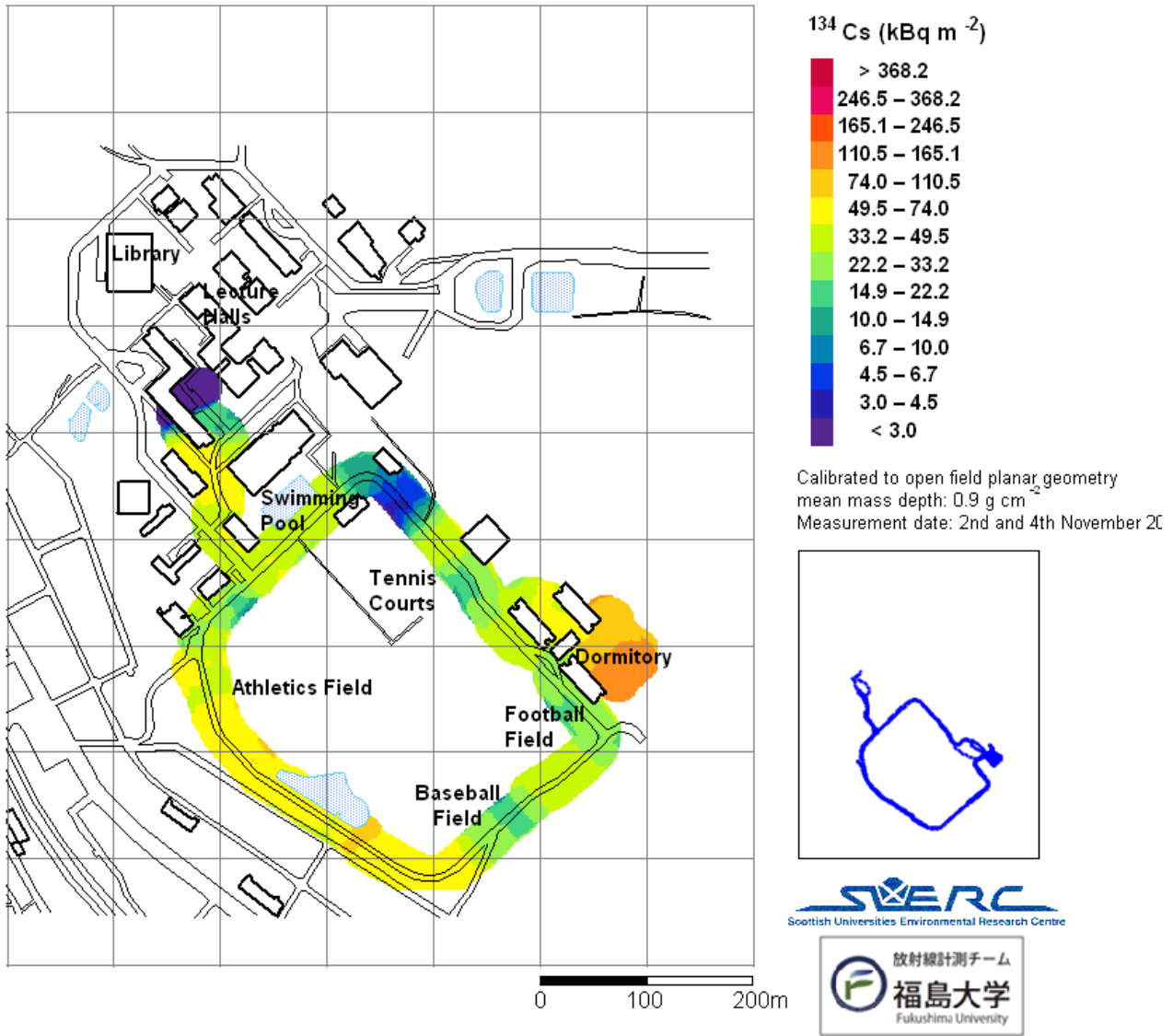


Figure 4.27: ^{134}Cs and ^{137}Cs activity per unit area and dose rate for Fukushima University, measured 2nd and 4th November 2012.



Athletics field. The central area has been remediated, with fresh turf laid, and has the among the lowest radiocaesium activity concentrations on the campus. The slight rise beyond the track, with the fence and light produces a slightly elevated linear feature on the map.



Tennis courts. The light brown court, has the among the lowest radiocaesium activity concentrations on the campus. The courts with the green surfaces have higher activity concentrations, similar to some unremediated locations.

In the foreground, a raised platform next to a dormitory building with ^{134}Cs activity concentrations above 100 kBq m^{-2} .



The raised platform next to a dormitory building.



Slight depression within trees outside computer laboratory which had radiocaesium activity concentrations ($>100 \text{ kBq m}^{-2} \text{ }^{134}\text{Cs}$)



Grassed and lightly wooded area outside the library, $>75 \text{ kBq m}^{-2} \text{ }^{134}\text{Cs}$.



Car park near baseball field, showing vegetated drain that has accumulated radiocaesium.

Figure 4.28: Photographs of parts of the Fukushima University campus referred to in the text, taken in July 2012.

The dose rate apportionments for the entire campus determined for each survey are given in Table 4.8 and Figure 4.29. It is noted that there is a small residual component in this apportionment, a mean mass depth of radiocaesium activity greater than the calibration (0.9 g cm^{-2}) would produce a residual. For a mean mass depth of 1.1 g cm^{-2} , the residual component would be less than 5%, with similar measurement uncertainties.

	March 2012	June 2012	July 2012	November 2012 [†]
Dose Rate $\mu\text{Gy h}^{-1}$	0.380 ± 0.007	0.483 ± 0.012	0.496 ± 0.005	0.554 ± 0.009
$^{238}\text{U} + ^{235}\text{U}$ series	$1.79 \pm 0.10 \%$	$1.45 \pm 0.14 \%$	$1.33 \pm 0.03 \%$	$1.34 \pm 0.15 \%$
^{232}Th series	$2.49 \pm 0.11 \%$	$2.07 \pm 0.12 \%$	$2.32 \pm 0.04 \%$	$2.03 \pm 0.15 \%$
$^{40}\text{K} + ^{87}\text{Rb}$	$4.77 \pm 0.07 \%$	$4.21 \pm 0.10 \%$	$3.71 \pm 0.02 \%$	$3.73 \pm 0.12 \%$
^{137}Cs	$29.71 \pm 1.79 \%$	$32.97 \pm 0.95 \%$	$32.83 \pm 1.87 \%$	$35.70 \pm 2.12 \%$
^{134}Cs	$61.24 \pm 3.74 \%$	$59.30 \pm 1.75 \%$	$59.82 \pm 2.45 \%$	$57.21 \pm 3.38 \%$
Residual	$3.2 \pm 7.1 \%$	$0.5 \pm 3.7 \%$	$1.6 \pm 5.4 \%$	$10.8 \pm 7.1 \%$

[†] Some data collected with mismatched gain, natural activity concentrations taken as the mean of the previous surveys

Table 4.8: Dose rate apportionment for the four data sets from Fukushima University.

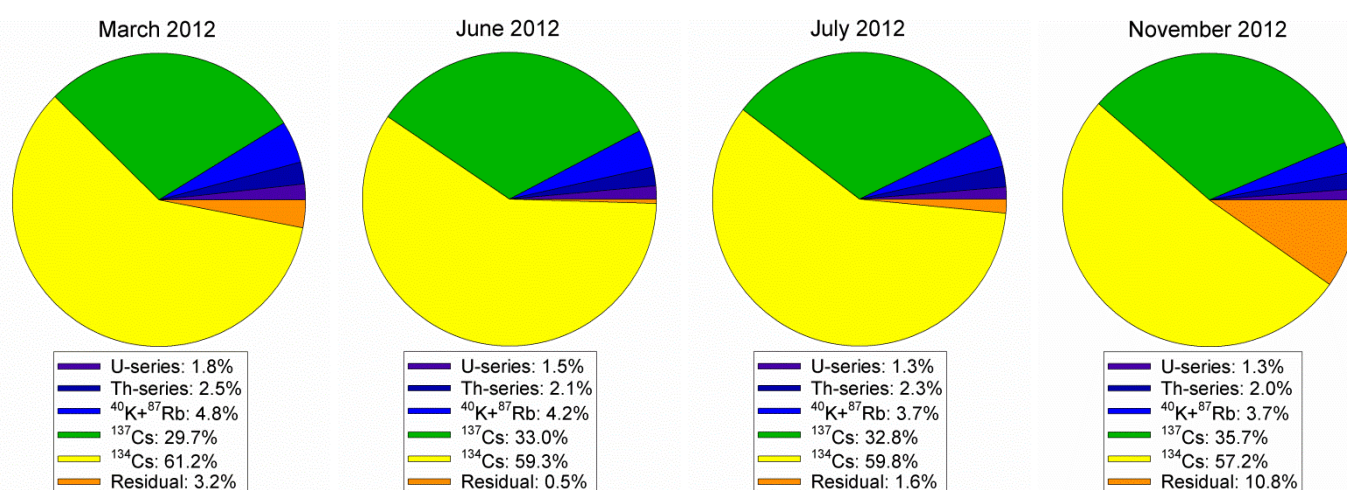


Figure 4.29: Dose rate apportionment for the four data sets from Fukushima University.

4.2.2 Evaluation of Remediation

The campus at Fukushima University had been partially remediated prior to the survey in July 2012. Soil had been removed from the athletics and other sports fields, with remediation on the paved area in the vicinity of the lecture theatres and other central buildings and tennis courts. Areas of the campus with lower occupancy had not been remediated at the time of the survey. The remediated areas are shown on Figure 4.30.

The data has been regridded onto a $10 \times 10 \text{ m}$ grid, and the remediated and unremediated areas separated. The distributions of ^{134}Cs activity per unit area for the total area, the unremediated and remediated areas are shown in Figure 4.31, with the corresponding summary statistics in Table 4.9. The ^{137}Cs and dose rate show similar distributions. The dose rate apportionments for the remediated and unremediated areas are given in Table 4.10 and Figure 4.32.

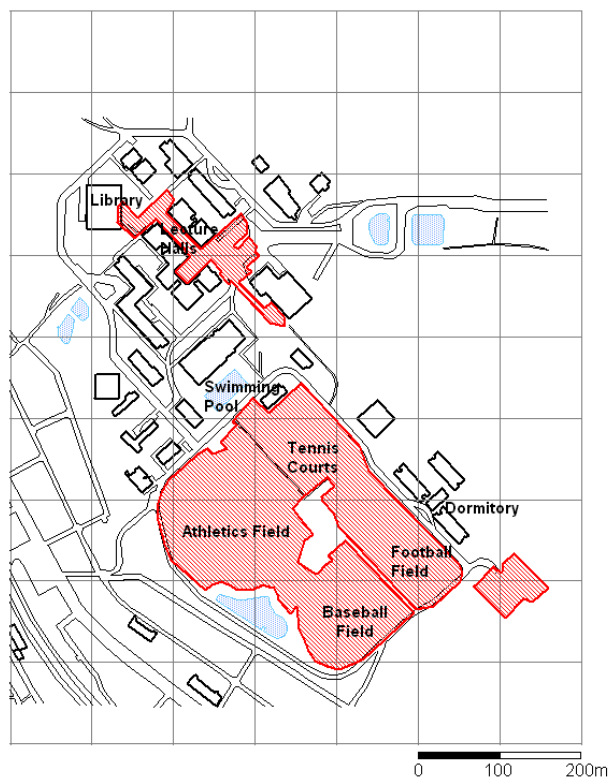


Figure 4.30: Areas of the Fukushima Campus that had been remediated by the July 2012 survey.

Area	Number		Mean	Standard Deviation	10 th Percentile	Median	90 th Percentile
All data	1884 188400 m ²	¹³⁷ Cs kBq m ⁻²	96.6	60.5	17.5	94.9	174.8
		¹³⁴ Cs kBq m ⁻²	63.5	40.3	10.8	63.0	114.8
		Dose rate μGy h ⁻¹	0.468	0.274	0.109	0.464	0.817
Unremediated	1306 130600 m ²	¹³⁷ Cs kBq m ⁻²	121.4	51.9	56.7	117.2	189.9
		¹³⁴ Cs kBq m ⁻²	80.0	34.6	37.8	76.8	124.3
		Dose rate μGy h ⁻¹	0.581	0.235	0.296	0.561	0.873
Remediated exc. tennis courts	542 54200 m ²	¹³⁷ Cs kBq m ⁻²	36.9	32.9	9.2	27.7	76.2
		¹³⁴ Cs kBq m ⁻²	23.8	21.8	4.9	17.7	48.6
		Dose rate μGy h ⁻¹	0.196	0.147	0.076	0.152	0.359
Tennis courts	36 3600 m ²	¹³⁷ Cs kBq m ⁻²	95.5	40.0	49.1	79.8	148.5
		¹³⁴ Cs kBq m ⁻²	62.3	27.6	30.6	51.6	99.8
		Dose rate μGy h ⁻¹	0.448	0.180	0.239	0.376	0.695

Table 4.9: Summary statistics for the regridded July 2012 Fukushima University survey, for the total area, the unremediated areas, and the remediated areas separating the tennis courts from the other areas.

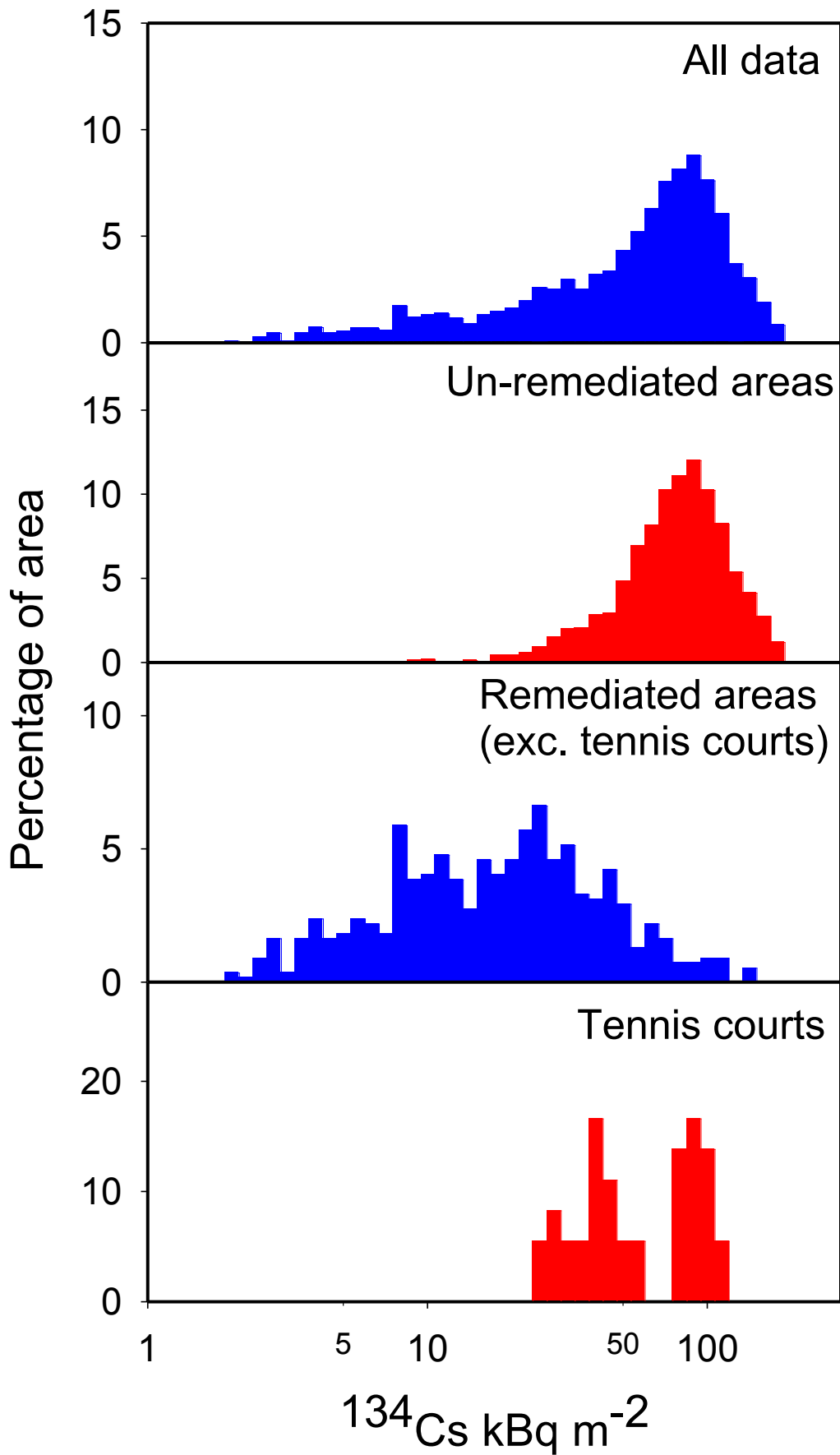


Figure 4.31: ^{134}Cs activity per unit area for the total data set for the July 2012 survey of Fukushima University, and for the unremediated and remediated areas with the tennis courts. The ^{137}Cs and dose rate show very similar distributions.

	Total Area	Unremediated	Remediated
Dose Rate $\mu\text{Gy h}^{-1}$	0.496 ± 0.005	0.581 ± 0.007	0.196 ± 0.006
$^{238}\text{U} + ^{235}\text{U}$ series	$1.33 \pm 0.03 \%$	$1.18 \pm 0.03 \%$	$2.99 \pm 0.10 \%$
^{232}Th series	$2.32 \pm 0.04 \%$	$1.95 \pm 0.03 \%$	$6.54 \pm 0.10 \%$
$^{40}\text{K} + ^{87}\text{Rb}$	$3.71 \pm 0.02 \%$	$3.34 \pm 0.02 \%$	$8.92 \pm 0.14 \%$
^{137}Cs	$32.83 \pm 1.87 \%$	$33.13 \pm 0.38 \%$	$29.20 \pm 1.12 \%$
^{134}Cs	$59.82 \pm 2.45 \%$	$60.39 \pm 0.70 \%$	$52.34 \pm 2.03 \%$
Residual	$1.6 \pm 5.4 \%$	$1.84 \pm 1.42\%$	$-0.40 \pm 4.19 \%$

Table 4.10: Dose rate apportionment for the remediated and unremediated (excluding the tennis courts) areas from the July 2012 Fukushima University survey.

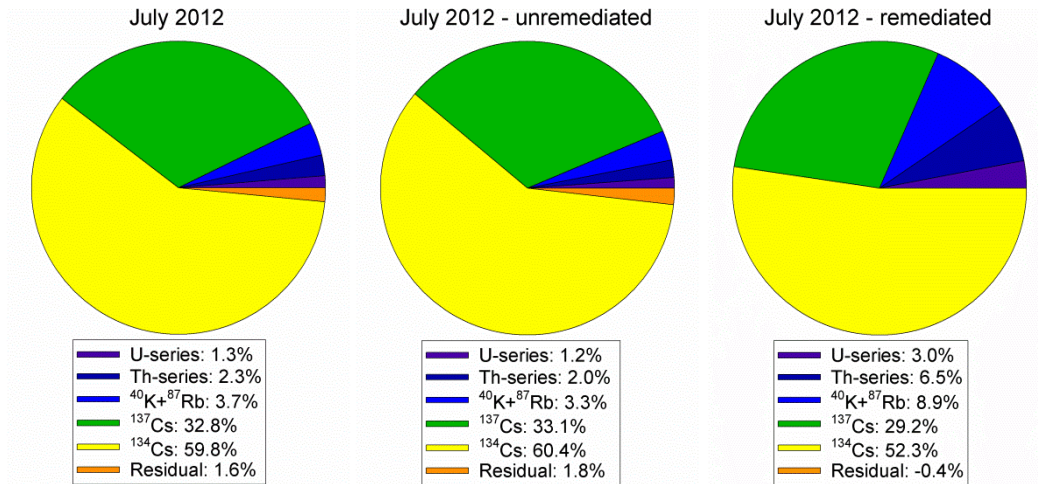


Figure 4.32: Dose rate apportionment for the remediated and unremediated (excluding the tennis courts) areas from the July 2012 Fukushima University survey.

4.2.3 Fukushima Iizaka Survey

The backpack system was demonstrated during a conference held in Paruse Iizaka, Fukushima City in May 2012. On the 20th May, a series of demonstrations collected data starting from one of the hotels used for the conference and the conference venue. Spectra were recorded with 5s integration time, over a total distance of almost 5.5 km with small areas surveyed including a shrine at Yawata and a children's play park at Furudate. The ^{134}Cs and ^{137}Cs activity per unit area and dose rate for the entire data set is shown in Figure 4.34.

During the course of the demonstration surveys, some small areas within Iizaka were surveyed in greater detail. These included a shrine at Yawata and a children's play area at Furudate. The ^{134}Cs and ^{137}Cs activity per unit area and dose rate for these small areas are shown in Figures 4.35 and 4.36.

The dose rate apportionments calculated for the entire survey and the smaller surveys at the Yawata Shrine and Furudate play area are given in Table 4.11 and Figure 4.37. These also include a dose rate apportionment for data collected inside the conference venue. At Yawata and Furudate, the contribution of radiocaesium to the dose rate is higher than for the survey as a whole. Inside the conference venue the dose rate is very much lower, and dominated by natural activity with radiocaesium contributing 15% of the dose rate. Within the enclosed geometry of the building the open field calibration assumption is no longer valid, and the

estimated activity concentrations will be incorrectly calibrated. This results in the large negative residual within the dose rate apportionment.



Figure 4.33: Photographs associated with the Fukushima Iizaka surveys, 20th May 2012.

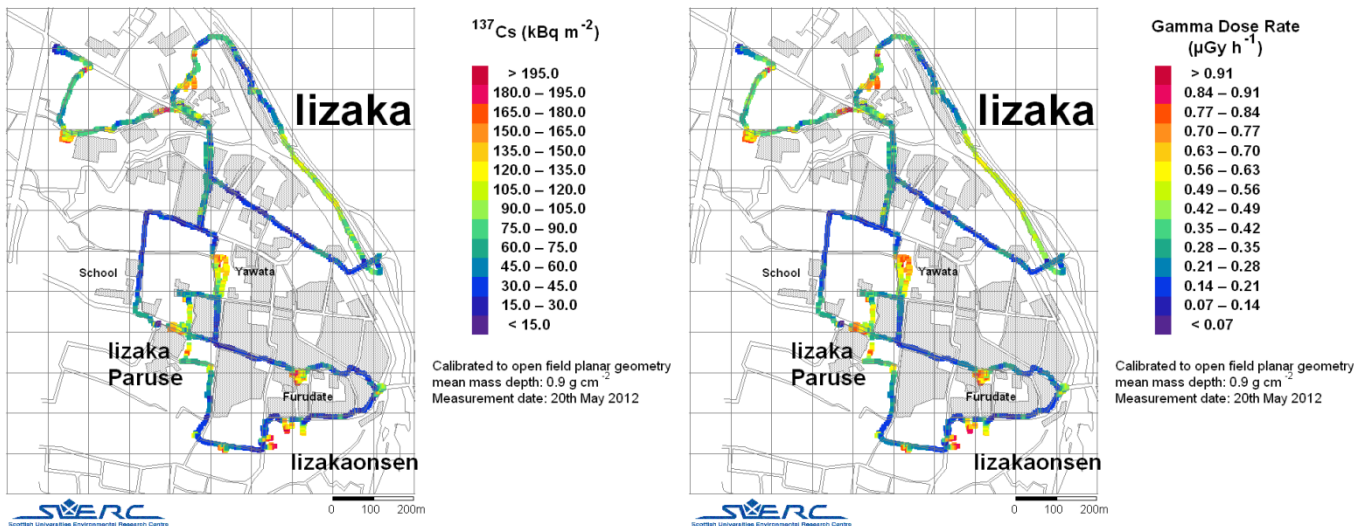
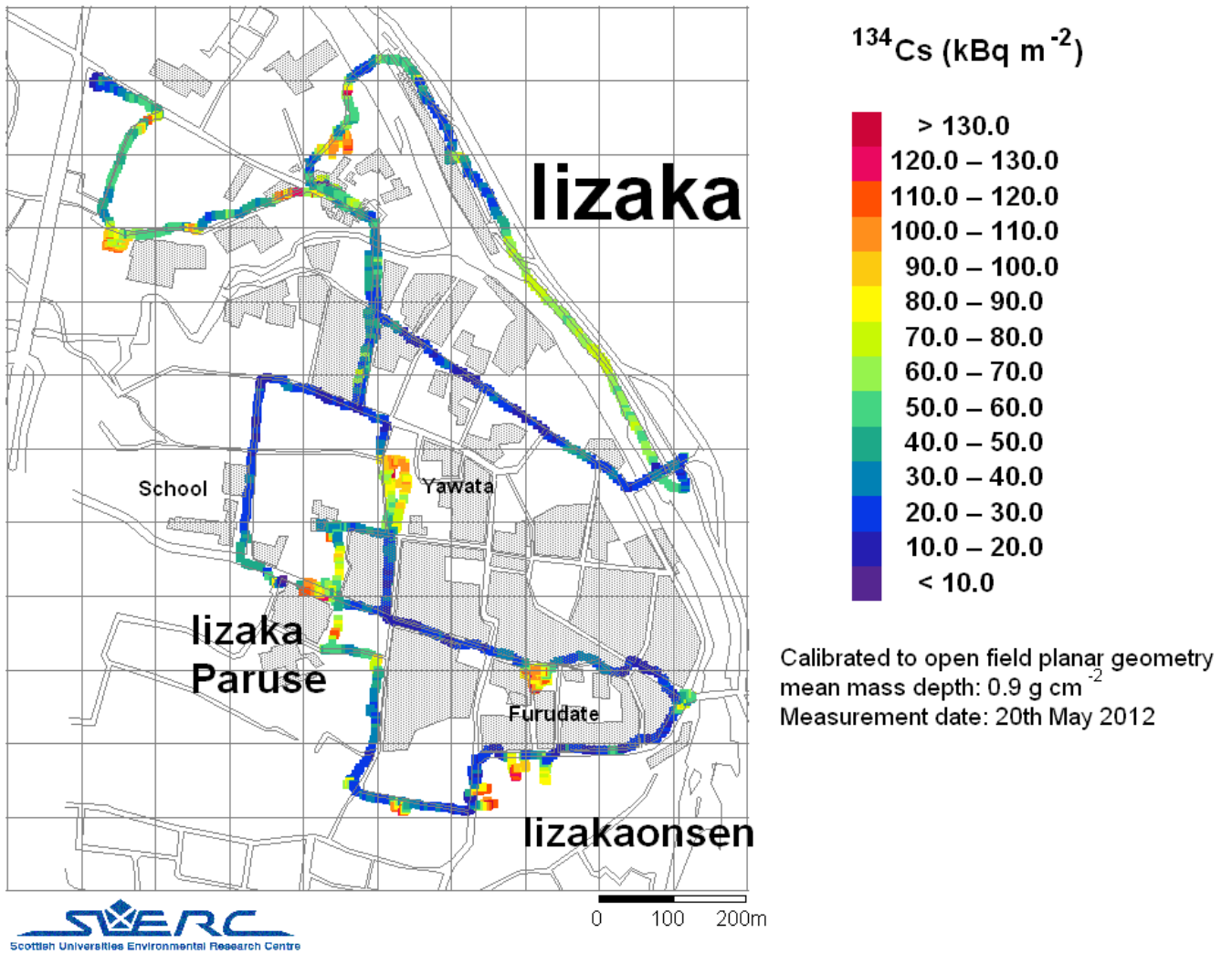
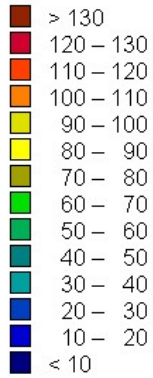


Figure 4.34: ^{134}Cs and ^{137}Cs activity per unit area and dose rate for the demonstration surveys around Lizaka, 20th May 2012.



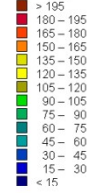
^{134}Cs kBq m⁻²



Calibrated to open field planar geometry
 mean mass depth: 0.9 g cm⁻²
 Measurement date: 20th May 2012



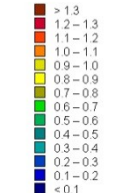
^{137}Cs kBq m⁻²



Calibrated to open field planar geometry
 mean mass depth: 0.9 g cm⁻²
 Measurement date: 20th May 2012



Dose rate μGy h⁻¹



Calibrated to open field planar geometry
 mean mass depth: 0.9 g cm⁻²
 Measurement date: 20th May 2012



Figure 4.35: ^{134}Cs and ^{137}Cs activity per unit area and dose rate around a children's play park at Furudate, 20th May 2012, on Google Earth image.

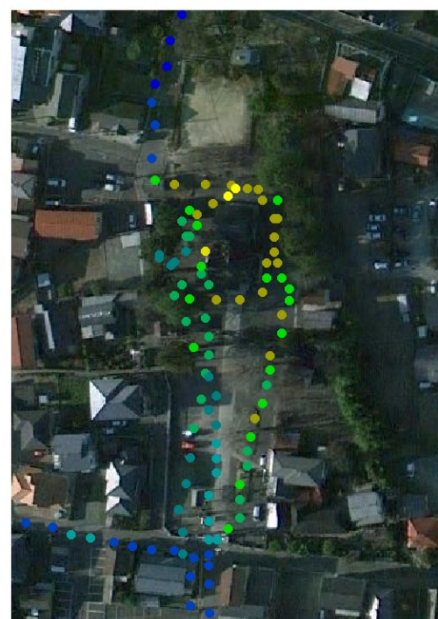


Figure 4.36: ¹³⁴Cs and ¹³⁷Cs activity per unit area and dose rate around a shrine at Yawata, 20th May 2012, on Google Earth image.

	Inside	All data (outside)	Furudate	Yawata
Dose Rate $\mu\text{Gy h}^{-1}$	0.027 ± 0.001	0.406 ± 0.005	0.682 ± 0.020	0.548 ± 0.017
$^{238}\text{U} + ^{235}\text{U}$ series	$22.7 \pm 2.6 \%$	$1.92 \pm 0.06 \%$	$0.97 \pm 0.16 \%$	$1.54 \pm 0.16 \%$
^{232}Th series	$22.2 \pm 2.3 \%$	$2.71 \pm 0.05 \%$	$2.73 \pm 0.23 \%$	$2.01 \pm 0.18 \%$
$^{40}\text{K} + ^{87}\text{Rb}$	$39.1 \pm 1.3\%$	$5.25 \pm 0.04\%$	$4.28 \pm 0.15 \%$	$4.18 \pm 0.12 \%$
^{137}Cs	$6.9 \pm 1.1 \%$	$31.15 \pm 1.81 \%$	$31.81 \pm 2.03 \%$	$32.66 \pm 2.16 \%$
^{134}Cs	$9.1 \pm 1.3 \%$	$58.97 \pm 3.41 \%$	$60.22 \pm 3.04 \%$	$59.61 \pm 3.08 \%$
Residual	$-21.3 \pm 9.5 \%$	$0.60 \pm 6.62 \%$	$-0.64 \pm 6.70 \%$	$2.61 \pm 6.83 \%$

Table 4.11: Dose rate apportionment for the data collected around Iizaka, 20th May 2012, inside the conference venue and the small survey areas at Furudate and Yawata.

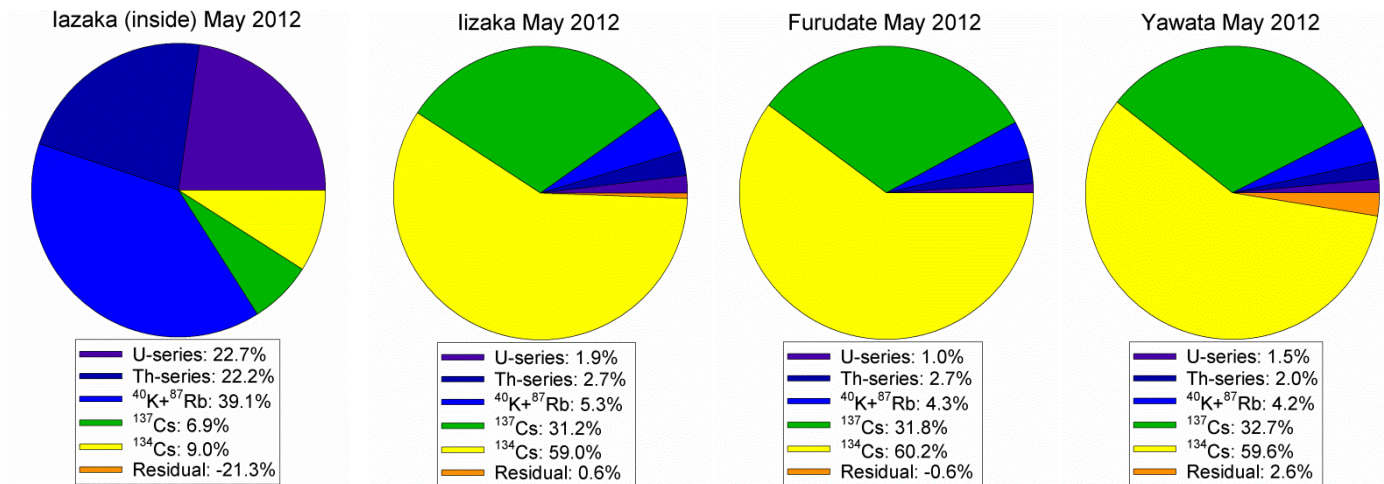


Figure 4.37: Dose rate apportionment for the data collected around Iizaka, 20th May 2012, inside the conference venue and the small survey areas at Furudate and Yawata.

4.2.4 Discussion of Fukushima University and Fukushima Iizaka Surveys

The SUERC Portable Gamma Spectrometry system has been used to collect high quality data from the campus of Fukushima University on four occasions in 2012, and from part of Fukushima city. These surveys of urbanised areas have demonstrated the capability of backpack systems in collecting data in locations where people spend their time. The surveys have demonstrated the variation in activity concentration and dose rate within such environments, with hard surfaces such as roads and pavements being generally lower activity areas compared to vegetated surfaces as a result of activity being removed by the action of rain and street cleaning. The environments surveyed inside buildings show much lower activity concentrations, with anthropogenic contributions to the dose rate often being less than 20%.

The maps of these detailed surveys show locations with locally enhanced activity concentrations. Monitoring of the system during survey usually allowed these features to be identified precisely and reported in near real time prior to checks on data quality and final analysis. Such information is vital in identifying areas of higher dose rate, especially in areas of higher occupancy, allowing the prioritisation of remediation programmes to target limited resource to where it would have the most effect.

The surveys of the university campus, in particular the July survey that covered the majority of the campus, has allowed the effectiveness of the remediation work conducted on the campus to be evaluated. This was done by comparing remediated with unremediated areas, repeat surveys of an area before and after remediation would provide a more direct method of evaluating remediation.

Areas on the university campus that were remediated by removal of top soil and replacement with uncontaminated top soil has been very effective at reducing the radiocaesium activity concentrations and associated anthropogenic dose rates to very low levels. Radiation from adjacent unremediated areas still contributes to dose rates at the edges of these areas. Remediation by power-washing the surfaces had a more varied effectiveness. On some surfaces this has resulted in significant reductions in radiocaesium activity concentrations. On other surfaces, most notably artificial surfaces on tennis courts, this method of remediation has reduced the activity concentrations by very small amounts.

4.3 Fruit Tree Cultivation

Fruit cultivation is a major component of the economy of Fukushima Prefecture that has been severely affected by the accidents at Fukushima Daiichi. Fukushima Prefecture operate a Fruit Tree Research Institute in the northern part of Fukushima city, which received a substantial deposition of activity following the accidents. An arrangement has been established with staff at the research institute, allowing the demonstration of the SUERC system at the institute orchards, and at orchards in more severely affected areas.

Activity transfer to fruit is a major concern. Following the Chernobyl accident there was a considerable increase in knowledge of radionuclides transfer to trees and between different parts of trees. Studies of temperate forests in Europe has shown that during the early phase (lasting 4-5 years) radiocaesium contamination in trees is primarily due to foliar interception by the canopy with translocation from foliar surfaces to structural components of the tree. (Baldini *et.al.* 1987, Antonopoulos-Domis *et.al.* 1991, Calmon *et.al.* 2009). Transfer of radionuclides from soil to fruit are primarily dominated by soil classification, with plant species a second order effect with those species with higher metabolic activity characterised by higher transfer factors if soil differences are minimised (Carini 2001, Baldini *et.al.* 1987). The applicability of prior studies to the particular varieties of fruit grown in Japan, and the soil types, has yet to be determined. It has been shown that immediately after the accident there was transfer from deposition on bark, which had not previously been observed. As the activity migrates further into the soil, especially as it enters the rooting zone of the trees, transfer from soil would be expected.

Mapping the deposition in fruit orchards allows the ratio of activity concentrations in fruit and on the ground to be measured. This is important data to help understand transfer processes, and hence develop methods to reduce such transfer that would be of a considerable benefit to fruit farmers in the area. Repeat measurements will also allow for the evaluation of remediation methods to reduce the activity available for transfer to fruit. Mapping of deposition also allows the evaluation of external doses to workers in the orchards.

Data were collected at the Fukushima Prefecture Fruit Tree Research Institute on four occasions, in March, May, July and November 2012. In July and November, data were also collected at some fruit cultivation areas in other parts of Fukushima Prefecture in

collaboration with staff at the research institute. Measurements have also been conducted at the AFFRC at Tsukuba in March and November 2012. Summary statistics for these measurements are given in Table 4.12.

Date and number of measurements		Mean	Std. Dev.	10 th %tile	Median	90 th %tile
Fruit Tree Research Institute						
March 2012 308	¹³⁷ Cs kBq m ⁻²	240.6	40.3	190.1	245.6	285.7
	¹³⁴ Cs kBq m ⁻²	178.9	28.2	145.0	183.2	206.4
	Dose rate µGy h ⁻¹	1.219	0.180	0.973	1.250	1.390
May 2012 1756	¹³⁷ Cs kBq m ⁻²	237.3	48.4	179.8	239.7	295.0
	¹³⁴ Cs kBq m ⁻²	164.3	32.4	124.6	166.6	203.8
	Dose rate µGy h ⁻¹	1.149	0.208	0.892	1.170	1.390
July 2012 843	¹³⁷ Cs kBq m ⁻²	234.3	51.5	149.0	243.5	290.3
	¹³⁴ Cs kBq m ⁻²	155.2	34.7	96.7	162.3	192.3
	Dose rate µGy h ⁻¹	1.102	0.226	0.711	1.150	1.340
Nov 2012 923	¹³⁷ Cs kBq m ⁻²	235.0	52.7	152.4	245.7	293.1
	¹³⁴ Cs kBq m ⁻²	142.9	32.2	90.8	149.0	178.8
	Dose rate µGy h ⁻¹	1.045	0.217	0.691	1.100	1.280
Mt Shinobu July 2012 552	¹³⁷ Cs kBq m ⁻²	257.5	97.0	105.3	272.6	379.5
	¹³⁴ Cs kBq m ⁻²	171.0	66.2	68.0	182.0	249.1
	Dose rate µGy h ⁻¹	1.235	0.444	0.549	1.320	1.759
Mt Shinobu Nov 2012 268	¹³⁷ Cs kBq m ⁻²	292.6	65.1	215.5	296.3	368.5
	¹³⁴ Cs kBq m ⁻²	177.1	40.7	129.7	180.1	224.3
	Dose rate µGy h ⁻¹	1.311	0.286	0.955	1.330	1.670
Date July 2012 355	¹³⁷ Cs kBq m ⁻²	291.2	110.3	146.0	271.3	449.5
	¹³⁴ Cs kBq m ⁻²	187.6	77.2	84.5	173.2	301.0
	Dose rate µGy h ⁻¹	1.449	0.514	0.763	1.350	2.180
Date Nov 2012 299	¹³⁷ Cs kBq m ⁻²	464.7	59.5	387.3	466.1	546.0
	¹³⁴ Cs kBq m ⁻²	286.4	37.4	237.2	285.3	335.9
	Dose rate µGy h ⁻¹	2.074	0.241	1.740	2.070	2.400
AFFRC						
March 2012 109	¹³⁷ Cs kBq m ⁻²	29.5	10.3	17.0	28.8	41.5
	¹³⁴ Cs kBq m ⁻²	22.7	6.9	14.5	23.3	29.8
	Dose rate µGy h ⁻¹	0.176	0.038	0.143	0.174	0.208
Nov 2012 775	¹³⁷ Cs kBq m ⁻²	19.8	6.9	10.6	19.7	28.8
	¹³⁴ Cs kBq m ⁻²	12.8	4.2	7.5	13.0	18.2
	Dose rate µGy h ⁻¹	0.122	0.028	0.088	0.123	0.153

Table 4.12: Summary statistics for the backpack surveys of areas of fruit cultivation in 2012: the Fukushima Prefecture Fruit Tree Research Institute in March, May, July and November; fruit cultivation areas at Mount Shinobu and near Date in July and November; the AFFRC at Tsukuba in March and November.

4.3.1 Fruit Tree Research Institute

The Fukushima Prefecture Fruit Tree Research Institute is located at Iojimae in the northern part of Fukushima City. The institute has a large number of experimental plots growing different varieties of fruit trees.

An exploratory survey on the 8th March 2012 collected data from a small area of orchards near the main buildings. The ^{134}Cs activity per unit area from this survey is shown in Figure 4.42, with the ^{137}Cs activity per unit area and dose rate shown in Figure 4.43. The survey showed that even within the small area of the site covered there was considerable variation in deposited activity.



Figure 4.38: Radiometric data collection by Mamoru Sato and his team using the SUERC system, 8th March 2012.

Following the remediation symposium held in Paruse Iizaka in May 2012, a more extensive survey of the institute was conducted covering a much larger portion of the site. The ^{134}Cs activity distribution from this survey is shown in Figure 4.44, with the ^{137}Cs activity per unit area and dose rate shown in Figure 4.45. The same area was surveyed again on the 12th July 2012, with investigation of an unplanted area near the south western boundary of the institute as a potential calibration site. The ^{134}Cs activity distribution from this survey is shown in Figure 4.46, with the ^{137}Cs activity per unit area and dose rate shown in Figure 4.47. For both of these surveys, control measurements on the lawn in front of the main buildings and by the gate house were conducted to allow for evaluation of environmental conditions (principally soil water content) to aid interpretation of the changes in deposition between surveys as a result of natural environmental processes and deliberate decontamination trials.

On the 3rd November 2012 samples were collected from the calibration site, and data collected from some of the areas surveyed in May and July. The ^{134}Cs activity distribution from this survey is shown in Figure 4.48, with the ^{137}Cs activity per unit area and dose rate shown in Figure 4.49.

The mean ^{134}Cs and ^{137}Cs activity per unit area and dose rate for all the measurements in each survey are shown in Figure 4.50. These show the decline in activity concentration and dose rate over the entire measurement period, consistent with the physical decay of ^{134}Cs with a half life of 2.065 years and ^{137}Cs with a half life of 30.04 years. Taking the entire data set for each survey does not account for the differences in the areas surveyed on each occasion. Some of the experimental plots on the site were surveyed on three different occasions, these plots are indicated in Figure 4.51. The mean activity concentrations and dose rates for these plots are shown in Figure 4.52. Most of these show a decline in activity consistent with the physical half lives of ^{134}Cs and ^{137}Cs . The data for plots 3-1 and 3-2 (which are apple trees) show a more rapid decline in activity concentration. These plots have had some soil removal.

The dose rate apportionments (Table 4.13 and Figure 4.53) show a gradual reduction in the contribution of ^{134}Cs to the dose rate, with compensatory increases in the contribution of ^{137}Cs and the natural activity, as would be expected with the shorter half life of ^{134}Cs .



Indicating zeolite pads, deployed to intercept radiocaesium before penetration to greater depth in the soil



Figure 4.39: Radiometric survey at the Fruit Tree Research Institute, 21st May 2102.



Figure 4.40: Radiometric surveys at the Fruit Tree Research Institute, 12th July 2012.



Figure 4.41: Radiometric surveys at the fruit tree institute, 3rd November 2012.

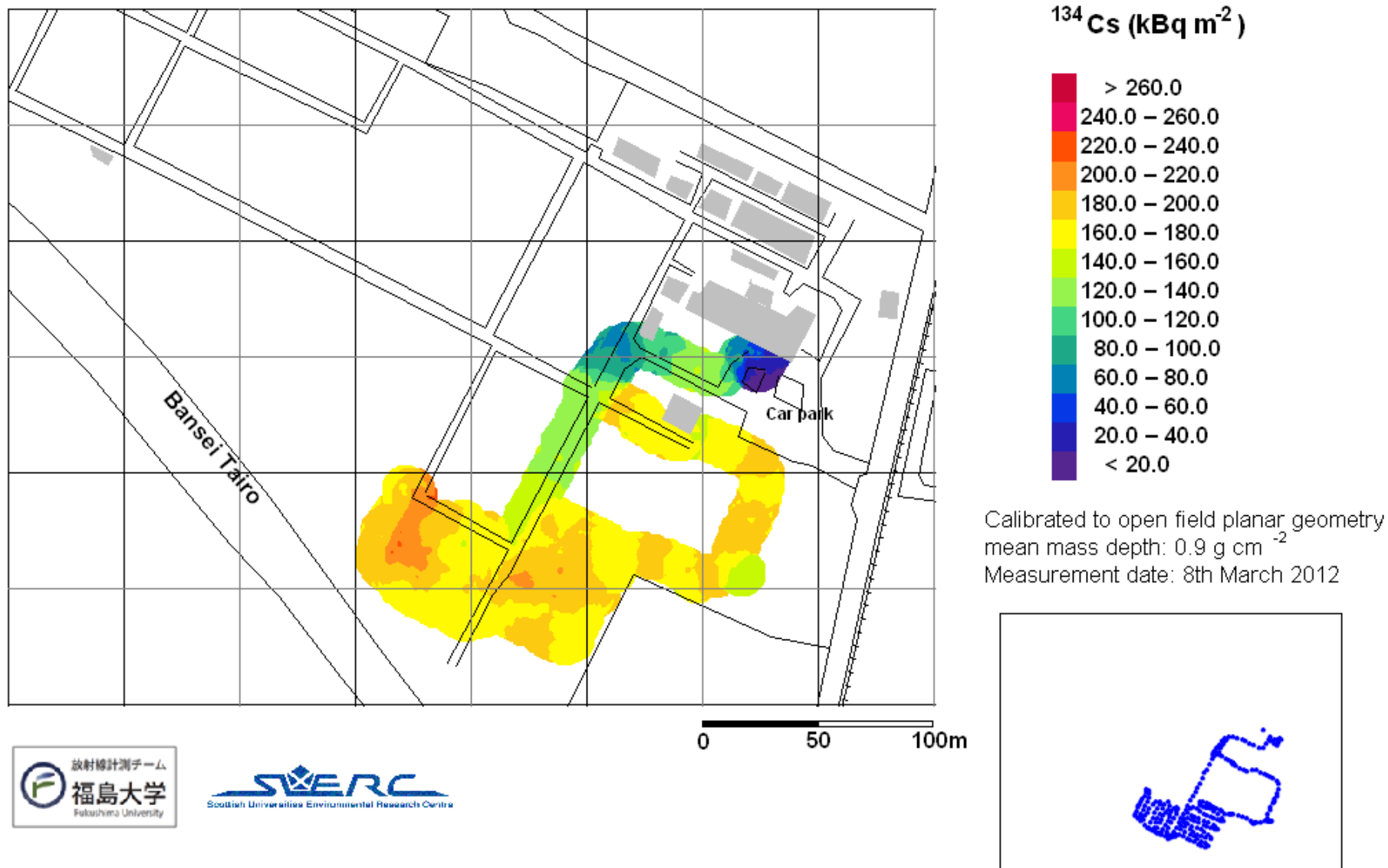


Figure 4.42: ^{134}Cs activity per unit area for the Fruit Tree Research Institute, measured 8th March 2012.

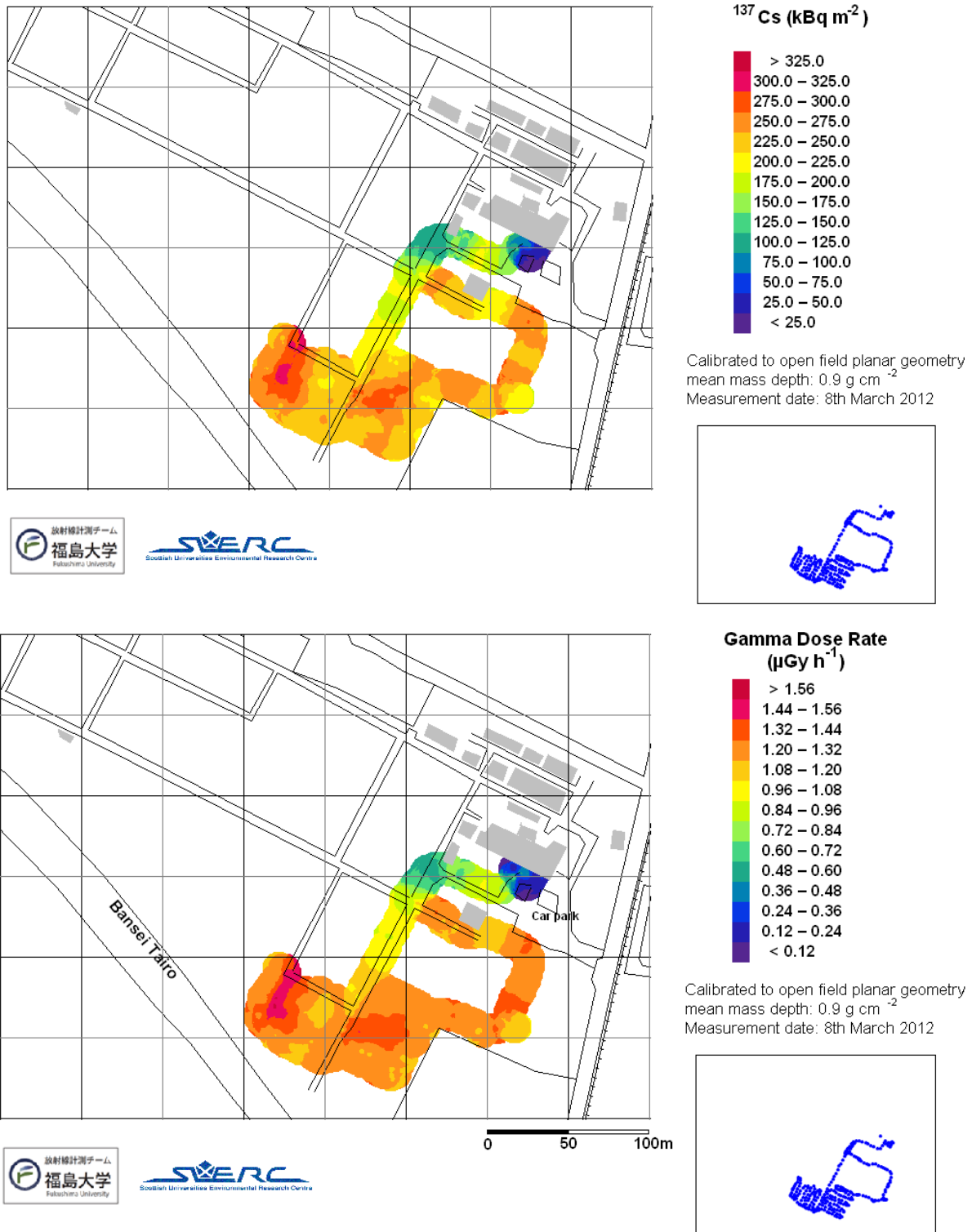


Figure 4.43: ^{137}Cs activity per unit area and dose rate for the Fruit Tree Research Institute, measured 8th March 2012.

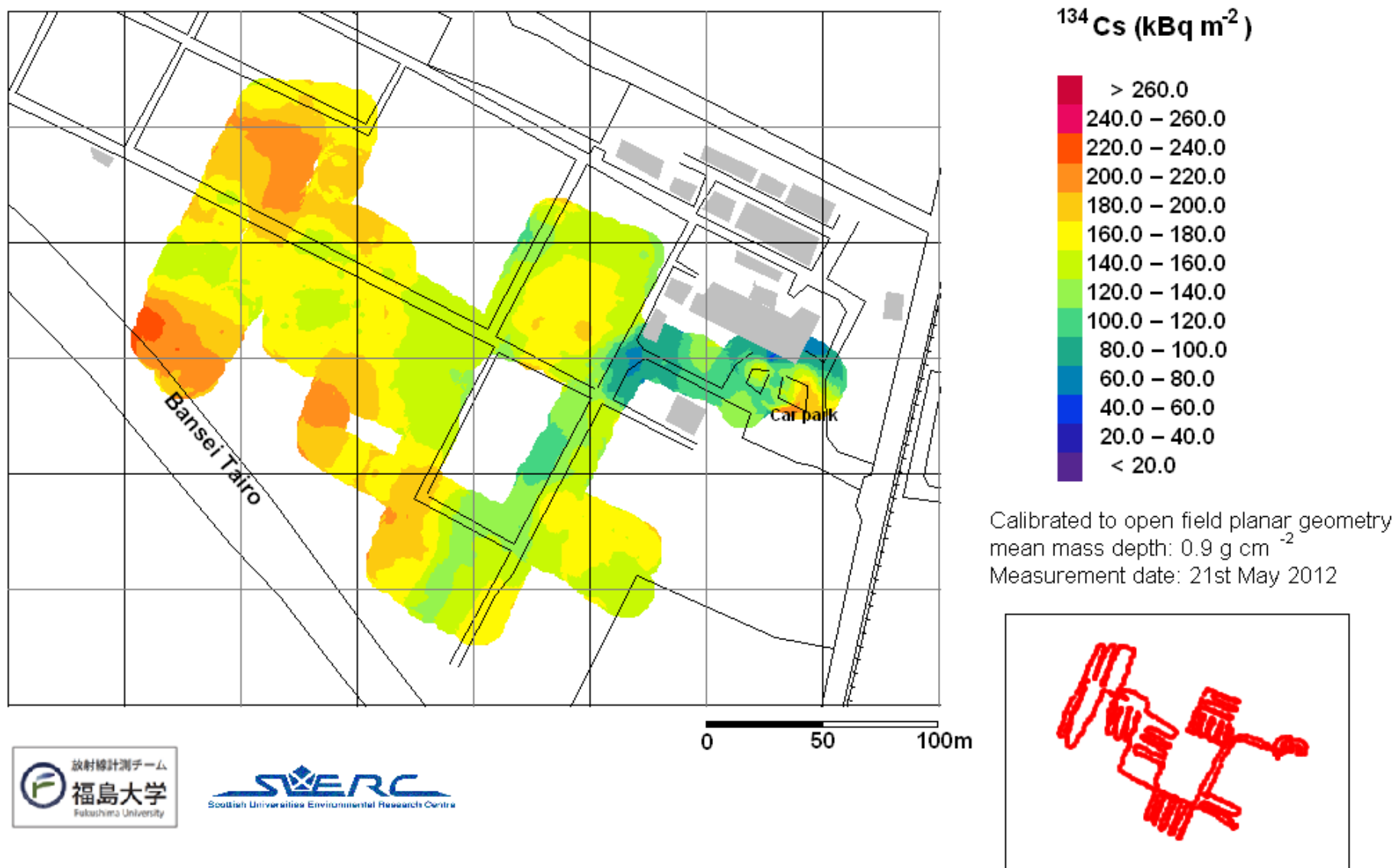
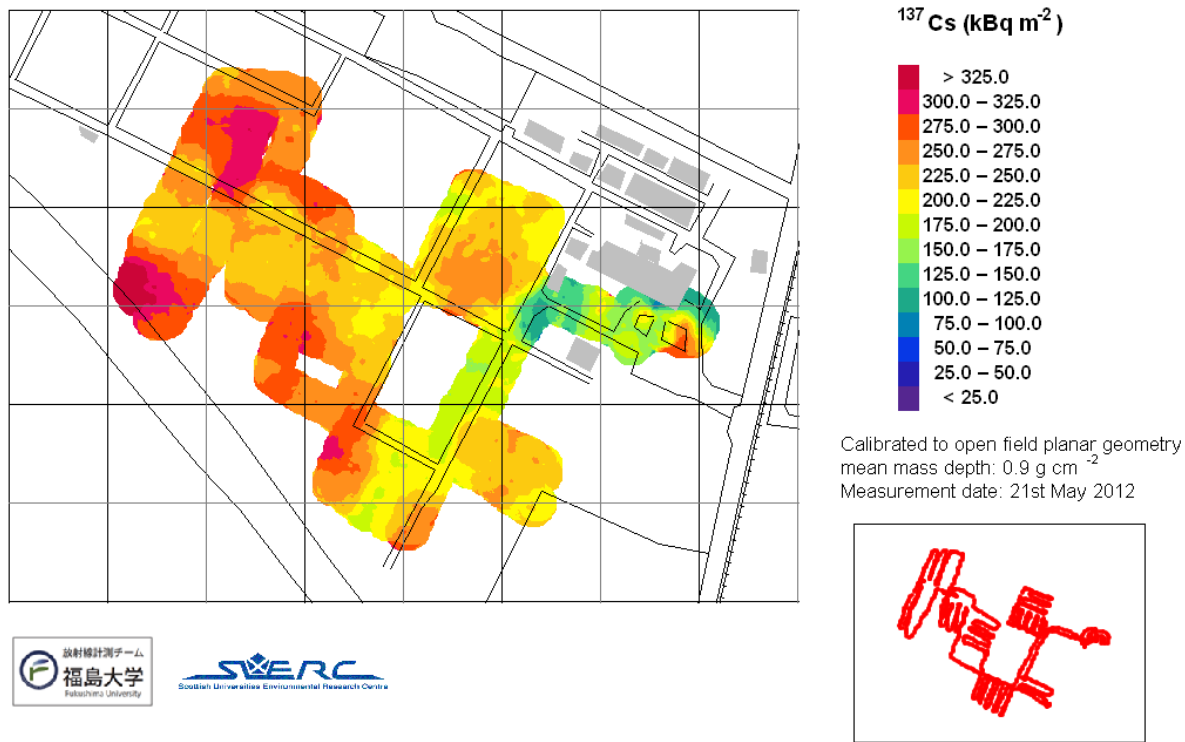
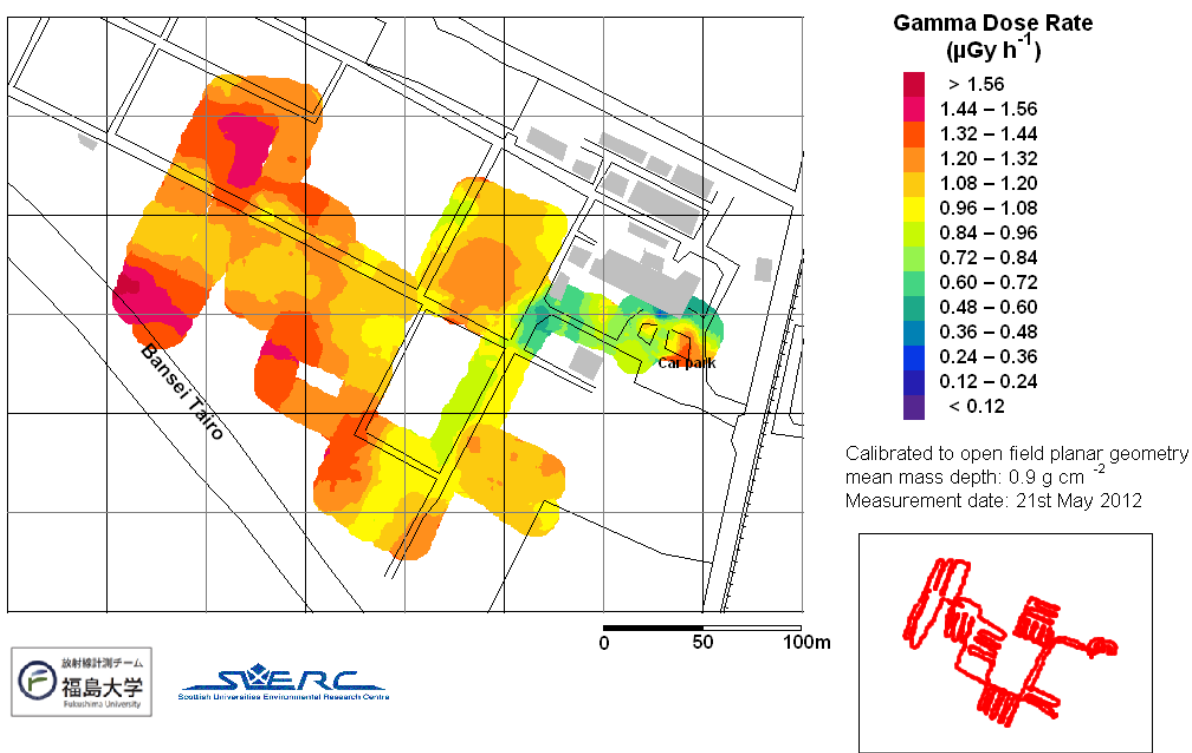


Figure 4.44: ^{134}Cs activity per unit area for the Fruit Tree Research Institute, measured 21st May 2012.



放射線計測チーム
福島大学
Fukushima University

SWERC
Scottish Universities Environmental Research Centre



放射線計測チーム
福島大学
Fukushima University

SWERC
Scottish Universities Environmental Research Centre

Figure 4.45: ^{137}Cs activity per unit area and dose rate for the Fruit Tree Research Institute, measured 21st May 2012.

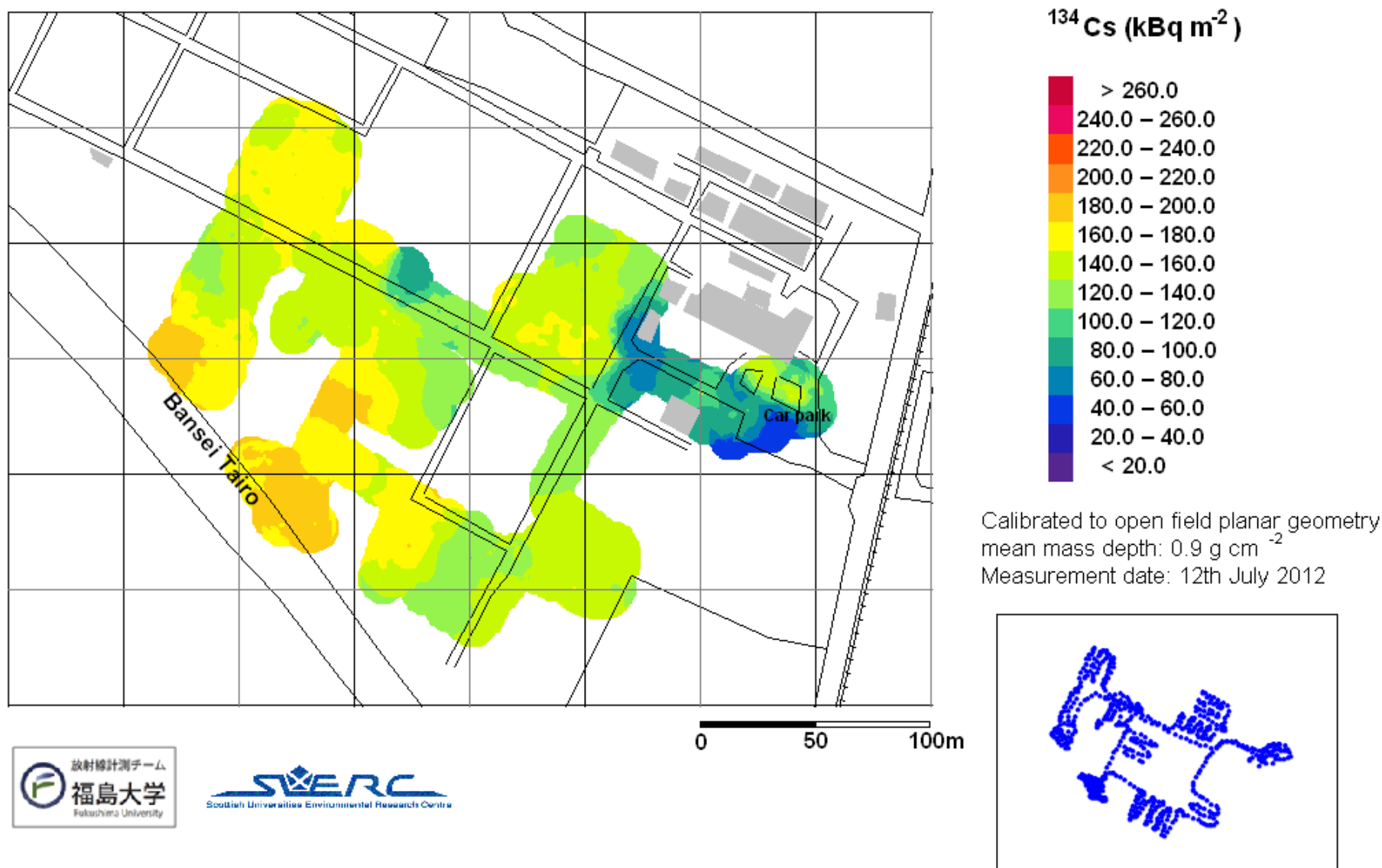


Figure 4.46: ^{134}Cs activity per unit area for the Fruit Tree Research Institute, measured 12th July 2012.

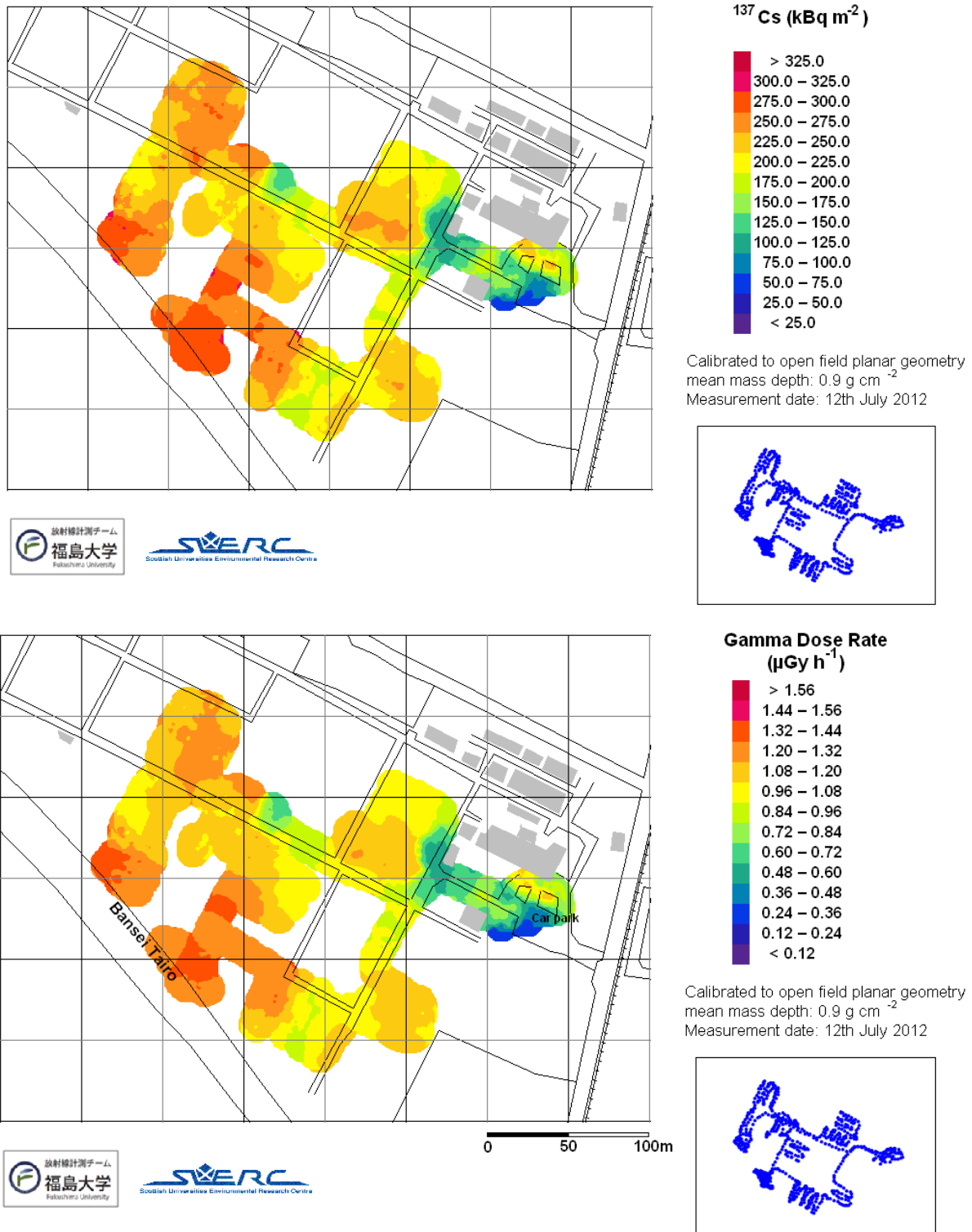


Figure 4.47: ^{137}Cs activity per unit area and dose rate for the Fruit Tree Research Institute, measured 12th July 2012.

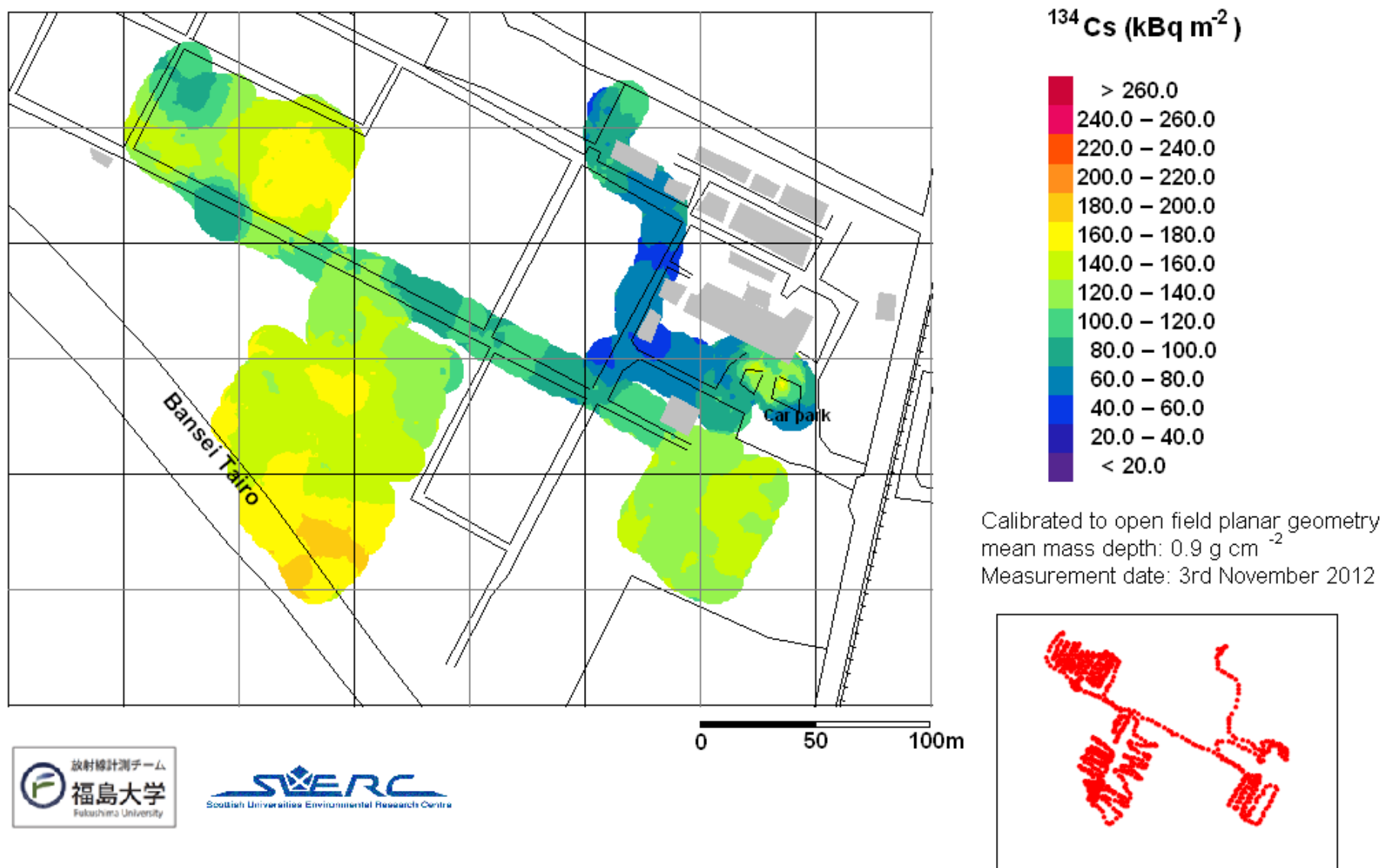


Figure 4.48: ^{134}Cs activity per unit area for the Fruit Tree Research Institute, measured 3rd November 2012.

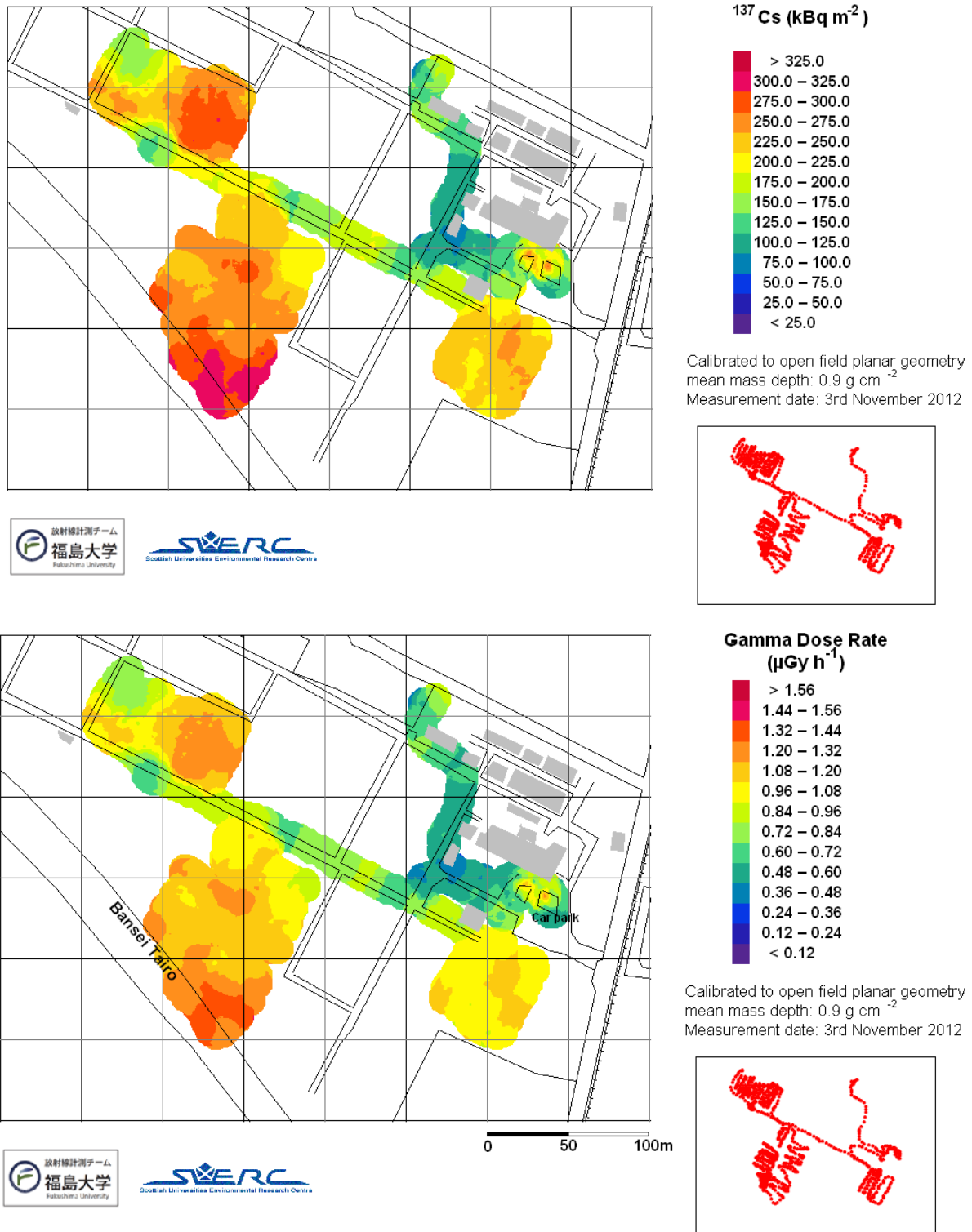


Figure 4.49: ^{137}Cs activity per unit area and dose rate for the Fruit Tree Research Institute, measured 3rd November 2012.

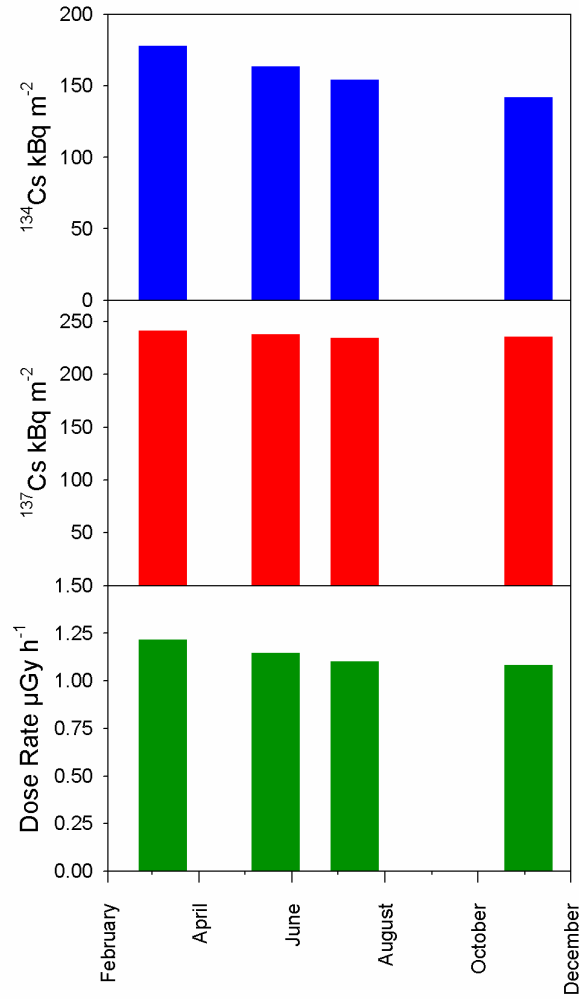


Figure 4.50: Time dependence of ^{134}Cs , ^{137}Cs and dose rate from all areas on the Fruit Tree research centre mapped in March, May, July and November 2012.

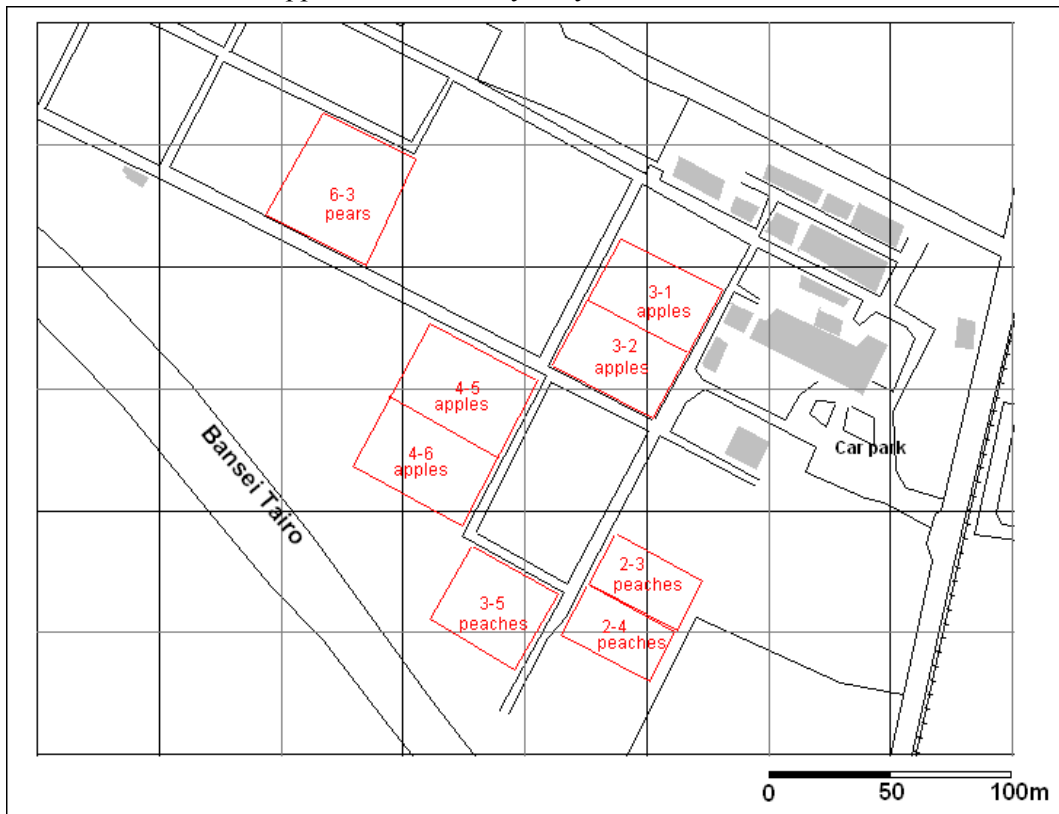


Figure 4.51: Fruit cultivation plots within the research station

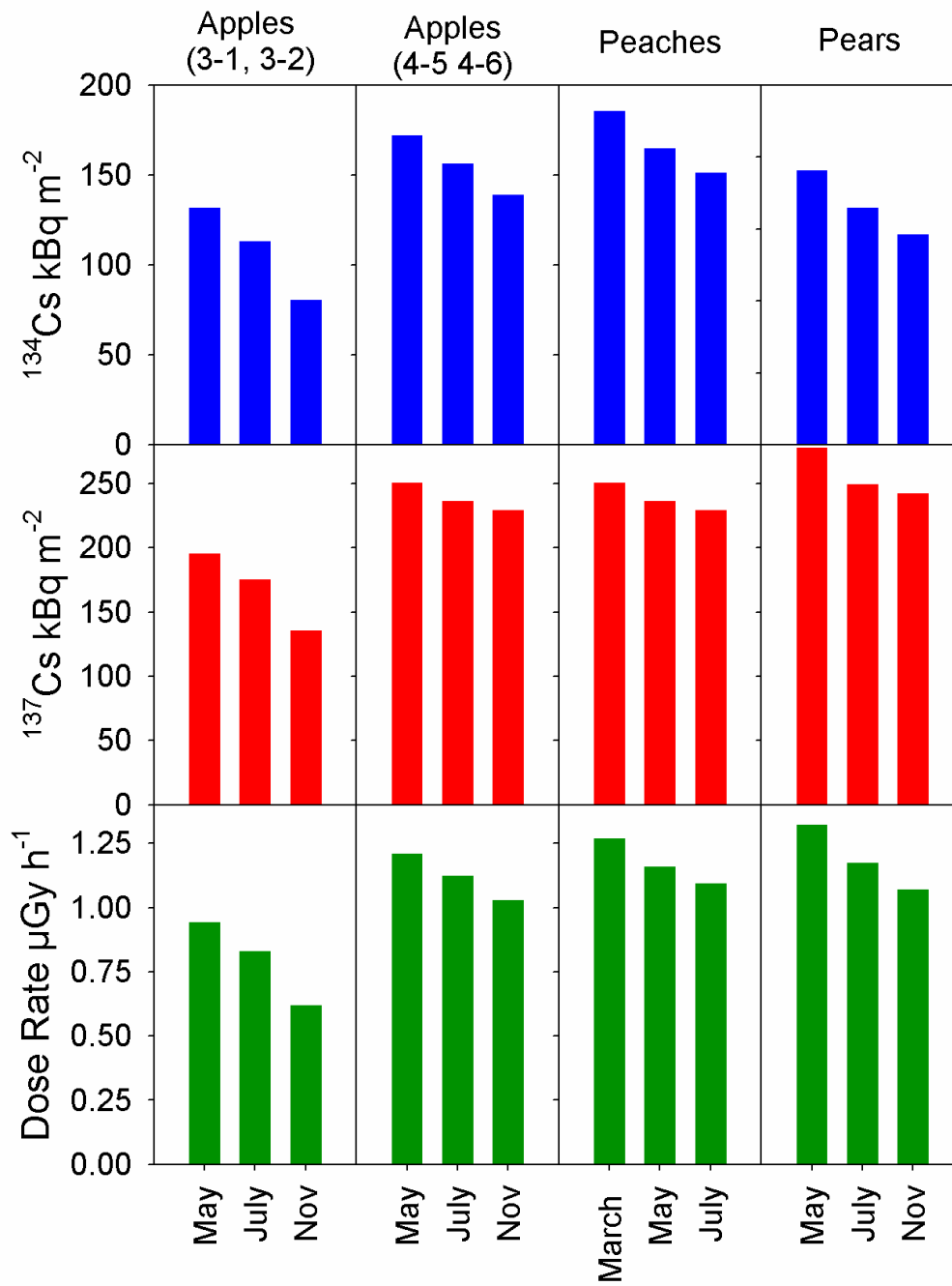


Figure 4.52: Time dependence of mean ^{134}Cs , ^{137}Cs activities and dose rates from the individual cultivation areas within the research institute (Figure 4.51).

	March 2012	May 2012	July 2012	November 2012
Dose Rate $\mu\text{Gy h}^{-1}$	1.218 ± 0.001	1.148 ± 0.005	1.101 ± 0.008	1.084 ± 0.007
$^{238}\text{U} + ^{235}\text{U}$ series	$0.58 \pm 0.04 \%$	$0.66 \pm 0.03 \%$	$0.91 \pm 0.03 \%$	$0.74 \pm 0.03 \%$
^{232}Th series	$0.94 \pm 0.05 \%$	$1.03 \pm 0.03 \%$	$1.02 \pm 0.04 \%$	$1.09 \pm 0.02 \%$
$^{40}\text{K} + ^{87}\text{Rb}$	$2.09 \pm 0.04 \%$	$2.16 \pm 0.02 \%$	$2.23 \pm 0.02 \%$	$2.53 \pm 0.02 \%$
^{137}Cs	$31.58 \pm 1.81 \%$	$33.01 \pm 1.88 \%$	$33.88 \pm 1.94 \%$	$35.71 \pm 2.04 \%$
^{134}Cs	$64.81 \pm 2.66 \%$	$63.14 \pm 2.54 \%$	$61.96 \pm 2.52 \%$	$59.94 \pm 2.43 \%$
Residual	$2.78 \pm 5.61 \%$	$2.67 \pm 5.51 \%$	$2.36 \pm 5.55 \%$	$5.88 \pm 5.53 \%$

Table 4.13: Dose rate apportionment for the four data sets from the Fruit Tree Research Institute.

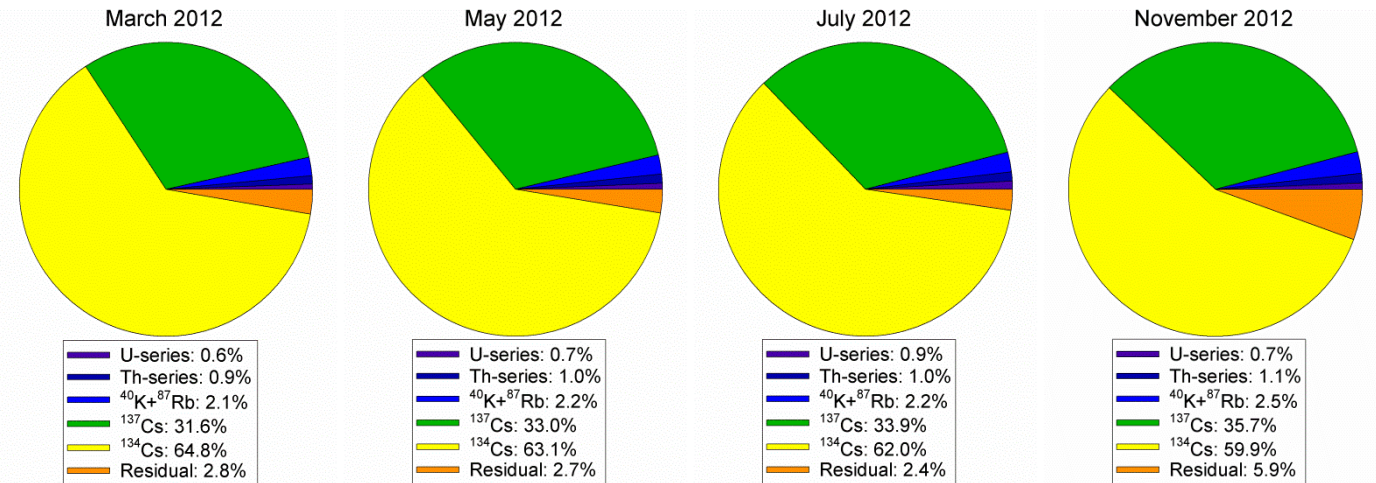


Figure 4.53: Dose rate apportionment for the four data sets from the Fruit Tree Research Institute.

4.3.2 Fruit Cultivation Areas in Fukushima Prefecture

In collaboration with staff from the Fruit Tree Research Institute, exploratory surveys of other areas of fruit cultivation in Fukushima Prefecture have been conducted. In July 2012 data were collected from citrus groves on Mount Shinobu and two areas near Date, with further data collected from Mount Shinobu and orchards near Date in November 2012.

On the 12th July 2012, data were collected around citrus groves on Mount Shinobu and in the vicinity of the viewpoint and childrens play areas nearer the summit. The GPS system registered incorrect positions during this survey, which has required a reconstruction of estimated positions using a small number of control points of known location. The reconstructed positions are within 20m of the most likely positions for each measurement. On the 3rd November 2012 additional data was collected from adjacent citrus groves on Mount Shinobu. The distribution of ^{134}Cs activity per unit area for the July survey of the citrus groves is shown in Figure 4.56, with the ^{137}Cs and dose rate shown in Figure 4.57. The corresponding distributions for the November 2012 surveys are shown in Figures 4.58 and 4.59. The ^{134}Cs , ^{137}Cs activity per unit area and dose rate for the survey of the viewpoint and play area nearer the summit in July 2012 are shown in Figure 4.60.

On the 24th of July two areas of fruit cultivation near Date were surveyed. The first was just south of Hashirazawa, in the south east of Date city. The second was at Ryozenmachi Shimooguni, about 8km further south. A persimmon orchard just south of the second site was

also surveyed on the 3rd November 2012. The ¹³⁴Cs and ¹³⁷Cs activity per unit area and dose rate for each of these areas are shown in Figures 4.61 to 4.63.



Citrus groves, Mount Shinobu, 12th July 2012



3rd November 2012



Play area on Mount Shinobu, $>250 \text{ kBq m}^{-2} \text{ }^{134}\text{Cs}$



Figure 4.54: Photographs of Mount Shinobu taken in July and November 2012.



Figure 4.55: Persimmon orchard near Ryozenmachi Shimooguni, 3rd November 2012.

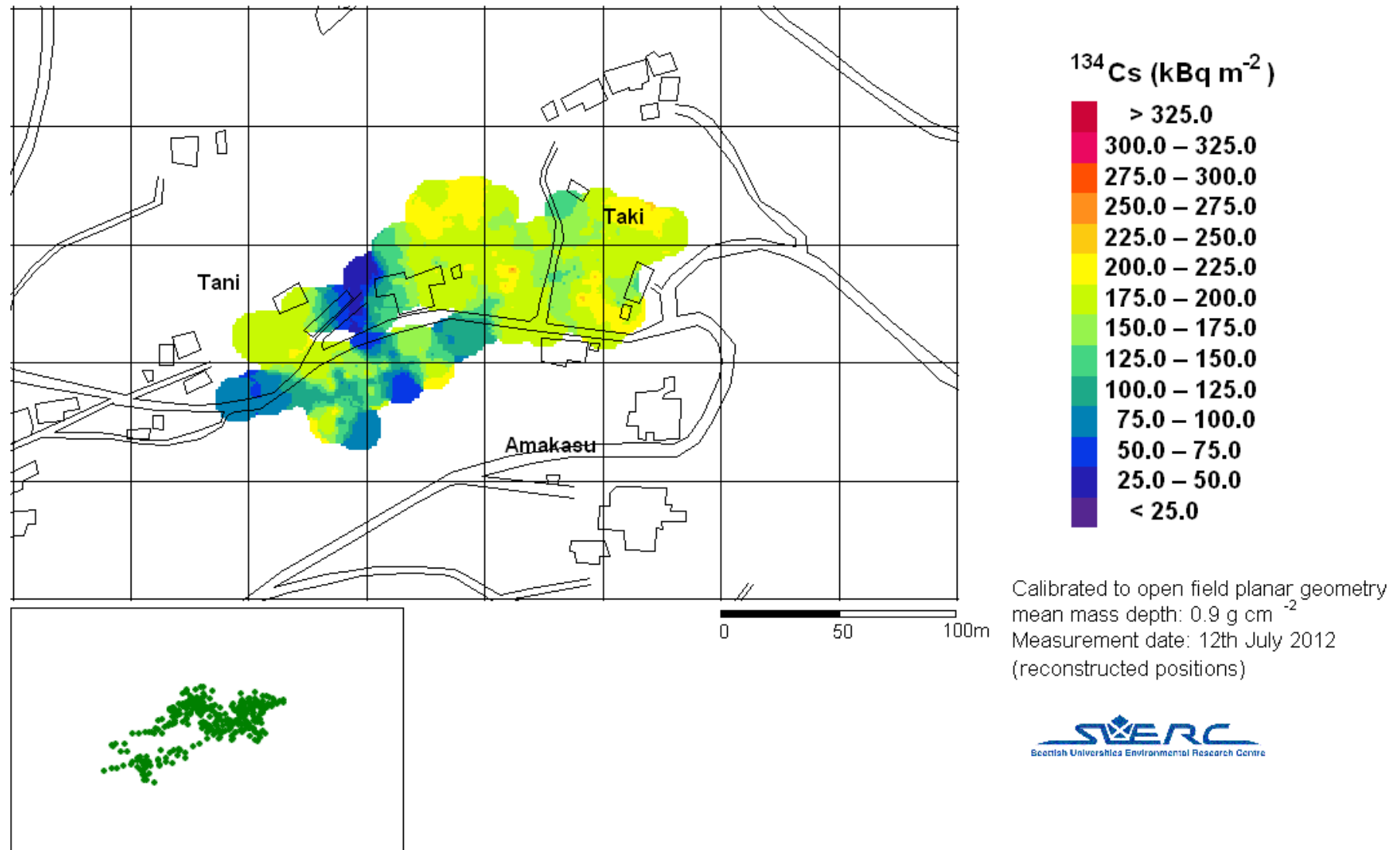


Figure 4.56: ^{134}Cs activity per unit area distribution for citrus groves on Mount Shinobu, 12th July 2012. Positions have been reconstructed from GPS locations with poor precision to within $\pm 20\text{m}$.

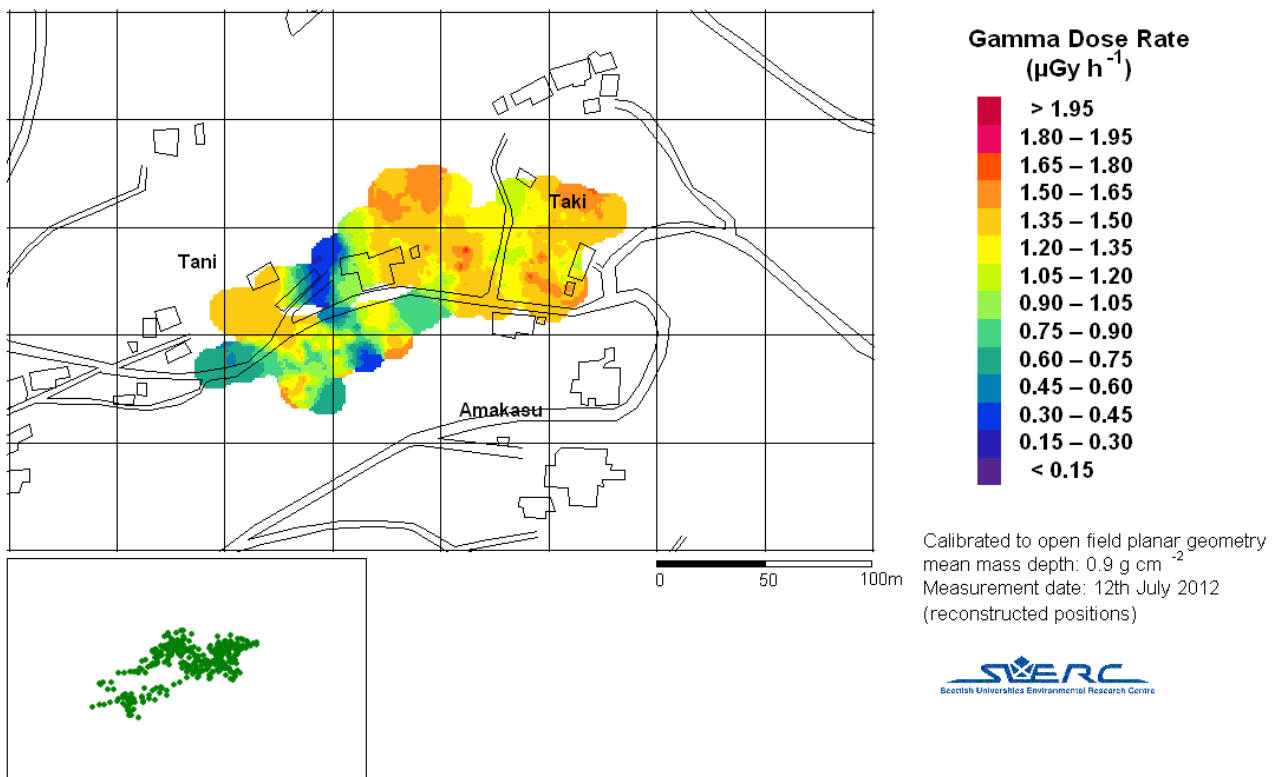
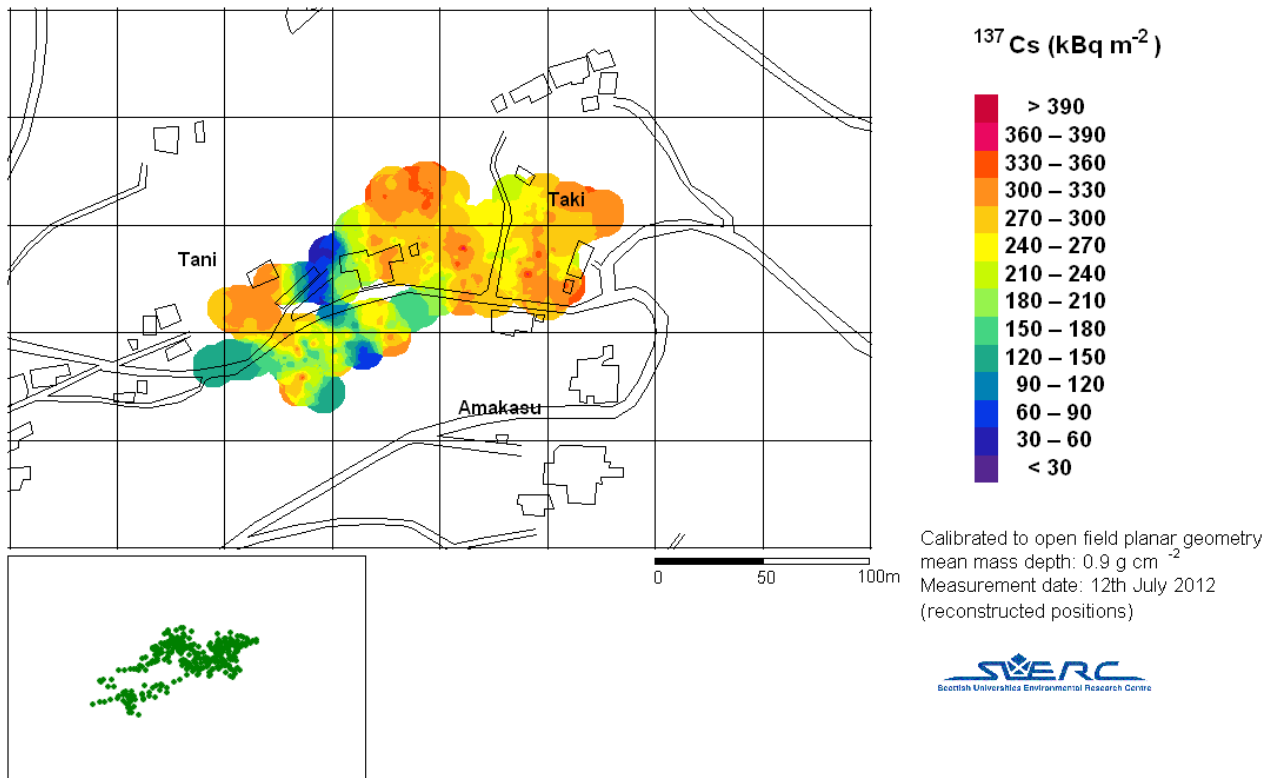


Figure 4.57: ^{137}Cs activity per unit area and dose rate distribution for citrus groves on Mount Shinobu, 12th July 2012. Positions have been reconstructed from GPS locations with poor precision to within $\pm 20\text{m}$

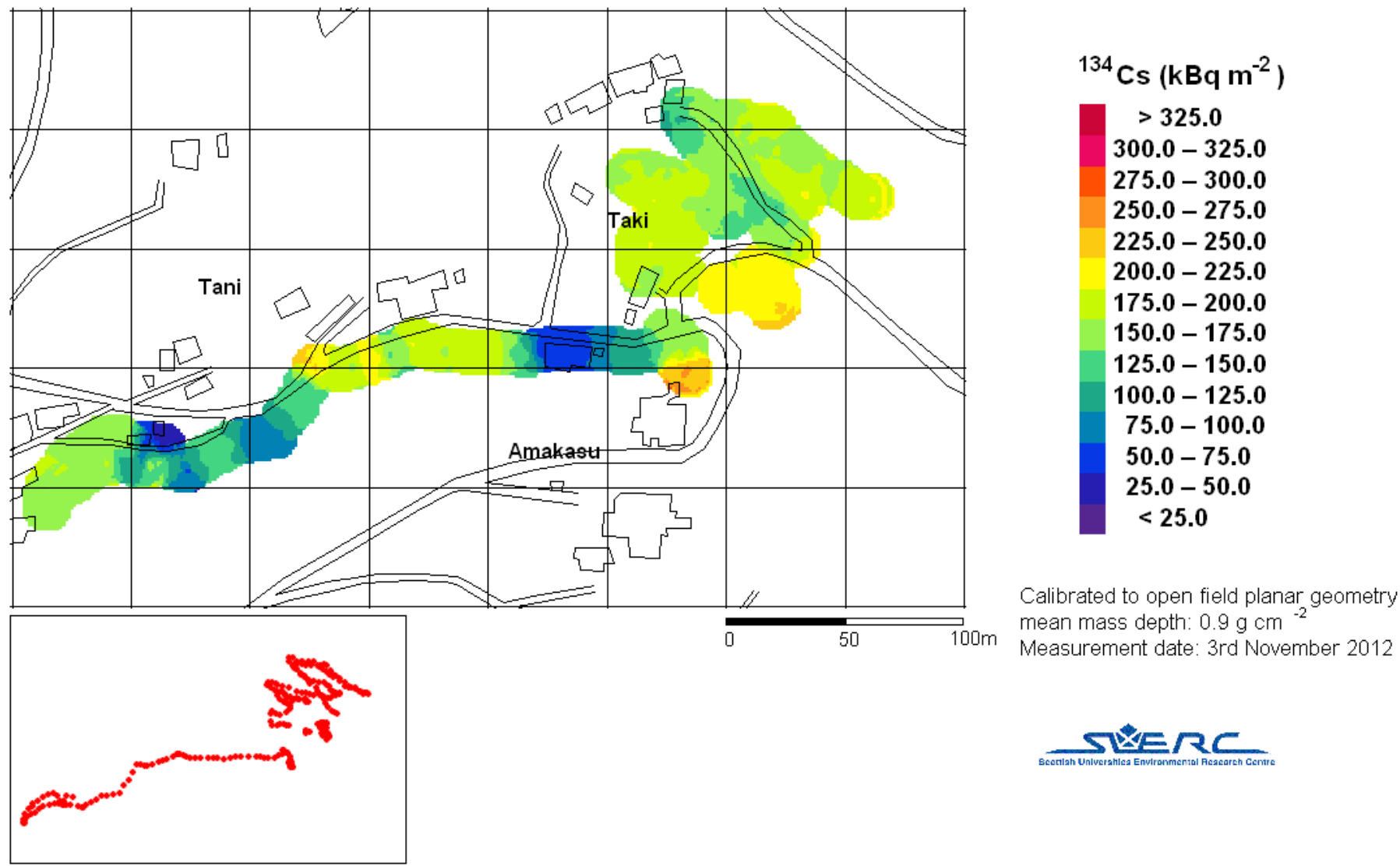


Figure 4.58: ^{134}Cs activity per unit area distribution for citrus groves on Mount Shinobu, 3rd November 2012.

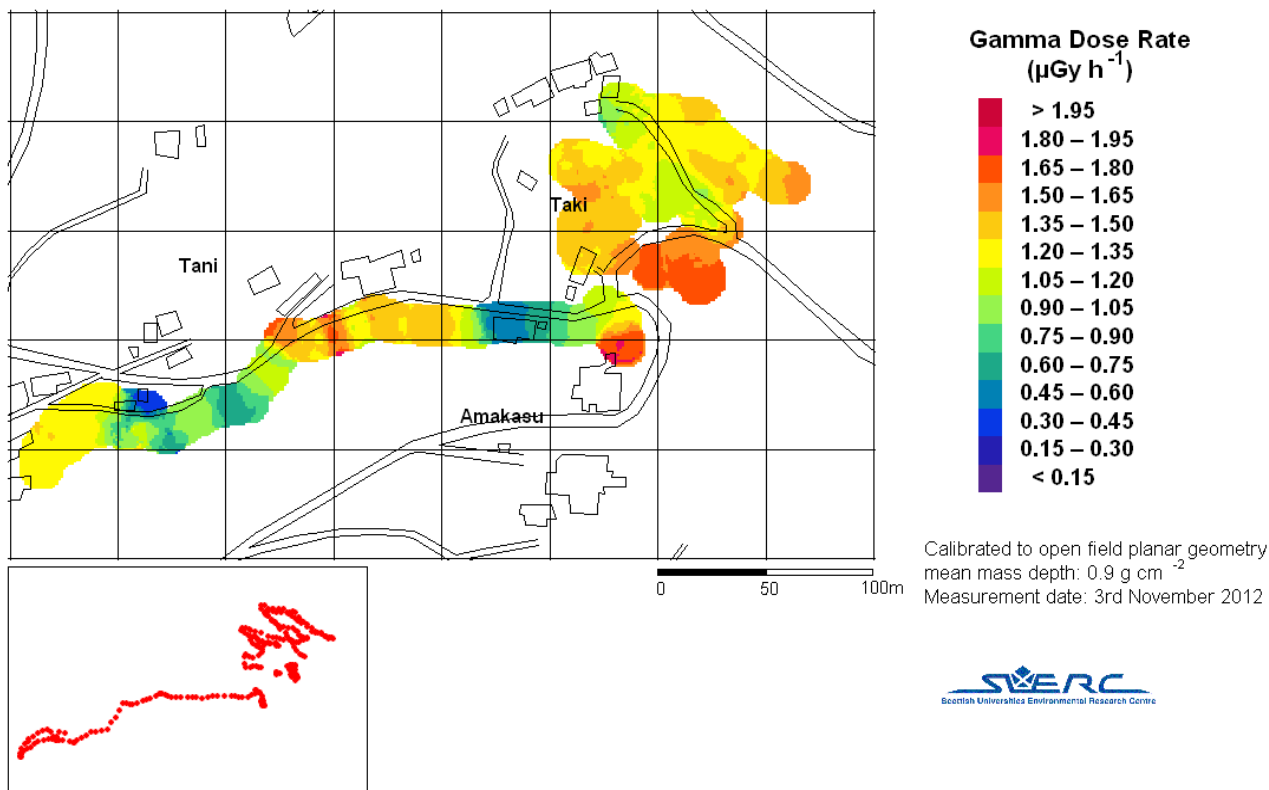
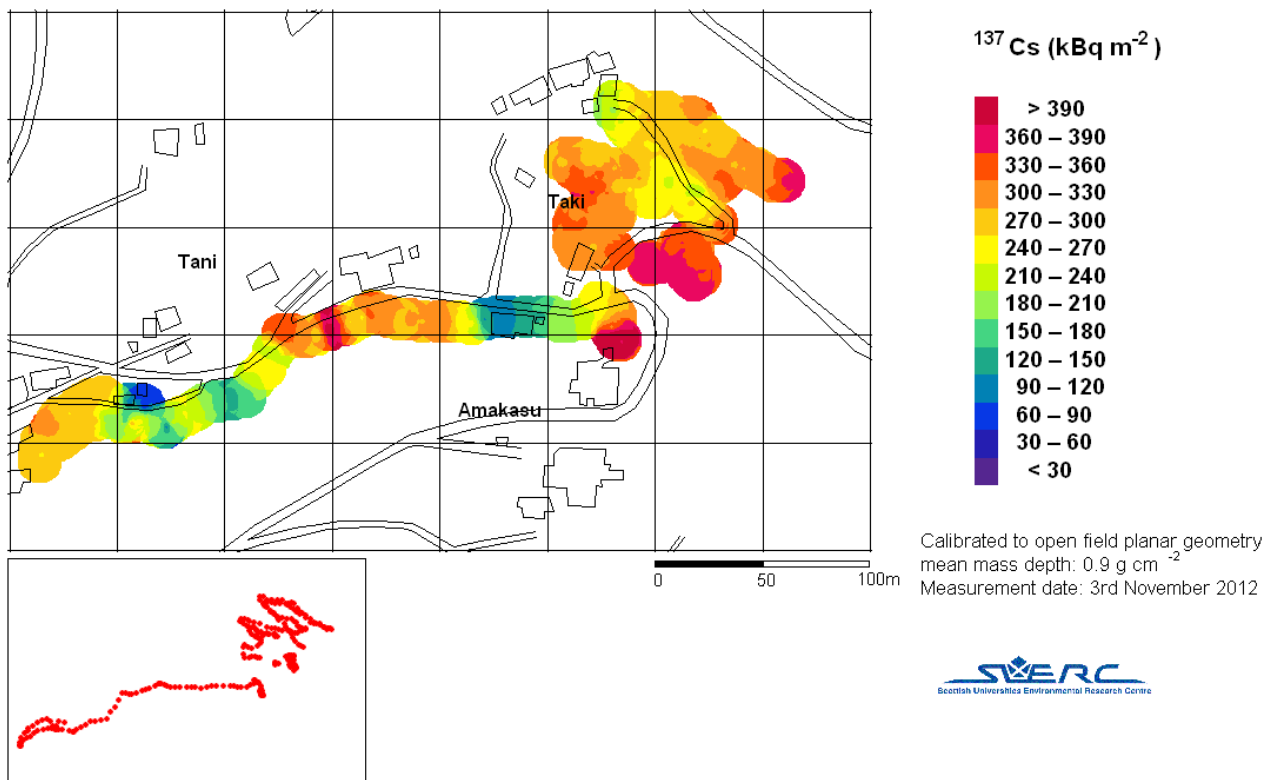


Figure 4.59: ^{137}Cs activity per unit area and dose rate distribution for citrus groves on Mount Shinobu, 3rd November 2012.

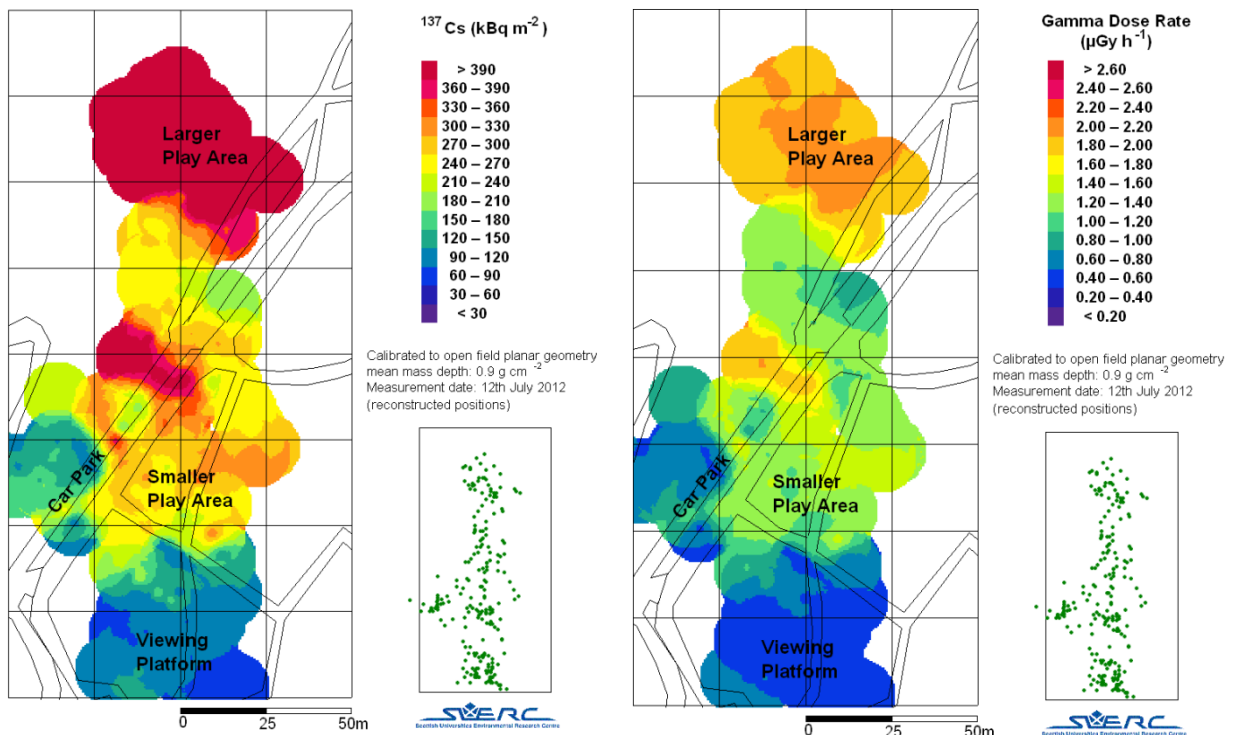
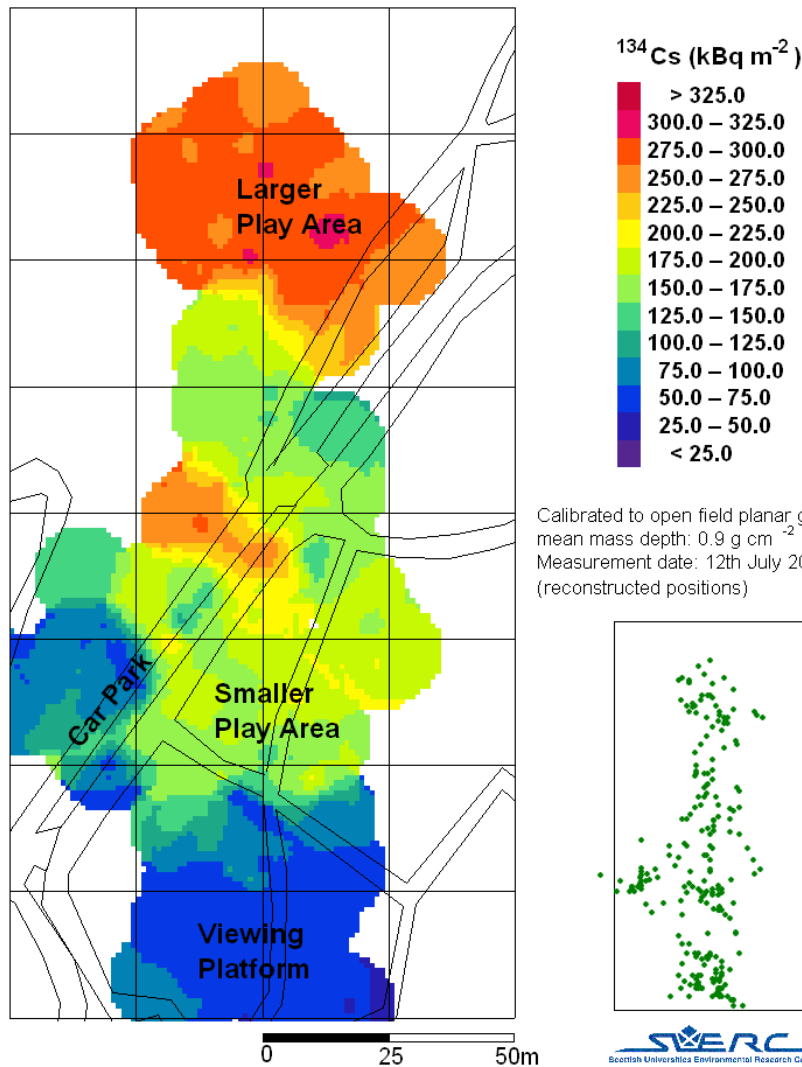


Figure 4.60: ^{134}Cs and ^{137}Cs activity per unit area and dose rate distribution for the viewpoint and playparks on Mount Shinobu, 12th July 2012. Positions have been reconstructed from GPS locations with poor precision to within $\pm 20\text{m}$.

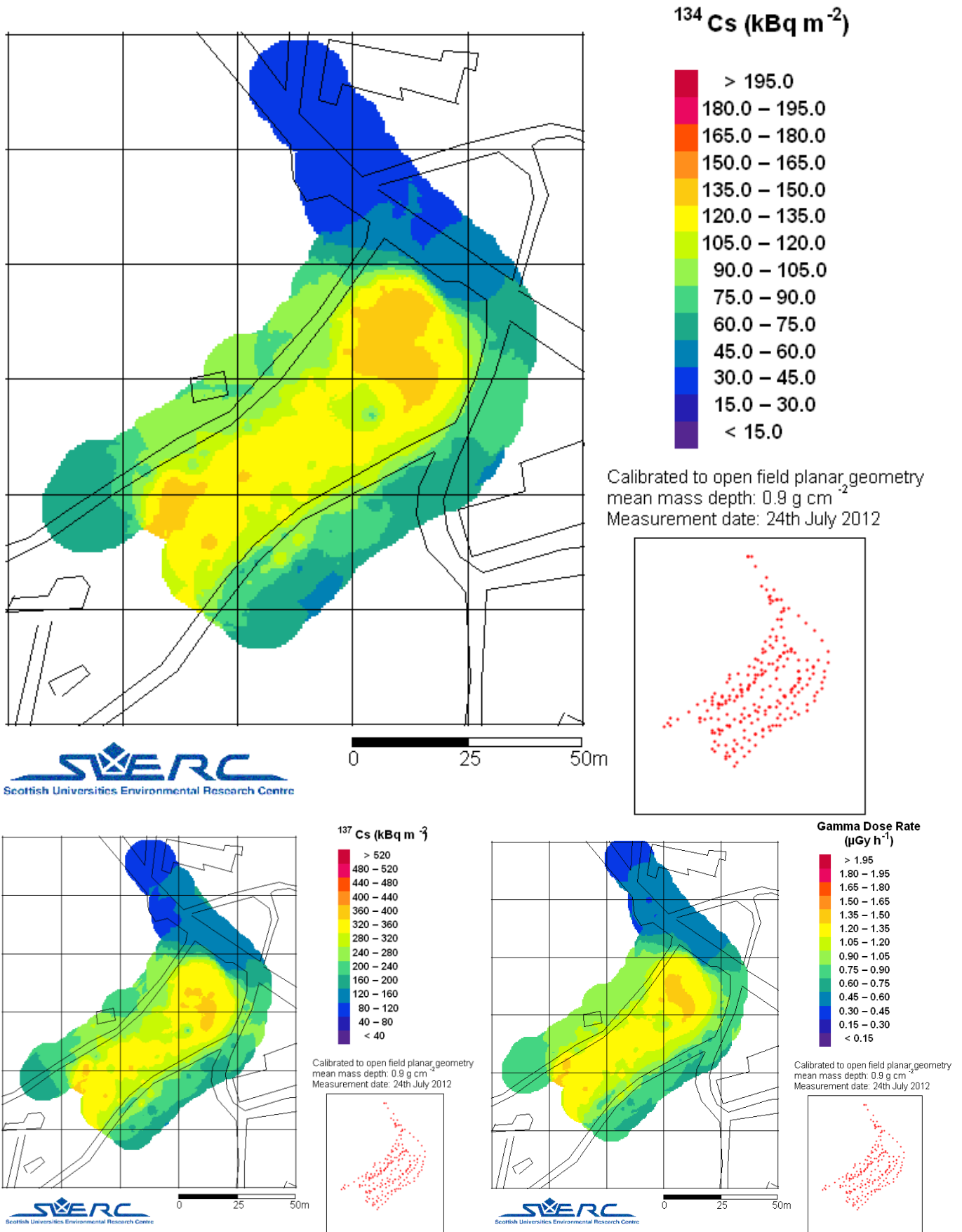


Figure 4.61: ^{134}Cs and ^{137}Cs activity per unit area and dose rate on an area of fruit cultivation near Hashirazawa, measured 24th July 2012.

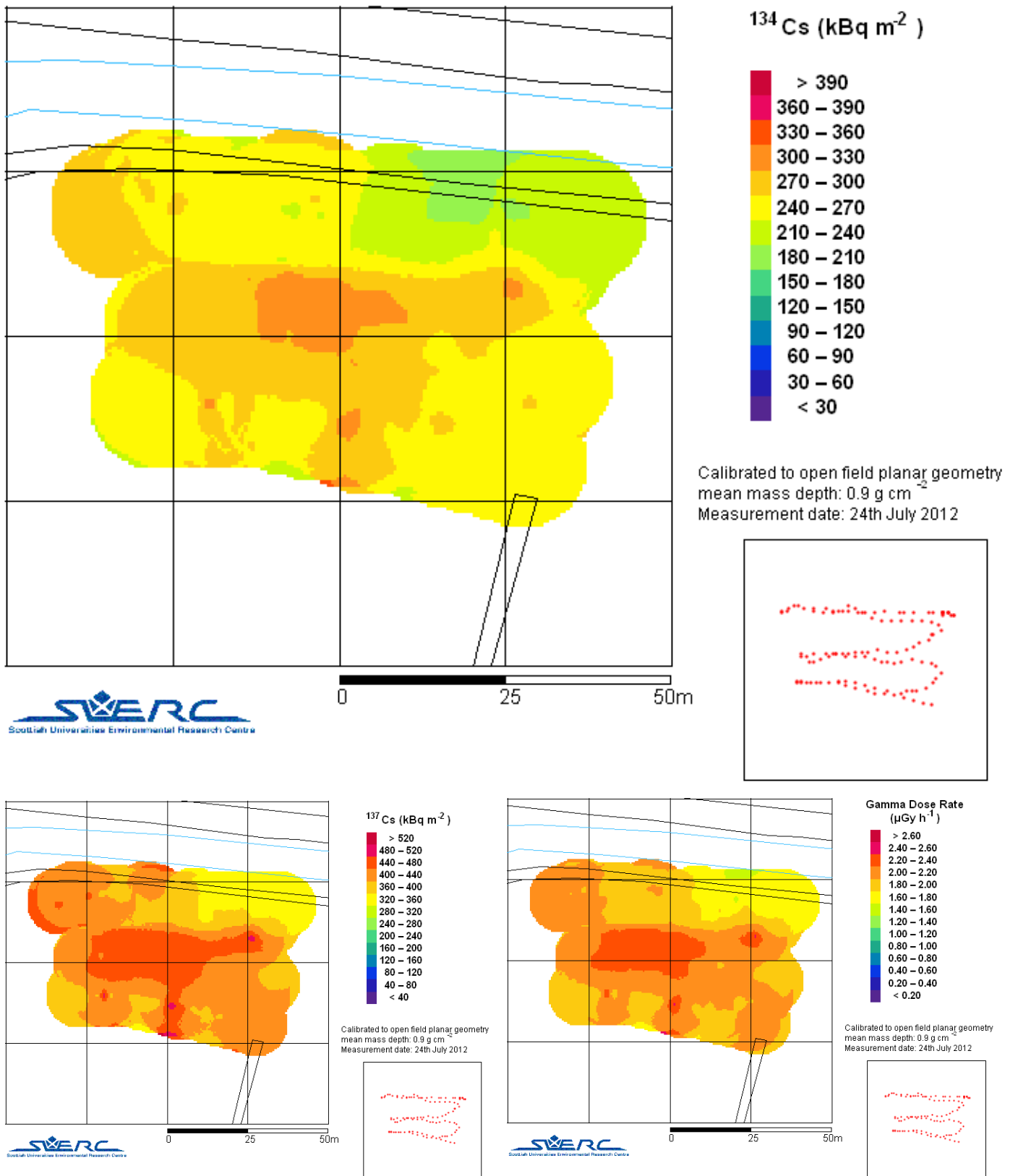


Figure 4.62: ^{134}Cs and ^{137}Cs activity per unit area and dose rate on an area of fruit cultivation near Ryozenmachi Shimooguni, measured 24th July 2012.

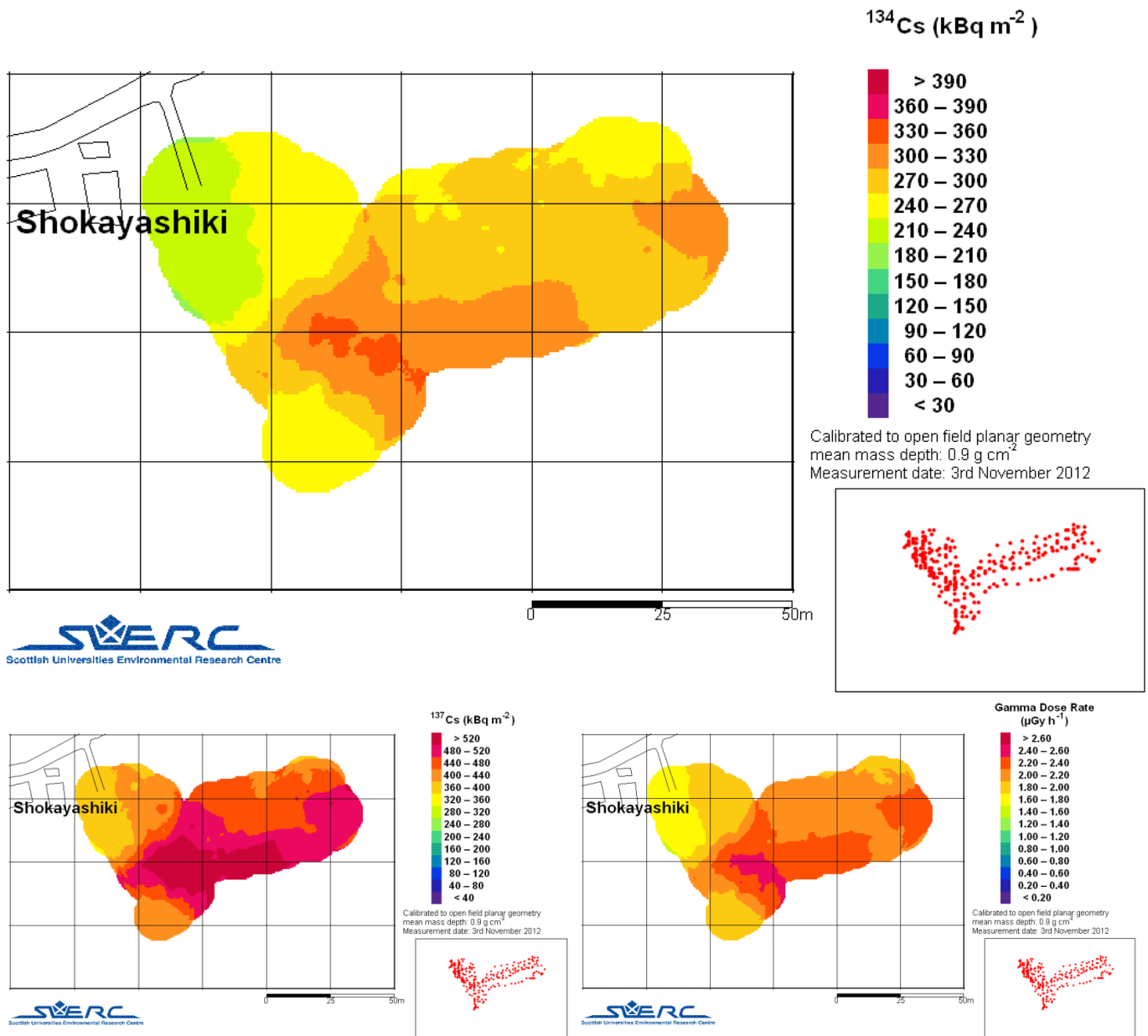


Figure 4.63: ^{134}Cs and ^{137}Cs activity per unit area and dose rate on an area of fruit cultivation near Ryozenmachi Shimooguni, measured 3rd November 2012.

4.3.3 Tsukuba

On the 3rd March 2012, an exploratory survey was conducted of the AFFRC at Tsukuba. The data include measurements inside the laboratory buildings and some plots outside. On the 5th November 2012, the system was again used to collect data at AFFRC, and the neighbouring NIRE site, summary statistics for these surveys are given in Table 4.12.

For the exploratory survey in March the data were logged without positional information. The average spectrum recorded outside the building is shown in Figure 4.64, with the distinctive high yield gamma rays of ^{134}Cs and ^{137}Cs , and gamma rays from natural radionuclides, clearly evident. Data recorded inside the buildings show low levels of radiocaesium (mean \pm standard deviation for ^{137}Cs 1.3 ± 1.9 , and for ^{134}Cs 1.5 ± 1.2 kBq m⁻²) and dose rate (0.058 ± 0.005 $\mu\text{Gy h}^{-1}$). Outside the buildings, the activity concentrations and dose rate are much higher (^{137}Cs 29.5 ± 10.3 , ^{134}Cs 22.7 ± 6.9 , dose rate 0.176 ± 0.038).

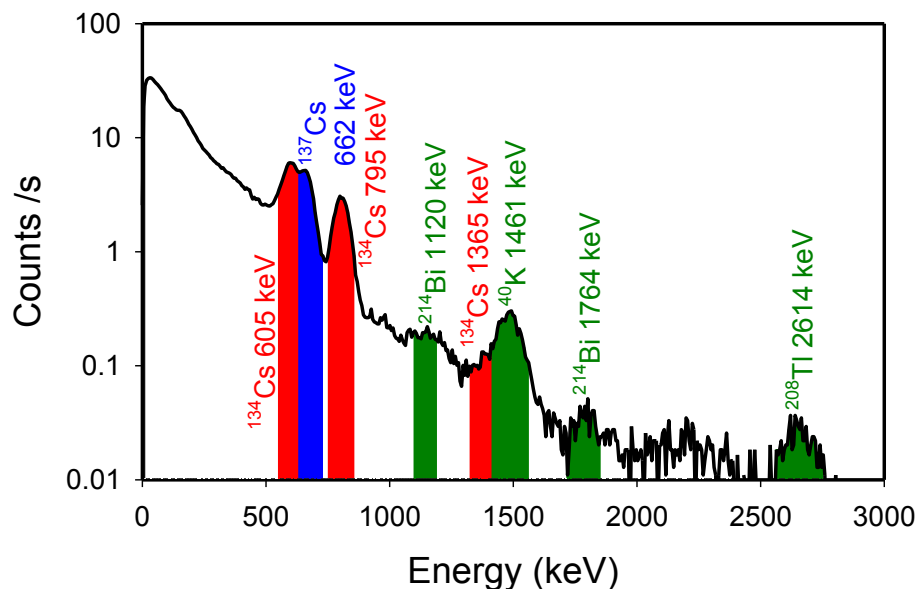


Figure 4.64: Average spectrum for data recorded at AFFRC, Tsukuba, in March 2012.



Figure 4.65: Demonstration of SUERC radiometric system at Tsukuba, 5th November 2012, with difference in activity concentrations on grass and hard surfaces apparent.



Area of experimental plots where soil has been removed



Figure 4.66: Radiometric surveys on test plots at NIRE, AFFRC, Tsukuba, 5th November 2012.

The distribution of ^{134}Cs and ^{137}Cs activity per unit area and dose rate measured in November is shown in Figures 4.67 and 4.68 for the two sites. The NIRE site survey covered two experimental plots. On one of these two square sections had been remediated by removal of soil, on the other plot soil had been removed from a narrow strip. The effect of this decontamination is clearly evident in Figure 4.68. The higher levels of radiocaesium activity concentrations and dose rate associated with trees along the edges of these plots are also apparent. This may represent increased deposition in these areas as a result of interception by the trees, or a change in source geometry if the trees contain significant concentrations of radiocaesium.

The dose rate apportionment for the data collected at Tsukuba in March and November 2012 is given in Table 4.14 and Figure 4.69. The two data sets cover slightly different areas, nevertheless there is a reduction in the contribution to dose rate from anthropogenic activity between the two surveys, from 75% to 70%, reflecting the reduction in mean activity per unit area between the two surveys.

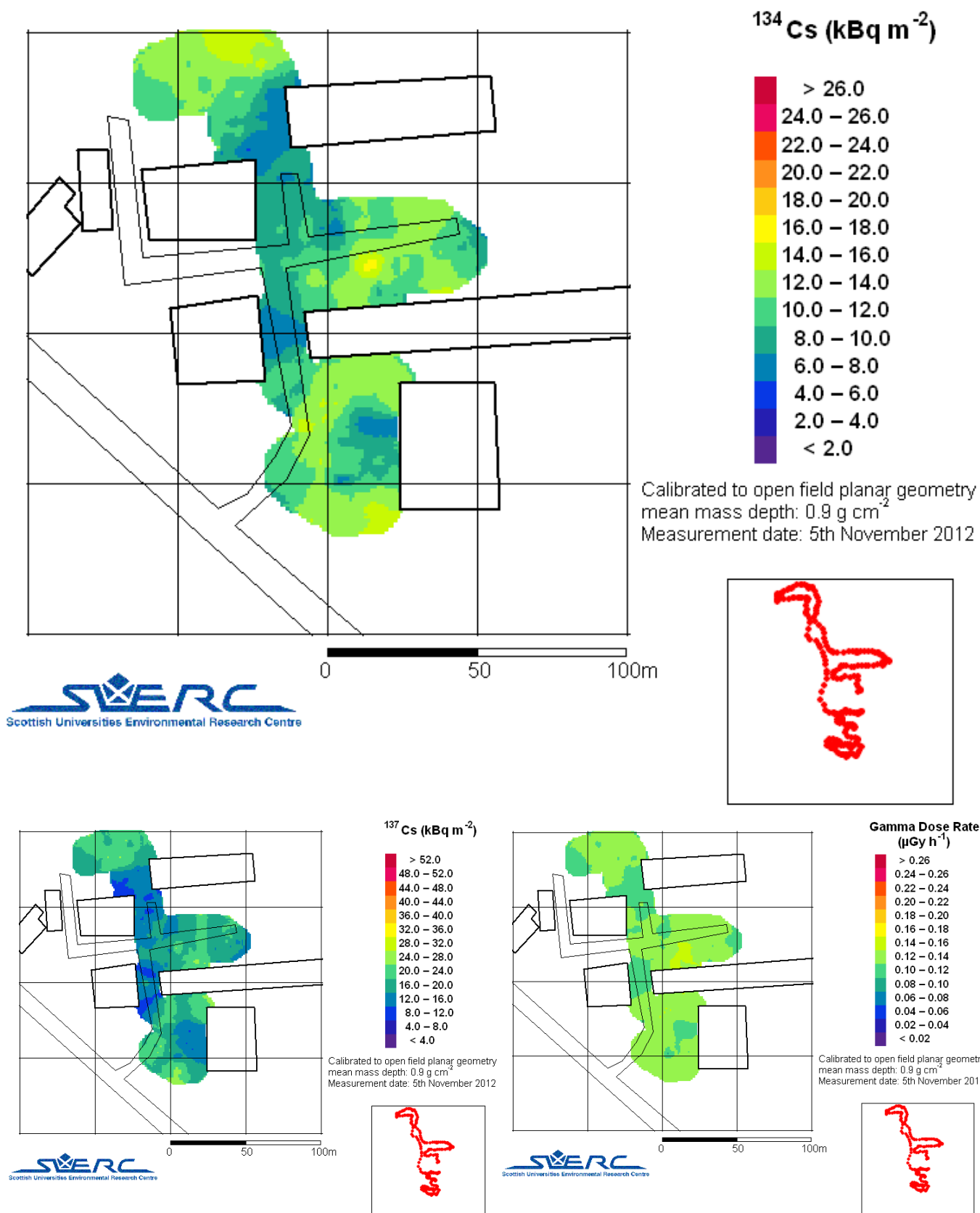


Figure 4.67: ^{134}Cs and ^{137}Cs activity per unit area and dose rate for the NFRE, Tsukuba, measured 5th November 2012.

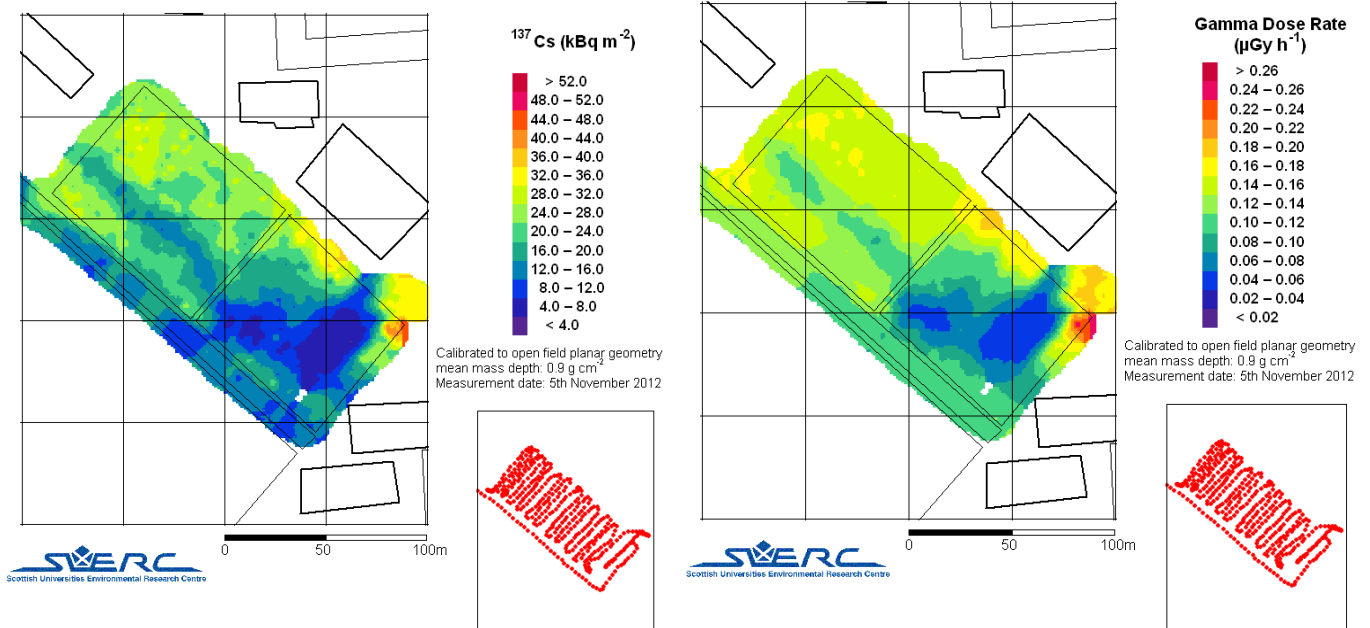
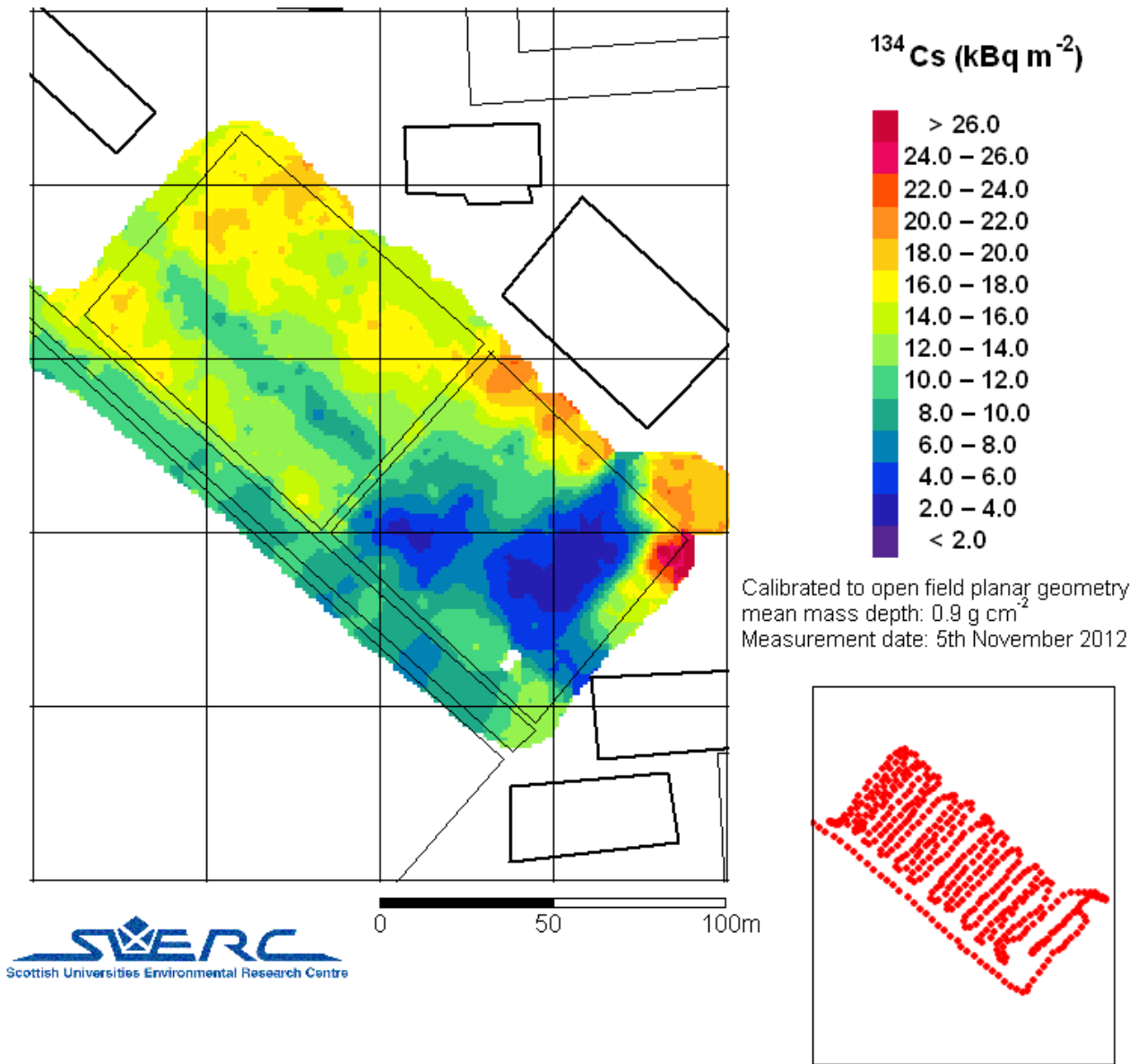


Figure 4.68: ^{134}Cs and ^{137}Cs activity per unit area and dose rate for the NIRE, Tsukuba, measured 5th November 2012.

	March 2012 (outside)	March 2012 (inside)	November 2012
Dose Rate $\mu\text{Gy h}^{-1}$	0.176 ± 0.003	0.058 ± 0.001	0.128 ± 0.007
$^{238}\text{U} + ^{235}\text{U}$ series	$4.97 \pm 0.45 \%$	$36.6 \pm 3.1 \%$	$5.78 \pm 0.45 \%$
^{232}Th series	$8.29 \pm 0.52 \%$	$33.8 \pm 2.8 \%$	$11.4 \pm 0.8 \%$
$^{40}\text{K} + ^{87}\text{Rb}$	$10.7 \pm 0.5 \%$	$14.9 \pm 1.8 \%$	$13.5 \pm 0.8 \%$
^{137}Cs	$24.4 \pm 1.6 \%$	$3.6 \pm 0.7 \%$	$24.9 \pm 1.5 \%$
^{134}Cs	$51.6 \pm 3.1 \%$	$11.1 \pm 1.6 \%$	$44.5 \pm 2.5 \%$
Residual	$-6.6 \pm 7.0 \%$	$3.5 \pm 11.2 \%$	$3.5 \pm 6.8 \%$

Table 4.14: Dose rate apportionment for the two data sets from Tsukuba.

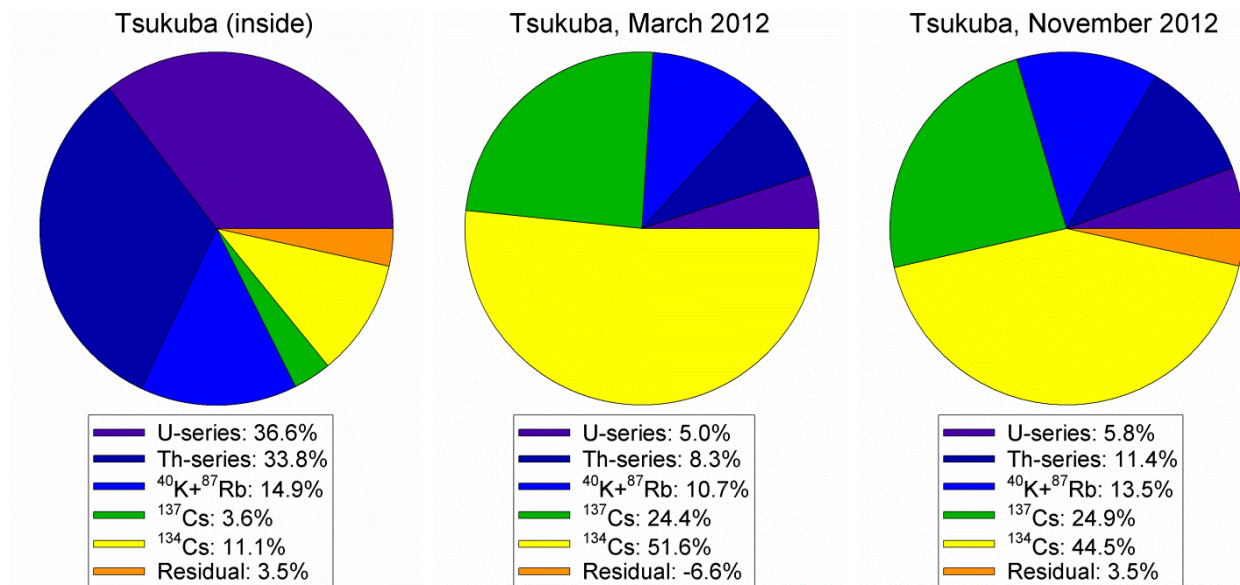


Figure 4.69: Dose rate apportionment for the March and November 2012 data sets from Tsukuba. In March 2012 the interior dose rate (left hand side) from accident nuclides represent a smaller proportion than outside (centre) the NFRI building. By November the decay of ^{134}Cs can also be seen (right hand side).

4.3.4 Discussion of Surveys of Areas of Fruit Cultivation

The surveys of fruit cultivation areas have demonstrated the high spatial resolution achievable with backpack systems. In more sparse orchards, the survey resolution allows deposition to be evaluated for individual trees. The radiometric data can thus be linked directly with data for the activity concentrations in the fruit from individual trees.

There is a complex system of routes for uptake of radioactivity by the trees, and subsequent transportation to the edible portions of the fruit. Direct deposition onto the tree is known to be one route of uptake, with post-Chernobyl studies showing uptake through leaves. Deciduous trees in Japan had not started growing new leaves after the winter at the time of the Fukushima Daiichi accidents, and so this is not a significant route of uptake of initial deposition. However, direct deposition onto bark has been shown to be a route of uptake. Following the initial deposition of activity in March 2011, some of the activity deposited directly onto the trees would have been removed by rain action and other processes, initially to the soil below the tree. Further deposition onto the trees would require resuspension of activity from the local environment.

As time passes since the accidents, activity deposited onto the surface of soils will migrate to greater depth in the soil column, with lateral migration of activity also possible. Repeat surveys, with some associated soil core sampling, will allow the rate of migration to be assessed. As the activity reaches greater depths it will intercept the rooting zone of the trees, and hence be more available for uptake by the roots. Thus, over time the uptake pathways will change.

4.4 Assessment of Radionuclide Ratio

The relative concentration of radionuclides within a nuclear reactor is a function of the fuel history of that particular reactor. Even within a single reactor different fuel elements will have experienced different neutron radiation fluxes and durations, and so it is expected that the radionuclide concentrations in different parts of a reactor core will vary. In a reactor, post shut down heating is primarily powered by the decay of fission products. Older fuel has a higher concentration of longer lived fission products compared to newer fuel, and will generate more post shut down heating than newer fuel that has experienced a similar recent radiation flux. In older fuel short lived fission and activation products will be saturated, or closer to saturation, than longer lived isotopes which will continue to grow in. Thus, it is expected that activity ratios for short lived isotopes to longer lived isotopes will be lower in older fuel. In particular, the $^{134}\text{Cs}:$ ^{137}Cs ratio for older fuel is, to first order, expected to be lower than in younger fuel. At the Fukushima Daiichi plant, reactor 1 had the oldest fuel at the time of the accident, followed by reactor 3 and then reactor 2. This resulted in greater post shut down heating in the reactors with older fuel, and the sequence of accidents followed this sequence with the reactor generating most heat releasing activity first.

Sections from four air filters collected at Tsukuba in March 2011 have been given sent to SUERC for ^{129}I analysis. As part of the characterisation of these samples, they were measured using high resolution gamma spectrometry methods to better than 1% precision on the ^{137}Cs peak count rate. Measurements were conducted on a thin n-type Ge (LoAx) detector with a cosmic-ray suppression system, with measurement times of 300 to 500 thousand seconds per sample. The count rates for the three dominant peaks from ^{137}Cs and ^{134}Cs are given in Table 4.15, with the associated ratios of count rates also shown in Figure 4.70. The count rate ratios vary by 7%, significantly larger than the measurement uncertainties. The first filter sample has the lowest ratio, the two filters collected 12h apart on the 16th March have ratios that are statistically indistinguishable, the filter collected on the 23rd March has the highest ratio. This clearly illustrates that different phases of release had different isotopic compositions. The ratios follow the expected sequence of releases, with earlier releases having a lower $^{134}\text{Cs}:$ ^{137}Cs ratio as would be expected from older, and hence hotter, fuel.

Filter #	Collected	Peak Count Rates /ks						Count rate ratios			
		^{137}Cs 662keV		^{134}Cs 604keV		^{134}Cs 795keV		604:662		795:662	
1	16:10 15 th March	126.9 ± 0.7	78.2 ± 0.6	49.5 ± 0.5			0.616 ± 0.006	0.390 ± 0.004			
2	01:15 16 th March	139.3 ± 1.3	88.3 ± 1.1	55.2 ± 0.8			0.633 ± 0.010	0.396 ± 0.007			
3	13:10 16 th March	59.0 ± 0.5	37.1 ± 0.4	23.4 ± 0.3			0.629 ± 0.008	0.396 ± 0.006			
8	00:30 23 rd March	44.4 ± 0.3	29.0 ± 0.3	18.5 ± 0.2			0.653 ± 0.007	0.417 ± 0.005			

Table 4.15: Count rates for the 662keV (^{137}Cs) and 604keV and 795keV (^{134}Cs) peaks with associated ratios for air filter samples collected at Tsukuba in March 2011, measured at SUERC in January 2013.

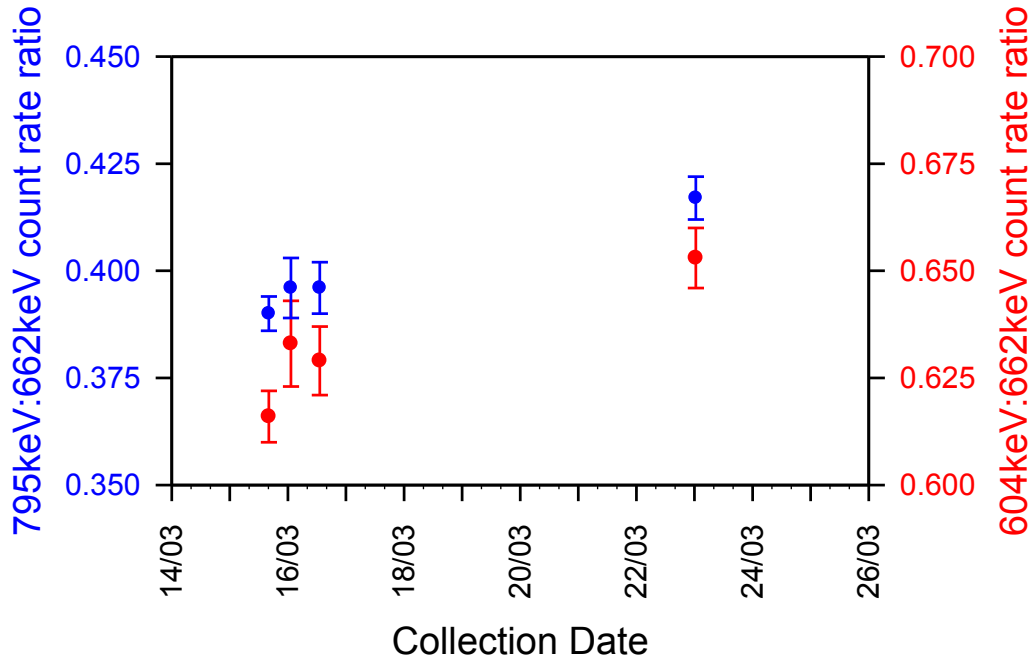


Figure 4.70: Count rate ratios of ^{134}Cs emissions (604keV in red, and 795keV in blue) to the ^{137}Cs 662keV peak, for air filter samples collected at Tsukuba in March 2011, measured at SUERC in January 2013.

Standards were prepared by dispensing measured volumes of ^{137}Cs solution and a uranium ore (CANMET BL-3, Ingles *et.al.* 1977) onto filter papers with the same dimensions as the air filter samples. Relationships between count rates for peaks in the uranium decay series were used to calculate a detector efficiency curve, normalised to the measured efficiency at 662keV. These were used to calculate the total activity for ^{134}Cs and ^{137}Cs on each air filter sample, without accounting for cascade summing in ^{134}Cs . These calculated activities and associated activity ratios are given in Table 4.16. These are all slightly lower than the activity ratios for soil samples at the Fukushima University calibration site, which are comparable to other soil sample analyses (Section 3.2.3), although a 5-10% cascade summing effect would be sufficient to bring these into line with these.

Filter #	Activity (Bq)		^{134}Cs : ^{137}Cs activity ratio	
	^{134}Cs	^{137}Cs	January 2013	15/03/2011
1	4.63 ± 0.07	9.49 ± 0.16	0.488 ± 0.011	0.87 ± 0.02
2	5.18 ± 0.09	10.41 ± 0.19	0.498 ± 0.012	0.89 ± 0.02
3	2.19 ± 0.04	4.41 ± 0.08	0.496 ± 0.012	0.88 ± 0.02
8	1.72 ± 0.03	3.32 ± 0.06	0.519 ± 0.012	0.92 ± 0.02

Table 4.16: Activities for ^{134}Cs and ^{137}Cs in the samples of air filter material analysed at SUERC, with associated ratios at time of measurement (16-23rd January 2013) and decay corrected to 15th March 2011. Note that the ^{134}Cs activities are calculated without accounting for cascade summing, and are hence underestimates of the activity.

A meta analysis of results from high resolution gamma spectrometry analysis of soil samples show ratios of ^{134}Cs to ^{137}Cs activity that vary by less than 15%, with some evidence of regional variation (Yamana 2013). Median values and ranges of histogrammed data analysed are given in Table 4.17.

Area	1 st March 2012			15 th March 2011		
	Median	10 th %ile	90 th %ile	Median	10 th %ile	90 th %ile
Total	0.78	0.70	0.90	1.05	0.95	1.22
A	0.77	0.70	0.84	1.04	0.95	1.14
B	0.81	0.75	0.86	1.09	1.01	1.16
C	0.78	0.70	0.85	1.05	0.95	1.15
D	0.81	0.73	0.85	1.09	0.99	1.15
E	0.81	0.72	0.89	1.09	0.97	1.20
F	0.81	0.73	0.88	1.09	0.99	1.19
G	0.70	0.66	0.86	0.95	0.89	1.16
H	0.77	0.72	0.88	1.04	0.97	1.19
I	0.77	0.72	0.86	1.04	0.97	1.16
J	0.82	0.74	0.91	1.11	1.00	1.23

Table 4.17: Median values of ^{134}Cs : ^{137}Cs activity ratios from Yamana (2013), as reported and with a decay correction to 15th March 2011.

During March and April 2011, rainwater was collected and analysed at SUERC. There was no rain between the 18th and 31st of March, when the first sample was collected that integrated the wet deposition during that rainfall and dry deposition over the previous 2 weeks. This first sample was measured on a 50% relative efficiency GMX detector, with a measurement over a weekend early in April 2011. Activity concentrations for this sample were calculated as $2.8 \pm 0.4 \text{ Bq kg}^{-1}$ ^{131}I , $0.90 \pm 0.20 \text{ Bq kg}^{-1}$ ^{137}Cs and $0.52 \pm 0.17 \text{ Bq kg}^{-1}$ ^{134}Cs . The ^{134}Cs : ^{137}Cs activity ratio for this sample was 0.57 ± 0.22 , significantly lower than the samples collected in Japan. Subsequent water samples were counted for insufficient periods to give precise activity concentration ratios. Although a contribution of old radiocaesium collected by the cloud on route from Japan, or accumulated on the roof at SUERC, can not be ruled out it does appear that activity in this sample is derived from an early release from the Fukushima Daiichi Nuclear Power Plant with a significantly lower ^{134}Cs : ^{137}Cs activity ratio compared to the releases that resulted in terrestrial deposition in Japan.

The ability of radiometric systems to quantify activity concentrations of different radionuclides over a large area, where weather patterns during the accidents are likely to have deposited material from different phases of release in different places, allows an assessment of the uniformity of the radionuclide concentrations to be made. The data reported from the airborne surveys have not been processed using fully spectral methods, and probably do not reflect activity concentration ratios. In principal, the lower altitude data may be re-analysed using fully spectral methods that could provide information on isotopic composition. The ground based data collected using the SUERC Portable Gamma Spectrometry system were all collected after shorter lived radionuclides (eg: ^{131}I , ^{132}I) had decayed well below detection limits, and so only the radionuclides with longer half lives (^{134}Cs and ^{137}Cs) are measured.

4.4.1 Vehicular survey results

The vehicular surveys in March and July 2012 covered a large area of Fukushima Prefecture, with the survey in March entering the exclusion zone and collecting data south of Fukushima Daiichi away from the main deposition plume. These surveys allow an assessment of spatial variability of isotope ratio over a relatively large area around the Fukushima Daiichi plant.

Figures 4.71 and 4.72 show the $^{134}\text{Cs}:^{137}\text{Cs}$ activity ratio for the March and July surveys. The weighted mean and standard deviations for these ratios, as measured and decay corrected to 15th March 2011, are given in Table 4.18. For the March 2012 survey, spectral distortion was observed in the vicinity of the Fukushima Daiichi Nuclear Power Plant which may affect the quality of the data processing. It is noted that in this area there is a significant increase in the $^{134}\text{Cs}:^{137}\text{Cs}$ ratio, as can be seen in Figure 4.71. Table 4.18 includes the mean and standard deviations for the survey excluding these points, resulting in a small reduction in the mean ratio and a larger reduction in standard deviation.

Figure 4.71 shows an enhanced activity ratio just north of Minamisoma. This is associated with a section of the survey where the gain was very much higher than for the bulk of the survey, and the gain stabilisation failed to adjust these few points. In the July 2012 survey, Figure 4.72, the precise road to the north of Minamisoma followed in March was not taken, nevertheless there is no indication of a substantial variation in activity ratio in the vicinity of Minamisoma. It is concluded that this feature is most likely to be an artefact due to the gain instability at that point. Figure 4.70 also shows an increased activity ratio to the north of Iwaki.

To reduce uncertainties in the measurements of activity ratio, the data for the two surveys have been regridded into 1x1 km cells. These reduce the uncertainties on the activity ratios in each cell to ± 0.05 and ± 0.03 for the March and July surveys respectively. The weighted mean and standard deviation for the regridded data sets are also included in Table 4.18.

Survey and date	Number	Weighted mean	
		Measured	Decay Corrected
March 2012 (all data)	3974	0.75 ± 0.13	1.02 ± 0.18
March 2012 (excl. NPP vicinity)	3157	0.71 ± 0.09	0.97 ± 0.12
July 2012	5539	0.64 ± 0.08	0.97 ± 0.12
March 2012 (all data)	155	0.76 ± 0.12	1.03 ± 0.16
March 2012 (excl. NPP vicinity)	140	0.73 ± 0.05	0.99 ± 0.06
July 2012	142	0.66 ± 0.03	1.00 ± 0.04

Table 4.18: Weighted mean and standard deviation $^{134}\text{Cs}:^{137}\text{Cs}$ activity ratio determined from vehicular measurements in March and July 2012, for the date measured and decay corrected to 15th March 2011. Values at the top are for individual measurements, with values for regridded data below. The March data are presented for the whole survey, and excluding those data in the immediate vicinity of the Fukushima Daiichi Nuclear Power Plant where spectral distortion may affect the analysis.

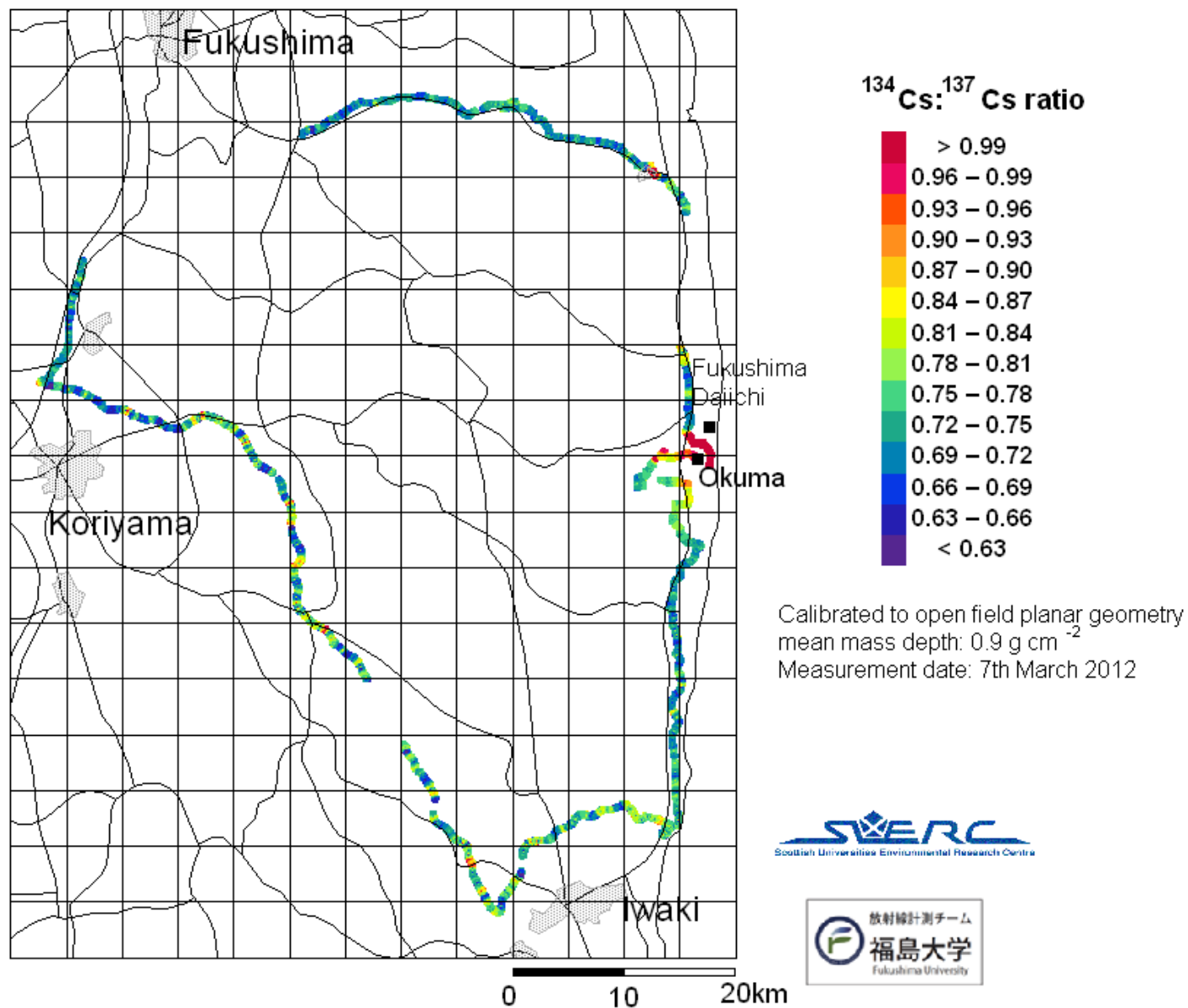


Figure 4.71: $^{134}\text{Cs} : ^{137}\text{Cs}$ activity ratio determined from vehicular survey using the SUERC Portable Gamma Spectrometry System in March 2012. Measurement uncertainties are typically ± 0.10 - 0.20

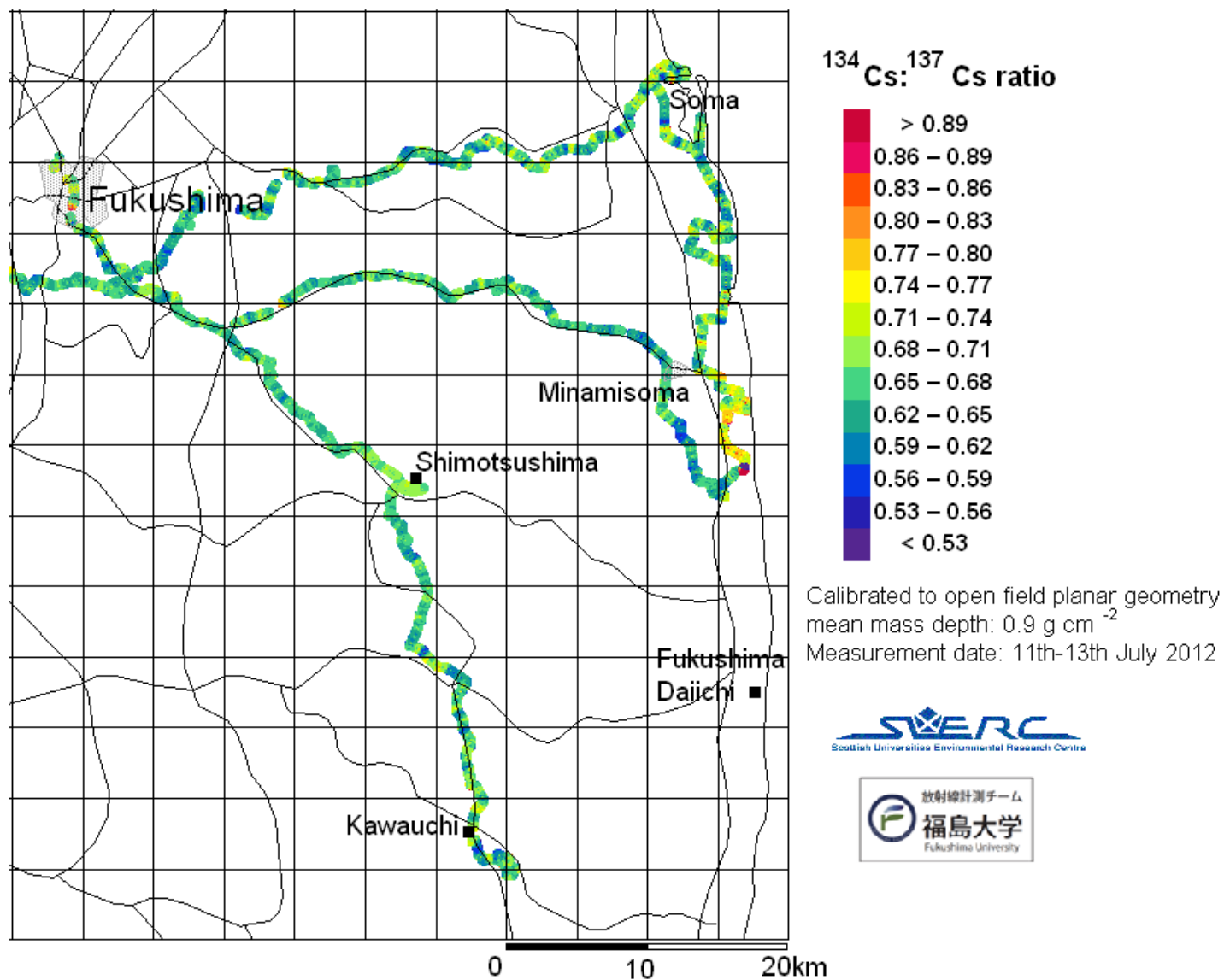


Figure 4.72: $^{134}\text{Cs} : ^{137}\text{Cs}$ activity ratio determined from vehicular survey using the SUERC Portable Gamma Spectrometry System in July 2012. Measurement uncertainties are typically ± 0.05 - 0.10

4.4.2 Backpack measurements

The backpack surveys can also be evaluated to produce measurements of the isotopic ratio. The average activity ratios measured for some of these surveys are given in Table 4.18, again with the values decay corrected to 15th March 2011. The uncertainties associated with individual measurements are ± 0.2 - 0.3 at Tsukuba and ± 0.1 - 0.2 at Fukushima. Spectral regridding improves the measurement precision, and activity ratios for some data sets following regridding are also presented in Table 4.19. The standard deviations in Table 4.19 are consistent with measurement uncertainty, and within measurement uncertainties the ratios at all locations are the same.

Survey and date	Number	Weighted mean	
		Measured	Decay Corrected
Tsukuba March 2012	107	0.71 \pm 0.10	0.97 \pm 0.13
Fukushima Uni March 2012	599	0.71 \pm 0.10	0.97 \pm 0.13
FTRI March 2012	305	0.73 \pm 0.05	0.99 \pm 0.08
Iizaka May 2012	1512	0.66 \pm 0.09	0.96 \pm 0.12
FTRI May 2012	1756	0.67 \pm 0.07	0.97 \pm 0.10
Fukushima Uni July 2012	4700	0.64 \pm 0.08	0.96 \pm 0.12
FTRI July 2012	843	0.65 \pm 0.04	1.13 \pm 0.07
Date, July 2012	355	0.62 \pm 0.06	0.98 \pm 0.10
Tsukuba Nov 2012	736	0.58 \pm 0.14	0.97 \pm 0.23
Date, Nov 2012	299	0.61 \pm 0.03	1.01 \pm 0.04
Fukushima Uni July 2012	1883	0.64 \pm 0.04	0.97 \pm 0.07
(unremediated only)	1306	0.65 \pm 0.04	0.98 \pm 0.05
Tsukuba Nov 2012	324	0.62 \pm 0.07	1.04 \pm 0.12

Table 4.19: Weighted mean and standard deviation $^{134}\text{Cs}:^{137}\text{Cs}$ activity ratio determined from backpack measurements in 2012, for the date measured and decay corrected to 15th March 2011. Data in the top half of the table are for individual measurements, with regridded data in the bottom half.

The spatial distribution of the activity ratio can also be mapped for the backpack data. Figures 4.73 and 4.74 show the $^{134}\text{Cs}:^{137}\text{Cs}$ activity ratio for the surveys of the university campus in March and July 2012. The initial analysis of the March data, prior to gain stabilisation, indicated some locations with significantly different activity ratios. Figure 4.73 still shows a few locations with activity ratios significantly higher or lower than the average. Figure 4.74 shows some areas with significantly reduced activity ratio, corresponding to areas which have been remediated with much lower activity concentrations. The consistently low activity ratios in these areas indicate a residual ^{137}Cs signal, either from Chernobyl and weapons testing activity in the deeper soil that was not removed or the soil imported to replace the removed soil, or from very small biases in the analysis algorithm. With the exception of these remediated areas, the July survey shows no areas where the activity ratio deviates significantly from the average.

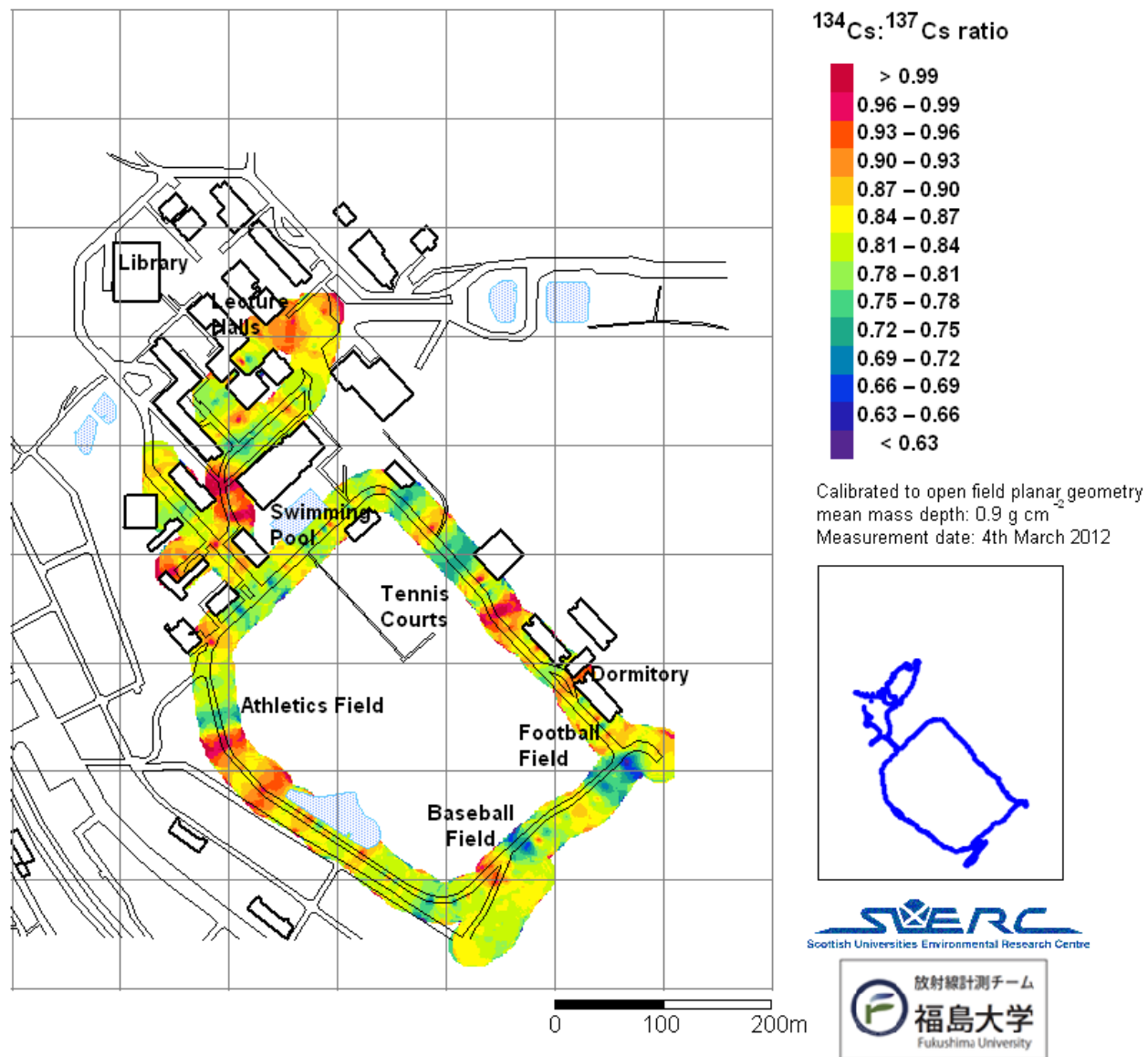


Figure 4.73: $^{134}\text{Cs} : ^{137}\text{Cs}$ activity ratio for the March 2012 survey of the Fukushima University campus. Uncertainties on individual measurements are typically ± 0.1 .

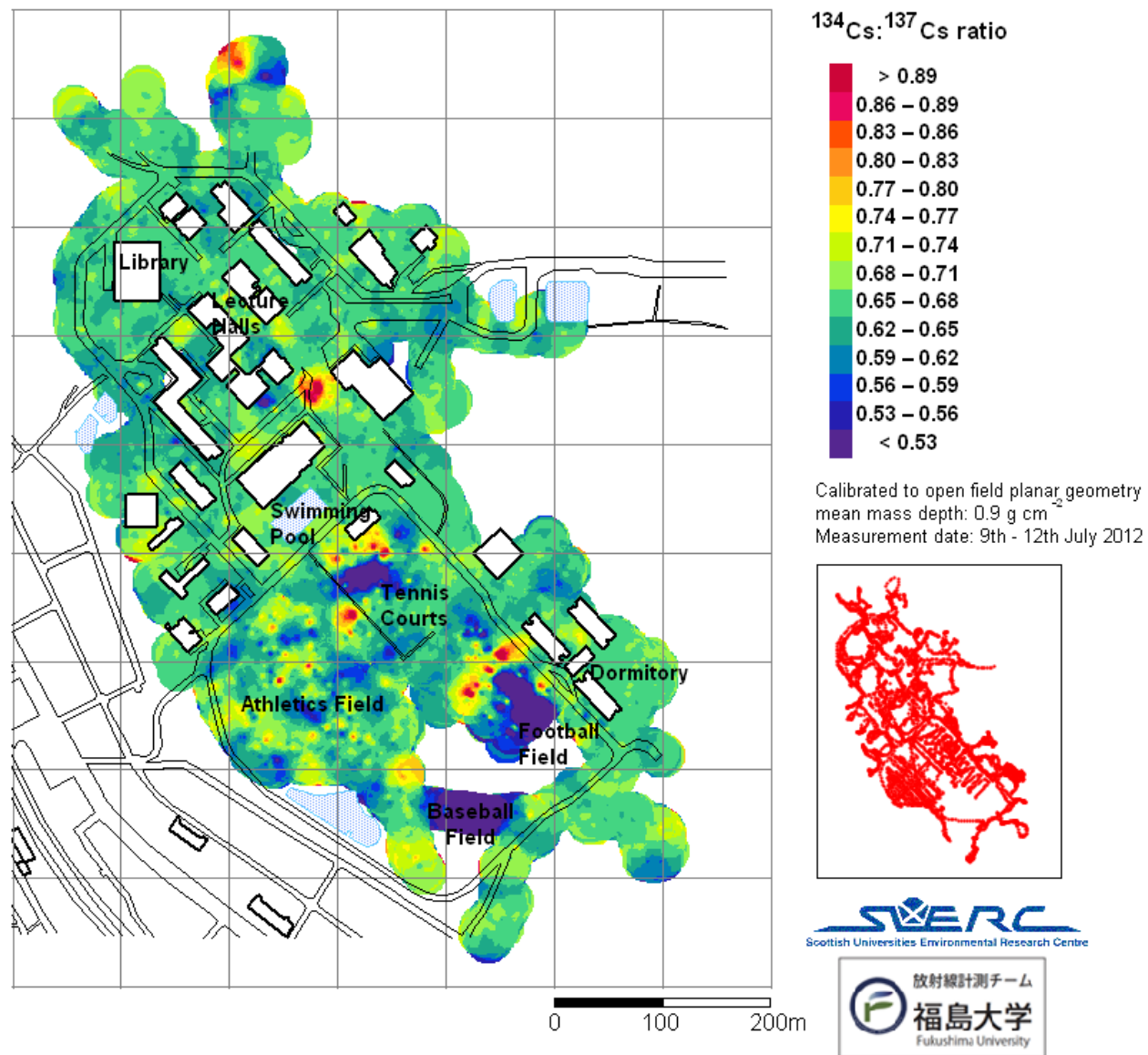


Figure 4.74: $^{134}\text{Cs}:^{137}\text{Cs}$ activity ratio for the July 2012 survey of the Fukushima University campus. Uncertainties on individual measurements are typically ± 0.1 .

4.4.3 Discussion of Radionuclide Ratios

Measurements of air filters have demonstrated that different releases from the reactors were characterised by different ratios of ^{134}Cs : ^{137}Cs activity, as would be expected from a series of releases from reactors with different radiation histories, with differences of 7-8% across the few days of samples measured. A water sample collected from the roof at SUERC after deposition from the first activity reaching the UK showed an activity ratio considerably lower than observed in samples collected in Japan.

Measurements using the SUERC Portable Gamma Spectrometry system from vehicles and as backpacks show a dispersion in the radiocaesium activity ratio of 10-15%. A meta-analysis of soil samples collected in Japan (Yamana 2013) has shown a similar dispersion of activity ratio.

The spread in observed isotope ratios may be partly explained by measurement precision, however it appears that there is some variation in isotope ratio reflecting different phases of release during the accidents, from different reactors and cooling ponds. However, the variation is a lot less than would be expected from multiple sources. This suggests that the terrestrial deposition was dominated by activity released from a single reactor core, and that the material released had been mixed within the reactor building prior to release.

5. Discussion and Conclusions

In collaboration with partner organisations in Japan, radiometric surveys have been conducted by the Scottish Universities Environmental Research Centre (SUERC) using the SUERC Portable Gamma Spectrometry System during four visits to Japan in March, May, July and November 2012. SUERC left a system with the Faculty of Symbiotic Sciences at Fukushima University. The system has been used in a vehicle to collect data from surveys along roads, mostly in Fukushima Prefecture, in March and July 2012 with short vehicular surveys at other times. With the system deployed as a backpack, urbanised areas have been surveyed at Fukushima University and parts of Fukushima city and orchards surveyed at the Fukushima Prefecture Fruit Tree Research Institute, farms in Fukushima Prefecture and also agriculture test plots at Tsukuba. Calibration sites have been developed at Fukushima University and the Fruit Tree Research Institute. The results of this work have been presented, and the relevance of such measurements to assisting recovery from nuclear accidents identified.

Calibration sites have been established at Fukushima University and the Fukushima Prefecture Fruit Tree Research Institute. These have been extensively sampled, with the samples measured by high resolution gamma spectrometry methods along with international reference materials. Analysis of the samples from the Fruit Tree Research Institute is ongoing. The sampling and analysis produces recommended values for the activity concentrations and dose rates on the sites, traceable to international reference materials. The sites can be used to validate the performance of ground based instruments to known activity distributions that are expected to be similar to survey conditions. These sites will be used to verify performance of the SUERC systems used in future work in Japan, and are available for the validation of the performance of any other instrument.

Radiometric systems deployed vehicles allow measurements to be conducted over regional scale areas relatively quickly. The SUERC Portable Gamma Spectrometry system has a relatively small detector compared to more conventional vehicular systems. The system was deployed in a vehicle collecting data for a survey on the 7th March 2012 that covered a route from Fukushima city to the Fukushima Daiichi NPP passing through Date and Iitate districts, then heading south towards Iwaki before returning to Fukushima City via Koriyama. A further extensive carborne survey was conducted on the 11th and 13th July, collecting data between Fukushima University and Kawauchi (11th July) and from Fukushima City to Minamisoma, then to Soma before returning to Fukushima City (13th July).

These surveys have reproduced the regional scale deposition patterns recorded using airborne systems. The March survey in particular showed the ability of the system to collect useful data over a very wide range of activity concentrations and dose rates. The surveys have demonstrated the ability of small gamma spectrometry systems to conduct regional scale deposition mapping from vehicles, and to be removed from those vehicles for small scale backpack mapping of features as required.

Radiometric systems deployed as backpacks provide a means of producing detailed surveys, collecting data in locations where people spend their time. This can be used to identify small locations with locally high activity concentrations, allowing targeted remediation. Surveys conducted following remediation allows the evaluation of the effectiveness of remediation. During the course of 2012 the SUERC system was used to collect data from urbanised areas,

the Fukushima University campus on four occasions and also in Fukushima Iizaka, to evaluate the effectiveness of this system to such roles.

These surveys have demonstrated the capability of backpack systems to collect spatially detailed data, with monitoring of the system during survey allowing features to be identified and reported in near real time. The surveys have demonstrated the variability of activity concentration and dose rate within urbanised environments. Hard surfaces such as roads and pavements generally have lower activity concentrations compared to vegetated surfaces, as a result of activity being removed by the action of rain and street cleaning. Inside buildings, the surveys have shown much lower activity concentrations, with anthropogenic contributions to the dose rate often being less than 20%.

The university campus surveys, in particular the July, has allowed the evaluation of the effectiveness of the remediation work by comparing remediated with unremediated areas. A more direct method of evaluating remediation would be by repeat surveys before and after remediation. Remediation by the replacement of top soil with uncontaminated material has been very effective at reducing the radiocaesium activity concentrations to very low levels. Remediation by power-washing the surfaces had a more varied effectiveness, with in some places significant reductions in radiocaesium activity concentrations whereas other surfaces, most notably artificial surfaces on tennis courts, reductions in the activity concentrations have been very small.

With fruit cultivation a major component of the local economy, transfer of activity to fruit is a major concern. Measurements of activity concentrations in fruit and on the ground provides useful data to assist in understanding the complex processes that transfer activity to trees, and to the edible parts of fruit. Repeat measurements of deposited activity allow for the evaluation of remediation methods to reduce the activity available for transfer to fruit. Mapping of deposition also allows the evaluation of external doses to workers in the orchards. The SUERC system has been used to map deposition at the Fukushima Prefecture Fruit Tree Research Institute on four occasions in 2012, at some fruit orchards in other parts of Fukushima Prefecture and also at the AFFRC at Tsukuba.

The high spatial resolution achievable with backpack systems allows deposition to be evaluated for individual trees in more sparse orchards. This allows radiometric data to be linked directly with activity concentrations in the fruit from individual trees.

The $^{134}\text{Cs}:$ ^{137}Cs activity ratios have been determined from measurements conducted with the SUERC Portable Gamma Spectrometry system operated as a backpack and for vehicular survey. These show small variations in activity ratio, with dispersions of 10-15% around a ratio of 1.00 (decay corrected to 15th March 2011). Analysis of data from soil samples and air filters have shown similar activity ratios and dispersions.

The spread in observed isotope ratios may be partly explained by measurement precision, however it appears that there is some variation in isotope ratio reflecting different phases of release during the accidents, from different reactors and cooling ponds. However, the variation is a lot less than would be expected from multiple sources. This suggests that the terrestrial deposition was dominated by activity released from a single reactor core, and that the material released had been mixed within the reactor building prior to release.

The work reported here has demonstrated the capabilities of small, fully spectroscopy instruments similar to the SUERC Portable Gamma Spectrometry system in environmental assessments of areas contaminated by fallout from the Fukushima Daiichi reactor accidents. Such systems can be deployed as backpacks or from vehicles, and are able to quantify activity concentrations for deposited radionuclides in a few seconds per measurement.

During this work conducted in Japan, a fruitful working relationship has developed between UK experts from the SUERC Environmental Physics Group and the School of Physics and Astronomy at Glasgow University, and scientists at several research institutions in Japan. We will continue to work together, supporting the ongoing work in Japan.

References

- Aage H.K., Korsbech U., Bargholz K., Hovgaard J. (2006). Carborne gamma-ray spectrometry. Calibration and applications. *Applied Radiation and Isotopes* **64**, 948–956.
- Aage H.K., Kuukankorpi S., Moring M., Smolander P., Toivonen H. (2009a). *Urban Gamma Spectrometry: Report 1*. Roskilde, Denmark: NKS Secretariat. NKS-190. ISBN 978-87-7893-257-0
- Aage H.K., Kuukankorpi S., Moring M., Smolander P., Toivonen H. (2009b). *Urban Gamma Spectrometry: Report 2*. Roskilde, Denmark: NKS Secretariat. NKS-191. ISBN 978-87-7893-258-7
- Abal'yan T.G. *et.al.* (1971). The application of aerial surveys to study the snow cover in the mountain region of the Varzob River (in Russian). *Proceedings of the Hydrometeorological Centre, Leningrad*.
- Aitken M.J. (1983). Dose Rate Data in SI Units, PACT 9, 69-76.
- Allyson J.D. (1994). *Environmental Gamma Ray Spectrometry: Simulation of Absolute Calibration of In-situ and Airborne Spectrometry for Natural and Anthropogenic Sources*. PhD Thesis, University of Glasgow.
- Allyson J.D., Sanderson D.C.W. (1998), Monte Carlo Simulation of Environmental Airborne Gamma-Spectrometry. *J Environ Rad* **38**, 259-282.
- Allyson J.D., Sanderson D.C.W. (2001). Spectral deconvolution and operational use of stripping ratios in airborne radiometrics. *J. Environ. Radioact.* **53**, 351–363.
- Antonopoulos-Domis M., Clouvas A., Gagianas A. (1991). Radiocesium dynamics in fruit trees following the Chernobyl accident. *Health Physics* **61**, 837-842.
- Baldini E., Bettoli M.G., Tubertini O. (1987). Effects of the Chernobyl pollution on some fruit trees. *Advances in Horticultural Science* **1**, 77-79.
- Bé M.M., Christé V., Dulieu C., Mougeot X., Chechev V.P., Kondev F.G., Nichols A.L., Huang X., Wang B. (2013). *Table of Radionuclides (Vol. 7 – A = 14 to 245)*. Bureau International des Poids et Mesures. Monograph BIPM-5.
- Beck H.L., Decampo J., Gogolak C. (1972). *In-situ Ge(Li) and NaI(Tl) gamma-ray spectrometry*. Health and Safety Laboratory, U.S. Atomic Energy Commission. Report: HASL-258.
- Bissell V.C., Peck E.L. (1973). Monitoring snow water equivalent by using natural soil radioactivity. *Wat. Resour. Res.* **9**, 885-890.
- Bourgeois Ch., Guillot L., Broudieu J.C., Mette M., Gutierrez S., Abt D., Jannic H. (2003). AGS Exercise Team Report for CEA, France. In: Sanderson, D.C.W., Cresswell, A.J., Lang, J.J. (Eds.). *An International Comparison of Airborne and Ground Based Gamma Ray Spectrometry. Results of the ECCOMAGS Exercise held 24th May–4th June 2002, Dumfries*

and Galloway, Scotland. University of Glasgow, Glasgow. ISBN 0-85261-783-6, pp. 207–220.

Bristow Q. (1978). The application of airborne gamma-ray spectrometry in the search for radioactive debris from the Russian satellite Cosmos 954 (Operation "Morning Light"). *Geol. Surv. Can. Paper* **78-1B**, 151-162.

Buchanan E. (2013). *Simulating the Operator in Portable Gamma-Ray Spectrometry*. Project report for School of Physics and Astronomy, University of Glasgow, MSci project.

Bucher, B., Rybach, L., Schwarz, G. (2000). Environmental mapping: comparison of ground and airborne spectrometry results under alpine conditions. In: Sanderson, D.C.W., McLeod, J.J. (Eds.), *Recent Applications and Developments in Mobile and Airborne Gamma Spectrometry. Proceedings of the RADMAGS Symposium, University of Stirling, 15-18 June 1998*, SURRC, University of Glasgow.

Calmon P., Thiry Y., Zibold G., Rantavaara A., Fesenko S. (2009). Transfer parameter values in temperate forest ecosystems: a review. *Journal of Environmental Radioactivity* **100**, 757-766.

Carini F. (2001). Radionuclide transfer from soil to fruit. *Journal of Environmental Radioactivity* **52**, 237-279.

Chino M., Nakayama H., Nagai H., Terada H., Katata G., Yamazawa H. (2011). Preliminary estimation of release amounts of ¹³¹I and ¹³⁷Cs accidentally discharged from the Fukushima Daiichi nuclear power plant into the atmosphere. *Journal of Nuclear Science and Technology* **48**, 1129–1134.

Cresswell A.J., Allyson J.D., Sanderson D.C.W. (2001). A code to simulate nuclear reactor inventories and associated gamma-ray spectra. *J Environ Rad* **53**, 399-410.

Cresswell A.J., Sanderson D.C.W., White D.C. (2006). ¹³⁷Cs measurement uncertainties and detection limits for airborne gamma spectrometry (AGS) data analysed using a spectral windows method. *Applied Radiation and Isotopes* **64** 247–253.

Cresswell A.J., Sanderson D.C.W. (2012). Evaluating airborne and ground based gamma spectrometry methods for detecting particulate radioactivity in the environment: A case study of Irish Sea beaches. *Science of the Total Environment* **437**, 285-296.

Cresswell A.J., Sanderson D.C.W., Harrold M., Kirley B., Mitchell C., Weir A. (2013). Demonstration of lightweight gamma spectrometry systems in urban environments. *Journal of Environmental Radioactivity* **124**, 22-28.

Dahl J.B., Odegaard H. (1970). Aerial measurements of water equivalent of snow deposits by means of natural radioactivity in the ground. *Isotope Hydrology 1970*. IAEA, Vienna.

Dickson B.L. (2004). Recent advances in aerial gamma-ray surveying. *J Environ Rad* **76**, 225–236.

ECCOMAGS (2002). *Deliverable D2: Measurement Protocols*. Report for EC 5th Framework Project FIKR-CT-2000-20098.

Grasty R.L. (1980). The search for Cosmos-954. In: *Search Theory and Applications*. Plenum Press, New York. pp 211-220.

Grasty R.L., Hovgaard J., Multala J. (1996). Airborne gamma-ray measurements in the Chernobyl plume. *Fourth International Workshop on "Real-time computing of the environmental consequences of an accidental release from a nuclear installation*.

Guillot, L. (2003). *Spectral Analysis Workgroup Report*. Deliverable D6: Workgroup Report, 3-43. ECCOMAGS Project Report ECCO-2003-WrkgrpRprt-vs1.2.

Harrold M. (2011). *Statistical Descriptors For Mobile Gamma Spectrometry*. Project report for School of Physics and Astronomy, University of Glasgow.

He Q., Walling D.E. (2003). Testing distributed soil erosion and sediment delivery models using ¹³⁷Cs measurements. *Hydrol. Process.* **17**, 901–916

Hjerpe T., Samuelsson C. (2006). Shielded and unshielded geometries in the search for orphan sources. *Applied Radiation and Isotopes* **64**, 551–555.

Honda M.C., Aono T., Aoyama M., Hamajima Y., Kawakami H., Kitamura M., Masumoto Y., Miyazawa Y., Takigawa M., Saino T. (2012). Dispersion of artificial caesium-134 and -137 in the western North Pacific one month after the Fukushima accident. *Geochemical Journal* **46**, e1-e9.

Hovgaard, J., Scott, E.M. (1997). RESUME-95: results of an international field test of mobile equipment for emergency response. *Radiat. Prot. Dosimetry* **73**, 219-224.

Hovgaard, J. (1998). *Airborne Gamma-ray Spectrometry, Statistical Analysis of Airborne Gamma-ray Spectra*. Ph.D. Thesis, Technical University of Denmark.

Hovgaard, J., 2000. NASVD – a new method for processing airborne spectral gamma ray. In: Sanderson, D.C.W., McLeod, J.J. (Eds.), *Recent Applications and Developments in Mobile and Airborne Gamma Spectrometry. Proceedings of the International Symposium (RADMAGS 98), University of Stirling, Scotland, 15–18 June 1998*. University of Glasgow, Glasgow. ISBN 0-85261-685-6, pp. 86–87.

Ingles J.C., Sutarno R., Bowman W.S., and Faye G.H. (1977). *Radioactive Ores DH -1, DL-1, BL-1, BL-2, BL-3 and BL-4 - Certified Reference Materials*. CANMET report 77-64.

International Atomic Energy Agency (1988). *The Radiological Accident in Goiânia*. IAEA, Vienna. STI/PUB/815. ISBN 92-0-129088-8.

International Atomic Energy Agency (1991). *Airborne Gamma Ray Spectrometer Surveying*. IAEA, Vienna. Technical Reports Series 323.

International Atomic Energy Agency (2003). *Guidelines for Radioelement Mapping Using Gamma Ray Spectrometry Data*. IAEA, Vienna. IAEA-TECDOC-1363.

International Commission on Radiation Units and Measurements (1994). *Gamma-ray spectrometry in the environment*. ICRU Report No. 53. ISBN 0-913394-52-1.

Investigation Committee on the Accident at Fukushima Nuclear Power Stations of Tokyo Electric Power Company, ICANPS (2011). *Interim Report*. Downloaded from <http://www.cas.go.jp/jp/seisaku/icanps/eng/>

Japan Nuclear Energy Safety Organisation, JNES (2011). JNES-RE-Report Series. JNES-RE-2011-0002. <http://www.jnes.go.jp/content/000119740.pdf>

Kanai Y. (2012). Monitoring of aerosols in Tsukuba after Fukushima nuclear power plant incident in 2011. *Journal of Environmental Radioactivity* **111**, 33-37.

Katata G., Ota M., Terada H., Chino M., Nagai H. (2012a). Atmospheric discharge and dispersion of radionuclides during the Fukushima Dai-ichi Nuclear Power Plant accident. Part I: Source term estimation and local-scale atmospheric dispersion in early phase of the accident. *Journal of Environmental Radioactivity* **109**, 103-113.

Katata G., Terada H., Nagai H. Chino M. (2012b). Numerical reconstruction of high dose rate zones due to the Fukushima Dai-ichi Nuclear Power Plant accident. *Journal of Environmental Radioactivity* **111**, 2-12.

Kato H., Onda Y., Teramaga M. (2012). Depth distribution of ^{137}Cs , ^{134}Cs and ^{131}I in soil profile after Fukushima Dai-ichi nuclear power plant accident. *Journal of Environmental Radioactivity* **111**, 59-64.

Kirley B. (2011). *Mobile Gamma Spectrometry: a least squares fitting approach*. Project report for School of Physics and Astronomy, University of Glasgow.

Kock P., Samuelsson C. (2011). Comparison of airborne and terrestrial gamma spectrometry measurements - evaluation of three areas in southern Sweden. *Journal of Environmental Radioactivity* **102**, 605-613.

Kuittinen R., Vironmäki J. (1980). Aircraft gamma-ray spectrometry in snow water equivalent measurement. *Hydrological Sciences Bulletin* **25**, 63-75.

Lindahl I., Haabrekke H. (1986). *Determination of radioactive fallout after the Chernobyl accident*. NGU/R-86.160.

Løvborg L., Kirkegaard P. (1974). Response of 3"x 3" NaI(Tl) detectors to terrestrial gamma radiation. *Nuclear Instruments and Methods* **121**, 239-251.

Lyons C., Colton D. (2012). Aerial measuring system in Japan. *Health Physics* **102**, 509-515.

Mellander H. (1989). *Airborne gamma spectrometric measurements of the fallout over Sweden after the nuclear reactor accident at Chernobyl, USSR*. IAEA/NENF/NM-89-1.

Mellander, H., Aage, H.K., Karlsson, S., Korsbech, U., Lauritzen, B., Smethurst, M. (2002). *Mobile Gamma Spectrometry. Evaluation of the Resume 99 Exercise*. NKS-56. NKS, Roskilde, ISBN 87-7893-111-8.

Mercier N., Falguères C. (2007). Field gamma dose-rate measurement with a NaI(Tl) detector: re-evaluation of the "threshold" technique. *Ancient TL* **25**, 1-4.

Ministry of Education, Culture, Sports, Science and Technology (2011). *Results of Airborne Monitoring by the Ministry of Education, Culture, Sports, Science and Technology and the U.S. Department of Energy*. MEXT, May 6 2011.

Ministry of Education, Culture, Sports, Science and Technology (2012a). *Results of Airborne Monitoring Survey by MEXT in the Kyushu Region and Okinawa Prefecture*. MEXT May 11 2012.

Ministry of Education, Culture, Sports, Science and Technology (2012b). (i) *Results of Airborne Monitoring Survey in Hokkaido* and (ii) *Revision to the Results of Airborne Monitoring Survey over the Eastern Part of Japan with Detailed Consideration of the Influence of Natural Radionuclides*. MEXT, July 27 2012.

Mitchell C., Weir A. (2010). *A Study of Environmental Radioactivity*. Project report for School of Physics and Astronomy, University of Glasgow.

Nagaoka T., Togawa O., Moriuchi S., Rybalko S.I., Sukhoruchkin A.K., Kazakov S.V. (1994) Radiation state of environment in the 30-km zone of Chernobyl NPP, water objects. *Proceeding of the Second Steering Conference Relating to the 'Agreement on the Implementation of Research at the Chernobyl Centre for International Research' between CHECIR and JAERI*. pp 10-26.

The National Diet of Japan (2012). *The official report of the Fukushima Nuclear Accident Independent Investigation Commission*.

<http://warp.da.ndl.go.jp/info:ndljp/pid/3856371/naaic.go.jp/en/index.html>

Nuclear and Industrial Safety Agency (NISA)/Ministry of Economy, Trade and Industry (2011a). *INES (the International Nuclear and Radiological Event Scale) Rating on the Events in Fukushima Dai-ichi Nuclear Power Station by the Tohoku District - off the Pacific Ocean Earthquake*. News Release, April 12, 2011.

Nuclear and Industrial Safety Agency (NISA)/Ministry of Economy, Trade and Industry (2011b). *Regarding the Evaluation of the Conditions on Reactor Cores of Unit 1, 2 and 3 related to the Accident at Fukushima Dai-ichi Nuclear Power Station, Tokyo Electric Power Co. Inc.* News Release, June 6, 2011.

NEA (2006), *The JEFF-3.1 Nuclear Data Library*, JEFF Report 21, Nuclear Energy Agency, Organisation For Economic Co-Operation And Development, ISBN 92-64-02314-3.

Nikiforov M.V., Pegoev N.N., Stroganov A.N. (1980). Aerial gamma survey of snow cover and soil moisture. *Hydrological Sciences Bulletin* **25**, 85-91.

Nordic Nuclear Safety Research, NKS (1997). *RESUME-95: Rapid Environmental Surveying Using Mobile Equipment*. Copenhagen: NKS. ISBN 87-7893-014-6.

Ohno T., Muramatsu Y., Miura Y., Oda K., Inagawa N., Ogawa H., Yamazaki A., Toyama C., Sato M. (2012). Depth profiles of radioactive cesium and iodine released from the Fukushima Daiichi nuclear power plant in different agricultural fields and forests. *Geochemical Journal* **46**, 287-295.

Office for Nuclear Regulation (2011). *Japanese earthquake and tsunami: Implications for the UK nuclear industry. Final Report*. ONR Report ONR-REP-11-002 revision 2.

Paatero P. (1964). DRIFT – a drift correcting computer subroutine for nuclear spectroscopy. *Nucl. Instr. & Methods* **31**, 360.

Peck E.L., Carroll T.R., Vandemark S.C. (1980). Operational aerial snow surveying in the United States. *Hydrological Sciences Bulletin* **25**, 51-62.

Saito K., Sakamoto R., Tsutsumi M., Nagaoka T., Moriuchi S. (1988). Prompt estimation of release rates of gaseous radioactivity from a nuclear plant using an aerial survey. *Radiation Protection Dosimetry* **22**, 77-85.

Saito K. (1991). External doses due to terrestrial gamma rays on the snow cover. *Radiation Protection Dosimetry* **35**, 31-39.

Sanderson D.C.W, Scott E.M., Baxter M.S., Preston T. (1988) *A Feasibility Study of Airborne Radiometric Survey for UK Fallout*. SURRC Report. <http://eprints.gla.ac.uk/57366/>

Sanderson D.C.W, Scott E.M. (1989). *Aerial Radiometric Survey in West Cumbria in 1988*. MAFF Report N611. <http://eprints.gla.ac.uk/57332/>

Sanderson D.C.W, East B.W., Scott E.M. (1989). *Aerial Radiometric Survey of Parts of North Wales in July 1989*. SURRC Report. <http://eprints.gla.ac.uk/57596/>

Sanderson D. C. W., Allyson J. D., Martin E., Tyler A. N., Scott E.M. (1990a). *An Airborne Gamma ray Survey of Three Ayrshire Districts*. SURRC Report for the district councils of Cunninghame, Kilmarnock & Loudoun, and Kyle & Carrick. <http://eprints.gla.ac.uk/57634/>

Sanderson D. C. W., Allyson J. D., Cairns K.J., MacDonald P.A. (1990b). *A Brief Aerial Survey in the Vicinity of Sellafield in September 1990*. SURRC Report. <http://eprints.gla.ac.uk/57750/>

Sanderson D. C. W., Allyson J. D., Tyler A. N. (1992a). *An Aerial Gamma Ray Survey of Chapelcross and its Surroundings in February 1992*. SURRC Report for British Nuclear Fuels plc. <http://eprints.gla.ac.uk/58260/>

Sanderson D. C. W., Allyson J. D., Tyler A. N., Murphy S. (1992b). *An Aerial Gamma Ray Survey of Springfields and the Ribble Estuary in September 1992*. SURRC Report for British Nuclear Fuels plc. <http://eprints.gla.ac.uk/57327/>

Sanderson D. C. W., Allyson J. D., Tyler A. N., Ni Riain S., Murphy S. (1993). *An Airborne Gamma Ray Survey of Parts of SW Scotland in February 1993. Final Report*. SURRC Report for the Scottish Office Environment Department (HMIPI). <http://eprints.gla.ac.uk/59483/>

Sanderson D. C. W., Allyson J. D., Tyler A. N. (1994a). Rapid quantification and mapping of radiometric data for anthropogenic and technically enhanced natural nuclides. In: *Application of Uranium Exploration Data and Techniques in Environmental Studies*. IAEA, Vienna. pp 197-216. IAEA TECDOC-827.

Sanderson D. C. W., Allyson J. D., Tyler A. N., Scott E. M (1994b). Environmental applications of airborne gamma spectrometry. In: *Application of uranium exploration data and techniques in environmental studies*. IAEA, Vienna. pp 71-91. IAEA TECDOC-827.

Sanderson D.C.W., Allyson J.D., Ni Riain S., Gordon G., Murphy S., Fisk S. (1994c). *An Aerial Gamma Ray Survey of Torness Nuclear Power Station on 27th-30th March 1994*. SURRC Report for Scottish Nuclear Limited. <http://eprints.gla.ac.uk/58355/>

Sanderson D.C.W., Allyson J.D., Gordon G., Murphy S., Tyler A. N., Fisk S. (1994d). *An Aerial Gamma Ray Survey of Hunterston Nuclear Power Station in 14-15 April and 4 May 1994*. SURRC Report for Scottish Nuclear Limited. <http://eprints.gla.ac.uk/39213/>

Sanderson D.C.W., Cresswell A.J., Allyson J.D., McConville P. (1997a). *Experimental Measurements and Computer Simulation of Fission Product Gamma-ray Spectra*. DETR/RAS/97.002. <http://eprints.gla.ac.uk/58978/>

Sanderson D.C.W., Allyson J.D., Cresswell A.J., McConville P. (1997b). *An Airborne and Vehicular Gamma Survey of Greenham Common, Newbury District and Surrounding Areas*. SURRC Report for Newbury District Council and Basingstoke & Deane Borough Council. <http://eprints.gla.ac.uk/58456/>

Sanderson D.C.W., Allyson J.D., Cresswell A.J. (1997c). *An Aerial Gamma ray Survey of the Surrounding Area of Sizewell Nuclear Power Station. 1 October – 3 October 1996*. SURRC Report IMC REF: RP/GNSR/5031. <http://eprints.gla.ac.uk/56976/>

Sanderson D.C.W., Allyson J.D., McConville P., Murphy S., Smith J. (1997d). Airborne gamma ray measurements conducted during an international trial in Finland. *RESUME-95: Rapid Environmental Surveying Using Mobile Equipment*. Copenhagen:NKS. ISBN 87-7893-014-6. pp. 235-254.

Sanderson D.C.W., Allyson J.D., Cresswell A.J. (1998). *An Investigation of Off-site Radiation Levels at Harwell and Rutherford Appleton Laboratory Following Airborne Gamma Spectrometry in 1996*. SURRC Report for Vale of White Horse District Council. <http://eprints.gla.ac.uk/39214/>

Sanderson, D.C.W., McLeod J.J (1999). *Final Report of EC Concerted Action Contract No. F14P-CT95-0017*.

Sanderson, D.C.W., McLeod J.J. (1999). *European Coordination of Environmental Airborne Gamma Ray Spectrometry*. Final Report of EC Concerted Action: Contract No. F14P-CT95-0017.

Sanderson, D.C.W., Cresswell, A.J., White D.C., Murphy S., McLeod J. (2001). *Investigation of Spatial and Temporal Aspects of Airborne Gamma Spectrometry. Final Report*. SURRC Report for DETR. Report No. DETR/RAS/01.001. <http://eprints.gla.ac.uk/39224/>

Sanderson, D.C.W., Cresswell, A.J., Lang, J.J. (eds.) (2003). *An International Comparison of Airborne and Ground Based Gamma Ray Spectrometry. Results of the ECCOMAGS 2002 Exercise held 24th May to 4th June 2002, Dumfries and Galloway, Scotland*. Glasgow: University of Glasgow. ISBN 0 85261 783 6.

Sanderson D.C.W., Cresswell A.J., Scott E.M., Lang J.J. (2004). Demonstrating the European Capability for Airborne Gamma Spectrometry: results from the ECCOMAGS Exercise. *Radiation Protection Dosimetry*, **109**, 119-125.

Sanderson D.C.W., Cresswell A.J., White D.C. (2008). The effect of flight line spacing on inventory and spatial feature characteristics of airborne gamma-ray spectrometry data. *International Journal of Remote Sensing* **29**, 31-46.

Sanderson D.C.W., Cresswell A.J. (2010). *Modelling Gamma Spectrometry Systems For Use in Beach Monitoring Near Sellafield*. SUERC report for Sellafield Sites Ltd. <http://eprints.gla.ac.uk/45876/>

Shanks A., Fournier S., Shanks S. (2012). Challenges in determining the isotopic mixture for the Fukushima Daiichi Nuclear Power Plant accident. *Health Physics* **102**, 527-534.

Storm E., Israel H. I. (1970) Photon cross sections from 1 keV to 100 MeV for elements Z = 1-100. *Nuclear Data Tables A* **7**, 565-681.

Stukin E.D. (1991). Characteristics of primary and secondary caesium-radionuclide contamination of the countryside following the Chernobyl NPP accident. *Seminar on Comparative Assessment of the Environmental Impact of Radionuclides Released During Three Major Nuclear Accidents: Kyshtym, Windscale, Chernobyl. 1-5 Oct 1990*. Commission of the European Communities, Luxembourg, vol 1, 255-300. EUR—13574 (V.1).

Sugimoto J. (2013). Accident of Fukushima Daiichi Nuclear Power Plant - sequences, FP released, lessons learned. *Proceedings of the International Symposium on Environmental monitoring and dose estimation of residents after accident of TEPCO's Fukushima Daiichi Nuclear Power Stations*. KUR Research Program for Scientific Basis of Nuclear Safety Report Series 4. KURRI-KR-186. pp 2-23.

Tagami K, Uchida S., Uchihori Y., Ishii N., Kitamura H., Shirakawa Y. (2011). Specific activity and activity ratios of radionuclides in soil collected about 20km from the Fukushima Daiichi nuclear power plant: radionuclide release to the south and southwest. *Science of the Total Environment* **409**, 4885-4888.

Tazoe H., Hosoda M., Sorimachi A., Nakata A., Yoshida M.A., Tokonami S., Yamada M. (2012). Radioactive pollution from Fukushima Daiichi nuclear power plant in the terrestrial environment. *Radiation Protection Dosimetry* **152**, 198-203.

Terada H., Katata G., Chino M., Nagai H. (2012). Atmospheric discharge and dispersion of radionuclides during the Fukushima Dai-ichi Nuclear Power Plant accident. Part II: verification of the source term and analysis of regional-scale atmospheric dispersion. *J. Environ. Radioact.* **112**, 141-154.

Tyler A.N. (1994). *Environmental Influences on Gamma Ray Spectrometry*. PhD Thesis, University of Glasgow.

Tyler, A.N., Sanderson, D.C.W., Scott, E.M., Allyson, J.D. (1996). Accounting for spatial variability and fields of view in environmental gamma ray spectrometry. *J. Environ. Radioact.* **33**, 213-235.

Walling D.E., He Q. (1999). Improved models for estimating soil erosion rates from cesium-137 measurements. *Journal of Environmental Quality* **28**, 611-622.

Walling D.E., He Q., Appleby P.G. (2002). Conversion models for use in soil-erosion, soil-redistribution and sedimentation investigations. In: Zapata F. (ed) *Handbook for the Assessment of Soil Erosion and Sedimentation using Environmental Radionuclides*. Kluwer Academic Publishers, Dordrecht, Netherlands. pp 111-164.

WHO (2012). *Preliminary dose estimation from the nuclear accident after the 2011 Great East Japan earthquake and tsunami*. World Health Organisation ISBN 978 92 4 150366 2.

WHO (2013). *Health risk assessment from the nuclear accident after the 2011 Great East Japan earthquake and tsunami, based on a preliminary dose estimation*. World Health Organisation ISBN 978 92 4 150513 0.

Williams D., Cambray R.S., Maskell S.C. (1958). *An airborne radiometric survey of the Windscale area, October 19-22 1957*. EL/R2438, UKAEA.

Winkelmann, I., Endrulat H.J., Fouasnon S., Gesewsky P., Haubelt R., Klipfer P., Köhler H., Kohl R., Kucheida D., Müller M.K., Neumann P., Schmidt H., Vogl K., Weimer S., Wildermuth H., Winkler S., Wirth E., Wolff S. (1987). *Radioactivity measurements in the Federal Republic of Germany after the Chernobyl accident*. ISH-148/90.

Yamana H. (2013). Implication of the isotopic ratios of radionuclides observed in the contaminated areas surrounding Fukushima-Daiichi NPP. *Proceedings of the International Symposium on environmental monitoring and dose estimation of residents after accident of TEPCO's Fukushima Daiichi Nuclear Power Stations*. KUR Research Program for Scientific Basis of Nuclear Safety, Report Series 4. KURRI-KR-186. pp 84-96.



University
of Glasgow

The University of Glasgow, charity number SC004401

ISBN 978-0-85261-937-7



9 780852 619377 >